RISING STARS: OPHTHALMOLOGY 2021

EDITED BY: Jorge L. Alió Del Barrio and Daniel Ting
PUBLISHED IN: Frontiers in Medicine

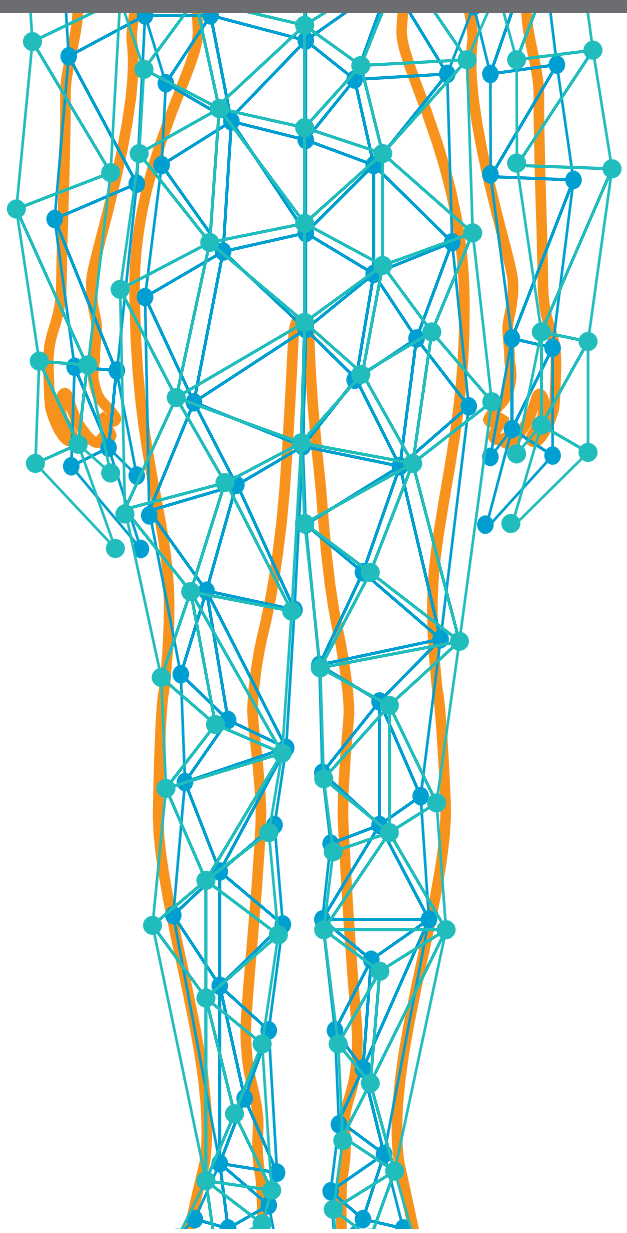

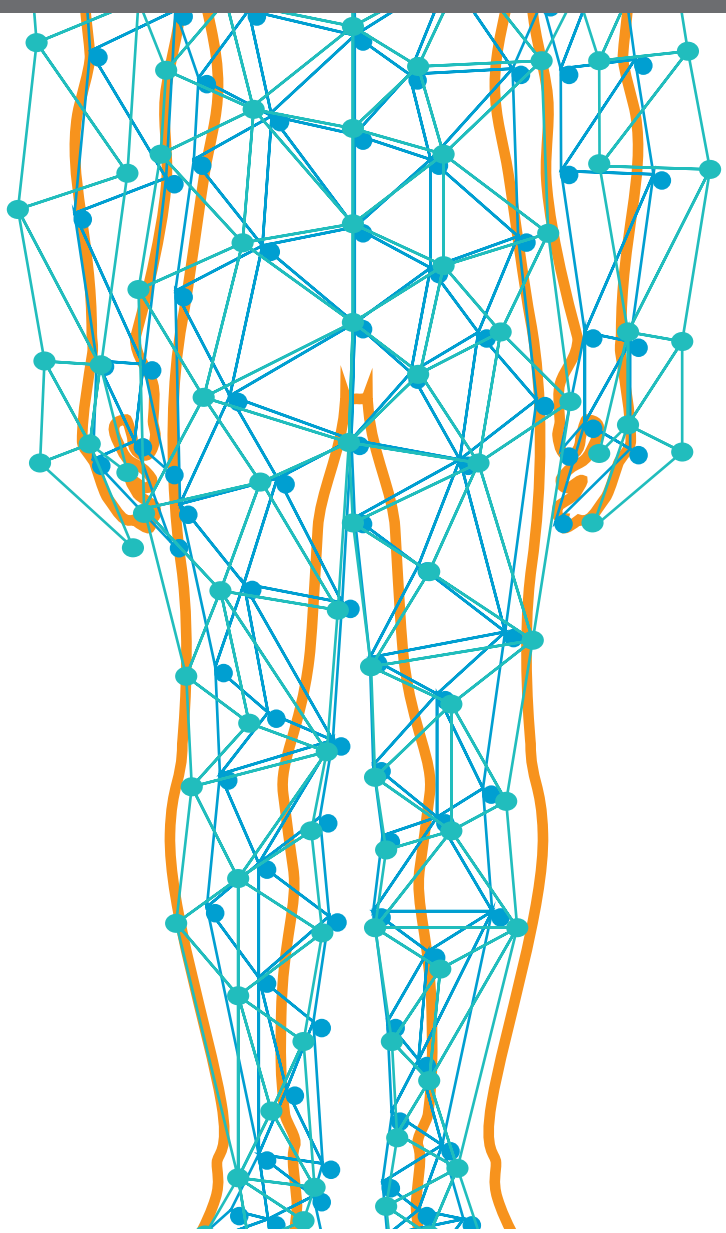

frontiers Research Topics

ISSN 1664-8714
ISBN 978-2-83250-557-1
DOI 10.3389/978-2-83250-557-1

About Frontiers

Frontiers is more than just an open-access publisher of scholarly articles: it is a pioneering approach to the world of academia, radically improving the way scholarly research is managed. The grand vision of Frontiers is a world where all people have an equal opportunity to seek, share and generate knowledge. Frontiers provides immediate and permanent online open access to all its publications, but this alone is not enough to realize our grand goals.

Frontiers Journal Series

The Frontiers Journal Series is a multi-tier and interdisciplinary set of open-access, online journals, promising a paradigm shift from the current review, selection and dissemination processes in academic publishing. All Frontiers journals are driven by researchers for researchers; therefore, they constitute a service to the scholarly community. At the same time, the Frontiers Journal Series operates on a revolutionary invention, the tiered publishing system, initially addressing specific communities of scholars, and gradually climbing up to broader public understanding, thus serving the interests of the lay society, too.

Dedication to Quality

Each Frontiers article is a landmark of the highest quality, thanks to genuinely collaborative interactions between authors and review editors, who include some of the world's best academicians. Research must be certified by peers before entering a stream of knowledge that may eventually reach the public - and shape society; therefore, Frontiers only applies the most rigorous and unbiased reviews.
Frontiers revolutionizes research publishing by freely delivering the most outstanding research, evaluated with no bias from both the academic and social point of view. By applying the most advanced information technologies, Frontiers is catapulting scholarly publishing into a new generation.

What are Frontiers Research Topics?

Frontiers Research Topics are very popular trademarks of the Frontiers Journals Series: they are collections of at least ten articles, all centered on a particular subject. With their unique mix of varied contributions from Original Research to Review Articles, Frontiers Research Topics unify the most influential researchers, the latest key findings and historical advances in a hot research area! Find out more on how to host your own Frontiers Research Topic or contribute to one as an author by contacting the Frontiers Editorial Office: frontiersin.org/about/contact

RISING STARS: OPHTHALMOLOGY 2021

Topic Editors:
Jorge L. Alió Del Barrio, Miguel Hernández University of Elche, Spain
Daniel Ting, Singapore National Eye Center, Singapore

Citation: Alio Del Barrio, J. L., Ting, D., eds. (2022). Rising Stars: Ophthalmology 2021. Lausanne: Frontiers Media SA. doi: 10.3389/978-2-83250-557-1

Table of Contents

frontiers in Medicine

SYSTEMATIC REVIEW
published: 03 December 2021
doi: 10.3389/fmed.2021.718724

Cost of Myopia Correction: A Systematic Review

*Li Lian Foo [1,2,3], Carla Lanca [2,4,5], Chee Wai Wong [1,2,3], Daniel Ting [1,2,3], Ecosse Lamoureux [2,3], Seang-Mei Saw [2,3,6] and Marcus Ang [1,2,3]**

[1] Singapore National Eye Centre, Singapore, Singapore, [2] Singapore Eye Research Institute, Singapore, Singapore, [3] Duke–NUS Medical School, National University of Singapore, Singapore, Singapore, [4] Escola Superior de Tecnologia da Saúde de Lisboa (ESTeSL), Instituto Politécnico de Lisboa, Lisboa, Portugal, [5] Comprehensive Health Research Center (CHRC), Escola Nacional de Saúde Pública, Universidade Nova de Lisboa, Lisboa, Portugal, [6] NUS Saw Swee Hock School of Public Health, Singapore, Singapore

Myopia is one of the leading causes of visual impairment globally. Despite increasing prevalence and incidence, the associated cost of treatment remains unclear. Health care spending is a major concern in many countries and understanding the cost of myopia correction is the first step eluding to the overall cost of myopia treatment. As cost of treatment will reduce the burden of cost of illness, this will aid in future cost-benefit analysis and the allocation of healthcare resources, including considerations in integrating eye care (refractive correction with spectacles) into universal health coverage (UHC). We performed a systematic review to determine the economic costs of myopia correction. However, there were few studies for direct comparison. Costs related to myopia correction were mainly direct with few indirect costs. Annual prevalence-based direct costs for myopia ranged from $14-26 (USA), $56 (Iran) and $199 (Singapore) per capita, respectively (population: 274.63 million, 75.15 million and 3.79 million, respectively). Annually, the direct costs of contact lens were $198.30-$378.10 while spectacles and refractive surgeries were $342.50 and $19.10, respectively. This review provides an insight to the cost of myopia correction. Myopia costs are high from nation-wide perspectives because of the high prevalence of myopia, with contact lenses being the more expensive option. Without further interventions, the burden of illness of myopia will increase substantially with the projected increase in prevalence worldwide. Future studies will be necessary to generate more homogenous cost data and provide a complete picture of the global economic cost of myopia.

Keywords: myopia, costs, spectacles, contact lenses, refractive surgeries declaration

OPEN ACCESS

Edited by:
Yuanbo Liang,
Affiliated Eye Hospital of Wenzhou Medical University, China

Reviewed by:
Michael Mimouni,
Rambam Health Care Campus, Israel
Shiming Li,
Capital Medical University, China

***Correspondence:**
Marcus Ang
marcus.ang@singhealth.com.sg

Specialty section:
This article was submitted to Ophthalmology, a section of the journal Frontiers in Medicine

Received: *01 June 2021*
Accepted: *11 November 2021*
Published: *03 December 2021*

Citation:
Foo LL, Lanca C, Wong CW, Ting D, Lamoureux E, Saw S-M and Ang M (2021) Cost of Myopia Correction: A Systematic Review. Front. Med. 8:718724. doi: 10.3389/fmed.2021.718724

INTRODUCTION

Myopia is one of the leading causes of visual impairment in the world (1, 2). The prevalence of myopia ranges from 15 to 49% in adult populations, and ranges from 20 to 90% in children, adolescents and young adults (3–7). Studies estimate that myopia will affect 50% (4.7 billion) of the world's population by 2050, with 10% (1 billion) having high myopia (≤-5.00 Dioptres) (8–10) Correction of myopia with spectacles, contact lenses and refractive surgeries therefore play an increasingly important role in society, as uncorrected myopia results in reduction of visual acuity leading to impaired visual functioning (11).

However, there are significant costs associated with optical correction, treatment to retard myopia progression and treatment of myopia related complications, including pathologic myopia, cataract, glaucoma and retinal detachment (12–16). With increasing demand for the limited healthcare resources globally, an understanding of the economic cost associated with the treatment of myopia is important for further cost-benefit analysis and policy making decisions. This will aid and justify in the allocation of invaluable healthcare resources to the treatment of myopia, in order to reduce the economic burden of this illness.

We aim to perform an evidence-based review of the economic costs associated with the correction of myopia.

SOURCES AND METHODS OF LITERATURE SEARCH

We conducted a systematic review of relevant literature articles in accordance with the Preferred Reporting Items for Systematic Reviews and Meta-analysis (PRISMA) guidelines (17). Several electronic databases (PubMed, ScienceDirect, Cochrane Library, and Web of Science databases) were searched to identify English language articles up to 29 February 2020 on costs associated with myopia correction treatment. The search used the keywords "myopia," "short-sightedness" or "near-sightedness" combined with "cost" or "economic burden." Original full-text articles in English were included if costs were quantified in relation to myopia correction, including: myopia correction (spectacles, contact lenses, refractive surgeries). 8,492 titles were retrieved through database searching. Forty five relevant records were reviewed with 12 records excluded (9 duplicates and 3 with no full-text available). Fifteen full-text articles were assessed for eligibility with 2 non-English articles excluded (articles in German). Articles that did not fulfill the inclusion criteria were excluded. Five eligible full-text articles were included in this review (18–22). The review article selection process is illustrated as a flowchart in **Figure 1.** The Asian studies comprised of 2 from Singapore while the non-Asian studies comprised of one from each of the following countries: United States of America (USA), Iran and Spain.

A 20-items Consensus Health Economic Criteria (CHEC)-extended checklist was used to evaluate the overall quality of included studies (23, 24). Scoring was performed by assigning a score of 1 (yes), 0 (no), 2 (not applicable) to each item and the total scores were summed to generate the overall quality score (0–100%). The total quality score for each study was categorized into low, moderate, good and excellent with cut-off value of <50, 51–75, 76–95 and >95, respectively. Only moderate, good and excellent quality studies were included as higher scores denote lower risk of bias. Two independent reviewers conducted the assessment (LLF and CL) and the interrater-agreement was evaluated using κ from STATA/IC 11.1 (25). The interpretation of the κ was based on a scale which indicates poor, slight, fair, moderate, substantial and perfect agreement with κ levels <0.0, 0.0–0.20, 0.21–0.40, 0.41–0.60, 0.61–0.80 and ≥0.81, respectively (26). Of the included studies, 4 were good in quality (76.5–95) and 1 was excellent (100). The interrater-reliability κ was moderate in 1 study (0.44), substantial in 2 studies (0.63, 0.64) and perfect in 2 studies (1, 1).

Examples of costs assessed included optical correction devices/procedures (spectacles, contact lenses, refractive surgeries), visits to professional services (transportation and fees) and time spent and loss of productivity while seeking treatment.

All costs are quoted in US dollars ($). Conversion rate used was Euro to USD = 1:1.12 (22, 27) and Pound sterling to USD = 1:1.31 (28), using average 2019 exchange rates (29).

RESULTS

The costs for myopia correction are shown in **Table 1**.

The average direct costs of myopia correction in Singapore children aged 12–17 years from the SCORM study (Singapore Cohort study of the Risk factors of Myopia) were $147.80 per year per myopia patient, $82.10 per pair of spectacles and $378.10 per year for contact lenses (18).

In Singapore adults aged ≥40 years, the mean direct cost of myopia correction was $709 per year per patient. This estimate translates into an annual economic burden of $755 million in Singapore. Refractive correction, comprising of optometry visits, spectacles and contact lenses, were the most significant, accounting for 65.2% of the total costs (19). The remaining costs comprise of refractive surgeries and complications related to it as well as contact lens use.

In USA, the annual direct country-wide cost of correcting distance vision impairment was estimated to be between $3.9 and $7.2 billion, with $780 million per annum for persons >age 65 years (33). The National Health and Nutrition Examination Survey (NHANES) was an ongoing, nationally representative survey of 14,203 participants aged ≥ 12 years (32, 33). The cost calculations were based on single-vision spectacles, without including other refractive correction options. Hence, this cost would be much higher if contact lenses and refractive surgeries were taken into account. As the annual costs from the earlier Singapore study were based on all forms of corrections, direct comparison is inequitable. In addition, due to the study's methodology for distant vision correction, subjects with pure astigmatism without myopia were also included in the cost calculations.

In two other studies (21, 22), the costs of refractive correction were computed by including other refractive errors (hyperopia and astigmatism). While the costs of each modality for myopia correction alone could not be determined, they provide insights to the general cost for refractive correction in the country.

In a Spanish study, the direct cost of spectacles, contact lenses and LASIK were evaluated (22). It was reported that the total direct (medical and non-medical) cost over 10, 20, and 30 years (5% discount rate) for contact lens was $3019.64; 4723.21; 5779.46, LASIK was $3341.96; 3368.75; 3385.71 and spectacles was $1091.07; 1623.21; 1960.71 (22). This was a

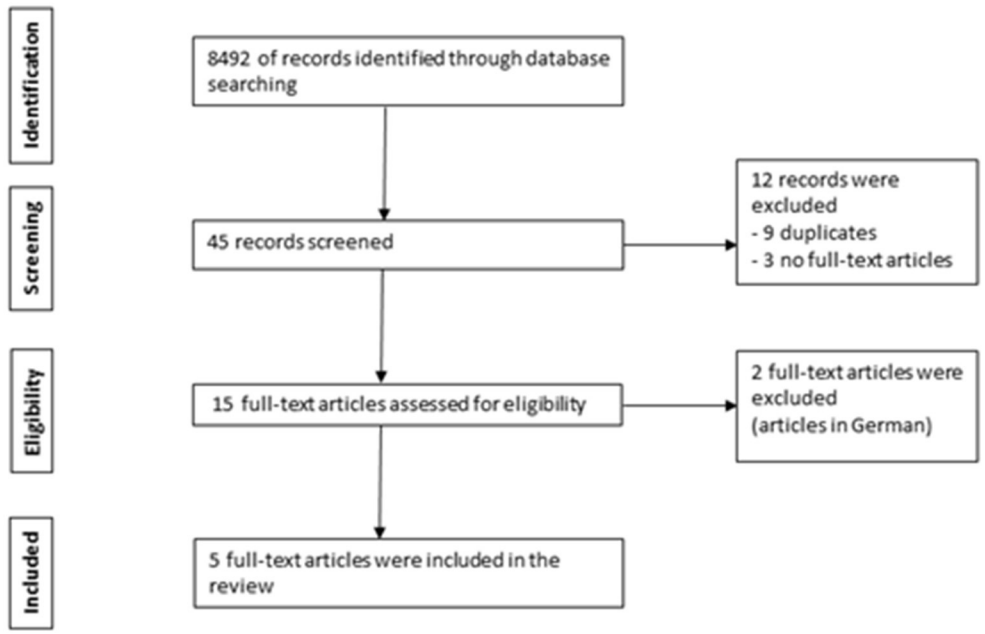

FIGURE 1 | Flowchart of the review article selection process.

small study of 40 subjects from one city in Alicante, with 80% myopes (12.5% hyperopes and 42.5% astigmatic). This study was conducted in 2002 and hence costs might not be representative of the current market, particularly the cost of cleaning and fitting contact lens and transport system with technological advancements.

In a recent Iranian study, 120 subjects aged $\geq$ 23 years were interviewed in a hospital and the lifetime direct costs of spectacles, contact lenses and refractive surgeries were \$9373.50, \$5203.10, and \$568.10, respectively (21). The annual direct costs of refractive correction per patient and for each of the three modalities were \$309, \$342.50, \$198.30, and \$19.10, respectively. Annually, direct cost of myopia correction was estimated to be \$4.2 billion in Iran. Indirect costs in this study were estimated using the human capital approach, by ascertaining lost productivity due to the complication, maintenance, repair and travel costs as a measure of patient's and caregiver's lost earnings (34). Annually, the indirect costs were \$12112.10, \$3045.20, and \$113.60, respectively with the main bulk contributed by patient's and caregiver's opportunity cost. However, it was not clear from the study regarding the basis and role of caregiver's costs calculation in optical correction and no justification was offered for the high indirect costs from spectacles, considering it is least prone to complications. In addition, cost calculations for each refractive correction modality were generalized to all forms of refractive errors, it was challenging to estimate the cost generated from myopia only.

Out of the three groups of myopia correction modalities reported in the studies (18, 21, 22), contact lens and spectacles appeared to be generally more costly than refractive surgeries **(Figure 2)**. Annually, the direct costs of contact lens and spectacles were \$198.30-\$378.10 and \$342.50, respectively while refractive surgeries was \$19.10 (18, 21).

In Singapore, while the annual direct cost of myopia correction to the individual is the lowest compared to diabetic retinopathy and wet age-related macular degeneration (AMD) (18, 19, 35, 36), the nation's annual direct cost of myopia correction (\$755 million) alone far exceeded other ocular diseases including acute primary angle closure glaucoma (\$0.26–0.29 million), dry eyes (\$1.51–1.52 million) and wet AMD (\$96.8–120.7 million) **(Table 2)** (18, 19, 35, 36, 41, 42).

DISCUSSION

In this review, we found 5 studies addressing the cost of myopia correction (18, 19, 21, 22, 33), which are generally direct costs from spectacles, contact lens and refractive surgeries. The per capita annual cost of myopia correction was low in USA, moderate in Iran and high in Singapore. Indirect costs in myopia correction are mainly related to complications, particularly with contact lens use, including cost of treatment, loss of productivity secondary to complications and its associated travel costs (21). We found that the annual direct costs of myopia correction in USA, Iran and Singapore were substantial at \$3.9–7.2 billion, \$4.2 billion and \$755 million, respectively. This translated to \$14–26 (USA), \$56 (Iran) and \$199 (Singapore) per capita, respectively (population: 274.63 million, 75.15 million and 3.79 million, respectively) (19, 21, 43). Most costs related to myopia correction were direct costs, with contact lens appearing to be generally more costly compared to other modalities.

TABLE 1 | Summary table of reviewed articles (treatment of Myopia-Myopia correction: $n = 5$).

Treatment of Myopia (Myopia correction)											
No	**References**	**Year**	**Country**	**Type of study**	**Costs**	**Sample size (*n*)**	**Age (Years)**	**Method of ascertaining cost**	**Prevalence of Myopia (%)**	**Direct cost ($)**	**Indirect cost ($)**
1	Ruiz-Moreno and Roura (27)	2009	Singapore	Cross-sectional study	Myopia correction	301	12–17	Parent and Self questionnaire	NA	Annual direct cost Mean (Per patient) = $147.8 ± 209.1 (CI, $124.3–172.1) Median (Per patient) = $83.3 Mean cost per pair of spectacles $82.1 ± 40.8 (CI, $77.8–86.5) Mean annual cost of contact lenses $378.1 ± 377.1 (CI, $281.4–474.6).	NA
2	Zheng YF et al. (30)	2013	Singapore	Cross-sectional study	Myopia correction	113	52.6 ± 7.8	Questionnaire	Age 0-4 = 10% 5–9 = 30% 10–14 = 60% 15–24 = 80% 25–39 = 90% 40–49 = 45% 50–59 = 35% 60–80+ =30%	Annual direct cost Mean (Per patient) = $709 Annual direct cost Singapore = $755 million Urban Asia = $328 billion Lifetime per capita cost (disease of 0–80 years) $232–17,020	
3	Vitale S et al. (31)	2006	USA	Cross-sectional	Myopia correction	13211	≥12	NHANES and fees schedule and expenditure data	NA	Annual direct cost All = $3.9–7.2 billion Persons age > 65 = $780 million	NA
4	Morgan et al. (7)	2002	Spain	Cross-sectional	Myopia correction	40 (80% Myopia)	Mean 32	Questionnaire markov model	NA	Total direct cost* (10, 20 and 30 years) LASIK = $ 3341.96; 3368.75; 3385.71 Spectacles = $ 1091.07; 1623.21; 1960.71 Contact lens = $ 3019.64; 4723.21; 5779.46	NA

(Continued)

TABLE 1 | Continued

Treatment of Myopia (Myopia correction)											
No	**References**	**Year**	**Country**	**Type of study**	**Costs**	**Sample size (*n*)**	**Age (Years)**	**Method of ascertaining cost**	**Prevalence of Myopia (%)**	**Direct cost ($)**	**Indirect cost ($)**
5	Malec et al. (32)	2018	Iran	Cross-sectional	Myopia correction	120 (60.83% Myopia)	≥23	Interview	Age < 14 = 3.6% 15–19 = 16.5% 20–29 = 22.0% >60 = 32.8%	Total annual direct cost* Spectacles = $342.5 ± 8.41 Contact lenses = $198.30 ± 0.12 Refractive surgery = $19.10 ± 1.2 Lifetime direct cost* Spectacles = $9373.5 ± 230.1 Contact lenses = $5203.10 ± 256.3 Refractive surgery = $568.1 ± 64.6 Annual direct cost* Mean (Per patient) = $309 Annual direct cost All ages = $4.2 billion Persons age < 14 = $196 million Persons age 15-19 = $337 million Persons age 20-29 = $3043 million Persons age > 60 = $628.55 million Annual and lifetime total costs* (direct and indirect) Spectacles = $12454.6; 340754.10, Contact lenses = $3243.5; 84965.30 Refractive surgery = $132.7; 3357.20	Total annual indirect cost* Spectacles = $12112.10 Contact lenses = $3045.20 Refractive surgery = $113.60 Lifetime indirect cost* Spectacles = $331380.60 Contact lenses = $79762.20 Refractive surgery = $2789.10

**Include all types of refractive error (myopia, hyperopia and astigmatism).*

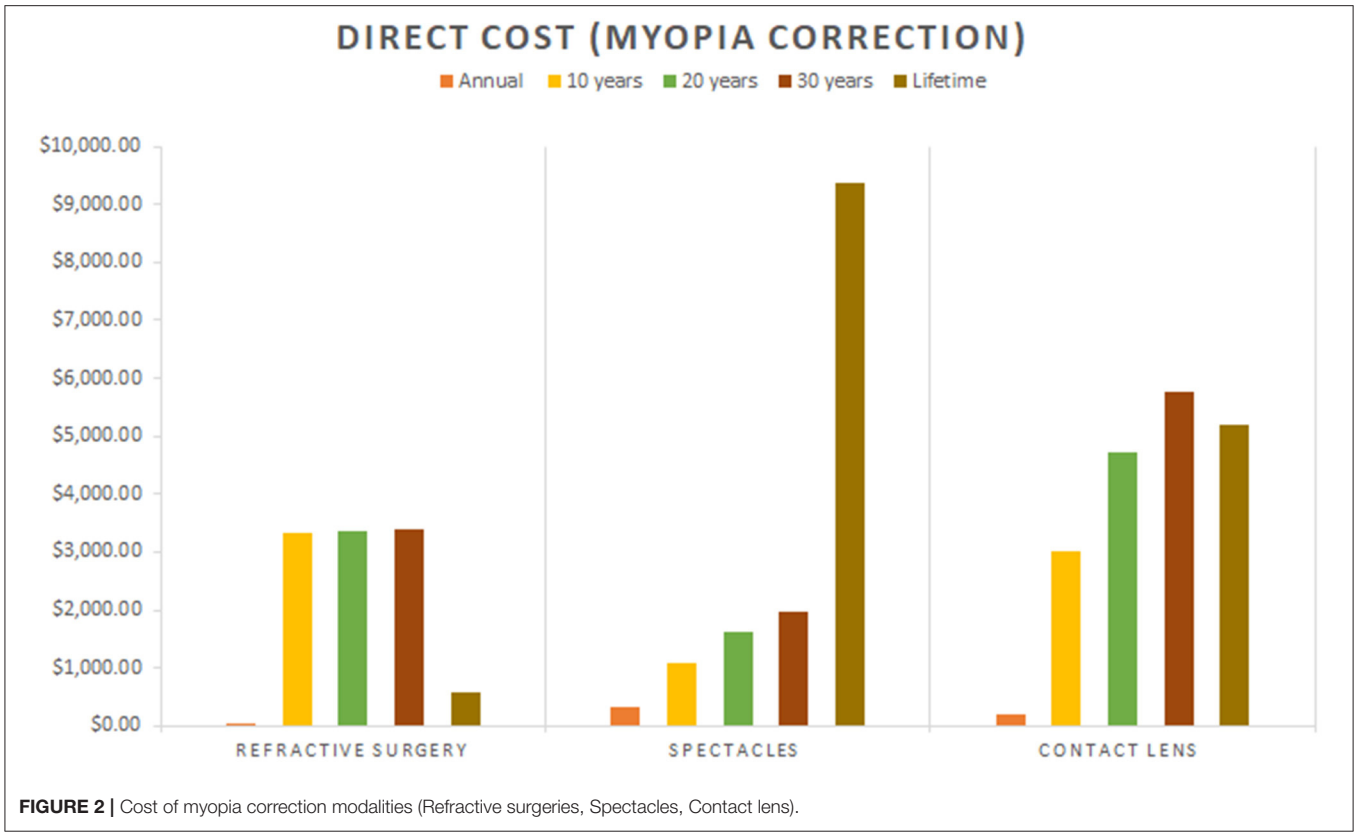

FIGURE 2 | Cost of myopia correction modalities (Refractive surgeries, Spectacles, Contact lens).

TABLE 2 | Cost of ocular diseases in Singapore.

Eye diseases in Singapore	Annual direct cost in Singapore ($)	Mean annual direct cost per patient ($)
Diabetic retinopathy (37)	NA	$863.65–2660.15
Acute primary angle closure glaucoma (38)	$0.26–0.29 million	NA
Dry eyes (39)	$1.51–1.52 million*	NA
Wet AMD (40)	$96.8–120.7 million	$6902.20
Myopia correction (27, 30)	$755 million	$147.80–709

**Singapore National Eye Centre only.*

We found few studies to adequately address this topic and limited studies using similar costs definitions for comparison. Firstly, there was a limited representation of studies globally, with 2 from Asia (Singapore) and 3 from Europe (Spain), USA and Middle East (Iran), respectively. Secondly, different methodologies and cost definitions were used for cost calculations and many studies did not assessed indirect costs in detail.

The World Health Organization (WHO) considers spectacles or contact lenses as functioning interventions (44), with spectacles being also considered as an assistive device which is part of the WHO Priority Assistive Products List (45). As health care spending is a major concern in many countries, understanding the cost of myopia correction is the first step eluding to the overall cost of myopia treatment. Moreover, among the worldwide population with moderate or severe vision impairment, uncorrected refractive error was the highest at 116.3 to 123.7 million (46, 47), with the cost of coverage gap for unaddressed refractive error and cataract estimated to be $14.3 billion globally (45). As cost of treatment will reduce the burden of cost of illness, this will aid in future cost-benefit analysis and the allocation of healthcare resources, including considerations in integrating eye care (refractive correction with spectacles) into universal health coverage (UHC) (45). This is particularly important in Asian developing countries where there is high prevalence of myopia with low accessibility to spectacles.

Although the cost of myopia to an individual may not be very high, the cost of myopia to the nation is one of the highest as the prevalence of myopia is higher than many other diseases. The high prevalence of myopia plays an important role in determining the economic cost of the treatment of myopia in each country. In East and Southeast Asia, the

prevalence of myopia was reported to be as high as 80–90% in adolescents of age of 17–18 (7). In contrast, 20–40% was reported in developed western countries (7, 20, 40, 48–50). Hence while the magnitude of direct cost of refractive correction was greater in USA and Iran than in Singapore, the per capita cost was lesser at $14–26 and $56 vs. $199 (19, 31).

Other factors that could account for variation in costs include country-specific costs, different methodologies, study subject's characteristics (including age), timeline, varying costs of living and socioeconomic status. However, due to limited studies available, it would be challenging to explore the influence of these factors. As the governments in most countries are unlikely to be able to monitor spectacle or contact lens sales, future cost data can be obtained by considering cross-sectional rapid assessment protocols, targeting for instance high schools.

In Singapore, although the annual direct cost of myopia correction to the individual is lowest amongst diabetic retinopathy and wet AMD (18, 19, 35, 36), the nation's annual direct cost of myopia correction alone far exceeded other ocular diseases including acute primary angle closure glaucoma, dry eyes and AMD (18, 19, 35, 36, 41, 42). This finding is not surprising and is attributed to the high prevalence of myopia in the country, with myopia expected to remain as the most common ocular condition with 2.393 million cases in 2040 (51).

Out of the three groups of myopia correction modalities, contact lens and spectacles seemed to be generally more costly than refractive surgery (18, 21, 22), with the exception of 1 study which did not justify the inclusion of high patient and caregiver opportunity costs from spectacles use (21). This is excluding the indirect costs of contact lens related complications (e.g., infective keratitis), including cost of treatment, loss of productivity secondary to complications and its associated travel costs. However, this cost is expected to be dynamic in view of technological advancement, economic forces, occupational and recreational requirements, individuals paying premium for factors such as aesthetics and quality as well as free or subsidized refractive correction by the government.

Contact lenses were mainly prescribed for the correction of myopia, with proportion as high as 94% (52). The three key cost components of contact lens wear are the professional fees, the cost of lenses and the cost of lens care solutions (38, 39). Spherical lenses have the lowest overall cost, followed by toric and multifocal lenses (39), with the true cost of lens wear (cost-per-wear) dependent on the frequency of use (38, 39). Generally, daily replacement contact lenses are more cost-effective on a part-time usage, while reusable lenses are more cost-effective on a full-time usage (38). With contact lens gaining popularity among the teenagers and young adults (52), together with the high prevalence of myopia in this age-group (3–7), the nation-wide costs of contact lenses are expected to rise in the near future.

We have reviewed the costs of optical correction of myopia. However, since the cost and burden to the nation is high, treatments to slow myopia progression and measures to prevent myopia and high myopia (including outdoor programs) are important to reduce the prevalence of myopia and subsequent costs of illness, including burden related to its complications.

Atropine eyedrops have shown strong evidence in myopia control while Orthokeratology, myopic defocus multizone contact lenses and spectacles have shown some effect (30, 37, 53–57). However, there is currently no literature reporting the treatment costs generated from Atropine use in children (53, 54). The use of myopia control treatment modalities will inevitably incur costs including equipment, professional services and the management of complications, particularly infective keratitis with contact lens use. Further studies, including cost-effectiveness randomized control trials of treatments for myopia progression will be necessary to evaluate this knowledge deficit.

LIMITATIONS

For myopia correction, differentiating costs of optometry visits and refractive correction devices was difficult due to difference in studie's methodology. Another limitation includes the presence recall and non-response bias from retrospective design studies and the use of questionnaires/interviews. In addition, cost data reported in older studies may not be a reliable reflection of today's costs, due to various economic factors. Details of indirect costs were lacking. There were few studies available in the literature with limited representation globally.

FURTHER STUDIES

Future studies will be necessary to generate a more homogenous cost data and provide a more complete picture of the global economic cost of myopia treatment. These include cost of illness analysis, programmatic costs of spectacles correction in rural areas by non-governmental organizations and cost-effectiveness randomized control trials of treatments for myopia progression.

CONCLUSION

Our systematic review provides insight on the costs of myopia correction. Annual prevalence-based direct costs for myopia correction are substantial, ranging from US$14–26 (USA), $56 (Iran) to $199 (Singapore) per capita. In Singapore, the annual direct cost of myopia correction alone far exceeded the costs of other ocular diseases including acute primary angle closure glaucoma, dry eyes and wet AMD due to high prevalence of disease. Without further interventions, the economic burden of illness of myopia will increase substantially with the projected increase in prevalence worldwide. Hence, myopia control treatment in children and measures to prevent myopia and high myopia will play an increasingly important role to reduce prevalence and costs of illness. Future studies will be necessary to generate a more homogenous cost data and provide a complete picture of the global economic cost of myopia.

DATA AVAILABILITY STATEMENT

The original contributions presented in the study are included in the article/**Supplementary Material**, further inquiries can be directed to the corresponding authors.

AUTHOR CONTRIBUTIONS

LF, CL, and S-MS: conception and design of study. LF, CL, CW, DT, EL, and MA: analysis and/or interpretation of data. LF, CL, S-MS, and MA: drafting the manuscript. CW, DT, EL, S-MS, and MA: revising the manuscript critically for important intellectual content. All authors contributed to the article and approved the submitted version.

SUPPLEMENTARY MATERIAL

The Supplementary Material for this article can be found online at: https://www.frontiersin.org/articles/10.3389/fmed.2021.718724/full#supplementary-material

REFERENCES

1. Pararajasegaram R. VISION 2020-the right to sight: from strategies to action. *Am J Ophthalmol.* (1999) 128:359–60. doi: 10.1016/S0002-9394(99)00251-2
2. Holden BA, Wilson DA, Jong M, Sankaridurg P, Fricke TR, Smith EL, et al. Myopia: a growing global problem with sight-threatening complications. *Community eye health.* (2015) 28:35.
3. Pan CW, Ramamurthy D, Saw SM. Worldwide prevalence and risk factors for myopia. *Ophthalmic Physiol Opt.* (2012) 32:3–16. doi: 10.1111/j.1475-1313.2011.00884.x
4. Lim DH, Han J, Chung TY, Kang S, Yim HW, Epidemiologic Survey Committee of the Korean Ophthalmologic Society. The high prevalence of myopia in Korean children with influence of parental refractive errors: the 2008-2012 Korean national health and nutrition examination survey. *PLoS ONE.* (2018) 13:e0207690. doi: 10.1371/journal.pone.0207690
5. Belete GT, Anbesse DH, Tsegaye AT, Hussen MS. Prevalence and associated factors of myopia among high school students in Gondar town, northwest Ethiopia, 2016. *Clinical optometry.* (2017) 9:11–8. doi: 10.2147/OPTO.S120485
6. Xie Z, Long Y, Wang J, Li Q, Zhang Q. Prevalence of myopia and associated risk factors among primary students in Chongqing: multilevel modeling. *BMC Ophthalmol.* (2020) 20:146. doi: 10.1186/s12886-020-01410-3
7. Morgan IG, Ohno-Matsui K, Saw SM. Myopia. *Lancet.* (2012) 379:1739–48. doi: 10.1016/S0140-6736(12)60272-4
8. Modjtahedi BS, Ferris FL, Hunter DG, Fong DS. Public health burden and potential interventions for myopia. *Ophthalmology.* (2018) 125:628–30. doi: 10.1016/j.ophtha.2018.01.033
9. Holden BA, Fricke TR, Wilson DA, Jong M, Naidoo KS, Sankaridurg P, et al. Global prevalence of myopia and high myopia and temporal trends from 2000 through 2050. *Ophthalmology.* (2016) 123:1036–42. doi: 10.1016/j.ophtha.2016.01.006
10. Chia A, Lu QS. Tan D. Five-year clinical trial on atropine for the treatment of myopia 2: myopia control with atropine 001% eyedrops. *Ophthalmology.* (2016) 123:391–9. doi: 10.1016/j.ophtha.2015.07.004
11. Naidoo KS, Fricke TR, Frick KD, Jong M, Naduvilath TJ, Resnikoff S, et al. Potential lost productivity resulting from the global burden of myopia: systematic review, meta-analysis, and modeling. *Ophthalmology.* (2019) 126:338–46. doi: 10.1016/j.ophtha.2018.10.029
12. Marcus MW, de Vries MM, Junoy Montolio FG, Jansonius NM. Myopia as a risk factor for open-angle glaucoma: a systematic review and meta-analysis. *Ophthalmology.* (2011) 118:1989–94. doi: 10.1016/j.ophtha.2011.03.012
13. Bechrakis NE, Dimmer A. [Rhegmatogenous retinal detachment: Epidemiology and risk factors]. *Ophthalmologe.* (2018) 115:163–78. doi: 10.1007/s00347-017-0647-z
14. Praveen MR, Vasavada AR, Jani UD, Trivedi RH, Choudhary PK. Prevalence of cataract type in relation to axial length in subjects with high myopia and emmetropia in an Indian population. *Am J Ophthalmol.* (2008) 145:176–81. doi: 10.1016/j.ajo.2007.07.043
15. Saw SM, Gazzard G, Shih-Yen EC, Chua WH. Myopia and associated pathological complications. *Ophthalmic Physiol Opt.* (2005) 25:381–91. doi: 10.1111/j.1475-1313.2005.00298.x
16. Saw SM, Matsumura S, Hoang QV. Prevention and management of myopia and myopic pathology. *Invest Ophthalmol Vis Sci.* (2019) 60:488–99. doi: 10.1167/iovs.18-25221
17. Moher D, Liberati A, Tetzlaff J, Altman DG, Group P. Preferred reporting items for systematic reviews and meta-analyses: the PRISMA statement. *J Clin Epidemiol.* (2009) 62:1006–12. doi: 10.1016/j.jclinepi.2009.06.005
18. Lim MC, Gazzard G, Sim EL, Tong L, Saw SM. Direct costs of myopia in Singapore. *Eye.* (2009) 23:1086–9. doi: 10.1038/eye.2008.225
19. Zheng YF, Pan CW, Chay J, Wong TY, Finkelstein E, Saw SM. The economic cost of myopia in adults aged over 40 years in Singapore. *Invest Ophthalmol Vis Sci.* (2013) 54:7532–7. doi: 10.1167/iovs.13-12795
20. Vitale S, Ellwein L, Cotch MF, Ferris FL, Sperduto R. Prevalence of refractive error in the United States, 1999-2004. *Arch Ophthalmol.* (2008) 126:1111–9. doi: 10.1001/archopht.126.8.1111
21. Mohammadi SF, Alinia C, Tavakkoli M, Lashay A, Chams H. Refractive surgery: the most cost-saving technique in refractive errors correction. *Int J Ophthalmol.* (2018) 11:1013–9.
22. Berdeaux G, Alio JL, Martinez JM, Magaz S, Badia X. Socioeconomic aspects of laser *in situ* keratomileusis, eyeglasses, and contact lenses in mild to moderate myopia. *J Cataract Refract Surg.* (2002) 28:1914–23. doi: 10.1016/S0886-3350(02)01496-7
23. Evers S, Goossens M, de Vet H, van Tulder M, Ament A. Criteria list for assessment of methodological quality of economic evaluations: consensus on health economic criteria. *Int J Technol Assess Health Care.* (2005) 21:240–5. doi: 10.1017/S0266462305050324
24. *Consensus Health Economic Criteria-CHEC list*. Available online: https://hsr.mumc.maastrichtuniversity.nl/consensus-health-economic-criteria-chec-list.
25. Brennan RL, Prediger DJ. Coefficient kappa: some uses, misuses, and alternatives. *Educ Psychol Meas.* (1981) 41:687–99. doi: 10.1177/001316448104100307
26. Landis JR, Koch GG. The measurement of observer agreement for categorical data. *Biometrics.* (1977) 33:159–74. doi: 10.2307/2529310
27. Ruiz-Moreno JM, Roura M. en representacion del grupo del estudio M. Cost of myopic patients with and without myopic choroidal neovascularization. *Arch Soc Esp Oftalmol.* (2016) 91:265–72. doi: 10.1016/j.oftal.2016.01.013
28. Claxton L, Malcolm B, Taylor M, Haig J, Leteneux C. Ranibizumab, verteporfin photodynamic therapy or observation for the treatment of myopic choroidal neovascularization: cost effectiveness in the UK. *Drugs Aging.* (2014) 31:837–48. doi: 10.1007/s40266-014-0216-y
29. *Monetary Authority of Singapore (MAS).* Available online at: https://www.mas.gov.sg/
30. Pineles SL, Kraker RT, VanderVeen DK, Hutchinson AK, Galvin JA, Wilson LB, et al. Atropine for the prevention of myopia progression in children: a report by the American Academy of Ophthalmology. *Ophthalmology.* (2017) 124:1857–66. doi: 10.1016/j.ophtha.2017.05.032
31. *Worldometer Elaboration of data by United Nations, Department of Economic and Social Affairs, Population Division.*
32. Malec D, Davis WW, Cao X. Model-based small area estimates of overweight prevalence using sample selection adjustment. *Stat Med.*

(1999) 18:3189–200. doi: 10.1002/(sici)1097-0258(19991215)18:23<3189::aid-sim309>3.0.co;2-c
33. Vitale S, Cotch MF, Sperduto R, Ellwein L. Costs of refractive correction of distance vision impairment in the United States, 1999-2002. *Ophthalmology.* (2006) 113:2163–70. doi: 10.1016/j.ophtha.2006.06.033
34. Kigozi J, Jowett S, Lewis M, Barton P, Coast J. Estimating productivity costs using the friction cost approach in practice: a systematic review. *Eur J Health Econ.* (2016) 17:31–44. doi: 10.1007/s10198-014-0652-y
35. Saxena N, George PP, Hoon HB, Han LT, Onn YS. Burden of wet age-related macular degeneration and its economic implications in Singapore in the year 2030. *Ophthalmic Epidemiol.* (2016) 23:232–7. doi: 10.1080/09286586.2016.1193617
36. Zhang X, Low S, Kumari N, Wang J, Ang K, Yeo D, et al. Direct medical cost associated with diabetic retinopathy severity in type 2 diabetes in Singapore. *PLoS ONE.* (2017) 12:e0180949. doi: 10.1371/journal.pone.0180949
37. Joachimsen L, Bohringer D, Gross NJ, Reich M, Stifter J, Reinhard T, et al. A pilot study on the efficacy and safety of 0.01% atropine in German school children with progressive myopia. *Ophthalmol Ther.* (2019) 8:427–33. doi: 10.1007/s40123-019-0194-6
38. Efron SE, Efron N, Morgan PB, Morgan SL, A. theoretical model for comparing UK costs of contact lens replacement modalities. *Cont Lens Anterior Eye.* (2012) 35:28–34. doi: 10.1016/j.clae.2011.07.006
39. Efron N, Efron SE, Morgan PB, Morgan SL, A. 'cost-per-wear' model based on contact lens replacement frequency. *Clin Exp Optom.* (2010) 93:253–60. doi: 10.1111/j.1444-0938.2010.00488.x
40. Vitale S, Sperduto RD, Ferris FL, III. Increased prevalence of myopia in the United States between 1971–1972 and 1999–2004. *Arch Ophthalmol.* (2009) 127:1632–9. doi: 10.1001/archophthalmol.2009.303
41. Waduthantri S, Yong SS, Tan CH, Shen L, Lee MX, Nagarajan S, et al. Cost of dry eye treatment in an Asian clinic setting. *PLoS ONE.* (2012) 7:e37711. doi: 10.1371/journal.pone.0037711
42. Wang JC, Chew PT. What is the direct cost of treatment of acute primary angle closure glaucoma? the Singapore model. *Clin Exp Ophthalmol.* (2004) 32:578–83. doi: 10.1111/j.1442-9071.2004.00906.x
43. Klein RJ SC. Age adjustment using the 2000 projected U.S. population. *Healthy People 2010 Stat Notes.* (2001) 20:1–10. doi: 10.1037/e583772012-001
44. WHO. *Western Pacific Regional Strategy for Health Systems Based on the Values of Primary Health Care.* World Health Organization (2010).
45. World Health Organization. *World Report on Vision Switzerland.* (2019).
46. Flaxman SR, Bourne RRA, Resnikoff S, Ackland P, Braithwaite T, Cicinelli MV, et al. Global causes of blindness and distance vision impairment 1990-2020: a systematic review and meta-analysis. *Lancet Glob Health.* (2017) 5:e1221–34. doi: 10.1016/S2214-109X(17)30393-5
47. Bourne RRA, Flaxman SR, Braithwaite T, Cicinelli MV, Das A, Jonas JB, et al. Magnitude, temporal trends, and projections of the global prevalence of blindness and distance and near vision impairment: a systematic review and meta-analysis. *Lancet Glob Health.* (2017) 5:e888–97. doi: 10.1016/S2214-109X(17)30293-0
48. Cumberland PM, Bao Y, Hysi PG, Foster PJ, Hammond CJ, Rahi JS, et al. Frequency and distribution of refractive error in adult life: methodology and findings of the UK Biobank Study. *PLoS ONE.* (2015) 10:e0139780. doi: 10.1371/journal.pone.0139780
49. Pan CW, Dirani M, Cheng CY, Wong TY, Saw SM. The age-specific prevalence of myopia in Asia: a meta-analysis. *Optom Vis Sci.* (2015) 92:258–66. doi: 10.1097/OPX.0000000000000516
50. Williams KM, Verhoeven VJ, Cumberland P, Bertelsen G, Wolfram C, Buitendijk GH, et al. Prevalence of refractive error in Europe: the European Eye Epidemiology (E(3)) Consortium. *Eur J Epidemiol.* (2015) 30:305–15. doi: 10.1007/s10654-015-0010-0
51. Ansah JP, Koh V, de Korne DF, Bayer S, Pan C, Thiyagarajan J, et al. Projection of eye disease burden in Singapore. *Ann Acad Med Singapore.* (2018) 47:13–28.
52. Yung AM, Cho P, Yap M, A. market survey of contact lens practice in Hong Kong. *Clin Exp Optom.* (2005) 88:165–75. doi: 10.1111/j.1444-0938.2005.tb06690.x
53. Huang J, Wen D, Wang Q, McAlinden C, Flitcroft I, Chen H, et al. efficacy comparison of 16 interventions for myopia control in children: a network meta-analysis. *Ophthalmology.* (2016) 123:697–708. doi: 10.1016/j.ophtha.2015.11.010
54. Weiss RS, Park S. Recent updates on myopia control: preventing progression 1 diopter at a time. *Curr Opin Ophthalmol.* (2019) 30:215–9. doi: 10.1097/ICU.0000000000000571
55. Chia A, Chua WH, Cheung YB, Wong WL, Lingham A, Fong A, et al. Atropine for the treatment of childhood myopia: safety and efficacy of 0.5%, 01%, and 001% doses (Atropine for the Treatment of Myopia 2). *Ophthalmology.* (2012) 119:347–54. doi: 10.1016/j.ophtha.2011.07.031
56. Li FF, Yam JC. Low-concentration atropine eye drops for myopia progression. *Asia Pac J Ophthalmol.* (2019) 8:360–5. doi: 10.1097/APO.0000000000000256
57. Sacchi M, Serafino M, Villani E, Tagliabue E, Luccarelli S, Bonsignore F, et al. Efficacy of atropine 0.01% for the treatment of childhood myopia in European patients. *Acta Ophthalmol.* (2019) 97:e1136–40. doi: 10.1111/aos

Conflict of Interest: The authors declare that the research was conducted in the absence of any commercial or financial relationships that could be construed as a potential conflict of interest.

Publisher's Note: All claims expressed in this article are solely those of the authors and do not necessarily represent those of their affiliated organizations, or those of the publisher, the editors and the reviewers. Any product that may be evaluated in this article, or claim that may be made by its manufacturer, is not guaranteed or endorsed by the publisher.

frontiers in Medicine

ORIGINAL RESEARCH
published: 25 February 2022
doi: 10.3389/fmed.2022.834663

Corneal Biomechanics Differences Between Chinese and Caucasian Healthy Subjects

Riccardo Vinciguerra[1], Robert Herber[2], Yan Wang[3,4], Fengju Zhang[5], Xingtao Zhou[6], Ji Bai[7], Keming Yu[8], Shihao Chen[9], Xuejun Fang[10], Frederik Raiskup[2] and Paolo Vinciguerra[11,12]*

[1] Humanitas San Pio X Hospital, Milan, Italy, [2] Department of Ophthalmology, University Hospital Carl Gustav Carus, Dresden, Germany, [3] Tianjin Eye Hospital, Tianjin Key Laboratory of Ophthalmology and Visual Science, Nankai University Affiliated Eye Hospital, Tianjin, China, [4] Clinical College of Ophthalmology, Tianjin Medical University, Tianjin, China, [5] Beijing Tongren Eye Center, Beijing Tongren Hospital, Beijing Ophthalmology and Visual Sciences Key Lab, Capital Medical University, Beijing, China, [6] EYE & ENT Hospital of Fudan University, Shanghai, China, [7] BAI JI Ophthalmology, Chongqing, China, [8] Zhongshan Ophthalmic Center, Sun Yat-Sen University, Guangzhou, China, [9] Eye Hospital, Wenzhou Medical University, Zhejiang, China, [10] Shenyang Aier Eye Hospital, Shenyang, China, [11] Department of Biomedical Sciences, Humanitas University, Milan, Italy, [12] IRCCS Humanitas Research Hospital, Rozzano, Italy

Purpose: The aim of this study was to evaluate the difference between Caucasian and Chinese healthy subjects with regards to Corvis ST dynamic corneal response parameters (DCRs).

Methods: Two thousand eight hundred and eighty-nine healthy Caucasian and Chinese subjects were included in this multicenter retrospective study. Subsequently, Chinese eyes were matched to Caucasians by age, intraocular pressure (IOP), and Corneal Thickness (CCT) using a case-control matching algorithm. The DCRs assessed were Deformation Amplitude (DA) Applanation 1 velocity (A1v), integrated radius (1/R), deformation amplitude ratio (DAratio), stiffness parameter at applanation 1 (SPA1), ARTh (Ambrósio's Relational Thickness to the horizontal profile), and the novel Stress Strain Index (SSI).

Results: After age-, CCT-, and IOP- matching, 503 Chinese were assigned to 452 Caucasians participants. Statistical analysis showed a statistical significant difference between Chinese and Caucasian Healthy subjects in the values of SPA1 ($p = 0.008$), Arth ($p = 0.008$), and SSI ($p < 0.001$). Conversely, DA, A1v, DAratio, and 1/R were not significantly different between the two ethnical groups ($p > 0.05$).

Conclusion: We found significant differences in the values of the DCRs provided by the Corvis ST between Chinese and Caucasian healthy subjects.

Keywords: biomechanics, cornea, keratoconus, CBI, IOP (intraocular pressure)

OPEN ACCESS

Edited by:
Jorge L. Alió Del Barrio, Miguel Hernández University of Elche, Spain

Reviewed by:
Mo Ziaei, The University of Auckland, New Zealand
Alessandro Arrigo, San Raffaele Hospital (IRCCS), Italy

****Correspondence:***
Riccardo Vinciguerra
vinciguerra.riccardo@gmail.com

Specialty section:
This article was submitted to Ophthalmology, a section of the journal Frontiers in Medicine

Received: *13 December 2021*
Accepted: *31 January 2022*
Published: *25 February 2022*

Citation:
Vinciguerra R, Herber R, Wang Y, Zhang F, Zhou X, Bai J, Yu K, Chen S, Fang X, Raiskup F and Vinciguerra P (2022) Corneal Biomechanics Differences Between Chinese and Caucasian Healthy Subjects. Front. Med. 9:834663. doi: 10.3389/fmed.2022.834663

INTRODUCTION

Ethnical differences in ocular metrics are well-known since many years and include central corneal thickness (1), corneal curvature (2), anterior chamber depth (3), and axial length (4).

In the last years, corneal biomechanics showed to play an important role for the diagnosis and management of keratoconus (5–9) post refractive surgery ectasia (10), cross-linking effect (11), measurement of intraocular pressure (12, 13), and glaucoma (14, 15).

Two instruments are commercially available to measure corneal biomechanics, the Ocular Response Analyzer (ORA, Reichert Inc., Depew, NY) (16) which measures corneal deformation during a bi-directional applanation method induced by an air jet, and produces appraisals of corneal hysteresis and corneal resistance factor, together with a set of 36 waveform-derived parameters (17–19). The Corvis ST (OCULUS Optikgeräte GmbH; Wetzlar, Germany) evaluates the reaction of the cornea to an air puff *via* an ultra-high speed (UHS) Scheimpflug camera, and uses the acquired image sequence to generate estimates of IOP and deformation response parameters (DCRs) (20).

The native software of the Corvis ST includes normative values for each DCRs which were derived from a mixed south American and Caucasian population (21). Very few population studies have been published with regards to DCRs values in other ethnical populations (22–24) and none of them evaluated the difference between two different ethnical groups.

The aim of this study was to assess the difference between Caucasian and Chinese healthy subjects with regards to Corvis ST DCRs.

METHODS

Two thousand eight hundred and eighty-nine healthy Caucasian and Chinese patients were included in this multicenter retrospective study. Caucasian subjects were recruited from Vincieye Clinic in Milan, Italy and from the Department of Ophthalmology, University Hospital Carl Gustav Carus, Technical University, Dresden, Germany. Conversely, Chinese participants were included from Beijing Tongren Eye Center, Beijing Tongren Hospital, Capital Medical University, Beijing; Shenyang Aier Eye Hospital, Shenyang, Zhongshan Ophthalmic Center, Sun Yat-Sen University, Guangzhou; EYE&ENT Hospital of Fudan University, Shanghai; Eye Hospital, Wenzhou Medical University, Zhejiang; BAI JI Ophthalmology, Chongqing, and Tianjin Eye Hospital,Tianjin.

Each Institutional review board (IRB) either ruled that approval was not required for this record review study or specifically approved the study. The research was conducted according to the ethical standards set in the 1964 Declaration of Helsinki, revised in 2000. All patients signed an informed consent before using their data in the study. All subjects underwent to a complete ophthalmic examination, including the Corvis ST and Pentacam exams. The inclusion criteria of this study were the existence in the database of a Corvis ST and Pentacam exam, a Belin Ambrosio Enhanced Ectasia Index total deviation (BAD-D) <1.6 and a signed informed consent. Exclusion criteria were any earlier ocular surgery or disease, any concurrent or previous glaucoma or hypotonic therapies. All exams with the Corvis ST were acquired by the same experienced technicians and captured by automatic release to ensure the absence of user dependency. Only Corvis ST exams with quality score "OK" were included in the analysis. Only 1 eye per subject was randomly included in the database to exclude the bias of the relationship between bilateral eyes that could influence the analysis result.

The parameters that were included in the analysis were the following: Deformation Amplitude Deformation Amplitude (DA, the largest displacement of corneal apex in the anterior-posterior direction at the moment of highest concavity) Applanation 1 velocity (A1v the velocity of corneal apex at first applanation), integrated radius (1/R the amount of the corneal concave state over the time between applanation 1 and applanation 2), deformation amplitude ratio (DAratio, the ratio between the central deformation and the average of peripheral deformation determined at 2.00 mm), stiffness parameter at applanation 1 [SPA1 is defined as the resultant pressure at inward applanation divided by the corneal displacement (25)], ARTh (Ambrósio's Relational Thickness to the horizontal profile), which is based on the thickness profile in the temporal-nasal direction (26) and the novel Stress Strain Index [SSI, which measures biomechanical behavior of the cornea without influence of corneal thickness and intraocular pressure (27)]. Additonally, the bIOP intraocular pressure estimate was included as a corrected value that is less influenced by age, corneal thickness and other DCR parameters (28).

Statistical Analysis

The statistical analysis was performed with SPSS version 27 (IBM Corp. in Armonk, NY, USA). In this study Chinese eyes were matched by age, bIOP, and Central Corneal Thickness (CCT) using a case-control matching algorithm provided by SPSS (29).

Descriptive statistics were calculated for the DCRs described previously, additionally, differences between data were evaluated with analysis of variance (ANOVA). The chosen level of significance was $p < 0.05$.

RESULTS

After age-, CCT- and bIOP- matching, 503 Chinese were assigned to 452 Caucasians participants. Mean age-, CCT- and bIOP of Chinese were 30.2 ± 6.8 years, 542.7 ± 29.7 μm, and 15.8 ± 2.1 mmHg, respectively, whereas, Caucasians showed 31.1 ± 6.8 years, 547.9 ± 31.8 μm, and 15.6 ± 2.1 mmHg of mean values.

Table 1 shows mean baseline characteristics of the two groups.

Statistical analysis showed a statistical significant difference between Chinese and Caucasian Healthy subjects in the values of SPA1 (**Figure 1**, $p = 0.008$), Arth (**Figure 2**, $p = 0.008$) and SSI (**Figure 3**, $p < 0.001$). Conversely, DA ($p = 0.674$), A1v ($p = 0.373$), DAratio ($p = 0.656$), and 1/R (p

TABLE 1 | Baseline and demographic data of the study population.

Parameter	Caucasians	Chinese
Age	31.1 ± 0.3	30.2 ± 0.3
CCT	547.9 ± 31.8	542.7 ± 29.7
bIOP	15.5 ± 2.2	15.7 ± 2.1
Eye (%Right)	45.1%	49.9%

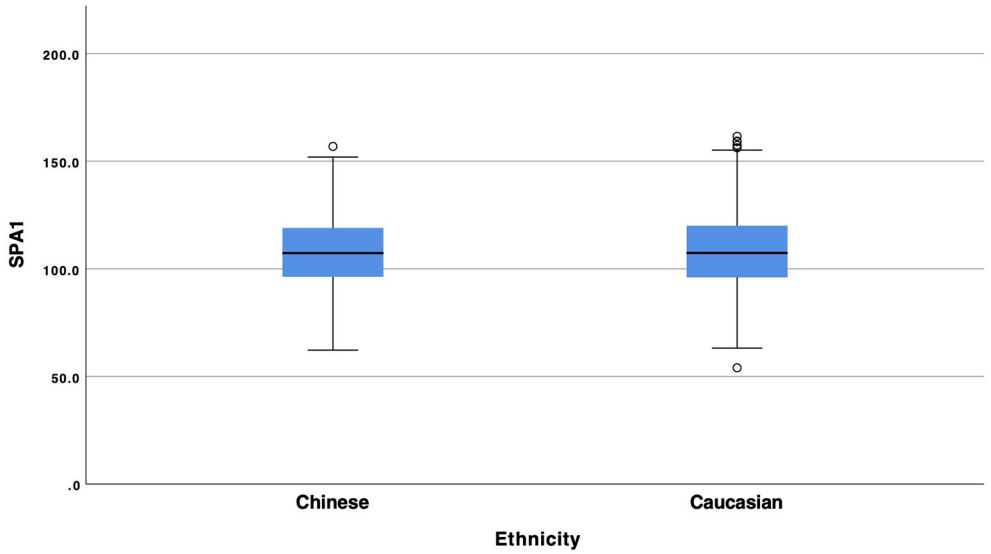

FIGURE 1 | Box and whiskers plot of SP-A1 of Chinese and Caucasian population.

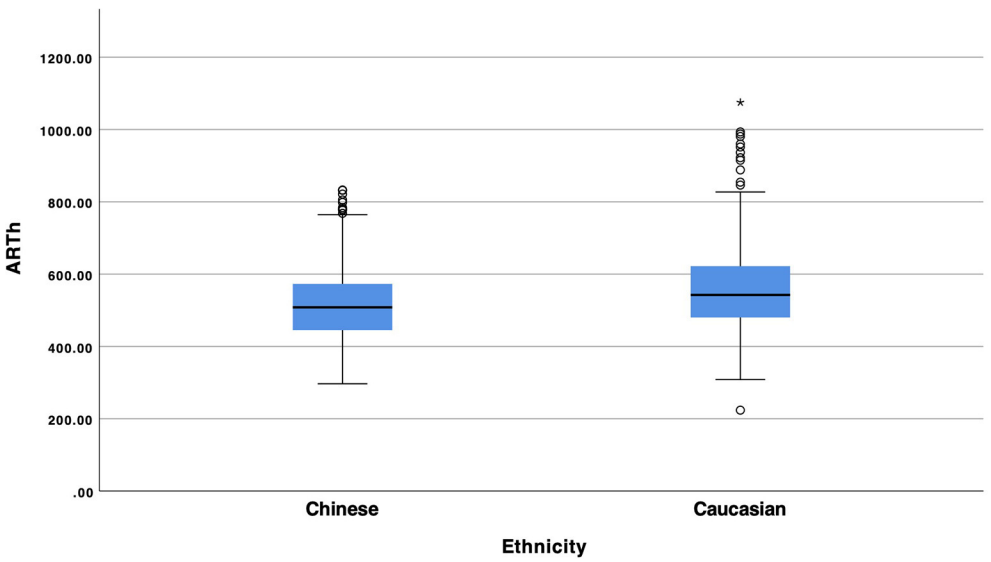

FIGURE 2 | Box and whiskers plot of Arth of Chinese and Caucasian population.

= 0.184) were not significantly different between the two ethnical groups. **Table 2** provides more details of the results of the ANOVA.

DISCUSSION

The evaluation of Ethnical variances in ocular metrics is not only important for the pure scientific knowledge but, more importantly, because a difference between two ethnicities could play a role in disease diagnosis.

The main finding of this study was the evidence that there is a significant difference in the values of the DCRs of the Corvis ST between Chinese and Caucasian population, more in details SPA1 and SSI which are pure biomechanical parameters and Arth which measures the thickness profile in the temporal-nasal direction.

It should be noted that these results are not due to the possible variance in age, IOP or corneal thickness between the two groups as they were specifically matched for these confounding factors. We decided not to match the patients for sex and refractive error to avoid decreasing too much the number of patients and we

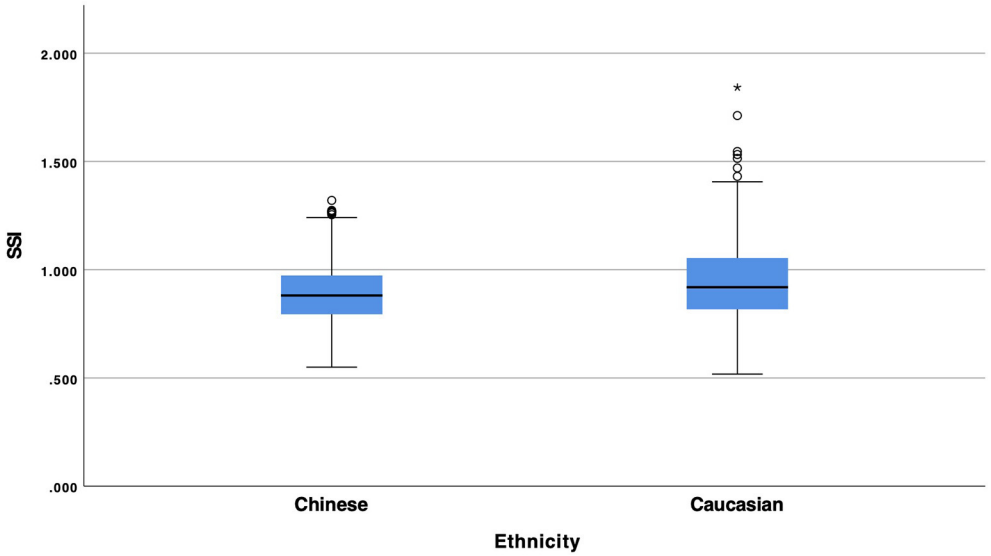

FIGURE 3 | Box and whiskers plot of SSI of Chinese and Caucasian population.

TABLE 2 | Number of cases, mean, standard deviation and p values of Corvis DCRs between Chinese and Caucasian population.

Parameters		*N*	Mean	Standard deviation	*p*-value
DA	Chinese	503	1.08485	0.102870	0.674
	Caucasian	452	1.07484	0.100243	
SPA1	Chinese	503	107.844	16.0351	**0.008**
	Caucasian	452	108.456	18.9433	
DARatio	Chinese	503	4.5317	0.45785	0.656
	Caucasian	452	4.3025	0.46629	
ARTh	Chinese	503	518.7264	100.13527	**0.008**
	Caucasian	452	563.2689	120.32852	
1/R	Chinese	503	8.5521	1.05437	0.184
	Caucasian	452	8.2790	1.17436	
A1v	Chinese	503	0.1517	0.01951	0.793
	Caucasian	452	0.1468	0.01883	
SSI	Chinese	503	0.88984	0.137459	**<0.0001**
	Caucasian	452	0.94163	0.186990	

Bold means significant values.

concentrated on age, IOP and CCT which are the most significant confounding factor for corneal biomechanics measurement (26).

It is the first time, to the authors' knowledge, that a large multicenter study was able to show a significant difference in corneal biomechanics (either Corvis ST or ORA) between two ethnical populations.

The importance of these results could be extremely high particularly in the sensitivity and the specificity of the Corvis Biomechanical Index (CBI) which includes all the three indices which were found to be different and was created basing on Caucasian and South American populations (8). We expect that this difference could play a significant role when screening a Chinese patient for refractive surgery that could lead potentially to false positives.

It is worth mentioning though only few studies on Chinese keratoconus patients assessed the sensitivity and specificity values of the CBI when compared to the original publication and they showed similar results (30, 31).

Further work of this group will focus on assessing the sensitivity and the specificity of CBI in Chinese keratoconus and to evaluate whether there is a need to improve the algorithm for this specific ethnic group.

In conclusion, we found significant differences in the values of the DCRs provided by the Corvis ST between Chinese and Caucasian healthy subjects. The presence of a case-control matching confirms this finding and excludes the influence of age, IOP, and CCT as confounding factors.

DATA AVAILABILITY STATEMENT

The datasets presented in this article are not readily available because it was not possible to be made public due to local laws.

ETHICS STATEMENT

Each Institutional Review Board (IRB) either ruled that approval was not required for this record review study or specifically approved the study. Written informed consent from the patients/participants was not required to participate in this study in accordance with the national legislation and the institutional requirements.

AUTHOR CONTRIBUTIONS

All authors listed have made a substantial, direct, and intellectual contribution to the work and approved it for publication.

REFERENCES

1. Aghaian E, Choe JE, Lin S, Stamper RL. Central corneal thickness of Caucasians, Chinese, Hispanics, Filipinos, African Americans, and Japanese in a glaucoma clinic. *Ophthalmology*. (2004) 111:2211–9. doi: 10.1016/j.ophtha.2004.06.013
2. Scheiman M, Gwiazda J, Zhang Q, Deng L, Fern K, Manny RE, et al. Longitudinal changes in corneal curvature and its relationship to axial length in the Correction of Myopia Evaluation Trial (COMET) cohort. *J Optom.* (2016) 9:13–21. doi: 10.1016/j.optom.2015.10.003
3. Wang D, Qi M, He M, Wu L, Lin S. Ethnic difference of the anterior chamber area and volume and its association with angle width. *Invest Ophthalmol Vis Sci.* (2012) 53:3139–44. doi: 10.1167/iovs.12-9776
4. Wang D, Amoozgar B, Porco T, Wang Z, Lin SC. Ethnic differences in lens parameters measured by ocular biometry in a cataract surgery population. *PLoS One.* (2017) 12:e0179836. doi: 10.1371/journal.pone.0179836
5. Ambrósio R, Correia FF, Lopes B, Salomão MQ, Luz A, Dawson DG, et al. Corneal biomechanics in ectatic diseases: refractive surgery implications. *Open Ophthalmol J.* (2017) 11:176–93. doi: 10.2174/1874364101711010176
6. Ambrosio R Jr, Lopes B, Faria-Correia F, Vinciguerra R, Vinciguerra P, Elsheikh A, et al. Ectasia detection by the assessment of corneal biomechanics. *Cornea.* (2016) 35:e18–20. doi: 10.1097/ICO.0000000000000875
7. Ambrosio R Jr, Lopes BT, Faria-Correia F, Salomao MQ, Buhren J, Roberts CJ, et al. Integration of scheimpflug-based corneal tomography and biomechanical assessments for enhancing ectasia detection. *J Refract Surg.* (2017) 33:434–43. doi: 10.3928/1081597X-20170426-02
8. Vinciguerra R, Ambrósio R, Elsheikh A, Roberts CJ, Lopes B, Morenghi E, et al. Detection of keratoconus with a new biomechanical index. *J Refract Surg.* (2016) 32:803–10. doi: 10.3928/1081597X-20160629-01
9. Vinciguerra R, Ambrósio R, Roberts CJ, Azzolini C, Vinciguerra P. Biomechanical characterization of subclinical keratoconus without topographic or tomographic abnormalities. *J Refract Surg.* (2017) 33:399–407. doi: 10.3928/1081597X-20170213-01
10. Vinciguerra R, Ambrosio R Jr, Elsheikh A, Hafezi F, Yong Kang DS, Kermani O, et al. Detection of post-laser vision correction ectasia with a new combined biomechanical index. *J Cataract Refract Surg.* (2021) 47:1314–8. doi: 10.1097/j.jcrs.0000000000000629
11. Vinciguerra R, Romano V, Arbabi EM, Brunner M, Willoughby CE, Batterbury M, et al. *In vivo* early corneal biomechanical changes after corneal cross-linking in patients with progressive keratoconus. *J Refract Surg.* (2017) 33:840–6. doi: 10.3928/1081597X-20170922-02
12. Chen KJ, Eliasy A, Vinciguerra R, Abass A, Lopes BT, Vinciguerra P, et al. Development and validation of a new intraocular pressure estimate for patients with soft corneas. *J Cataract Refract Surg.* (2019) 45:1316–23. doi: 10.1016/j.jcrs.2019.04.004
13. Eliasy A, Chen KJ, Vinciguerra R, Maklad O, Vinciguerra P, Ambrósio R, et al. *Ex-vivo* experimental validation of biomechanically-corrected intraocular pressure measurements on human eyes using the CorVis ST. *Exp Eye Res.* (2018) 175:98–102. doi: 10.1016/j.exer.2018.06.013
14. Qassim A, Mullany S, Abedi F, Marshall H, Hassall MM, Kolovos A, et al. Corneal stiffness parameters are predictive of structural and functional progression in glaucoma suspect eyes. *Ophthalmology.* (2021) 128:993–1004. doi: 10.1016/j.ophtha.2020.11.021
15. Vinciguerra R, Rehman S, Vallabh NA, Batterbury M, Czanner G, Choudhary A, et al. Corneal biomechanics and biomechanically corrected intraocular pressure in primary open-angle glaucoma, ocular hypertension and controls. *Br J Ophthalmol.* (2020) 104:121–6. doi: 10.1136/bjophthalmol-2018-313493
16. Luce DA. Determining *in vivo* biomechanical properties of the cornea with an ocular response analyzer. *J Cataract Refract Surg.* (2005) 31:156–62. doi: 10.1016/j.jcrs.2004.10.044
17. Roberts CJ. Concepts and misconceptions in corneal biomechanics. *J Cataract Refract Surg.* (2014) 40:862–9. doi: 10.1016/j.jcrs.2014.04.019
18. Mikielewicz M, Kotliar K, Barraquer RI, Michael R. Air-pulse corneal applanation signal curve parameters for the characterisation of keratoconus. *Br J Ophthalmol.* (2011) 95:793–8. doi: 10.1136/bjo.2010.188300
19. Hallahan KM, Sinha Roy A, Ambrosio R Jr, Salomao M, Dupps WJ Jr. Discriminant value of custom ocular response analyzer waveform derivatives in keratoconus. *Ophthalmology.* (2014) 121:459–68. doi: 10.1016/j.ophtha.2013.09.013
20. Ambrósio R Jr, Ramos I, Luz A, Faria FC, Steinmueller A, Krug M, et al. Dynamic ultra high speed Scheimpflug imaging for assessing corneal biomechanical properties. *Rev Bras Oftalmol.* (2013) 72:99–102. doi: 10.1590/S0034-72802013000200005
21. Vinciguerra R, Elsheikh A, Roberts CJ, Ambrósio R, Kang DSY, Lopes BT, et al. Influence of pachymetry and intraocular pressure on dynamic corneal response parameters in healthy patients. *J Refract Surg.* (2016) 32:550–61. doi: 10.3928/1081597X-20160524-01
22. Wang W, He M, He H, Zhang C, Jin H, Zhong X. Corneal biomechanical metrics of healthy Chinese adults using Corvis ST. *Cont Lens Anterior Eye.* (2017) 40:97–103. doi: 10.1016/j.clae.2016.12.003
23. Kenia VP, Kenia RV, Pirdankar OH. Age-related variation in corneal biomechanical parameters in healthy Indians. *Indian J Ophthalmol.* (2020) 68:2921–9. doi: 10.4103/ijo.IJO_2127_19
24. Salouti R, Bagheri M, Shamsi A, Zamani M. Corneal parameters in healthy subjects assessed by corvis ST. *J Ophthalmic Vis Res.* (2020) 15:24–31. doi: 10.18502/jovr.v15i1.5936
25. Roberts CJ, Mahmoud AM, Bons JP, Hossain A, Elsheikh A, Vinciguerra R, Vinciguerra P, Ambrosio R Jr. Introduction of two novel stiffness parameters and interpretation of air puff-induced biomechanical deformation parameters with a dynamic scheimpflug analyzer. *J Refract Surg.* (2017) 33:266–73. doi: 10.3928/1081597X-20161221-03
26. Vinciguerra R, Elsheikh A, Roberts CJ, Ambrosio R Jr, Kang DS, Lopes BT, et al. Influence of pachymetry and intraocular pressure on dynamic corneal response parameters in healthy patients. *J Refract Surg.* (2016) 32:550–61.
27. Eliasy A, Chen KJ, Vinciguerra R, Lopes BT, Abass A, Vinciguerra P, et al. Determination of corneal biomechanical behavior *in-vivo* for healthy eyes using CorVis ST tonometry: stress-strain index. *Front Bioeng Biotechnol.* (2019) 7:105. doi: 10.3389/fbioe.2019.00105
28. Joda AA, Shervin MM, Kook D, Elsheikh A. Development and validation of a correction equation for Corvis tonometry. *Comput Methods Biomech Biomed Eng.* (2016) 19:943–53. doi: 10.1080/10255842.2015.1077515
29. Niven DJ, Berthiaume LR, Fick GH, Laupland KB. Matched case-control studies: a review of reported statistical methodology. *Clin Epidemiol.* (2012) 4:99–110. doi: 10.2147/CLEP.S30816
30. Ren S, Xu L, Fan Q, Gu Y, Yang K. Accuracy of new Corvis ST parameters for detecting subclinical and clinical keratoconus eyes in a Chinese population. *Sci Rep.* (2021) 11:4962. doi: 10.1038/s41598-021-84370-y
31. Yang K, Xu L, Fan Q, Zhao D, Ren S. Repeatability and comparison of new Corvis ST parameters in normal and

keratoconus eyes. *Sci Rep*. (2019) 9:15379. doi: 10.1038/s41598-019-51502-4

Conflict of Interest: RV and PV are consultants for OCULUS Optikgeräte GmbH. OCULUS Optikgeräte GmbH did not take part in the design, analysis, or interpretation of the results.

The remaining authors declare that the research was conducted in the absence of any commercial or financial relationships that could be construed as a potential conflict of interest.

Publisher's Note: All claims expressed in this article are solely those of the authors and do not necessarily represent those of their affiliated organizations, or those of the publisher, the editors and the reviewers. Any product that may be evaluated in this article, or claim that may be made by its manufacturer, is not guaranteed or endorsed by the publisher.

frontiers in Medicine

ORIGINAL RESEARCH
published: 04 March 2022
doi: 10.3389/fmed.2022.843176

Associations Between the Macular Microvasculatures and Subclinical Atherosclerosis in Patients With Type 2 Diabetes: An Optical Coherence Tomography Angiography Study

Jooyoung Yoon[1], Hyo Joo Kang[2], Joo Yong Lee[1,2], June-Gone Kim[1,2], Young Hee Yoon[1,2], Chang Hee Jung[2,3†] and Yoon Jeon Kim[1,2*†]*

[1] Department of Ophthalmology, Asan Medical Center, College of Medicine, University of Ulsan, Seoul, South Korea, [2] Asan Diabetes Center, Asan Medical Center, Seoul, South Korea, [3] Department of Internal Medicine, Asan Medical Center, College of Medicine, University of Ulsan, Seoul, South Korea

Objective: To investigate the associations between the macular microvasculature assessed by optical coherence tomography angiography (OCTA) and subclinical atherosclerosis in patients with type 2 diabetes.

Methods: We included patients with type 2 diabetes who received comprehensive medical and ophthalmic evaluations, such as carotid ultrasonography and OCTA at a hospital-based diabetic clinic in a consecutive manner. Among them, 254 eyes with neither diabetic macular edema (DME) nor history of ophthalmic treatment from 254 patients were included. The presence of increased carotid intima-media thickness (IMT) (>1.0 mm) or carotid plaque was defined as subclinical atherosclerosis. OCTA characteristics focused on foveal avascular zone (FAZ) related parameters and parafoveal vessel density (VD) were compared in terms of subclinical atherosclerosis, and risk factors for subclinical atherosclerosis were identified using a multivariate logistic regression analysis.

Results: Subclinical atherosclerosis was observed in 148 patients (58.3%). The subclinical atherosclerosis group were older ($p < 0.001$), had a greater portion of patients who were men ($p = 0.001$) and who had hypertension ($p = 0.042$), had longer diabetes duration ($p = 0.014$), and lower VD around FAZ ($p = 0.010$), and parafoveal VD (all $p < 0.05$). In the multivariate logistic regression analysis, older age ($p \leq 0.001$), male sex ($p \leq 0.001$), lower VD around FAZ ($p = 0.043$), lower parafoveal VD of both superficial capillary plexus (SCP) ($p = 0.011$), and deep capillary plexus (DCP) ($p = 0.046$) were significant factors for subclinical atherosclerosis.

Conclusion: The decrease in VD around FAZ, and the VD loss in parafoveal area of both SCP and DCP were significantly associated with subclinical atherosclerosis in patients with type 2 diabetes, suggesting that common pathogenic mechanisms might predispose to diabetic micro- and macrovascular complications.

Keywords: carotid ultrasonography, optical coherence tomography angiography (OCTA), retinal microvasculatures, subclinical atherosclerosis, type 2 diabetes

OPEN ACCESS

Edited by:
Michele Lanza,
University of Campania Luigi Vanvitelli, Italy

Reviewed by:
Jacqueline Chua,
Singapore Eye Research Institute (SERI), Singapore
Haoyu Chen,
Shantou University and The Chinese University of Hong Kong, China
Rodrigo Lira,
Federal University of Pernambuco, Brazil
Ryo Mukai,
Gunma University, Japan
Lin Lu,
Sun Yat-sen University, China

***Correspondence:**
Yoon Jeon Kim
anne215@gmail.com
Chang Hee Jung
chjung0204@gmail.com

†These authors have contributed equally to this work

Specialty section:
This article was submitted to Ophthalmology, a section of the journal Frontiers in Medicine

Received: *25 December 2021*
Accepted: *01 February 2022*
Published: *04 March 2022*

Citation:
Yoon J, Kang HJ, Lee JY, Kim J-G, Yoon YH, Jung CH and Kim YJ (2022) Associations Between the Macular Microvasculatures and Subclinical Atherosclerosis in Patients With Type 2 Diabetes: An Optical Coherence Tomography Angiography Study. Front. Med. 9:843176. doi: 10.3389/fmed.2022.843176

INTRODUCTION

Carotid artery stenosis, an important, potentially life-threatening consequence of systemic atherosclerotic disease in the aging population, is responsible for 10–20% of the ischemic strokes, which are the second most common cause of death worldwide. Diabetes mellitus (DM), one of the major risk factors of carotid artery stenosis, results in systemic vascular complications: macro- and microvascular complications (1). Therefore, screening for the vascular abnormalities and prevention of irrecoverable damage in the high-risk patients are crucial to reduce the social and financial burden of DM (2). Traditionally, the macro- and microvascular complications of diabetes have been considered as the distinct and independent disorders. Recently, however, pathophysiological evidence and epidemiologic evidence suggest that these vascular complications may share common pathophysiological mechanisms (3).

Optical coherence tomography angiography (OCTA) is a new, non-invasive technology that enables the reproducible, quantitative assessment of the microcirculation of different retinal capillary layers (4–8). Unlike the fluorescein angiography, OCTA does not require intravenous dye to assess the retinal vasculature, and therefore causes less discomfort and pain, and is free from the potential systemic adverse effects (9). Characteristic retinal vascular alterations in OCTA have been well-described in patients with diabetic retinopathy (DR) from their early stage of diseases, and several reports showed that these changes were detectable even before the development of DR (10, 11). Recently, the clinical implications of the OCTA parameters for assessing associations with the carotid stenosis were investigated (12). However, not only carotid intima media thickness (IMT), but carotid plaque burden is also reported as a surrogate of atherosclerosis and predictor of future atherosclerotic cardiovascular diseases (13). Thus, we aimed

TABLE 1 | Baseline demographics and clinical characteristics of patients in this study.

	Total (n = 254)	Subclinical atherosclerosis (–) (n = 106)	Subclinical atherosclerosis (+) (n = 148)	P-value
Age (year)	57.6 ± 10.4	54.1 ± 11.2	60.1 ± 9.1	<0.001
Sex (male: female)	162: 92	55: 51	107: 41	0.001
Hypertension [*n* (%)]	115 (45.3)	40 (37.7)	75 (50.7)	0.041
DM duration (yr)	18.3 ± 8.1	16.8 ± 7.6	19.4 ± 8.3	0.013
DM treatment [*n* (%)]				0.630
OHA only	166 (65.4)	66 (62.3)	100 (67.6)	
Insulin	88 (34.5)	40 (37.7)	48 (32.4)	
Hyperlipidemia [*n* (%)]	141 (55.5)	52 (49.1)	89 (59.7)	0.256
Smoking status [*n* (%)]				0.325
Non-smoker	134 (52.8)	61 (57.5)	73 (49.3)	
Ex-smoker	69 (27.2)	27 (25.5)	42 (28.4)	
Current smoker	51 (20.1)	18 (17.0)	33 (22.3)	
HbA1C (%)	7.7 ± 1.3	7.6 ± 1.2	7.7 ± 1.4	0.517
Glucose (mg/dL)	145.2 ± 46.2	143.1 ± 46.9	146.7 ± 45.8	0.547
SBP (mmHg)	132.2 ± 18.0	131.8 ± 17.7	132.4 ± 18.3	0.768
DBP (mmHg)	74.4 ± 11.9	75.9 ± 10.7	73.4 ± 12.3	0.088
Total cholesterol (mg/dL)	145.5 ± 35.4	151.2 ± 34.2	141.3 ± 35.8	0.028
Triglyceride (mg/dL)	132.7 ± 72.9	135.2 ± 79.1	130.9 ± 68.3	0.641
HDL-cholesterol (mg/dL)	45.5 ± 10.9	46.8 ± 10.5	44.6 ± 11.2	0.122
LDL-cholesterol (mg/dL)	91.3 ± 28.5	95.0 ± 27.7	88.6 ± 28.9	0.074
UACR [*n* (%)]				0.149
Normal (<30 mcg/mg)	168 (66.1)	76 (71.7)	92 (62.2)	
Microalbuminuria (30∼300 mcg/mg)	63 (24.8)	20 (18.9)	43 (29.1)	
Albuminuria (>300 mcg/mg)	21 (8.3)	9 (8.5)	12 (8.1)	
Creatinine (mg/dL)	1.0 ± 0.6	1.0 ± 0.7	1.0 ± 0.6	0.800
eGFR (%)	82.5 ± 20.6	84.3 ± 21.4	81.2 ± 19.9	0.237
Carotid IMT (mm)	0.73 ± 0.02	0.69 ± 0.02	0.75 ± 0.01	0.014
Presence of carotid plaque [*n* (%)]	155 (61.0)	15 (14.1)	140 (94.6)	<0.001

DM, diabetes mellitus; OHA, oral hypoglycemic agent; SBP, systolic blood pressure; DBP, diastolic blood pressure; HDL, high density lipid; LDL, low density lipid; UACR, urine albumin to creatinine ratio; eGFR, estimated glomerular filtration rate; IMT, intima media thickness.

to compare the retinal microvascular changes measured with OCTA in patients with type 2 diabetes in terms of the presence of carotid artery disease detected by carotid ultrasonography (US), the early indicator of systemic subclinical atherosclerosis (14). In addition, systemic and ophthalmologic factors related to subclinical atherosclerosis were evaluated.

METHODS

The research adhered to the tenets of Declaration of Helsinki. The study was approved by the international research board of Asan Medical Center (IRB No. 2020-0014). Informed consent was waived due to the retrospective nature of the study.

Study Subjects

Patients with type 2 DM who received comprehensive medical and ophthalmic evaluations during the period from January 2017 to December 2019 at a hospital-based diabetic clinic (Asan Medical Center, Seoul, Korea) were selected by medical record review in a consecutive manner. Patients underwent vascular evaluation, such as carotid US, and ophthalmic evaluation, including OCTA at regular intervals based on their medical status, and those who had both carotid US and OCTA within 6 months interval were included in this retrospective observational study. We excluded patients if they had history of ophthalmic treatment, diabetic macular edema (DME), with concomitant ocular disease other than DR, or history of ocular trauma. For image qualities, those with poor OCTA quality, with a scan quality of 6 or less out of 10, were excluded. In addition, to minimize the possible errors in image analysis, proper segmentation without errors, and removal of projection artifact are carefully considered. When both eyes met the inclusion criteria, we included the right eye, and when only one eye of the two eyes satisfied the inclusion criteria, the corresponding eye was included in the study to include one eye for each patient.

At the initial visit of endocrinology, every patient underwent detailed medical and surgical history, such as medication information and duration for diabetes and hypertension, smoking habits, and alcoholic intake. In addition, at baseline and every visit, arterial blood pressure (BP), body weight, and height were measured, and body weight and height were used to calculate the body mass index (BMI), which was used for analysis. After overnight fasting, early morning blood samples were obtained and underwent a central, certified laboratory analysis. Measurements included were hemoglobin A1C (HbA1c), serum glucose level, several lipid parameters, and creatinine. HbA1c was measured using high-performance liquid chromatography (HPLC) of a Variant II Turbo (Bio-Rad Laboratories, Hercules, CA, USA). Fasting total cholesterol, high-density lipoprotein-cholesterol (HDL-C), low-density lipoprotein-cholesterol (LDL-C), and triglyceride (TG) were measured by using an enzymatic colorimetric method (Toshiba Medical Systems). Creatinine was measured by using the Jaffe method, and estimated glomerular filtration rate (eGFR) was calculated with the modified Modification of Diet in Renal Disease (MDRD) equation. In addition, urine tests were performed and urinary albumin-to-creatinine ratio (UACR) was calculated to determine the severity of albuminuria, using a photometric method of the Integra 800 system (Roche Diagnostics, Indianapolis, IN, USA) in a random spot urine collection.

At their initial visit and at each visit to a retina clinic, all patients underwent a comprehensive ophthalmologic examination that included a review of their ophthalmologic history, measurement of visual acuity, slit lamp biomicroscopy, and funduscopic examinations through dilated pupils by retinal specialists. The severity of DR was classified into 5 grades by the following criteria of the Early Treatment Diabetic Retinopathy Study (ETDRS): (1) no diabetic retinopathy—"no DR"; (2) mild non-proliferative diabetic retinopathy—"mild NPDR"; (3) moderate non-proliferative diabetic retinopathy—"moderate NPDR"; (4) severe non-proliferative diabetic retinopathy—"severe NPDR"; and (5) proliferative diabetic retinopathy—"PDR."

Optical Coherence Tomography Angiography

The RTVue XR Avanti (Optovue, Fremont, CA, USA) spectral-domain OCT device with phase 7 AngioVue software was used for the OCT and OCT angiography examination. A 3 mm × 3-mm macular scans centered on the fovea were acquired. Each OCTA en face image contains 304 × 304 pixels created from the intersection of the 304 vertical and the 304 horizontal B-scans. AngioVue software automatically segments the B-scan images into four layers: superficial capillary plexus (SCP), deep capillary plexus (DCP), outer retina, and choriocapillaris layer. The SCP layer was segmented with an inner boundary set at 3 μm beneath the internal limiting membrane and an outer boundary at 15 μm beneath the inner plexiform layer. The DCP layer was segmented with an inner boundary set at 15 μm beneath the inner plexiform layer and an outer boundary at 70 μm beneath the inner plexiform layer. Using SCP and DCP images, following parameters were measured with the integrated automated software. For FAZ related parameters, area (mm^2) and perimeter (mm) were measured and acircularity was calculated using those two parameters. In addition, vessel density (VD) around 300 μm boundary around FAZ and VD of each selected region (foveal and parafoveal area of four quadrants) were calculated as the percentage of area occupied by flowing blood vessels and was analyzed in both SCP and DCP, respectively.

Carotid Ultrasonography

Carotid artery examination was performed by a single specialized technician with patients in the supine position with the head elevated to 45 degrees and tilted to either side by 30 degrees and the operator seated at the head bed. High resolution ultrasound (HD 11 XE, Philips Healthcare, Andover MA) equipped with a high-frequency (5–12.5 MHz) linear transducer was used to acquire images of the left and right common carotid arteries. Carotid IMT scanning and reading was evaluated with the criteria of Mannheim Carotid Intima-Media Thickness Consensus (15). IMT was measured from the media-adventitia interface to the intima-lumen interface at the level of ∼0.5 cm below the carotid-artery bulb, over a 1-cm segment of the artery, and the degree of stenosis was assessed. The value obtained through a QLAB IMT-quantification software measurement plug-in (Philips Healthcare) was used in analysis (16). The upper

TABLE 2 | Baseline ophthalmologic characteristics and optical coherence tomography angiography (OCTA) parameters of patients.

	Total ($n = 254$)	Subclinical atherosclerosis (–) ($n = 106$)	Subclinical atherosclerosis (+) ($n = 148$)	*P*-value
BCVA (LogMAR)	0.07 ± 0.09	0.06 ± 0.08	0.08 ± 0.09	0.144
DR stage [*n* (%)]				0.159
No DR	33 (13.0)	18 (17.0)	15 (10.1)	
Mild NPDR	111 (43.7)	50 (47.2)	61 (41.2)	
Moderate NPDR	56 (22.1)	20 (18.9)	36 (24.3)	
Severe NPDR	42 (16.5)	13 (12.3)	29 (19.6)	
PDR	12 (4.7)	5 (4.7)	7 (4.7)	
FAZ parameters				
Area (mm^2)	0.38 ± 0.59	0.35 ± 0.11	0.40 ± 0.77	0.486
Perimeter (mm)	2.38 ± 0.43	2.43 ± 0.45	2.35 ± 0.41	0.161
VD around FAZ (%)	47.6 ± 3.7	48.3 ± 3.8	47.1 ± 3.6	0.009
Acircularity	1.16 ± 0.06	1.17 ± 0.07	1.16 ± 0.04	0.087
SCP parameters				
Fovea VD (%)	14.8 ± 5.1	14.5 ± 4.8	14.6 ± 5.4	0.817
Parafovea VD (%)	46.3 ± 3.7	47.2 ± 3.7	45.7 ± 3.6	0.002
DCP parameters				
Fovea VD (%)	27.5 ± 6.5	27.4 ± 6.2	27.7 ± 6.8	0.722
Parafovea VD (%)	49.9 ± 3.7	50.5 ± 3.5	49.5 ± 3.8	0.044
Scan quality	8.3 ± 2.2	8.2 ± 2.2	8.0 ± 2.0	0.075

BCVA, best corrected visual acuity; DR, diabetic retinopathy; NPDR, non-proliferative diabetic retinopathy; PDR, proliferative diabetic retinopathy; FAZ, foveal avascular zone; VD, vessel density; SCP, superficial capillary plexus; DCP, deep capillary plexus.

normal limit of IMT was 1.0 mm, and focal lesions with increased carotid IMT (>1.0 mm) or the presence of carotid plaque was defined as subclinical atherosclerosis (17).

Statistical Analysis

The following variables were analyzed in each patient: (i) demographic variables (i.e., age, sex, comorbidities with hypertension or hyperlipidemia, DM duration, and DM treatment), (ii) laboratory variables (i.e., carotid IMT, presence of carotid plaque, HbA1C, glucose, systolic BP (SBP) and diastolic BP (DBP), total cholesterol, TG, HDL and LDL-cholesterol, UACR, creatinine, and eGFR), (iii) ocular characteristics (i.e., BCVA and DR severity), and (iv) OCTA parameters (FAZ related parameters; area, perimeter, acircularity, and VD around FAZ, foveal and parafoveal VD in SCP and DCP).

Descriptive statistics were demonstrated in numbers and percentages for categorical variables and mean ± SD of continuous variables to present the baseline characteristics of study subjects. For comparison in terms of the presence of subclinical atherosclerosis (the subclinical atherosclerosis group and the non-subclinical atherosclerosis group), independent *t*-test or Mann–Whitney *U*-test was used depending on the normality of their distribution. Chi-squared test was used to compare the categorical data. To explore the factors significantly associated with subclinical atherosclerosis, logistic regression analyses were conducted. Univariate analyses were separately

TABLE 3 | Factors associated with the presence of subclinical atherosclerosis in patients with type 2 diabetes in univariate logistic analysis.

	Odds ratio (95% CI)	*P*-value
Demographics		
Age	1.06 (1.03–1.09)	<0.001
Sex		
Male	2.42 (1.43–4.09)	0.001
Female	1 (Ref)	
Hypertension	1.70 (1.02–2.82)	0.042
DM duration	1.04 (1.01–1.08)	0.014
DM treatment		
OHA only	1 (Ref)	
Insulin	0.78 (0.30–2.05)	0.613
Hyperlipidemia	1.23 (0.95–1.58)	0.165
Laboratory data		
HbA1C	1.07 (0.88–1.30)	0.515
Glucose	1.00 (1.00–1.01)	0.546
SBP	1.02 (0.99–1.03)	0.622
DBP	0.98 (0.95–1.04)	0.703
Total cholesterol	0.99 (0.99–1.00)	0.030
Triglyceride	1.00 (1.00–1.00)	0.640
HDL-cholesterol	0.98 (0.96–1.01)	0.123
LDL-cholesterol	0.99 (0.98–1.00)	0.076
UACR		
Normal	1 (Ref)	
Microalbuminuria	1.78 (0.96–3.27)	0.066
Albuminuria	1.10 (0.44–2.75)	0.836
Creatinine	1.06 (0.70–1.59)	0.800
eGFR	0.99 (0.98–1.01)	0.237
Ophthalmologic data		
BCVA (LogMAR)	9.03 (0.46–175.68)	0.146
DR stage		
No DR-mild NPDR	1 (Ref)	
Worse than moderate NPDR	2.16 (0.85–5.79)	0.075
OCT angiography parameters		
FAZ parameters		
Area (mm^2)	1.25 (0.61–2.56)	0.547
Perimeter (mm)	0.66 (0.36–1.19)	0.163
VD around FAZ (%)	0.91 (0.85–0.98)	0.010
Acircularity	0.02 (0.00–1.88)	0.092
SCP parameters		
Fovea VD (%)	1.01 (0.96–1.06)	0.816
Parafovea VD (%)	0.89 (0.83–0.96)	0.002
DCP parameters		
Fovea VD (%)	1.01 (0.97–1.05)	0.721
Parafovea VD (%)	0.93 (0.87–1.00)	0.045
Scan quality	0.92 (0.85–1.05)	0.116

DM, diabetes mellitus; OHA, oral hypoglycemic agent; SBP, systolic blood pressure; DBP, diastolic blood pressure; HDL, high density lipid; LDL, low density lipid; UACR, urine albumin to creatinine ratio; eGFR, estimated glomerular filtration rate; BCVA, best corrected visual acuity; DR, diabetic retinopathy; NPDR, non-proliferative diabetic retinopathy; PDR, proliferative diabetic retinopathy; OCT, optical coherence tomography; FAZ, foveal avascular zone; VD, vessel density; SCP, superficial capillary plexus; DCP, deep capillary plexus.

performed for each variable and those with $p < 0.1$ were included in the multivariate analysis with the forward elimination process. Odds ratios (*OR*s) with 95% *CI*s were calculated. All statistical analyses were performed using SPSS version 21.0 software (SPSS Inc., Chicago, IL, USA).

RESULTS

Of a total of 254 patients included in this analysis, 148 patients (58.3%) had subclinical atherosclerosis. Patients with subclinical atherosclerosis were older than those without (60.1 ± 9.1 vs. 54.1 ± 11.2 years, $p < 0.001$). Baseline characteristics in this study are summarized in **Table 1**. Patients with subclinical atherosclerosis had greater portion of male sex (72.3 vs. 52.9%, $p = 0.001$), hypertension (50.7 vs. 37.7%, $p = 0.041$), and longer duration of type 2 DM (19.4 ± 8.3 vs. 16.9 ± 7.6 years, $p = 0.013$). All the study participants were receiving either oral hypoglycemic agents or insulin injection or both, and the proportion of patients on insulin treatment and smoking status were not significantly different between the two groups. HbA1C, serum glucose, SBP, DBP, UACR, creatinine, and eGFR were not different between the two groups.

Regarding the ophthalmologic data, BCVA, DR stage, and OCTA signal strength were not significantly different in terms of subclinical atherosclerosis (**Table 2**). Whereas, the area, perimeter, and acircularity of FAZ were not different between the two groups, VD around FAZ was significantly more impaired in the subclinical atherosclerosis group (47.1 ± 3.6 vs. 48.3 ± 3.8, $p = 0.009$). While foveal VD in the SCP and DCP was not different between two groups, parafoveal VD in the SCP (45.7 ± 3.6 vs. 47.2 ± 3.7, P = 0.002) and DCP (49.5 ± 3.6 vs. 50.5 ± 3.5, P = 0.044) was significantly reduced in the subclinical atherosclerosis group. There was no significant difference in scan quality in terms of subclinical atherosclerosis to identify the factors associated with presence of the subclinical atherosclerosis, univariate and multivariate logistic regression analyses were conducted including the baseline variables and OCTA parameters. In the univariate analysis (**Table 3**), old age [$OR = 1.06$ (95% *CI* 1.03–1.09), $p < 0.001$], male sex [$OR = 2.42$ (95% *CI* 1.43–4.09), $p = 0.001$], longer duration of DM [$OR = 1.04$ (95% *CI* 1.01–1.08), $p = 0.014$], and the presence of hypertension [$OR = 1.70$ (95% *CI* 1.02–2.82), $p = 0.042$] were associated with the presence of subclinical atherosclerosis. When all patients were divided into two groups according to DR severity, marginal association was confirmed in the univariate analysis [$OR = 2.16$ (95% *CI* 0.85–5.79), $p = 0.075$]. Among the OCTA parameters, decrease in foveal VD around FAZ [$OR = 0.91$ (95% *CI* 0.85–0.98), $p = 0.010$] and parafoveal VD in SCP [$OR = 0.89$ (95% *CI* 0.83–0.96), $p = 0.002$] and DCP [$OR = 0.93$ (95% *CI* 0.87–1.00), $p = 0.045$] was associated with subclinical atherosclerosis.

We performed three models of multivariate analyses (**Table 4**) to obviate the confounding effects of the multicollinearity of the OCTA parameters (correlation coefficients >0.8). Old age and male sex were consistently remained as the significant factors for subclinical atherosclerosis (all $p < 0.05$) in all three models. Low foveal VD around FAZ [$OR = 0.92$ (95% *CI* 0.86–1.00), $p = 0.043$], parafoveal VD in both SCP [$OR = 0.91$ (95% *CI* 0.85–0.98), $p = 0.011$], and DCP [$OR = 0.93$ (95% *CI* 0.86–1.00), $p = 0.046$] were significant factors for subclinical atherosclerosis in each of three models. **Figure 1** shows the different averages and distributions in the significant OCTA parameters according to the presence of subclinical atherosclerosis. And **Figure 2** demonstrated the difference in the foveal and parafoveal capillary vessel density of an age-sex matched control and a patient with subclinical atherosclerosis.

DISCUSSION

This study demonstrates that the decreases in VD of macular microvasculatures were associated and the presence of subclinical atherosclerosis in type 2 DM, suggesting associations between macro- and microvascular diabetes complications. Based on our findings, the alterations of macular microvasculatures in OCTA which are implicative of higher risk of subclinical atherosclerosis, could be used as one of the non-invasive imaging biomarkers for the higher risk of macrovascular diseases which requires careful monitoring.

Our results showing the associations between the carotid disease and retinal vasculatures in diabetes were in line with the

TABLE 4 | Factors significantly associated with the presence of subclinical atherosclerosis in patients with type 2 diabetes in multivariate logistic analysis.

	Model 1 including foveal VD around FAZ		Model 2 including SCP Parafovea VD		Model 3 including DCP Parafovea VD	
	Odds ratio (95% CI)	*P*-value	Odds ratio (95% CI)	*P*-value	Odds ratio (95% CI)	*P*-value
Age (year)	1.06 (1.03–1.10)	<0.001	1.06 (1.03–1.09)	0.001	1.06 (1.03–1.10)	<0.001
Male sex	2.67 (1.51–4.75)	0.001	2.77 (1.56–4.93)	0.001	2.77 (1.56–4.90)	<0.001
DM duration (yr)	1.02 (0.98–1.06)	0.456	1.02 (0.98–1.06)	0.425	1.02 (0.98–1.06)	0.409
Hypertension	1.24 (0.71–2.18)	0.448	1.27 (0.72–2.23)	0.412	1.34 (0.76–2.35)	0.311
Foveal VD around FAZ	0.92 (0.86–1.00)	0.043				
SCP Parafovea VD			0.91 (0.84–0.98)	0.011		
DCP Parafovea VD					0.93 (0.86–1.00)	0.046

Model 1, 2, and 3 contains each of OCTA parameters which showed associations with subclinical atherosclerosis in univariate analyses.
DM, diabetes mellitus; VD, vessel density; FAZ, foveal avascular zone; SCP, superficial capillary plexus; DCP, deep capillary plexus.

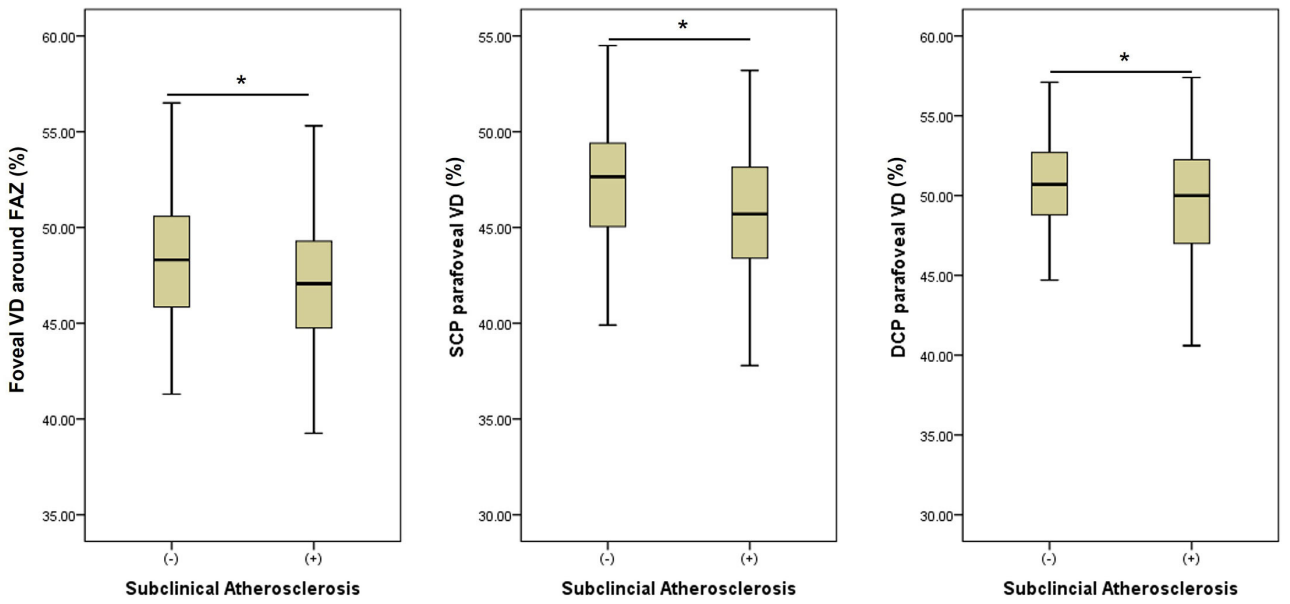

FIGURE 1 | Bar graphs showing the different averages and 95% distributions of the significantly associated optical coherence tomography angiography (OCTA) parameters (foveal vessel density (VD) around foveal avascular zone (FAZ) and parafoveal VD in superficial and deep capillary plexuses (DCP) according to the presence of subclinical atherosclerosis. An asterisk means a statistical significance ($p < 0.05$) between two groups in an independent *t*-test. VD, vessel density; FAZ, foveal avascular zone; SCP, superficial capillary plexus; DCP, deep capillary plexus.

previous studies that proved the increased cardiovascular risks in patients with DR. DR is an independent risk factor for carotid plaques, and the severity of carotid atherosclerosis correlates with the severity of microangiopathy. In this study, we could provide stronger evidence for those findings through access to a more sensitive retinal imaging modality than the conventionally used color fundus photography. Morphologic changes assessed by OCTA in DR, i.e., retinal microvasculature abnormalities, such as capillary dropout, reduced capillary VD, tortuous capillary branches, dilated average vascular caliber, FAZ enlargement, and irregular FAZ contour, were present before the beginning of the clinically diagnosed DR and become more obvious as DR progress. As a result, we revealed general reduction in VD in terms of subclinical atherosclerosis.

Interestingly, however, we could not find significant differences in area and contour of FAZ and foveal VD in terms of subclinical atherosclerosis. These differences imply that the overall hemodynamic changes of retinal vasculatures may reflect systemic risk factors related to subclinical atherosclerosis more sensitively, compared with the localized deformation of retinal vessels in FAZ. Moreover, foveal VD which means VD within a fovea centered circle of 1 mm diameter is mostly influenced by the FAZ area. In other words, when the FAZ area is large, the foveal VD is small, and when the FAZ area is small, the foveal VD is large. Therefore, parafoveal VD or VD around FAZ reflects vascular impairment more accurately than foveal VD, which is related to the FAZ area with large individual variability.

Our results showing the close associations between retinal microvasculature obtained by OCTA and diabetic macrovascular complications were in line with those by Drinkwater et al. (12). On the other hand, it is differentiated by the fact that not only carotid stenosis represented by carotid IMT thickening but also carotid plaque, which is a predictor of atherosclerotic cardiovascular diseases. Most of our patients classified as the subclinical atherosclerosis group had carotid plaques without IMT thickening. Moreover, when we evaluated the VD changes of each layer, we noted that parafoveal VDs in both SCP and DCP were all correlated with subclinical atherosclerosis. These results were different from their study which concluded that the decrease VD in only DCP correlates to the increased IMT and the grade of stenosis and VD in SCP did not show significant association with the carotid parameters (17). This difference primarily may be due to the different patient characteristics, particularly in the distribution of DR stages between two studies. While our study included the patients with variable stages of DR (13.1% patients with no DR), the study by Drinkwater et al. (12) mainly included the patients with no DR (83.8% patients with no DR). Since it is widely reported that the vascular changes in DCP occur in the early stage of DR (even before the development of DR) and those in SCP occur in the later stage, patients with no DR or early stage of DR might not have the significant changes in SCP (18). Rather, our data showed that the degree of association between subclinical atherosclerosis and reduction in VD was slightly higher in SCP compared with that of DCP. While metabolic diseases, i.e., diabetes mainly affect DCP with slower blood flow, where toxic materials take longer to contact the blood vessels, arterial diseases, i.e., hypertension, act more on precapillary arterioles where shear stress and oxidative stress work well (19).

The pathogenic mechanism of how carotid diseases associates with retinal microvascular disease is not well-established, although there are several hypotheses. Similar risk factors

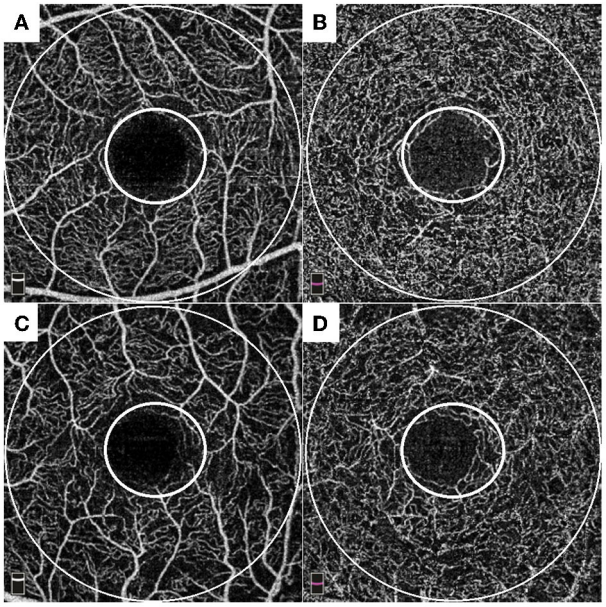

FIGURE 2 | Representative cases of an age-sex matched control **(A,B)** and a patient with subclinical atherosclerosis **(C,D)**. Each of small and large circles denote foveal and parafoveal area. Control: A 56-year- old male patient with 18-years history of diabetes showed 0.63 mm of carotid intima media thickness (IMT) with plaque-free in carotid ultrasonography (US). He had well-preserved foveal VD around foveal avascular zone FAZ (49.7%), parafoveal VD in superficial capillary plexus (49.3%), and parafoveal VD in deep capillary plexus (50.3%) in OCTA. A patient with subclinical atherosclerosis: a 57-year- old male patient with 5-years history of diabetes showed 1.11 mm of carotid IMT with plaque in carotid US. He had impaired foveal VD around FAZ (45.9%), parafoveal VD in superficial capillary plexus (40.8%), and parafoveal VD in deep capillary plexus (46.5%) in OCTA.

may contribute to both diseases. In addition, microcirculation damage caused by diabetes serves as the "common soil" for macro- and microangiopathy of diabetes, since diabetic macroangiopathy evolves from the microvascular damage within the major arterial wall (the vasa vasorum) (20). Recent evidence has shown that the vasa vasorum of the major vessels in patients with diabetes undergoes the similar process as the microvascular changes of the DR. Endothelial dysfunction and increase of vascular permeability occur at first, followed by hypoxia, which leads to the angiogenesis and neovascularization. Therefore, this shared vascular pathophysiology proves that microangiopathy and macroangiopathy of the diabetes are not entirely separated entities.

In our analysis, we could not confirm the differences in BP, blood lipid, glucose control level, and treatment thereof, known factors which affect retinal vasculatures, according to the presence of subclinical atherosclerosis. This can be explained by several reasons. First, this study was conducted on patients who had undergone medical treatment for BP, blood lipid, and glucose. The second reason is that the systemic clinical data included in this study were measured on the day of the visit to the internal medicine clinic, not on the exact date of OCTA acquisition. Considering the variability of medical indicators, the possibility that the time difference affected in the lack of associations cannot be excluded.

The present study has some limitations, including its retrospective nature of study design. The other limitation is that our measurements based on a small field of view (3 mm $\times$ 3 mm) of OCT angiography, which may not represent the whole retinal circulation. Despite these limitations, this approach could provide the important clinical implications of predicting the systemic status with widely available ocular images captured in a short time. The other strength of this study is that we focused only on patients with no DR or treatment naïve patients with DR to obviate the possible effects of ocular treatments on retinal vasculatures. Since previous studies reported changes in macular vasculatures after laser photocoagulation or intravitreal injections (21, 22), we believe that this point has an importance for the accurate analysis. In addition, to minimize the possible errors in image analysis, we included only patients with good OCTA image quality of scan quality $\geq$7, proper segmentation without errors, and the removal of projection artifact, which are all major factors that must be carefully considered in an OCTA imaging study. Last, the number of patients was sufficient for the analysis of risk factors for subclinical atherosclerosis.

In conclusion, we found that decreased VD around FAZ and parafoveal VD in OCTA were significantly associated with subclinical atherosclerosis with other risk factors, such as male sex and old age. Non-invasive *in vivo* retinal vascular imaging captured by OCTA could be used to assess DR but also as the early indicator of macrovascular complications, which suggests that diabetic microangiopathy and macroangiopathy may share the common pathophysiology. Therefore, ophthalmologists should keep in mind such close relationship between ocular changes and systemic diseases and consider evaluations for other comorbidities, such as carotid US, when they examine the patients with impaired macular vasculatures.

DATA AVAILABILITY STATEMENT

The raw data supporting the conclusions of this article will be made available by the authors, without undue reservation.

ETHICS STATEMENT

The studies involving human participants were reviewed and approved by Asan Medical Center IRB. Written informed consent for participation was not required for this study in accordance with the national legislation and the institutional requirements.

AUTHOR CONTRIBUTIONS

All authors listed have made a substantial, direct, and intellectual contribution to the work and approved it for publication.

FUNDING

This study was supported by a grant from the Technology Innovation Program (or Industrial Strategic Technology Development Program) (1415175064, Development of portable fundus imaging and diagnosis device equipped with artificial intelligence and edge computing) funded by the Ministry of Trade, Industry & Energy (MOTIE, South Korea), and the Asan Institute for Life Sciences (2020IP0103-1), Asan Medical Center, Seoul, South Korea.

REFERENCES

1. Nathan DM. Long-term complications of diabetes mellitus. *N Engl J Med.* (1993) 328:1676–85. doi: 10.1056/NEJM199306103282306
2. Zhang P, Gregg E. Global economic burden of diabetes and its implications. *Lancet Diab Endocrinol.* (2017) 5:404–5. doi: 10.1016/S2213-8587(17)30100-6
3. Krentz AJ, Clough G, Byrne CD. Interactions between microvascular and macrovascular disease in diabetes: pathophysiology and therapeutic implications. *Diab Obes Metab.* (2007) 9:781–91. doi: 10.1111/j.1463-1326.2007.00670.x
4. Agrawal R, Xin W, Keane PA, Chhablani J, Agarwal A. Optical coherence tomography angiography: a non-invasive tool to image end-arterial system. *Expert Rev Med Devices.* (2016) 3:519–21. doi: 10.1080/17434440.2016.1186540
5. Jia Y, Bailey ST, Wilson DJ, Tan O, Klein ML, Flaxel CJ, et al. Quantitative optical coherence tomography angiography of choroidal neovascularization in age-related macular degeneration. *Ophthalmology.* (2014) 121:1435–44. doi: 10.1016/j.ophtha.2014.01.034
6. Matsunaga D, Yi J, Puliafito CA, Kashani AH. OCT angiography in healthy human subjects. *Ophthal Surg Lasers Imaging Retina.* (2014) 45:510–5. doi: 10.3928/23258160-20141118-04
7. Spaide RF, Klancnik JM, Cooney MJ. Retinal vascular layers imaged by fluorescein angiography and optical coherence tomography angiography. *JAMA Ophthalmol.* (2015) 133:45–50. doi: 10.1001/jamaophthalmol.2014.3616
8. Spaide RF, Klancnik JM, Cooney MJ. Retinal vascular layers in macular telangiectasia type 2 imaged by optical coherence tomographic angiography. *JAMA Ophthalmol.* (2015) 133:66–73. doi: 10.1001/jamaophthalmol.2014.3950
9. Kwiterovich KA, Maguire MG, Murphy RP, Schachat AP, Bressler NM, Bressler SB, et al. Frequency of adverse systemic reactions after fluorescein angiography: results of a prospective study. *Ophthalmology.* (1991) 98:1139–42. doi: 10.1016/S0161-6420(91)32165-1
10. E.T.D.R.S.R. Group. Fluorescein angiographic risk factors for progression of diabetic retinopathy: ETDRS report number 13. *Ophthalmology.* (1991) 98:834–40. doi: 10.1016/S0161-6420(13)38015-4
11. E.T.D.R.S.R. Group. Classification of diabetic retinopathy from fluorescein angiograms: ETDRS report number 11. *Ophthalmology.* (1991) 98:807–22. doi: 10.1016/S0161-6420(13)38013-0
12. Drinkwater JJ, Chen FK, Brooks AM, Davis BT, Turner AW, Davis TM, et al. Carotid disease and retinal optical coherence tomography angiography parameters in type 2 diabetes: the fremantle diabetes study phase II. *Diabetes Care.* (2020) 43:3034–41. doi: 10.2337/dc20-0370
13. Sillesen H, Sartori S, Sandholt B, Baber U, Mehran R, Fuster V. Carotid plaque thickness and carotid plaque burden predict future cardiovascular events in asymptomatic adult Americans. *Eur Heart J Cardiovasc Imaging.* (2018) 19:1042–50. doi: 10.1093/ehjci/jex239
14. O'Leary DH, Polak JF, Kronmal RA, Manolio TA, Burke GL, Wolfson SK Jr. Carotid-artery intima and media thickness as a risk factor for myocardial infarction and stroke in older adults. *N Engl J Med.* (1999) 340:14–22. doi: 10.1056/NEJM199901073400103
15. Touboul PJ, Hennerici MG, Meairs S, Adams H, Amarenco P, Bornstein N, et al. Mannheim carotid intima-media thickness and plaque consensus (2004-2006-2011). An update on behalf of the advisory board of the 3rd, 4th and 5th watching the risk symposia, at the 13th, 15th and 20th European Stroke Conferences, Mannheim, Germany, 2004, Brussels, Belgium, 2006, and Hamburg, Germany, 2011. *Cerebrovasc Dis.* (2012) 34:290–6. doi: 10.1159/000343145
16. Jung CH, Lee WJ, Lee MJ, Kang YM, Jang JE, Leem J, et al. Association of serum angiopoietin-like protein 2 with carotid intima-media thickness in subjects with type 2 diabetes. *Cardiovasc Diabetol.* (2015) 14:35. doi: 10.1186/s12933-015-0198-z
17. Cobble M, Bale B. Carotid intima-media thickness: knowledge and application to everyday practice. *Postgraduate Med.* (2010) 122:10–8. doi: 10.3810/pgm.2010.01.2091
18. J Ting DSW, Tan GSW, Agrawal R, Yanagi Y, Sie NM, Wong CW, et al. Optical coherence tomographic angiography in type 2 diabetes and diabetic retinopathy. *JAMA Ophthalmol.* (2017) 135:306–12. doi: 10.1001/jamaophthalmol.2016.5877
19. Yang M, Park CS, Kim SH, Noh TW, Kim JH, Park S, et al. Dll4 Suppresses transcytosis for arterial blood-retinal barrier homeostasis. *Circ Res.* (2020) 126:767–83. doi: 10.1161/CIRCRESAHA.119.316476
20. Rubinat E, Ortega E, Traveset A, Arcidiacono MV, Alonso N, Betriu A, et al. Microangiopathy of common carotid vasa vasorum in type 1 diabetes mellitus. *Atherosclerosis.* (2015) 241:334–8. doi: 10.1016/j.atherosclerosis.2015.05.024
21. Kim YJ, Yeo JH, Son G, Kang H, Sung YS, Lee JY, et al. Efficacy of intravitreal AFlibercept injection For Improvement of retinal Nonperfusion In diabeTic retinopathY (AFFINITY study). *BMJ Open Diabetes Res Care.* (2020) 8:e001616. doi: 10.1136/bmjdrc-2020-001616
22. Fawzi AA, Fayed AE, Linsenmeier RA, Gao J, Yu F. Improved macular capillary flow on optical coherence tomography angiography after panretinal photocoagulation for proliferative diabetic retinopathy. *Am J Ophthalmol.* (2019) 206:217–27. doi: 10.1016/j.ajo.2019.04.032

Conflict of Interest: The authors declare that the research was conducted in the absence of any commercial or financial relationships that could be construed as a potential conflict of interest.

Publisher's Note: All claims expressed in this article are solely those of the authors and do not necessarily represent those of their affiliated organizations, or those of the publisher, the editors and the reviewers. Any product that may be evaluated in this article, or claim that may be made by its manufacturer, is not guaranteed or endorsed by the publisher.

frontiers in Medicine

ORIGINAL RESEARCH
published: 07 March 2022
doi: 10.3389/fmed.2022.830678

Anterior Segment Optical Coherence Tomography Angiography Following Trabecular Bypass Minimally Invasive Glaucoma Surgery

*Jinyuan Gan[1], Chelvin C. A. Sng[2,3], Mengyuan Ke[2], Chew Shi Chieh[3], Bingyao Tan[2,4,5], Leopold Schmetterer[1,2,3,4,5,6,7,8] and Marcus Ang[1,2]**

[1] Duke-NUS Graduate Medical School, Singapore, Singapore, [2] Singapore National Eye Centre, Singhealth, Singapore Eye Research Institute, Singapore, Singapore, [3] Department of Ophthalmology, National University Hospital, Singapore, Singapore, [4] SERI-NTU Advanced Ocular Engineering (STANCE), Singapore, Singapore, [5] School of Chemical and Biomedical Engineering, Nanyang Technological University, Singapore, Singapore, [6] Department of Clinical Pharmacology, Medical University of Vienna, Vienna, Austria, [7] Center for Medical Physics and Biomedical Engineering, Medical University of Vienna, Vienna, Austria, [8] Institute of Molecular and Clinical Ophthalmology, Basel, Switzerland

Objective: To assess anterior segment optical coherence tomography angiography (AS-OCTA) imaging of the episcleral vessels before and after trabecular bypass minimally invasive glaucoma surgery (MIGS).

Design: A prospective, clinical, single-centre, single-arm pilot feasibility study conducted at National University Hospital, Singapore.

Subjects: Patients with primary glaucomatous optic neuropathy undergoing Hydrus Microstent (Ivantis Inc., Irvine, CA, USA) implantation, who require at least one intra-ocular pressure-lowering medication. One or two eyes per patient may be enrolled.

Methods: We performed AS-OCTA (Nidek RS-3000 Advance 2, Gamagori, Japan) pre- and up to 6 months post-MIGS implantation using a standard protocol in all cornealimbal quadrants, to derive episcleral vessel densities (VD) using a previously described technique.

Main Outcome Measures: Episcleral VD pre- and post-surgery, in sectors with and without the implant.

Results: We obtained serial AS-OCTA images in 25 eyes undergoing MIGS implantation (23 subjects, mean age 70.3 ± 1.5, 61% female) with mean preoperative intraocular pressure (IOP) of 15.5 mmHg ± 4.0. We observed reductions in postoperative episcleral VD compared to preoperative VD at month 1 (mean difference −3.2, $p = 0.001$), month 3 (mean difference −2.94, $p = 0.004$) and month 6 (mean difference −2.19, $p = 0.039$) in sectors with implants (overall 6 month follow-up, $p = 0.011$). No significant changes were detected in episcleral VD in the sectors without implants ($p = 0.910$).

Conclusion: In our pilot study, AS-OCTA was able to detect changes in the episcleral VD following trabecular bypass MIGS, which may be a useful modality to evaluate surgical outcomes if validated in future studies.

Keywords: glaucoma, imaging, intraocular pressure, sclera, cornea, episclera

OPEN ACCESS

Edited by:
Jorge L. Alió Del Barrio, Miguel Hernández University of Elche, Spain

Reviewed by:
Miguel Teus, University of Alcalá, Spain
Harry Orlans, Imperial College London, United Kingdom

***Correspondence:**
Marcus Ang
marcus.ang@snec.com.sg

Specialty section:
This article was submitted to Ophthalmology, a section of the journal Frontiers in Medicine

Received: *07 December 2021*
Accepted: *27 January 2022*
Published: *07 March 2022*

Citation:
Gan J, Sng CCA, Ke M, Chieh CS, Tan B, Schmetterer L and Ang M (2022) Anterior Segment Optical Coherence Tomography Angiography Following Trabecular Bypass Minimally Invasive Glaucoma Surgery. Front. Med. 9:830678. doi: 10.3389/fmed.2022.830678

INTRODUCTION

Glaucoma is one of the leading causes of blindness worldwide (1). Increased intraocular pressure (IOP) is the main risk factor for glaucoma, and the mainstay of glaucoma treatment involves lowering of IOP (2, 3). The most common treatment involves the use of topical medications – however, these may be associated with adverse effects and poor compliance (4). Meanwhile conventional glaucoma surgeries such as trabeculectomy may effectively lower IOP, but can be associated with sight-threatening complications (5). To address these limitations, minimally invasive glaucoma surgery (MIGS) has gained popularity in recent years.

Currently, MIGS include a heterogeneous group of IOP-lowering devices and procedures that are generally less invasive and have a faster recovery time compared to traditional filtration surgery (6, 7). While MIGS is usually associated with a good safety profile, clinical results suggest variable efficacy in IOP reduction (8, 9). Both iStent (Glaukos, San Clemente, CA, USA) and Hydrus Microstent (Ivantis Inc., Irvine, CA, USA) are ab interno trabecular bypass products that increase aqueous outflow, with the latter scaffolding and dilating the Schlemm's canal as well. In a head-to-head study comparing Hydrus to iStent inject, the COMPARE study found Hydrus to have a greater rate of surgical success compared to iStent, with fewer subjects needing repeat glaucoma surgeries or medications (10).

When evaluating trabecular bypass MIGS devices, imaging the aqueous outflow tracts may be useful in understanding its efficacy. Aqueous angiography is a functional imaging technique utilising an ab interno approach with fluorescein or indocyanine green (ICG) as tracers, demonstrated in enucleated animal eyes (11, 12) and *in vivo* animal studies (13). However, aqueous angiography has limited clinical application as it is an invasive procedure that requires intraocular injection of dye, and is associated with potential complications such as infection and anaphylaxis (14). Recently, optical coherence tomography angiography (OCTA) has emerged as a non-invasive, rapid imaging technique that may be used to delineate vasculature in the anterior segment (15). While the role of anterior segment OCTA (AS-OCTA) has been described for episcleral, scleral and limbal vasculature (16–21), it has not been described specifically for the episcleral venous plexus in relation to MIGS to date (22). Thus, we conducted this pilot feasibility study to evaluate the role of AS-OCTA imaging following Hydrus Microstent implantation, to examine the potential effect of this trabecular bypass MIGS implant on episcleral vessel density.

Abbreviations: AHO, aqueous humour outflow; AS-OCTA, anterior segment optical coherence tomography angiography; BCVA, best-corrected visual acuity; FFT, Fast Fourier Transform; HVF, Humphrey Visual Field; ICG, indocyanine green; IOP, intraocular pressure; MD, mean deviation; MIGS, minimally invasive glaucoma surgery; OCTA, optical coherence tomography angiography; PACG, primary angle-closure glaucoma; POAG, primary open-angle glaucoma; VD, vessel density.

MATERIALS AND METHODS

This was a prospective single-centre case series of consecutive patients who underwent combined phacoemulsification with Hydrus Microstent implantation at the National University Hospital between May 2019 to Mar 2020. Approval was obtained from the National Healthcare Group Domain Specific Review Board (2016/00125) and the study was conducted in accordance with the tenets of the Declaration of Helsinki. Written informed consent was obtained from all patients prior to surgery.

Study Subjects

We included phakic subjects with primary glaucomatous optic neuropathy, as defined by Foster et al. (23), who required at least one intraocular-pressure lowering medication in this study. Exclusion criteria included advanced primary angle-closure glaucoma (PACG) (24) (as defined by cup-disc ratio $\geq$0.9 and/or a visual field defect within the central 10° of fixation), >180° of peripheral anterior synechiae, peripheral anterior synechiae in the target quadrant of Hydrus Microstent implantation, prior incisional glaucoma surgery, secondary glaucoma (including uveitic, neovascular, traumatic glaucoma, or glaucoma secondary to raised episcleral venous pressure) and any orbital, corneal, retinal or choroidal disease which may interfere with cataract extraction or Hydrus Microstent implantation.

Study Measures

Complete ophthalmic examination by a fellowship-trained glaucoma specialist (C. A. Sng) was performed pre-operatively and on day 1, week 1, and months 1, 3, and 6. This included the best corrected Snellen visual acuity (BCVA), IOP measurement with Goldmann applanation tonometry, and a detailed slit lamp examination of the anterior and posterior segments. Humphrey perimetry (Swedish Interative Threshold Algorithm Standard 24-2 algorithm, Humphrey Visual Field, HVF Analyzer II, Carl Zeiss Meditec, Inc., Dublin, California, USA) was performed pre-operatively and 6 months post-operatively, and the mean deviation (MD) was recorded.

Surgical Technique

All surgeries were performed under topical anaesthesia or peribulbar block. Phacoemulsification and intraocular lens implantation were performed via a clear corneal incision. To implant the Hydrus Microstent, the surgical microscope was tilted 30° towards the patient and the patient's head was tilted 45° nasally or inferiorly to allow direct visualisation of the angle structures with an intra-operative gonioscopy lens (Ocular Hill Open Access Surgical Gonioscopy [Left-Hand], Ocular Instruments, Bellevue, WA). An ophthalmic viscosurgical device was used to maintain the anterior chamber and widen the anterior chamber angle after phacoemulsification. The Hydrus Microstent was passed into the anterior chamber through a separate clear corneal incision (about 90 to 120° from the target site of Hydrus Microstent implantation) into the anterior chamber. The trabecular meshwork was incised with the tip of the device injector cannula and the Hydrus Microstent was inserted into the Schlemm's canal in the nasal or inferior

quadrant over a span of approximately 90°. The targeted quadrants were reported to contain greater aqueous humour outflow (AHO), and selection of quadrants was based on surgical accessibility through a clear corneal temporary incision, and surgical technique of Hydrus Microstent implantation (14, 25). After visual confirmation of correct device positioning with the Schlemm's canal, the device injector was withdrawn and the ophthalmic viscosurgical device was removed. The corneal incisions were hydrated with a balanced salt solution. Vision blue (D.O.R.C. Dutch Ophthalmic Research Center [International] B.V., Zuidland, The Netherlands) was injected into the anterior chamber and the presence of the blue dye in the conjunctival vessels was noted and videoed for manual segmentation and comparison with OCTA vessels.

Anterior Segment Imaging

Anterior segment imaging was performed pre-operatively and post-operatively at week 1, month 1, month 3, and month 6 using a digital slit-lamp camera (Topcon ATE-600, Nikon Corp) with a standard diffuse illumination (×10 magnification, flash power 4) for colour photography. Next, AS-OCTA of the episcleral vessels in all cornealimbal quadrants was conducted using a previously described scan protocol (26), using a spectral domain optical coherence tomography system (Nidek RS-3000 Advance 2, Gamagori, Japan) with a central wavelength of 880 nm, axial resolution of 7 um and transverse resolution of 15 um (anterior segment module). The eye tracker function was deactivated for imaging acquisition. The lens was moved close to the area of interest at the corneal surface before optimisation of the focal length and Z position to focus on the area of interest. The scan areas were divided into six sectors: Superior, superior nasal (right eye), nasal, inferior nasal, inferior, inferior temporal (left eye) and temporal directions i.e., six scans were acquired for each eye (**Figure 1**).

AS-OCTA Image Processing

Scans were segmented manually to produce AS-OCTA enface images of (a) episcleral and (b) conjunctival to scleral i.e., full segmentation scans for each eye, before image processing as previously described (27). Essentially, motion artefacts were first removed using Fiji-J (NIH, Bethesda, MD) with a Fast Fourier Transform (FFT) bandpass filter (tolerance of direction 90%). Next, the images were processed with MATLAB (The Mathworks, Inc., Natick, Massachusetts, USA) to segment vessels by removing the speckle noise using a median filter and Gaussian smoothing, then applying Frangi filter to enhance vessel features (**Figure 2**). Finally, local adaptive thresholding was used to binarize the images. The binary images were used to calculate the vessel densities (equation label) of corneal vessels within each sector. Vessel density is defined as the segmented vessels (in white pixel) divided by the sector area (total pixels) i.e., Vessel density $= 100 * P/A$; where $P = 1$ for white pixels representing blood vessels, $P = 0$ for black pixels representing the background, and A being the sector area. As a higher signal strength improves the reliability of measurement and allows for better reproducibility (28), we compared the sector with the highest OCTA vessel density with the control sectors. For consistent comparison, inferior and temporal sectors were used as controls for superior-nasal implants. Likewise superior and temporal sectors were used as controls for inferior-nasal implants, and superior and nasal sectors for inferior-temporal implants. These same sectors were kept consistent between visits. Thus, for each Hydrus Microstent sector we have 2 opposing sectors as controls. We confirmed that vessels derived from AS-OCTA images corresponded to episcleral outflow veins, we injected trypan blue (VisionBlue®) intra-operatively into the anterior chamber after Hydrus Microstent implantation to highlight episcleral venous vessels. Corresponding AS-OCTA images at 1 month were selected from sectors with and without the implant, and compared to the intra-operative images with highlighted vessels that were manually segmented and overlaid with ImageJ (**Figure 3**).

Statistical Analysis

Vessel densities obtained from control sectors without implants were compared to vessel densities from sectors with the Hydrus Microstent in the same eye, with serial comparison analysis performed over the follow-up period (**Figure 4**). Statistical analysis was performed using Statistical Program for Social Sciences version 27.0.1.0 for MacOS© (2020 SPSS© Inc. IBM Corp, USA). Percentage differences in vessel densities were evaluated using Friedman Test (serial measurements over follow-up) and Wilcoxon Signed Rank Test (paired, compared to baseline). All data were expressed as mean ± standard deviation (SD) when applicable, and $P < 0.05$ were considered statistically significant.

RESULTS

In this pilot study, we included 25 eyes from 23 subjects undergoing Hydrus Microstent implant surgeries. Patients' mean age was 70.3 ± 1.5 years, with 74% Chinese from our predominantly Asian population, while 61% were female. The mean pre-operative intraocular pressure (IOP) was 15.5 ± 4.0 mmHg, with eyes being on an average of 1.2 glaucoma medications pre-operation, and mean HVF MD was −4.9 ± 3.2 dB. We observed a reduction in mean post-operative IOP at 1 week (11.6 ± 3.1 mmHg, $P = 0.001$), 1 month (12.8 ± 3.1 mmHg, $P = 0.002$), 3 months (12.3 ± 3.2 mmHg, $P = 0.001$), and 6 months (12.5 ± 3.1 mmHg, $P = 0.002$)—none required IOP lowering medications post-operatively during follow-up. There were no significant post-operative complications such as hyphaemia, infection or progression of glaucoma; while no eyes required a repeat surgical procedure during the follow-up period.

All eyes had intra-operative identification of episcleral vessels after Hydrus Microstent implantation to confirm drainage of aqueous humour and intra-operative images were compared with corresponding AS-OCTA images at post-operative day 1 (**Figure 3**). At baseline, implant sectors have higher vessel densities compared to control sectors for both episcleral images ($p = 0.03$, mean difference of 2.12, 95% CI [0.13, 4.11]) and full-thickness scans ($p = 0.03$, mean difference of 2.21, 95% CI [0.19, 4.23]). We analysed the month 1 AS-OCTA images that clearly corresponded with trypan blue labelled vessels (6 sectors)

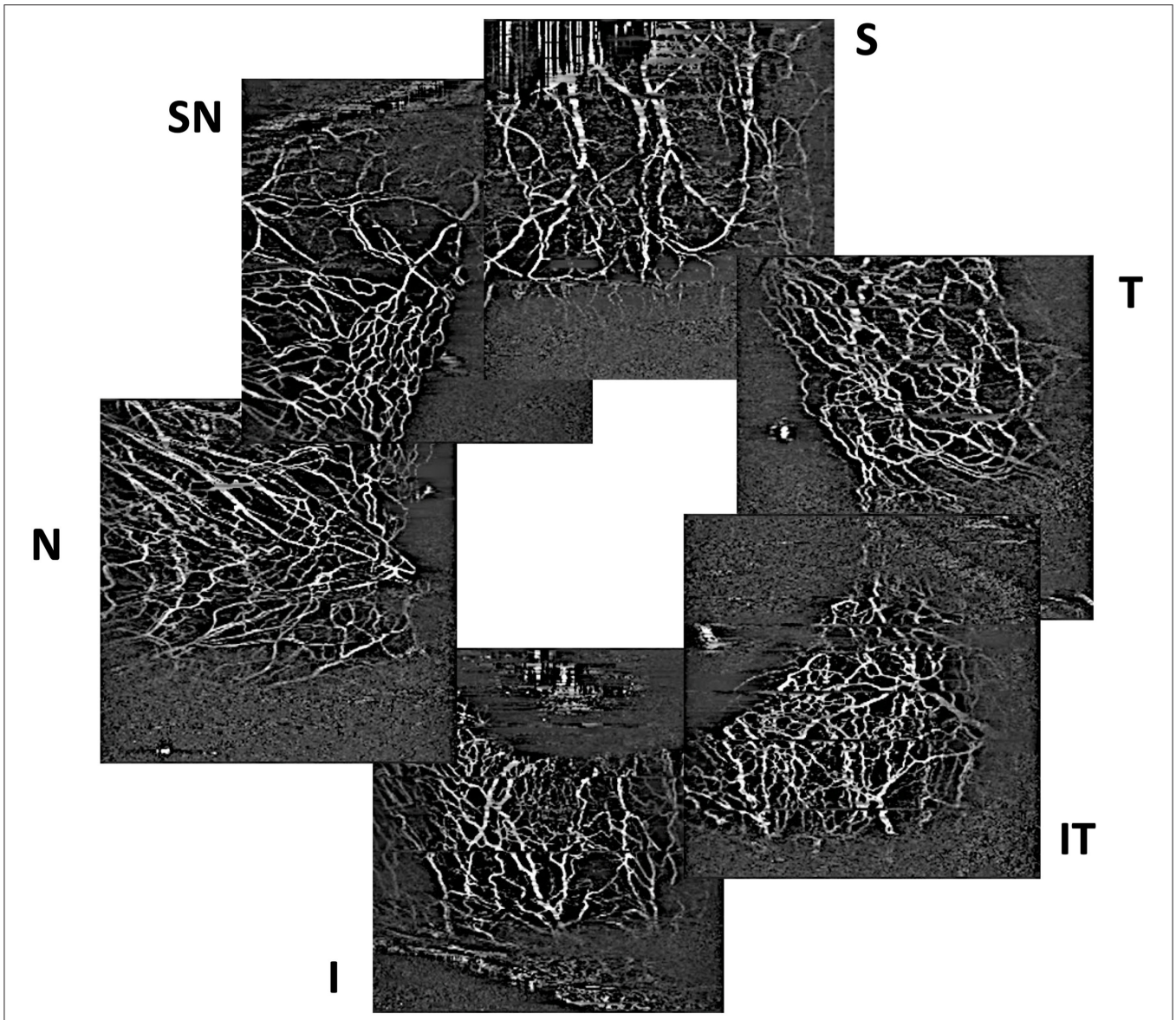

FIGURE 1 | Example of optical coherence tomography angiography scans of episcleral vessels acquired in sectors with the trabecular bypass minimally invasive glaucoma surgical device (S, superior; SN, superior nasal; N, nasal) and control sectors without the implant (I, inferior; IT, inferior temporal; T, temporal).

and observed a reduction in VD of trypan blue labelled vessels comparing sectors with the implant vs. control sectors with no implant (mean difference 1.35 ± 0.5 vs. 0.64 ± 0.2 respectively, $p = 0.008$). We also found that sectors with the Hydrus Microstent implanted showed significant reductions in episcleral vessel density over 6 months ($p = 0.011$), with specific reductions in VD observed at month 1 ($p = 0.001$, mean difference of −3.2, 95% CI [−1.14, −5.10]), month 3 ($p = 0.004$, mean difference of −2.94, 95% CI [−1.12, −4.76]) and month 6 ($p = 0.039$, mean difference of −2.19, 95% CI [−0.29, −4.08]) compared to pre-operative baseline. Meanwhile, control sectors remained unchanged at all time points compared to pre-operative vessel densities (**Table 1**).

Similar analysis for full segmentation of AS-OCTA scans i.e., conjunctival, episcleral and scleral layers showed a similar trend i.e., Hydrus Microstent sectors showed significant reduction in VD month 1 ($p = 0.001$, mean difference of −3.27, 95% CI −1.12, −5.42), month 3 ($p = 0.005$, mean difference of −3.24, 95% CI [−1.33, −5.15]) and month 6 ($p = 0.046$, mean difference of −2.18, 95% CI [−0.12, −4.25]) compared to baseline, while control sectors remained unchanged at all time points (**Table 2**). Of note, these differences were not significant at week 1 in both episcleral ($p = 0.326$, 95% CI −1.09, 3.07) and full segmentation scans ($p = 0.510$, 95% CI −1.45, 2.99).

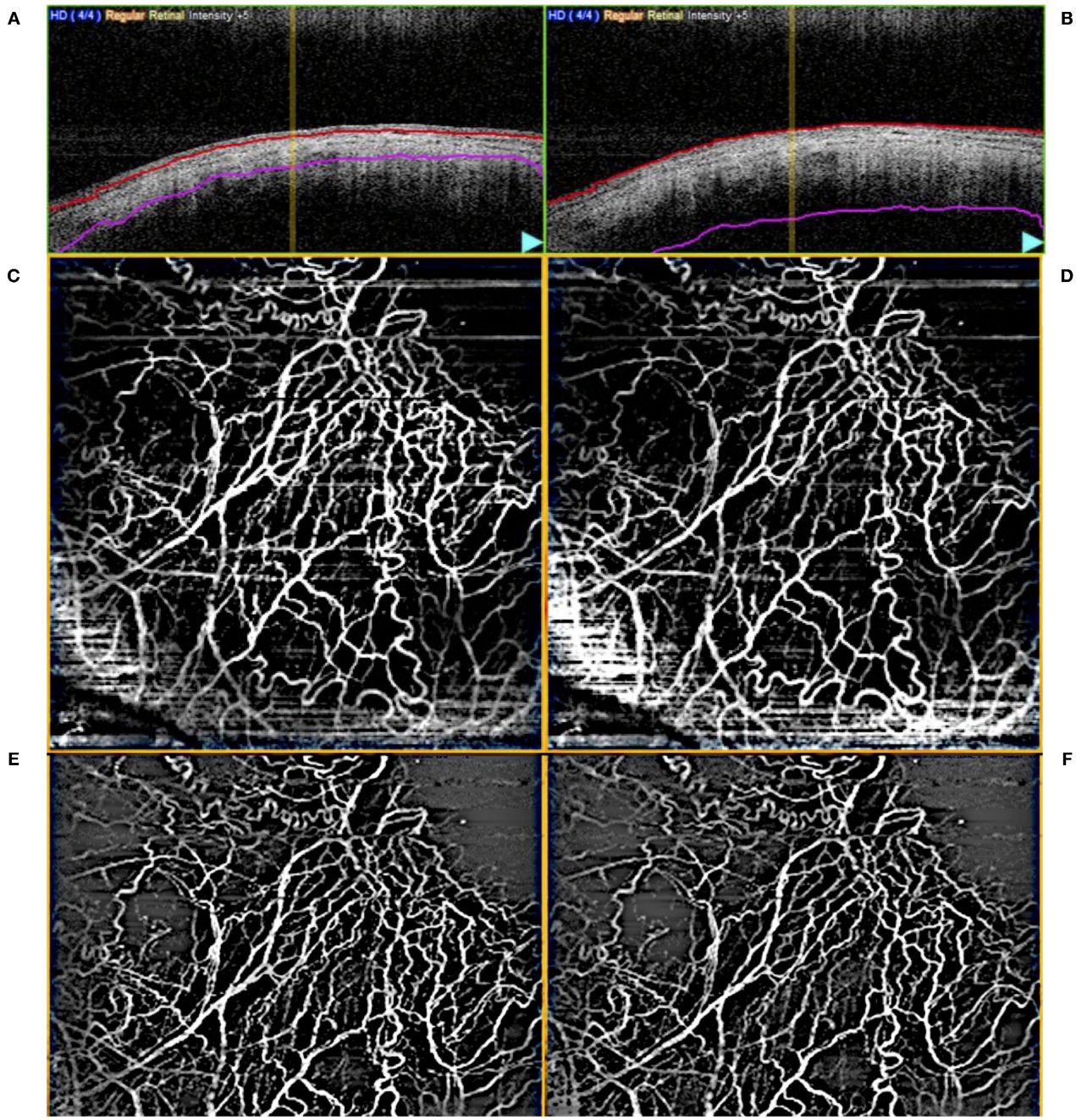

FIGURE 2 | Example of **(A)** episcleral and **(B)** full layer (conjunctival, episcleral, scleral) segmented optical coherence tomography angiography (AS-OCTA) images. Unprocessed en face AS-OCTA images of the **(C)** episcleral and **(D)** full layer vasculature, respectively, and after removal of artefacts [**(E,F)**, respectively].

DISCUSSION

In this pilot study, AS-OCTA detected a post-operative reduction in episcleral vessel density in sectors with the Hydrus Microstent implant compared to control sectors without implants. We correlated these vessels with intraoperative imaging that highlighted the aqueous outflow tracts using trypan blue. Our observations may seem counterintuitive since trabecular bypass MIGS devices such as the Hydrus Microstent are meant to enhance flow to collector channels (29). We postulate that the apparent reduction in AS-OCTA derived vessel density measurements may be attributed to increased aqueous humour flow in the episcleral veins, thereby reducing the signal intensity or phase differences detected by the AS-OCTA (30). Changes in vessel density in the control sectors could have been a result of cataract surgery itself, which may also increase aqueous flow

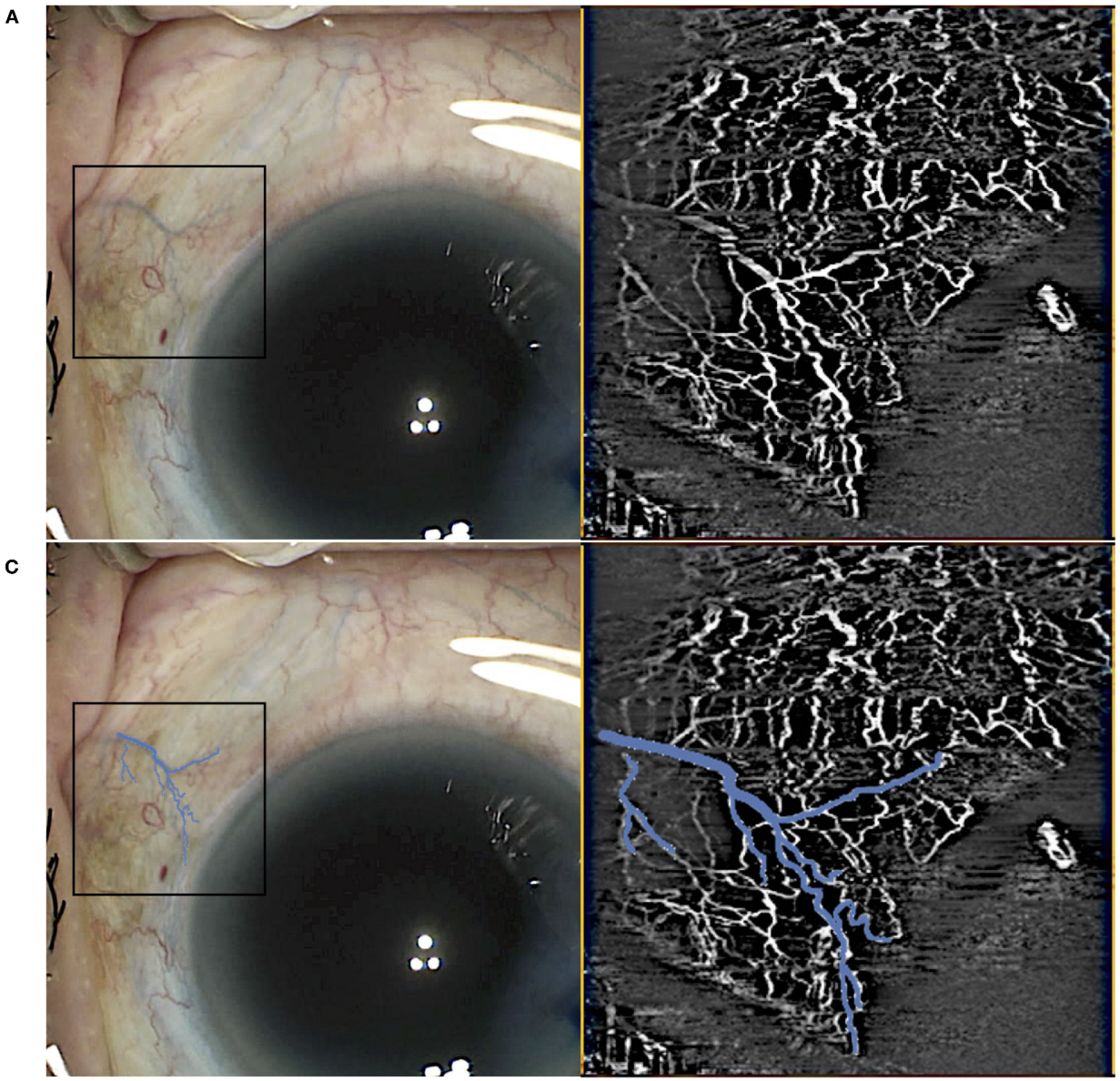

FIGURE 3 | Example of intraoperative identification of episcleral vessels using trypan blue immediately postimplant **(A)** with the corresponding optical coherence tomography angiography (OCTA) scan in the sector **(B)**. Trypan blue vessels in the region of interest were highlighted **(C)** with an overlay on the intraoperative images **(D)** before vessel density calculations.

to a lesser extent (31, 32). It is also possible that the Hydrus Microstent leads to changes in aqueous outflow in a differential manner, i.e., some vessels with greater aqueous flow, while others with decreased flow—leading to an overall AS-OCTA detection of decreased vessel density (33).

The reduction in vessel densities could also be due to the cessation of IOP-lowering medications, many of which are associated with hyperaemia (34). To control for potential confounders, we compared Hydrus Microstent sectors with control quadrants without the implant within the same eye, such that all quadrants were subjected to potential effects of medications and cataract surgery. However, we do recognise this study's limitations and cannot exclude any local quadrant effects of prostaglandin use if applicable (35). Lastly, vessel densities were found to be higher in sectors with Hydrus Microstent compared to control sectors at baseline. One explanation could be that Hydrus Microstent sectors included more inferior-nasal sectors, which were associated with the highest vessel volume of aqueous outflow channels out of all ocular sectors, and hence greater vessel densities (36, 37). Nonetheless, we recognise that AS-OCTA cannot directly detect aqueous outflow, but instead measures episcleral vessel density as a potential surrogate (38).

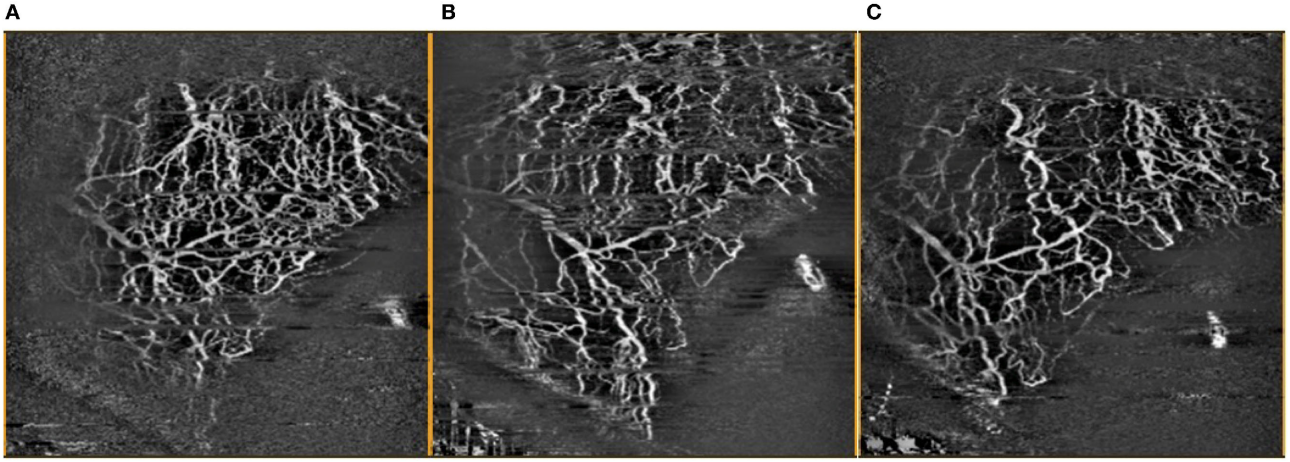

FIGURE 4 | Comparison of OCTA images of inferior temporal episcleral vessels taken **(A)** pre-operatively, **(B)** 1 month post-operatively, and **(C)** 3 months post-operatively, with artefacts removed.

TABLE 1 | Optical coherence tomography angiography vessel density measurements of episcleral vasculature in sectors with Hydrus Microstent implants and controls comparing pre-operative and post-operative week 1 and month 1, 3, and 6.

Assessment time-points	Vessel density Mean (±SD)	*P-value
Control		
Pre-operative ($n = 25$)	23.2 (4.3)	0.910**
Week 1 ($n = 25$)	23.0 (3.4)	0.946
Month 1 ($n = 23$)	23.3 (3.5)	0.976
Month 3 ($n = 16$)	22.8 (1.4)	0.538
Month 6 ($n = 13$)	24.0 (3.3)	0.917
Control		
Pre-operative ($n = 24$)	24.0 (4.4)	0.723**
Week 1 ($n = 25$)	23.0 (3.4)	0.241
Month 1 ($n = 23$)	23.3 (3.5)	0.114
Month 3 ($n = 16$)	23.2 (4.7)	0.836
Month 6 ($n = 13$)	23.0 (5.1)	0.552
Hydrus Microstent sector		
Pre-operative ($n = 25$)	25.6 (3.4)	0.011**
Week 1 ($n = 25$)	24.7 (3.9)	0.326
Month 1 ($n = 23$)	22.5 (3.4)	0.001
Month 3 ($n = 16$)	22.7 (2.8)	0.004
Month 6 ($n = 13$)	23.5 (3.1)	0.039

*Wilcoxon signed rank test (paired) comparing baseline VD to follow-up VD measurements.

**Friedman test for serial VD measurements over follow-up period (n = 25 eyes at baseline, 1 week and 1 month; n = 16 eyes beyond month 3).

TABLE 2 | Optical coherence tomography angiography vessel density measurements of overall vasculature (conjunctival, episcleral, scleral) in sectors with Hydrus Microstent implants and controls comparing pre-operative and post-operative week 1 and month 1, 3, and 6.

Assessment time-points	Vessel density Mean (±SD)	*P-value (compared to pre-operative)
Control		
Pre-operative ($n = 25$)	22.9 (4.4)	0.699**
Week 1 ($n = 25$)	22.8 (3.2)	0.757
Month 1 ($n = 23$)	23.1 (4.0)	0.761
Month 3 ($n = 16$)	23.1 (2.1)	0.717
Month 6 ($n = 13$)	24.4 (3.0)	0.701
Control		
Pre-operative ($n = 24$)	24.2 (4.3)	0.536**
Week 1 ($n = 25$)	23.2 (4.2)	0.153
Month 1 ($n = 23$)	23.2 (3.0)	0.153
Month 3 ($n = 16$)	23.3 (4.7)	0.301
Month 6 ($n = 13$)	24.0 (4.5)	0.601
Hydrus Microstent sector		
Pre-operative ($n = 25$)	25.7 (3.6)	0.021**
Week 1 ($n = 25$)	25.0 (4.2)	0.510
Month 1 ($n = 23$)	22.5 (3.8)	0.001
Month 3 ($n = 16$)	22.5 (2.9)	0.005
Month 6 ($n = 13$)	23.6 (3.5)	0.046

*Wilcoxon signed rank test (paired) comparing baseline VD to follow-up VD measurements.

**Friedman test for serial VD measurements over follow-up period (n = 25 eyes at baseline, 1 week and 1 month; n = 16 eyes beyond month 3).

As such, current AS-OCTA technology might not yet be an ideal imaging modality for the detection of conventional aqueous outflow. However, our study was a unique opportunity to confirm the location of the outflow tracts using trypan blue, and allowed us to compare pre- and post-procedure changes in vessel density in the sectors with the implant, vs. control sectors without any implant. Further validation studies using larger sampling sizes and alternative methods for aqueous outflow and episcleral vessel

delineation, such as aqueous angiography, are needed to confirm our observations.

Currently, imaging the aqueous outflow tracts are not performed in the clinical setting due to the need to inject a contrast agent into the anterior chamber. Thus, AS-OCTA could provide a non-invasive alternative to imaging the episcleral venous plexus as an adjunctive or surrogate for evaluating the aqueous outflow (39). The AS-OCTA has been previously shown to detect increased episcleral vessel density due to increased episcleral venous flow leading to raised intraocular pressure (40), or reduction in episcleral vessel density following anterior segment ischemia (41). Although a previous report suggested that AS-OCT (non-angiographic) imaging did not detect changes in aqueous outflow after successful trabecular-targeted MIGS (120-degree trabectome or 360-degree suture trabeculotomy) during 3 month follow-up (42), our study specifically examined AS-OCT angiography to delineate the episcleral venous plexus following trabecular bypass MIGS. As AS-OCTA imaging is rapid and non-contact, repeated serial post-operative scans can be taken for comparison (43), and may be useful for pre-operative assessment to guide trabecular bypass device placement.

Though MIGS has been viewed as a safe surgical option for lowering IOP in carefully selected eyes, variable efficacy has been attributed to non-optimal surgical placement (44). Traditionally MIGS devices are placed in the nasal angle (45), but pre-operative imaging assessment using modalities such as AS-OCTA may be able to optimise surgical planning and the location of device implantation. Past studies have demonstrated the non-uniform nature of AHO around the limbus, which may vary over time and differ between eyes (46). Hence it is unclear how these variations might affect the surgical outcomes and decision on the most optimal location for trabecular bypass MIGS. Nonetheless, this highlights the unmet need for an imaging modality to allow for preoperative assessment to individualise MIGS implantation for patients.

Despite the promising observations from our pilot study, we would like to highlight several challenges with using the AS-OCTA to image the episcleral venous plexus. Firstly, scan techniques will have to be adjusted for the anterior segment as these systems were originally designed for the posterior segment, hence anterior segment images are motion-sensitive and regions of interest are more difficult to match in serial scans (21). In our study, we recognise the limitations of manually segmenting the episcleral layers from AS-OCTA imaging to minimise effects from conjunctival vessels on our analysis, and thus correlated our images with intraoperative dye labelled vessels and observed reduction in overall vessel density from fully segmented scans as well. Secondly, AS-OCTA derived vessel density measurements may be underestimated due to limited detection of smaller vessels (47), or overestimated due to projection and motion artefacts (48). Thus, repeated serial measurements were performed to reduce random errors and confirm our observations. Thirdly, the AS-OCTA does not directly image the aqueous outflow tracts such as the Schlemm's canal and collector channels (49). Ideally we should perform aqueous angiography to assess the actual flow through the collector channels—thus the Hydrus implant may not increase the flow in the collector channels. However, we used the AS-OCTA imaging of the episcleral venous plexuses as a surrogate *in vivo*, as flow may be detected because the vessels are partially filled with both clear aqueous humour and blood; and we had further confirmed increased aqueous outflow using intraoperative imaging with trypan blue. Lastly, although we have excluded patients with advanced PACG, we have included patients with both mild to moderate PACG and primary open-angle glaucoma (POAG). Ideally we would have studies with larger sample sizes that exclude PACG eyes, but as this is a pilot study primarily focused on investigating the feasibility of using AS-OCTA for imaging of episcleral vessels pre- and post-MIGS, we have decided to include PACG eyes to aid in estimation purposes. Despite these limitations, our study suggests that AS-OCTA is a promising non-invasive imaging tool that is readily available in the clinics, that may be useful in assessing changes in episcleral vessel density secondary to trabecular bypass MIGS.

In summary, our pilot study suggests that AS-OCTA detects changes in episcleral vessel density before and after trabecular bypass MIGS implantation in sectors with the implant compared to control sectors. The reduction in episcleral vessel density is observed to occur over 3 to 6 months after surgery, which requires further validation in future studies to examine the potential clinical application of AS-OCTA imaging for this indication.

DATA AVAILABILITY STATEMENT

The raw data supporting the conclusions of this article will be made available by the authors, without undue reservation.

ETHICS STATEMENT

The studies involving human participants were reviewed and approved by National Healthcare Group Domain Specific Review Board. The patients/participants provided their written informed consent to participate in this study.

AUTHOR CONTRIBUTIONS

All authors substantial contributions to conception and design, acquisition of data, or analysis and interpretation of data, drafting the article or revising it critically for important intellectual content, and final approval of the version to be published.

FUNDING

This work was supported by Singapore Imaging Eye Network (SIENA), project no. NMRC/CG/C010A/2017_SERI and SERI-NTU Advanced Ocular Engineering (STANCE) Program.

REFERENCES

1. Bourne RR, Taylor HR, Flaxman SR, Keeffe J, Leasher J, Naidoo K, et al. Number of people blind or visually impaired by glaucoma worldwide and in world regions 1990 - 2010: a meta-analysis. *PLoS ONE*. (2016) 11:e0162229. doi: 10.1371/journal.pone.0162229
2. Blanco A, Bagnasci L, Bagnis A, Barton K, Baudouin C, Bengtsson B. European Glaucoma Society Terminology and Guidelines for Glaucoma, 4th Edition - Chapter 3: Treatment principles and options Supported by the EGS Foundation: Part 1: Foreword; Introduction; Glossary; Chapter 3 Treatment principles and options. *Br J Ophthalmol*. (2017) 101:130–95. doi: 10.1136/bjophthalmol-2016-EGSguideline.003
3. Lavia C, Dallorto L, Maule M, Ceccarelli M, Fea AM. Minimally-invasive glaucoma surgeries (MIGS) for open angle glaucoma: a systematic review and meta-analysis. *PLoS ONE*. (2017) 12:e0183142. doi: 10.1371/journal.pone.0183142
4. Le K, Saheb H. iStent trabecular micro-bypass stent for open-angle glaucoma. *Clin Ophthalmol*. (2014) 8:1937–45. doi: 10.2147/OPTH.S45920
5. Gedde SJ, Herndon LW, Brandt JD, Budenz DL, Feuer WJ, Schiffman JC, et al. Postoperative complications in the Tube Versus Trabeculectomy (TVT) study during five years of follow-up. *Am J Ophthalmol*. (2012) 153:804–14 e1. doi: 10.1016/j.ajo.2011.10.024
6. Meier KL, Greenfield DS, Hilmantel G, Kahook MY, Lin C, Rorer EM, et al. Special commentary: Food and Drug Administration and American Glaucoma Society co-sponsored workshop: the validity, reliability, and usability of glaucoma imaging devices. *Ophthalmology*. (2014) 121:2116–23. doi: 10.1016/j.ophtha.2014.05.024
7. Wang J, Barton K. Overview of MIGS. In: Sng CCA, Barton K, editors. *Minimally Invasive Glaucoma Surgery*. Singapore: Springer Singapore (2021). p. 1–10.
8. Minckler D, Mosaed S, Dustin L, Ms BF, Trabectome Study G. Trabectome (trabeculectomy-internal approach): additional experience and extended follow-up. *Trans Am Ophthalmol Soc*. (2008) 106:149–59; discussion 59–60.
9. Huang AS, Camp A, Xu BY, Penteado RC, Weinreb RN. Aqueous angiography: aqueous humor outflow imaging in live human subjects. *Ophthalmology*. (2017) 124:1249–51. doi: 10.1016/j.ophtha.2017.03.058
10. Ahmed IIK, Fea A, Au L, Ang RE, Harasymowycz P, Jampel HD, et al. A prospective randomized trial comparing hydrus and istent microinvasive glaucoma surgery implants for standalone treatment of open-angle glaucoma: the COMPARE study. *Ophthalmology*. (2020) 127:52–61. doi: 10.1016/j.ophtha.2019.04.034
11. Saraswathy S, Tan JC, Yu F, Francis BA, Hinton DR, Weinreb RN, et al. Aqueous angiography: real-time and physiologic aqueous humor outflow imaging. *PLoS ONE*. (2016) 11:e0147176. doi: 10.1371/journal.pone.0147176
12. Burn JB, Huang AS, Weber AJ, Komaromy AM, Pirie CG. Aqueous angiography in normal canine eyes. *Transl Vis Sci Technol*. (2020) 9:44. doi: 10.1167/tvst.9.9.44
13. Huang AS, Li M, Yang D, Wang H, Wang N, Weinreb RN. Aqueous angiography in living nonhuman primates shows segmental, pulsatile, and dynamic angiographic aqueous humor outflow. *Ophthalmology*. (2017) 124:793–803. doi: 10.1016/j.ophtha.2017.01.030
14. Huang AS, Francis BA, Weinreb RN. Structural and functional imaging of aqueous humour outflow: a review. *Clin Exp Ophthalmol*. (2018) 46:158–68. doi: 10.1111/ceo.13064
15. Ang M, Sim DA, Keane PA, Sng CC, Egan CA, Tufail A, et al. Optical coherence tomography angiography for anterior segment vasculature imaging. *Ophthalmology*. (2015) 122:1740–7. doi: 10.1016/j.ophtha.2015.05.017
16. Ang M, Cai Y, Tan AC. Swept source optical coherence tomography angiography for contact lens-related corneal vascularization. *J Ophthalmol*. (2016) 2016:9685297. doi: 10.1155/2016/9685297
17. Ang M, Devarajan K, Das S, Stanzel T, Tan A, Girard M, et al. Comparison of anterior segment optical coherence tomography angiography systems for corneal vascularisation. *Br J Ophthalmol*. (2018) 102:873–7. doi: 10.1136/bjophthalmol-2017-311072
18. Ang M, Devarajan K, Tan AC, Ke M, Tan B, Teo K, et al. Anterior segment optical coherence tomography angiography for iris vasculature in pigmented eyes. *Br J Ophthalmol*. (2020) 105:929–34. doi: 10.1136/bjophthalmol-2020-316930
19. Hau SC, Devarajan K, Ang M. Anterior segment optical coherence tomography angiography and optical coherence tomography in the evaluation of episcleritis and scleritis. *Ocul Immunol Inflamm*. (2019) 29:362–9. doi: 10.1080/09273948.2019.1682617
20. Liu YC, Devarajan K, Tan TE, Ang M, Mehta JS. Optical coherence tomography angiography for evaluation of reperfusion after pterygium surgery. *Am J Ophthalmol*. (2019) 207:151–8. doi: 10.1016/j.ajo.2019.04.003
21. Ang M, Baskaran M, Werkmeister RM, Chua J, Schmidl D, Aranha Dos Santos V, et al. Anterior segment optical coherence tomography. *Prog Retin Eye Res*. (2018) 66:132–56. doi: 10.1016/j.preteyeres.2018.04.002
22. Lee WD, Devarajan K, Chua J, Schmetterer L, Mehta JS, Ang M. Optical coherence tomography angiography for the anterior segment. *Eye and Vision*. (2019) 6:4. doi: 10.1186/s40662-019-0129-2
23. Foster PJ, Buhrmann R, Quigley HA, Johnson GJ. The definition and classification of glaucoma in prevalence surveys. *Br J Ophthalmol*. (2002) 86:238–42. doi: 10.1136/bjo.86.2.238
24. Canadian Ophthalmological Society Glaucoma Clinical Practice Guideline Expert C, Canadian Ophthalmological S. Canadian Ophthalmological Society evidence-based clinical practice guidelines for the management of glaucoma in the adult eye. *Can J Ophthalmol*. (2009) 44(Suppl. 1):S7–93. doi: 10.3129/i09.080
25. Pillunat LE, Erb C, Junemann AG, Kimmich F. Micro-invasive glaucoma surgery (MIGS): a review of surgical procedures using stents. *Clin Ophthalmol*. (2017) 11:1583–600. doi: 10.2147/OPTH.S135316
26. Tey KY, Gan J, Foo V, Tan B, Ke MY, Schmetterer L, et al. Role of anterior segment optical coherence tomography angiography in the assessment of acute chemical ocular injury: a pilot animal model study. *Sci Rep*. (2021) 11:16625. doi: 10.1038/s41598-021-96086-0
27. Ang M, Foo V, Ke M, Tan B, Tong L, Schmetterer L, et al. Role of anterior segment optical coherence tomography angiography in assessing limbal vasculature in acute chemical injury of the eye. *Br J Ophthalmol*. (2021). doi: 10.1136/bjophthalmol-2021-318847. [Epub ahead of print].
28. Lim HB, Kim YW, Nam KY, Ryu CK, Jo YJ, Kim JY. Signal strength as an important factor in the analysis of peripapillary microvascular density using optical coherence tomography angiography. *Sci Rep*. (2019) 9:16299. doi: 10.1038/s41598-019-52818-x
29. Gulati V, Fan S, Hays CL, Samuelson TW, Ahmed, II, et al. A novel 8-mm Schlemm's canal scaffold reduces outflow resistance in a human anterior segment perfusion model. *Invest Ophthalmol Vis Sci*. (2013) 54:1698–704. doi: 10.1167/iovs.12-11373
30. Hays CL, Gulati V, Fan S, Samuelson TW, Ahmed, II, et al. Improvement in outflow facility by two novel microinvasive glaucoma surgery implants. *Invest Ophthalmol Vis Sci*. (2014) 55:1893–900. doi: 10.1167/iovs.13-13353
31. Mansberger SL, Gordon MO, Jampel H, Bhorade A, Brandt JD, Wilson B, et al. Reduction in intraocular pressure after cataract extraction: the Ocular Hypertension Treatment Study. *Ophthalmology*. (2012) 119:1826–31. doi: 10.1016/j.ophtha.2012.02.050
32. Berdahl JP. Cataract surgery to lower intraocular pressure. *Middle East Afr J Ophthalmol*. (2009) 16:119–22. doi: 10.4103/0974-9233.56222
33. Larkin KA, Macneil RG, Dirain M, Sandesara B, Manini TM, Buford TW. Blood flow restriction enhances post-resistance exercise angiogenic gene expression. *Med Sci Sports Exerc*. (2012) 44:2077–83. doi: 10.1249/MSS.0b013e3182625928
34. Li F, Huang W, Zhang X. Efficacy and safety of different regimens for primary open-angle glaucoma or ocular hypertension: a systematic review and network meta-analysis. *Acta Ophthalmol*. (2018) 96:e277–84. doi: 10.1111/aos.13568
35. Akagi T, Uji A, Okamoto Y, Suda K, Kameda T, Nakanishi H, et al. Anterior segment optical coherence tomography angiography imaging of conjunctiva and intrasclera in treated primary open-angle glaucoma. *Am J Ophthalmol*. (2019) 208:313–22. doi: 10.1016/j.ajo.2019.05.008
36. Carreon T, van der Merwe E, Fellman RL, Johnstone M, Bhattacharya SK. Aqueous outflow - a continuum from trabecular meshwork to episcleral veins. *Prog Retin Eye Res*. (2017) 57:108–33. doi: 10.1016/j.preteyeres.2016.12.004
37. Akagi T, Uji A, Huang AS, Weinreb RN, Yamada T, Miyata M, et al. Conjunctival and intrascleral vasculatures assessed using anterior segment

optical coherence tomography angiography in normal eyes. *Am J Ophthalmol.* (2018) 196:1–9. doi: 10.1016/j.ajo.2018.08.009
38. Ang M, Cai Y, Shahipasand S, Sim DA, Keane PA, Sng CC, et al. En face optical coherence tomography angiography for corneal neovascularisation. *Br J Ophthalmol.* (2016) 100:616–21. doi: 10.1136/bjophthalmol-2015-307338
39. Stanzel TP, Devarajan K, Lwin NC, Yam GH, Schmetterer L, Mehta JS, et al. Comparison of optical coherence tomography angiography to indocyanine Green angiography and slit lamp photography for corneal vascularization in an animal model. *Sci Rep.* (2018) 8:11493. doi: 10.1038/s41598-018-29752-5
40. Ang M, Sng C, Milea D. Optical coherence tomography angiography in dural carotid-cavernous sinus fistula. *BMC Ophthalmol.* (2016) 16:93. doi: 10.1186/s12886-016-0278-1
41. Pineles SL, Chang MY, Oltra EL, Pihlblad MS, Davila-Gonzalez JP, Sauer TC, et al. Anterior segment ischemia: etiology, assessment, and management. *Eye.* (2018) 32:173–8. doi: 10.1038/eye.2017.248
42. Yoshikawa M, Akagi T, Uji A, Nakanishi H, Kameda T, Suda K, et al. Pilot study assessing the structural changes in posttrabecular aqueous humor outflow pathway after trabecular meshwork surgery using swept-source optical coherence tomography. *PLoS ONE.* (2018) 13:e0199739. doi: 10.1371/journal.pone.0199739
43. Ang M, Tan ACS, Cheung CMG, Keane PA, Dolz-Marco R, Sng CCA, et al. Optical coherence tomography angiography: a review of current and future clinical applications. *Graefes Arch Clin Exp Ophthalmol.* (2018) 256:237–45. doi: 10.1007/s00417-017-3896-2
44. Richter GM, Coleman AL. Minimally invasive glaucoma surgery: current status and future prospects. *Clin Ophthalmol.* (2016) 10:189–206. doi: 10.2147/OPTH.S80490
45. Huang AS, Penteado RC, Papoyan V, Voskanyan L, Weinreb RN. Aqueous angiographic outflow improvement after trabecular microbypass in glaucoma patients. *Ophthalmol Glaucoma.* (2019) 2:11–21. doi: 10.1016/j.ogla.2018.11.010
46. Huang AS, Saraswathy S, Dastiridou A, Begian A, Mohindroo C, Tan JC, et al. Aqueous angiography-mediated guidance of trabecular bypass improves angiographic outflow in human enucleated eyes. *Invest Ophthalmol Vis Sci.* (2016) 57:4558–65. doi: 10.1167/iovs.16-19644
47. Spaide RF, Fujimoto JG, Waheed NK. Image artifacts in optical coherence tomography angiography. *Retina.* (2015) 35:2163–80. doi: 10.1097/IAE.0000000000000765
48. Spaide RF, Fujimoto JG, Waheed NK, Sadda SR, Staurenghi G. Optical coherence tomography angiography. *Prog Retin Eye Res.* (2018) 64:1–55. doi: 10.1016/j.preteyeres.2017.11.003
49. Yao X, Tan B, Ho Y, Liu X, Wong D, chua j, et al. Full circumferential morphological analysis of schlemm's canal in human eyes using megahertz swept source OCT. *Biomedical Optics Express.* (2021) 12:3865–77. doi: 10.1364/BOE.426218

Conflict of Interest: The authors declare that the research was conducted in the absence of any commercial or financial relationships that could be construed as a potential conflict of interest.

Publisher's Note: All claims expressed in this article are solely those of the authors and do not necessarily represent those of their affiliated organizations, or those of the publisher, the editors and the reviewers. Any product that may be evaluated in this article, or claim that may be made by its manufacturer, is not guaranteed or endorsed by the publisher.

frontiers in Medicine

PERSPECTIVE
published: 11 March 2022
doi: 10.3389/fmed.2022.835804

Benefits of Integrating Telemedicine and Artificial Intelligence Into Outreach Eye Care: Stepwise Approach and Future Directions

Mark A. Chia[1,2] *and Angus W. Turner*[1,3]*

[1] Lions Outback Vision, Lions Eye Institute, Nedlands, WA, Australia, [2] Institute of Ophthalmology, Faculty of Brain Sciences, University College London, London, United Kingdom, [3] Centre for Ophthalmology and Visual Science, University of Western Australia, Nedlands, WA, Australia

Telemedicine has traditionally been applied within remote settings to overcome geographical barriers to healthcare access, providing an alternate means of connecting patients to specialist services. The coronavirus 2019 pandemic has rapidly expanded the use of telemedicine into metropolitan areas and enhanced global telemedicine capabilities. Through our experience of delivering real-time telemedicine over the past decade within a large outreach eye service, we have identified key themes for successful implementation which may be relevant to services facing common challenges. We present our journey toward establishing a comprehensive teleophthalmology model built on the principles of collaborative care, with a focus on delivering practical lessons for service design. Artificial intelligence is an emerging technology that has shown potential to further address resource limitations. We explore the applications of artificial intelligence and the need for targeted research within underserved settings in order to meet growing healthcare demands. Based on our rural telemedicine experience, we make the case that similar models may be adapted to urban settings with the aim of reducing surgical waitlists and improving efficiency.

Keywords: telemedicine, ophthalmology (MeSH), rural health services, indigenous health services, quality of health care (MeSH), artificial intelligence

OPEN ACCESS

Edited by:
Daniel Ting,
Singapore National Eye Centre, Singapore

Reviewed by:
Luigi Fontana,
IRCCS Local Health Authority of Reggio Emilia, Italy

***Correspondence:**
Angus W. Turner
angus.turner@gmail.com

Specialty section:
This article was submitted to Ophthalmology, a section of the journal Frontiers in Medicine

Received: *14 December 2021*
Accepted: *15 February 2022*
Published: *11 March 2022*

Citation:
Chia MA and Turner AW (2022) Benefits of Integrating Telemedicine and Artificial Intelligence Into Outreach Eye Care: Stepwise Approach and Future Directions. Front. Med. 9:835804. doi: 10.3389/fmed.2022.835804

INTRODUCTION

The delivery of equitable eye services for rural and remote communities represents a unique challenge to healthcare providers. Within Western Australia (WA), the integration of teleophthalmology into service delivery has played a pivotal role in addressing these challenges. Lions Outback Vision was established in 2010 at the Lions Eye Institute in Perth and now serves 51 communities with visiting optometry and/or ophthalmology. This article presents an overview of our journey toward the development of an integrated teleophthalmology model over the past decade, with a focus on the key lessons for building an effective telemedicine service. Beyond telemedicine, we consider the role of recent advancements in artificial intelligence (AI) and the pathway toward harnessing this technology for more equitable service provision in under-resourced settings. Finally, we make the case that outreach telemedicine models may be translated into urban areas to address the problem of burgeoning surgical waitlists. The coronavirus 2019 (COVID-19) pandemic has accelerated telemedicine capabilities across the globe and catapulted its applications beyond traditional geographic barriers to healthcare.

TELEMEDICINE INTEGRATION FOR OUTREACH EYE CARE

With an area of 2.65 million square kilometers, the state of WA would feature within the top 10 countries by size worldwide. Ninety percent of the population live within the southwest corner of the state, centered around the capital city where all tertiary services are located. The remaining population is scattered sparsely across outback WA, representing a significant challenge for eye care providers. Remote health services are frequently affected by high staff turnover, impacting on long-term stability. Furthermore, rural areas have a high proportion of Indigenous patients compared to metropolitan areas. Patient rurality and Indigenous status are both associated with a higher burden of vision impairment coupled with reduced access to eye care services (1).

Given the unique demography of WA, teleophthalmology has been a key and growing service element within Lions Outback Vision through both real-time videoconferencing and "store and forward" modalities **(Figure 1)**. In 2021, 25% (n = 1,825) of all ophthalmology appointments at our service were conducted though telemedicine. During face-to-face outreach specialist visits, 62% (n = 3,442) of appointments required specialist procedural management, representing a highly efficient clinical triage through collaboration with optometrists. The ability to waitlist surgical patients via videoconference at the time of primary-care assessment eliminates the waiting time for the initial specialist appointment with attendant logistical and cost implications. Moreover, teleophthalmology can also be delivered safely utilizing the correct expertise and case-selection, with a systematic review finding that diagnostic accuracy for real-time teleophthalmology was comparable to face-to-face consultation (2).

We believe that our experience in delivering real-time videoconference consults over the last decade may provide useful lessons for similar regions around the world. Through our history of service delivery, we have identified several key lessons in our journey. These include: 1) a focus on coordination of services at both regional and local community levels, 2) engagement with government funding agencies to align telemedicine-related financial incentives with the benefits they deliver, and 3) reducing barriers to telemedicine uptake through a range of service modifications, education, and support initiatives.

Coordination of Eye Services

Coordination between ophthalmology and optometry has been identified as an essential part of delivering effective outreach eye care. A cross-sectional case study of rural eye services in Australia demonstrated that higher levels of integration between optometrists and ophthalmologists led to improved surgical case rates, with trends toward increased clinical activity and reduced wait times (3). The primary screening and triage provided by optometrists funneled more patients with a higher concentration of pathology requiring procedural intervention to the limited number of specialist visits. Important elements of coordination were highlighted including: 1) service integration with optometry services to facilitate primary screening and triage, 2) involvement of local health staff such as Aboriginal Health Workers to support patient attendance, and 3) appointment of a Rural Eye Health Coordinator (REHC) to liaise between primary healthcare, regional hospitals, and visiting eye services.

In 2011, Lions Outback Vision implemented real-time videoconference teleophthalmology services that linked patients to an ophthalmologist and was facilitated by their primary healthcare provider. To build an evidence base, we conducted a series of studies designed to evaluate our service and found that several of the themes highlighted above regarding eye service coordination were also critical for telemedicine. A prospective clinical audit of 100 telemedicine consultations showed that 60% of referrals emanated from optometrists, despite there being no reimbursement for referral at that time, and the remainder of the referrals were generated from general practitioners (4). A survey of 109 patients who took part in telemedicine consultations found a high level of satisfaction, with 94% of patients indicating they were "satisfied" or "very satisfied" (5). Qualitative analysis of the factors contributing to satisfaction revealed that familiarity with staff at the patient-end was important, in part making up for any perceived impersonality due to the absence of face-to-face interaction. This again highlights the essential part that local community staff play in facilitating effective teleophthalmology.

The key role of REHCs has been demonstrated within our diabetic retinopathy screening program, which operates using a store-and-forward model (6). Following a period of declining screening activity in WA's Kimberley region, an REHC was appointed with the aim of providing high-level support for retinal screening and staff training. A retrospective audit comparing the period before and after the REHC's appointment showed an increase in screening coverage from 9 to 30%, with the number of screening sites increasing from 4 to 17 (6). This illustrates the positive impact that regional coordination can have on the effective delivery of teleophthalmology.

Alignment of Funding Incentives

A high degree of engagement with government funding bodies has been critical to the success of our telemedicine program, with the aim of ensuring that reimbursement sustains services and reflects the costs of high-quality service delivery. In 2011, the Commonwealth government introduced Medicare funding for both the referring doctor and specialist, with ∼50% loading above equivalent face-to-face visits to reflect the additional resources required for telemedicine consults. Limited reimbursement in the United States is a frequently cited reason for reduced uptake of teleophthalmology (7). In 2019, only 10 of 50 states had payment parity between telemedicine and office visits (7). In response to COVID-19, telemedicine was made more widely available through reimbursement at the same rate as in-person visits regardless of setting. Similarly, in Australia regulations have been temporarily relaxed to include funding for audio-only consultations as well as metropolitan settings.

Despite the introduction of sustainable funding, telemedicine uptake in WA was initially low, falling 74% below government targets in the first year that incentives became available (8). Our group conducted an analysis of structural and economic drivers within WA eye care services with the aim of increasing the impact

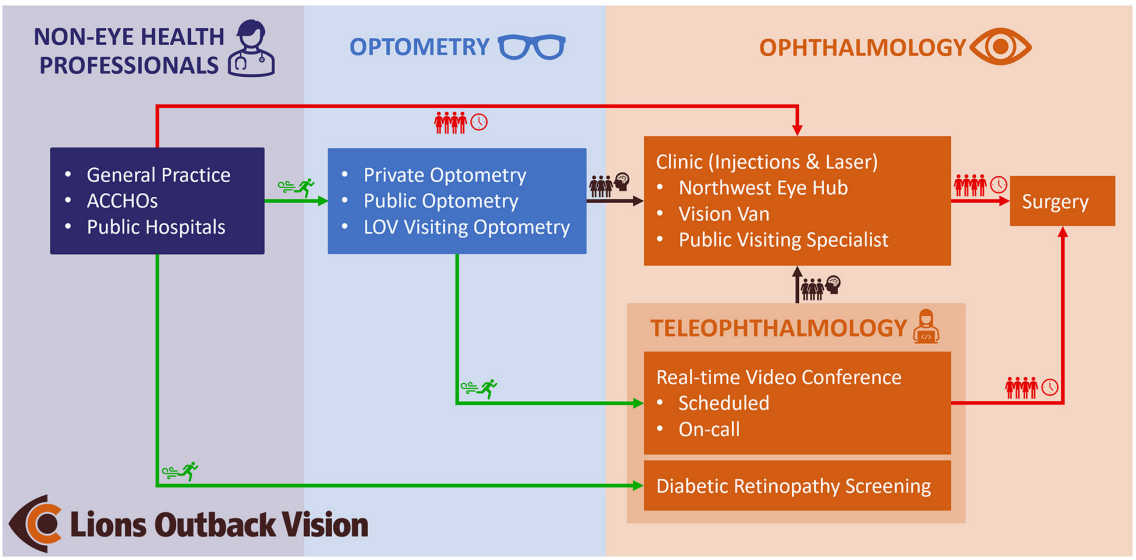

FIGURE 1 | Clinical pathway demonstrating the role of teleophthalmology within Lions Outback Vision. Teleophthalmology enables fast-track access (green) for patients to specialist care compared to traditional referral pathways which are congested (red). By diverting referrals from non-eye care professionals via optometry and diabetic retinal screening, specialist clinics can manage well-triaged pathology (brown). ACCHOs, Aboriginal Community Controlled Health Organizations; LOV, Lions Outback Vision.

of teleophthalmology in Australia (9). Based on clinical audits of 5,456 eye visits, an estimated 15% of urgent transfers and 24% of outreach consultations were assessed as being suitable for telemedicine, leading to an estimated annual cost-saving of $1.1 million. Additionally, to determine the initial capital expenditure required to facilitate basic teleophthalmology, we conducted a survey of ocular diagnostic and teleconference equipment available at optometrists, primary-care practices, and hospitals. Setup costs for primary-care practices were estimated at $20,500, compared to negligible costs for already well-equipped optometry practices.

Based on this finding, along with the reduced need for further eye-specific clinical training for optometrists, we concluded that facilitating optometrist-led teleophthalmology provided the most compelling economic case. A strategy document was created with recommendations for teleophthalmology in Australia and submitted to the Royal Australian and New Zealand College of Ophthalmologists and Optometry Australia. Amongst other strategic initiatives, successful advocacy resulted in the approval of new Medicare codes for optometrist-led rural telemedicine referrals in 2015. In the first year following approval, Lions Outback Vision received 709 teleophthalmology referrals facilitated by optometrists (10).

Addressing Barriers to Telemedicine Uptake

Despite the demonstrated benefits of telemedicine, there are numerous barriers that can limit widespread uptake. In addition to the financial barriers previously outlined, there are also a range of technical and logistical obstacles. Taking a proactive approach to addressing these challenges has been critical to developing our service model. We found that introducing a multi-faceted intervention increased teleophthalmology uptake at our service (11). Key elements of this intervention included awareness raising, educational resources, logistical support, an updated online booking system, and a funding mechanism to simulate Medicare payments prior to government implementation.

In the United States, restrictions on permitted videoconferencing software emerged as an important barrier to telemedicine uptake in the context of COVID-19 (7). In response, the Centers for Medicare and Medicaid Services removed penalties for technologies that were previously considered non-compliant, such as Facetime, Skype, and Google Hangout. In contrast, these types of technologies have been used for telemedicine in Australia since 2011. Our existing service remains agnostic to videoconference platforms in order to minimize barriers for the referrer. Multiple audits of our service have shown that freely available voice-over-Internet-Protocol services such as Skype and Facetime are commonly chosen by referrers, supporting the idea that familiarity and useability are critical factors (10, 11).

Scheduling three parties (patient, referrer and specialist) for synchronous telemedicine relies on availability and timeliness of participants to ensure minimal disruption to clinical workflow. In 2017, our service introduced on-call teleophthalmology services to complement the existing online booking system. When an optometrist is visiting a community or a patient has traveled a significant distance for an assessment, there is limited opportunity for a scheduled future telemedicine appointment. This alternative provided immediate access to the ophthalmologist, resulting in improved access for rural and Indigenous patients. A clinical audit showed that the proportion

of Indigenous patients in the on-call telemedicine cohort was 51.4%, compared to 8.7% in the online-booking telemedicine group (12). We found similar improvements in access for the most remote regions of WA, with 79.0% in the on-call service compared to 26.1% in the online-booking cohort. Of all telemedicine consultations in 2018, 27.8% made use of the on-call service, demonstrating high demand for the more flexible booking arrangement.

BEYOND TELEMEDICINE: THE ROLE OF AI IN RURAL EYE CARE

Rapid progress in AI technology has attracted interest due to its potential to perform complex medical tasks with supra-human performance. Deep learning is a type of AI utilizing multiple processing layers to learn representation of data with multiple levels of abstraction (13). Deep learning is particularly well-suited to image analysis tasks; hence, image-driven specialties like ophthalmology have become the frontrunners for medical AI. Advances in AI hold promise in helping bridge the widening gap between population eye care needs and trained human resources to meet these needs, particularly for underserved rural communities. A well-known limitation of AI is the tendency for algorithms to generalize poorly outside their research milieu (14). AI systems must therefore be trained on data from diverse populations and then rigorously validated within their intended settings.

Autonomous Diabetic Retinopathy Screening

Ophthalmic AI applications exist for numerous conditions, most commonly for diabetic retinopathy (DR), glaucoma, and age-related macular degeneration (AMD) (13). DR represents a growing burden for outreach eye services due to increasing prevalence, requirement for expensive imaging equipment, and the need for regular specialist intervention for optimal outcomes. It is therefore reassuring that much of the most promising progress toward real-world AI implementation has been for autonomous DR screening. Currently, two autonomous DR screening systems have been approved for use by Food and Drug Administration, following pivotal trials showing strong performance in real-world settings (15, 16). Both studies were conducted in the United States within majority white populations.

Our group was recently involved with a real-world validation study of a separate autonomous DR screening system evaluating 236 diabetic patients from Aboriginal Medical Services and endocrinology outpatient clinics (17). In addition to identifying referable DR, the system was also designed to screen for AMD and glaucoma, although performance was only assessed for DR screening. The system achieved a sensitivity and specificity of 96.9 and 87.7%, respectively, in detecting referable DR. Apart from investigating an at-risk ethnic group, other novel aspects of the study included: 1) the use of an offline AI system rather than a cloud-based system, as the latter is a notable barrier in some rural settings, 2) use of several types of retinal camera, and 3) evaluation of patient and clinician acceptability, which is frequently cited as a major limitation to AI uptake. Of 207 participants who completed a satisfaction questionnaire, 93.7% stated that they were either "satisfied" or "extremely satisfied". Clinicians most frequently noted that the AI system was easy to use, and that the real-time diagnostic report was helpful.

Research Potential at Australia's First Remote Eye Center

Despite the progress of ophthalmic AI applications, further study is required to ensure that AI technology delivers benefit to patients. In 2021, Lions Outback Vision opened the Northwest Eye Hub in the remote Kimberley town of Broome. As Australia's first permanent dedicated eye center located in a remote region, it holds significant potential for furthering AI research in this high-risk but under-studied population. Our decade-long history of working in partnership with local community leaders and health organizations means we are well-positioned to develop further collaborative research partnerships. The hub is equipped with state-of-the-art diagnostic equipment, which, in many cases, surpasses that of tertiary eye clinics. The center is staffed by two full-time ophthalmologists and a range of other health staff including Aboriginal Health Workers and optometrists. Our team is currently engaged in several AI projects focusing on DR screening, detecting macular edema, (18) and analyzing optical coherence tomography angiography linking systemic risk factors.

TRANSLATIONAL TELEMEDICINE: OUTBACK SOLUTIONS TO BIG CITY PROBLEMS

A significant "hidden" waitlist has been recently highlighted in Australia—the waiting time for initial specialist assessment (19). This pre-specialist assessment waiting time is often not publicly available and yet masks a burden of preventable diseases silently resulting in unknown levels of permanent blindness or unnecessarily prolonged visual impairment. An audit of cataract referrals from two metropolitan public hospitals in New South Wales found that two-thirds of patients were yet to have their initial hospital appointment in the year following referral (20).

The COVID-19 pandemic has elevated telemedicine in the consciousness of all health service providers attempting to bridge barriers to healthcare. The imperative for telemedicine in outback Australia over the last decade and the robust supporting evidence-base can be translated rapidly to urban settings. For eye care in Australia, optometrists represent an accessible, publicly funded, and well-equipped resource to help tackle population eye health needs. Collaborative care models involving community-based optometrists and virtual review by an ophthalmologist using "store-and-forward" telemedicine modalities have been demonstrated for glaucoma and diabetes clinics in Australia, leading to cost-savings and reduced wait times (21, 22). Exploring options for upscaling these models has the potential to further improve the capacity of public eye services.

Synchronous videoconferencing may also be utilized to consent patients for surgical management during their first

in-person contact point with the specialist, as shown within Lions Outback Vision. An audit of outreach surgery found that patients assessed through telemedicine waited half the length of time compared to those assessed in traditional outpatient clinics (23). Urban centers in the United Kingdom have explored comparable models involving community optometrists and telemedicine consultations to enable "one stop cataract surgery," demonstrating similar benefits (24, 25). Adapting these models to the Australian context will require careful consideration to safeguard informed consent, rigorous surgical risk-assessment, and effective use of theater-time, however the benefits warrant further exploration. Telemedicine provides a seamless path from primary care to surgical management, and enables expert medical input where required, establishing a cornerstone to collaborative care.

CONCLUSION

Within WA, integration of teleophthalmology has been a crucial component in enabling Lions Outback Vision to make progress toward equitable eye care delivery. Much of this headway has relied upon establishing collaborative care models with regional optometrists, maximizing the efficiency of in-person specialist visits. Key lessons from our service have the potential to be applied to areas that share similar geographical and logistical challenges. Looking forward, advances in AI have shown promise toward bridging the gap between expanding eye care demands and limited resources; however, further investigation within under-resourced settings is critical to future progress. Finally, following the acceleration of global telemedicine capabilities triggered by COVID-19, lessons from rural services may be applied to urban centers to curb rapidly growing surgical wait lists. There is a clarion call to harness telemedicine advances in collaborative care to preserve sight in both urban and rural settings.

DATA AVAILABILITY STATEMENT

The original contributions presented in the study are included in the article/supplementary material, further inquiries can be directed to the corresponding author.

AUTHOR CONTRIBUTIONS

MC and AT were involved in planning, researching, and drafting the manuscript. The final manuscript was reviewed and approved by both authors.

FUNDING

MC is completing a PhD at University College London funded by a General Sir John Monash Scholarship.

REFERENCES

1. Foreman J, Xie J, Keel S, van Wijngaarden P, Sandhu SS, Ang GS, et al. The prevalence and causes of vision loss in indigenous and non-indigenous Australians: the national eye health survey. *Ophthalmology*. (2017) 124:1743–52. doi: 10.1016/j.ophtha.2017.06.001
2. Tan IJ, Dobson LP, Bartnik S, Muir J, Turner AW. Real-time teleophthalmology versus face-to-face consultation: a systematic review. *J Telemed Telecare*. (2017) 23:629–38. doi: 10.1177/1357633X16660640
3. Turner AW, Mulholland WJ, Taylor HR. Coordination of outreach eye services in remote Australia. *Clin Experiment Ophthalmol*. (2011) 39:344–9. doi: 10.1111/j.1442-9071.2010.02474.x
4. Johnson KA, Meyer J, Yazar S, Turner AW. Real-time teleophthalmology in rural Western Australia. *Aust J Rural Health*. (2015) 23:142–9. doi: 10.1111/ajr.12150
5. Host BK, Turner AW, Muir J. Real-time teleophthalmology video consultation: an analysis of patient satisfaction in rural Western Australia. *Clin Exp Optom*. (2018) 101:129–34. doi: 10.1111/cxo.12535
6. Moynihan V, Turner A. Coordination of diabetic retinopathy screening in the Kimberley region of Western Australia. *Aust J Rural Health*. (2017) 25:110–5. doi: 10.1111/ajr.12290
7. Kalavar M, Hua H-U, Sridhar J. Teleophthalmology: an essential tool in the era of the novel coronavirus 2019. *Curr Opin Ophthalmol*. (2020) 31:366–73. doi: 10.1097/ICU.0000000000000689
8. Turner A, Razavi DH, Copeland S. *Increasing the Impact of Eye Telehealth in Rural and Remote Western Australia*. (2014). Available online at: https://www.outbackvision.com.au/wp-content/uploads/2020/04/increasing-the-impact-of-telehealth-for-eye-care-in-rural-and-remote-western-australia.pdf (accessed December 01, 2021).
9. Razavi H, Copeland SP, Turner AW. Increasing the impact of teleophthalmology in Australia: Analysis of structural and economic drivers in a state service. *Aust J Rural Health*. (2017) 25:45–52. doi: 10.1111/ajr.12277
10. Bartnik SE, Copeland SP, Aicken AJ, Turner AW. Optometry-facilitated teleophthalmology: an audit of the first year in Western Australia. *Clin Exp Optom*. (2018) 101:700–3. doi: 10.1111/cxo.12658
11. O'Day R, Smith C, Muir J, Turner A. Optometric use of a teleophthalmology service in rural Western Australia: comparison of two prospective audits. *Clin Exp Optom*. (2016) 99:163–7. doi: 10.1111/cxo.12334
12. Nguyen AA, Baker A, Turner AW. On-call telehealth for visiting optometry in regional Western Australia improves patient access to eye care. *Clin Exp Optom*. (2020) 103:393–4. doi: 10.1111/cxo.12979
13. Wang Z, Keane PA, Chiang M, Cheung CY, Wong TY, Ting DSW. Artificial intelligence and deep learning in ophthalmology. *Artif Intell Med*. (2021) 1–34. doi: 10.1007/978-3-030-58080-3_200-1
14. Ting DSW, Pasquale LR, Peng L, Campbell JP, Lee AY, Raman R, et al. Artificial intelligence and deep learning in ophthalmology. *Br J Ophthalmol*. (2019) 103:167–75. doi: 10.1136/bjophthalmol-2018-313173
15. Abràmoff MD, Lavin PT, Birch M, Shah N, Folk JC. Pivotal trial of an autonomous AI-based diagnostic system for detection of diabetic retinopathy in primary care offices. *Npj Digit Med*. (2018) 1:1–8. doi: 10.1038/s41746-018-0040-6
16. Ipp E, Liljenquist D, Bode B, Shah VN, Silverstein S, Regillo CD, et al. Pivotal evaluation of an artificial intelligence system for autonomous detection of referrable and vision-threatening diabetic retinopathy. *JAMA Netw Open*. (2021) 4:e2134254. doi: 10.1001/jamanetworkopen.2021.34254
17. Scheetz J, Koca D, McGuinness M, Holloway E, Tan Z, Zhu Z, et al. Real-world artificial intelligence-based opportunistic screening for diabetic retinopathy in endocrinology and indigenous healthcare settings in Australia. *Sci Rep*. (2021) 11:15808. doi: 10.1038/s41598-021-94178-5
18. Liu X, Ali TK, Singh P, Shah A, McKinney SM, Ruamviboonsuk P, et al. Deep learning to detect optical coherence tomography-derived diabetic macular edema from retinal photographs: a multicenter validation study. *Ophthalmol Retina*. (2022) : doi: 10.1016/j.oret.2021.12.021. [Epub ahead of print].

19. Huang-Lung J, Angell B, Palagyi A, Taylor H, White A, McCluskey P, et al. The true cost of hidden waiting times for cataract surgery in Australia. *Public Health Res Pract*. (2021) doi: 10.17061/phrp31342116. [Epub ahead of print].
20. Do VQ, McCluskey P, Palagyi A, Stapleton FJ, White A, Carnt N, et al. Are cataract surgery referrals to public hospitals in Australia poorly targeted? *Clin Experiment Ophthalmol*. (2018) 46:364–70. doi: 10.1111/ceo.13057
21. Ford BK, Angell B, Liew G, White AJR, Keay LJ. Improving patient access and reducing costs for glaucoma with integrated hospital and community care: a case study from Australia. *Int J Integr Care*. (2019) 19:5. doi: 10.5334/ijic.4642
22. Tahhan N, Ford BK, Angell B, Liew G, Nazarian J, Maberly G, et al. Evaluating the cost and wait-times of a task-sharing model of care for diabetic eye care: a case study from Australia. *BMJ Open*. (2020) 10:e036842. doi: 10.1136/bmjopen-2020-036842
23. McGlacken-Byrne A, Turner AW, Drinkwater J. Review of cataract surgery in rural north Western Australia with the Lions Outback Vision. *Clin Experiment Ophthalmol*. (2019) 47:802–3. doi: 10.1111/ceo.13481
24. Gaskell A, McLaughline A, Young E, McCristal K. Direct optometrist referral of cataract patients into a pilot 'one-stop'cataract surgery facility. *J R Coll Surg Edinb*. (2001) 46:1.
25. Dhillon N, Ghazal D, Harcourt J, Kumarasamy M. A proposed redesign of elective cataract services in Scotland – pilot project. *Eye*. (2021) 1–6. doi: 10.1038/s41433-021-01810-9

Conflict of Interest: The authors declare that the research was conducted in the absence of any commercial or financial relationships that could be construed as a potential conflict of interest.

Publisher's Note: All claims expressed in this article are solely those of the authors and do not necessarily represent those of their affiliated organizations, or those of the publisher, the editors and the reviewers. Any product that may be evaluated in this article, or claim that may be made by its manufacturer, is not guaranteed or endorsed by the publisher.

frontiers in Medicine

SYSTEMATIC REVIEW
published: 29 March 2022
doi: 10.3389/fmed.2022.857200

Effects of Combined Cataract Surgery on Outcomes of Descemet's Membrane Endothelial Keratoplasty: A Systematic Review and Meta-Analysis

Kai Yuan Tey[1,2], *Sarah Yingli Tan*[2], *Darren S. J. Ting*[3,4], *Jodhbir S. Mehta*[1,5,6] *and Marcus Ang*[1,5,6]*

[1] Singapore Eye Research Institute, Singapore, Singapore, [2] Tasmanian Medical School, University of Tasmania, Hobart, TAS, Australia, [3] Academic Ophthalmology, Division of Clinical Neuroscience, University of Nottingham, Nottingham, United Kingdom, [4] Department of Ophthalmology, Queen's Medical Centre, Nottingham, United Kingdom, [5] Singapore National Eye Center, Singapore, Singapore, [6] Duke-National University Singapore Graduate Medical School, Singapore, Singapore

OPEN ACCESS

Edited by:
Jorge L. Alió Del Barrio,
Miguel Hernández University of Elche, Spain

Reviewed by:
Jose Luis Guell,
Instituto de Microcirugía Ocular, Spain
Luis Fernández-Vega-Cueto,
Fernández-Vega Ophthalmological Institute, Spain
Asaf Achiron,
Tel Aviv University, Israel

***Correspondence:**
Marcus Ang
marcus.ang@snec.com.sg

Specialty section:
This article was submitted to Ophthalmology, a section of the journal Frontiers in Medicine

Received: 18 January 2022
Accepted: 04 March 2022
Published: 29 March 2022

Citation:
Tey KY, Tan SY, Ting DSJ, Mehta JS and Ang M (2022) Effects of Combined Cataract Surgery on Outcomes of Descemet's Membrane Endothelial Keratoplasty: A Systematic Review and Meta-Analysis. Front. Med. 9:857200. doi: 10.3389/fmed.2022.857200

Objective: A systematic review and meta-analysis of literature-to-date regarding the effects of combined cataract surgery on outcomes of DMEK.

Methods: Multiple electronic databases were searched, including Cochrane Library databases, PubMed, Web of Science, and ClinicalTrials.gov. The final search was updated on 10th February 2022. We included randomized controlled trials (RCTs), non-randomized studies and large case series (≥25 eyes) of DMEK (pseudophakic/phakic) and "triple DMEK". A total of 36 studies were included in this study. Meta-analyses were done with risk differences (RD) computed for dichotomous data and the mean difference (MD) for continuous data via random-effects model. Primary outcome measure: postoperative re-bubbling rate; secondary outcome measures: complete/partial graft detachment rate, best-corrected visual acuity (BCVA), endothelial cell loss (ECL), primary graft failure, and cystoid macular edema (CMO).

Results: A total of 11,401 eyes were included in this review. Based on non-randomized studies, triple DMEK demonstrated a better BCVA at 1-month postoperative than DMEK alone (MD 0.10 logMAR; 95% CI: 0.07–0.13; $p < 0.001$), though not statistically significant at 3–6 months postoperative (MD 0.07 logMAR; 95% CI: −0.01 to 0.15; $p = 0.08$). There was no significant difference in rebubbling, ECL, graft failures, and CMO postoperatively between the two groups ($p = 0.07$, $p = 0.40$, 0.06, and 0.54 respectively).

Conclusion: Our review suggests that DMEK has a similar post-operative complication risk compared to "triple DMEK" (low-quality evidence), with comparable visual outcome and graft survival rate at 6 months postoperative. High-quality RCTs specifically studying the outcomes of combined vs. staged DMEK are still warranted.

Systematic Review Registration: https://www.crd.york.ac.uk/prospero/display_record.php?ID=CRD42020173760, identifier: CRD42020173760.

Keywords: DMEK, cataract surgery, systematic review & meta-analysis, staged surgery, combined surgery, Descemet's membrane endothelial keratoplasty

INTRODUCTION

Cataract surgery is the most commonly performed elective surgery in the world, with >10 millions of cases being carried out each year (1). In addition, age-related corneal endothelial diseases (e.g., Fuchs endothelial corneal dystrophy; FECD) are common causes of visual impairment, and represent a leading indication for corneal transplantation (2–4). Therefore, with the aging global population, it is becoming increasingly common for patients to require treatment for co-existing age-related ocular diseases such as cataract and FECD.

FECD can lead to endothelial cell loss (ECL) with resultant corneal edema, ocular discomfort, and visual impairment (5). Once corneal decompensation sets in, corneal transplant serves as the mainstay of treatment for restoring the vision (6). In recent years, selective endothelial keratoplasty (EK) has been the treatment choice for managing corneal endothelial diseases (3, 4, 7). In EKs, the donor corneal tissue is inserted, and positioned against the posterior surface of the host cornea (8–10). In particular, Descemet's membrane endothelial keratoplasty (DMEK) involves the use of a manually prepared partial-thickness donor cornea containing only endothelium and Descemet membrane (11–13). DMEK has been shown to have superior postoperative visual acuity and lower graft rejection rate (14–17). Despite the established benefits, the adoption of DMEK is gaining popularity albeit slowly, owing to its steep surgical learning curve (16, 18–20).

The approach in managing a concomitant cataract with FECD can be done in various ways. One of the commonest approaches is to perform a combined DMEK and cataract surgery (i.e., "triple DMEK"). When compared to a staged DMEK procedure (i.e., cataract surgery followed by DMEK, or DMEK followed by cataract surgery), "triple DMEK" offers advantages such as improved cost-effectiveness, better intraoperative corneal clarity (due to simultaneous removal of the diseased and thickened endothelium and elimination of the risk of post-cataract surgery-induced corneal edema) and comparable clinical outcomes (8, 21). It was however also found that "triple DMEK" may be associated with a higher rate of postoperative complications such as graft detachment requiring postoperative re-bubbling (22–24). Overall, there is no consensus on whether to stage or combine DMEK with cataract surgery in patients who present with visually significant cataracts and FECD.

Thus, we performed a systematic review to appraise and compare the published evidence on the surgical outcomes of DMEK and "triple DMEK" procedures, which could help inform the future clinical practice on managing patients with co-existing corneal endothelial diseases and cataract. As graft detachment requiring postoperative re-bubbling is one of the most complications of DMEK, we have studied this as the main outcome measure of our systematic review.

MATERIALS AND METHODS

Eligibility Criteria for Considering Studies for This Review

We included publications in which the surgical outcomes of DMEK performed for the treatment of corneal endothelial dysfunction were reported. Studies that reported on the outcomes of eyes that had undergone surgeries other than DMEK or "triple DMEK" were excluded from the review. Studies that solely reported on the clinical outcomes of DMEK performed for previous graft failures (including repeat DMEK surgery) or specific high-risk disease groups (e.g., glaucoma, previous glaucoma filtration surgeries, cytomegalovirus retinitis, herpes simplex virus) were excluded. There were no restrictions on age, gender, or ethnic group. To avoid any duplication of the reporting of similar study populations, where the same group of investigators published several studies, earlier smaller studies were excluded if more recent larger studies reporting the same outcome measures were available. We included all randomized controlled trials (RCTs), non-randomized studies, and large prospective and retrospective case series ($n \geq 25$ eyes). Small case series (<25 eyes), letter, reviews, published abstracts, and laboratory-based studies were excluded from this review. The main outcome measure was the postoperative re-bubbling rate (at 0–6 months). Secondary outcome measures included graft detachment (including partial and complete detachment at 0–6 months), BCVA (at 1–6 months; in logarithm of the minimum angle of resolution, logMAR), graft failure (at 1–6 months), ECL (at 1–6 months), and cystoid macular edema (CME; at 1–6 months). Analysis of the literature and writing of the manuscript were performed in accordance with the Preferred Reporting Items for Systematic Reviews and Meta-Analyses (PRISMA) guidelines (http://www.prisma-statement.org/).

Search Methods for Identifying Studies

We conducted a literature search in multiple electronic databases, including Cochrane Library databases, PubMed, Web of Science, and ClinicalTrials.gov (www.clinicaltrials.gov). We did not set any restrictions on the date, language, or publication status in our electronic search. The search strategies for the relevant databases can be found in **Supplementary Appendix 1**. We also performed manual searches by reviewing the reference lists of relevant reports and reviews. The final search was updated on 10th February 2022. The protocol was registered at the Prospective Register for Systematic Reviews (PROSPERO; registration number: CRD42020173760). Distiller Systematic

Review (DSR) was used to manage the records identified and eligibility status.

Study Selection

The reviewers (K.Y.T and M.A) independently screened the titles and abstracts. Full reports of all titles that met the inclusion criteria or where there was uncertainty were obtained. Reviewers (K.Y.T and S.Y.T) then screened the full-text reports and additional information from the original investigators were sought after where necessary to resolve questions about the eligibility. We resolved any disagreement through discussion and any unresolved discussion was adjudicated by M.A. Reasons for excluding studies were recorded.

Data Collection and Risk of Bias Assessment

The following details of each study were extracted for this review: study participants' characteristics, location of study, study design, DMEK sub-groups, funding support (if any), and surgical outcome measures. Data on the following surgical outcome measures were included: re-bubbling rate, best-corrected visual acuity (BCVA), postoperative ECL, and complications including graft detachment. If only absolute numbers of the EC count were described, ECL was calculated by the method described by Hwang et al. (25). For descriptive and analytic purposes, visual outcome reported in Snellen visual acuity (VA) was converted to the respective logMAR (26). All outcome measures were ordinal data, except for mean BCVA and mean ECL (continuous data). The preferred unit of analysis was outcomes for eyes rather than individuals as some individuals had unilateral treatment or different treatments in each eye. For results that were reported in median, range and/or interquartile range, the mean and standard deviation were calculated using the method described by Luo et al. (27) and Wan et al. (28). Missing data were dealt per protocol, which is available in **Supplementary Appendix 2**.

Risk of bias was assessed by two authors (K.Y.T and S.Y.T) independently and any disagreement was adjudicated by M.A. Included randomized controlled trials (RCT) were assessed for risk of bias using Chapter 8 of the Cochrane Handbook for Systematic Reviews of Intervention (29). For non-randomized studies, we utilized the tool—Risk of Bias in non-randomized Studies—of Intervention (ROBINS-I) to evaluate the risk of bias in estimates (30). The study design of each article was also assessed and rated according to its level of evidence using a rating scale adapted from the Oxford Centre for Evidence-based Medicine (31). Funnel plots were analyzed to evaluate publication bias and small-study effects.

RCTs were judged for the selection bias, performance bias, detection bias, attrition bias, reporting bias and other sources of bias. Non-randomized studies were judged for confounding bias, selection bias, bias in classification of interventions, bias in deviation from intended interventions, bias due to missing data, bias in measurement of outcome and bias in selection of the reported results. Non-comparative case series was not assessed for risk of bias in view of the inherent high risk of bias.

Quality of evidence of each study was assessed by one author (K.Y.T) using the Grading of Recommendations Assessment, Development and Evaluation (GRADE) tool (32). Each study was graded as either high, moderate, low or very low based on the study design, study limitations, consistency of results, directness of evidence, precision, treatment effect and reporting bias.

Data Synthesis and Analysis

A meta-analysis was performed if there were sufficient similarities in the reporting of outcome measures in different studies. The meta-analyses for comparison between both "triple DMEK" and DMEK alone were performed using Review Manager (Version 5.3) by Cochrane. Meta-analyses were done by computing the risk differences for dichotomous data and the mean difference for continuous data using a random-effects model. For single-arm studies (i.e., "triple DMEK" or DMEK alone), the overall effect was studied using Open Meta-Analyst [OpenMetaAnalyst for Windows 8 (64-bit) (built 04/06/2015) by Brown University]. Random-effects model was used in view of the anticipated heterogeneity in study design, patient cohort and surgical aspects (including surgeon's experience and surgical technique). Where zeros caused problems with the computation of effects or standard errors, 0.5 was added to all cells for that study. Statistical heterogeneity (I^2) was defined as mild (0–40%), moderate (30–60%), substantial (50–90%), and considerable (75–100%) (33).

RESULTS

Literature Search and Study Characteristics

The electronic searches yielded a total of 873 records, and 42 additional records were identified through manual hand searching of bibliography (see **Figure 1** for the PRISMA flow diagram). After deduplication, 815 abstracts were screened and a further 683 records were removed. Full-text copies of 132 articles were obtained and reviewed. After excluding 96 ineligible studies, 36 studies (n = 11,401 eyes) were included in this systematic review. These included 17 non-randomized studies comparing DMEK alone to "triple DMEK" (n = 8,304 eyes) with a mean follow-up duration of 12.8 ± 15.9 months (ranged, 6–60 months) (21, 22, 34–48), 14 studies on DMEK (n = 2,609 eyes) with a mean follow-up duration of 20.0 ± 21.9 months (ranged, 3–42 months) (49–62), and five studies on "triple DMEK" (n = 495 eyes) with a mean follow-up duration of 8.0 ± 3.4 months (ranged, 6–12 months) (63–67). Studies included were conducted at The Netherland (12 studies), Germany (nine studies), United States of America (seven studies), Canada (two studies), Egypt (one study), France (one study), Italy (one study), Nepal (one study), Spain (one study), United Kingdom (one study), and a multicenter study (23 countries). The surgical outcomes reported in studies included are summarized in **Supplementary Appendix 3**. Subgroup analysis comparing "triple DMEK" with phakic DMEK or pseudophakic DMEK alone was not possible due to due to limited numbers and heterogeneous study design (21, 34–36, 44).

Level of Evidence, Quality of Evidence and the Risks of Bias of Included Studies

The level of evidence assessed could be found in **Supplementary Appendix 3**. Of all the 17 studies that compared

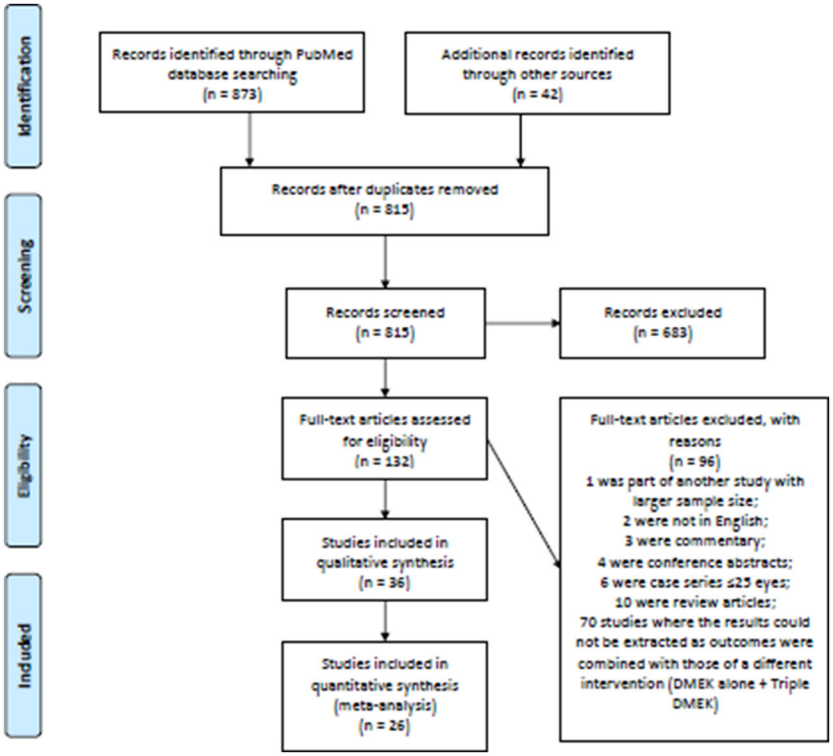

FIGURE 1 | Preferred reporting items for systematic reviews and meta-analyses (PRISMA) flow diagram.

DMEK alone and "triple DMEK", eight (47.1%) were rated as level II evidence, three (17.6%) were rated as level III evidence, and six (35.3%) were rated as level IV evidence. Of all the 14 DMEK alone studies, two (14.3%) were rated as level II evidence and 12 (85.7%) were rated as level IV evidence. Of all the five "triple DMEK" studies, all (100%) were rated as level IV evidence.

Similarly, the quality of evidence assessed could be found in **Supplementary Appendix 3**. Of all the 17 studies that compared DMEK alone and "triple DMEK", nine (52.9%) were graded as moderate quality of evidence and eight (47.1%) were graded as low quality. Of all the DMEK alone studies, 14 (100%) were graded as low quality evidence, and of all the five "triple DMEK" studies, all (100%) were graded as low quality.

Based on all 17 non-randomized studies, the risk of bias assessment considered one (5.9%) study as low risk, 13 (76.5%) studies as moderate risk, and three (17.6%) studies as high risk. **Figure 2** summarizes the judgments of each risk of bias domain presented as overall percentages across all included studies and **Figure 3** summarizes the authors' judgments of each risk of bias item for each included comparative study.

Surgical Outcomes

Summary of the outcomes of meta-analysis of various surgical outcomes could be found in **Table 1** (for non-randomized studies) and **Table 2** (for non-comparative studies).

Postoperative Re-bubbling Rate

Eight comparative studies (n = 2,799 eyes), which included 1,408 DMEK eyes and 1,391 "triple DMEK" eyes, reported the postoperative re-bubbling rate (21, 22, 34, 35, 39, 43, 45, 48), Re-bubbling was reported in 316 (22.4%) DMEK eyes and 381 (27.4%) "triple DMEK" eyes. The meta-analysis demonstrated that there was no statistical difference between DMEK alone and "triple DMEK" in terms of postoperative re-bubbling rate (RD −0.06; 95% CI: −0.13 to 0.00; I^2 = 73%; p = 0.07; **Figure 4A**). Based on the findings of non-comparative studies, the overall re-bubbling rate following DMEK was estimated at 3.9% (95% CI: 1.9–5.8; n = 950 eyes from five studies; **Figure 4B**) (52, 55, 58, 59, 62). No relevant data was available from "triple DMEK" studies.

Graft Detachment

There was insufficient data regarding graft detachment among the comparative studies for meta-analysis. One study, which included 131 DMEK and 101 "triple DMEK" eyes, reported 12.9 and 10.1% of partial and complete graft detachment following DMEK, respectively, whilst there were 10.7 and 11.9% eyes with partial and complete graft detachment following "triple DMEK", respectively, with no statistical difference observed between both groups (p = 0.78) (43).

Amongst the non-comparative DMEK studies, four studies (n = 1,085 eyes) and five studies (n = 1,152 eyes) that reported the rate of complete and partial graft detachments postoperatively respectively (52, 58, 59, 61, 62). The overall rate of complete and

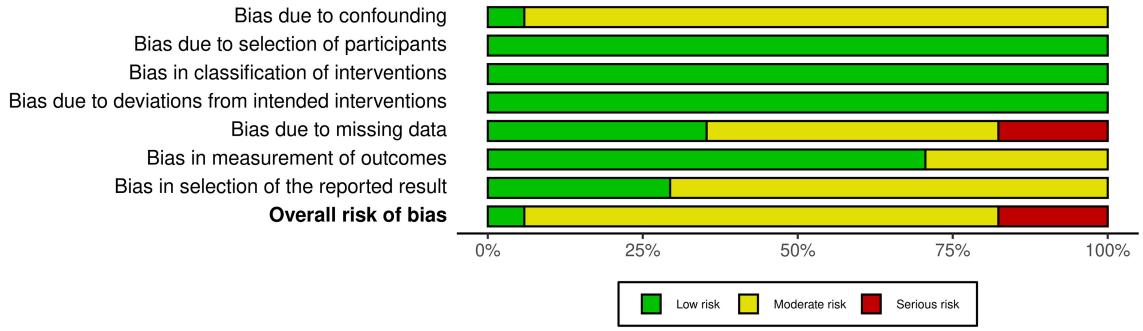

FIGURE 2 | Summary of the judgments of each risk of bias domain presented as percentages across all included studies.

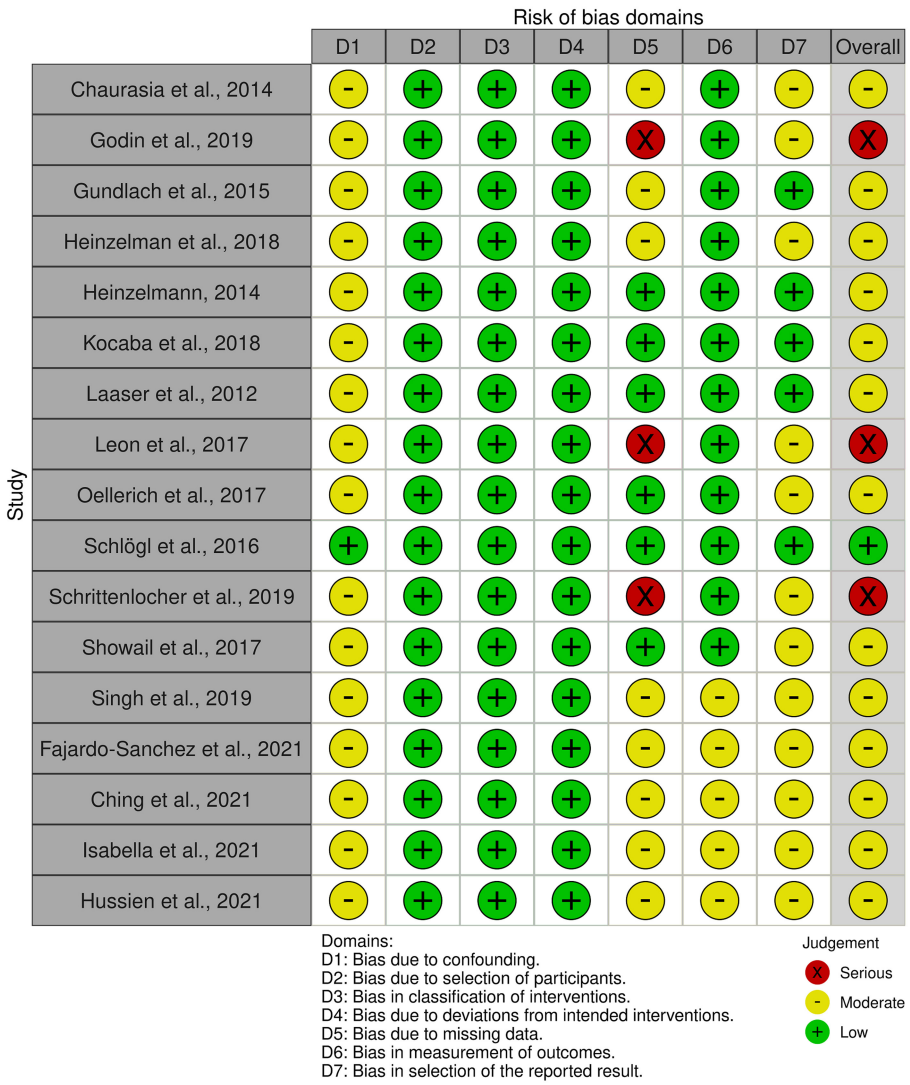

FIGURE 3 | Authors' judgments of each risk of bias item for each included comparative study.

partial graft detachment was 8.3% (95% CI: 4.2–12.4) and 8.3% (95% CI: 5.1–11.5), respectively (**Figures 4C,D**). There was no data on graft detachment amongst the non-comparative "triple DMEK" studies.

TABLE 1 | Summary of meta-analysis result of each surgical outcomes in the non-randomized studies (non-randomized studies).

Surgical outcomes	Number of studies, *n*	Number of eyes included, *n* (DMEK only vs. "triple DMEK")	Effect Measure, MD/RD (95% CI)	I^2, %	*p*-value	Level of evidences
Postoperative re-bubbling rate	8	2,799 (1,408 vs. 1,391)	RD −0.06 (−0.13 to 0.00)	76	0.07	6 Level 2 2 Level 3 2 Level 4
Best corrected visual acuity, LogMAR at 1-month	2	435 (243 vs. 192)	MD 0.10 (0.07–0.13)	0	<0.001	1 Level 2 1 Level 4
Best corrected visual acuity, LogMAR at 3–6 month	5	769 (393 vs. 376)	MD 0.07 (−0.01 to 0.15)	88	0.08	2 Level 2 1 Level 1 2 Level 2
Endothelial cell loss at 3- month	2	154 (60 vs. 94)	MD −3.24 (−9.30 to 2.81)	78	0.29	1 Level 2 1 Level 4
Endothelial cell loss at 6-month	2	297 (142 vs. 155)	MD 2.93 (−3.94 to 9.79)	49	0.40	1 Level 2 1 Level 4
Primary graft failure	7	1,414 (807 vs. 607)	MD 0.01 (−0.02 to 0.05)	34	0.44	4 Level 2 1 Level 3 2 Level 4
Cystoid macular edema	5	1,013 (573 vs. 440)	RD 0.00 (−0.02 to 0.01)	0	0.70	3 Level 2 1 Level 3 1 Level 4
Posterior capsular rupture	2	235 (117 vs. 118)	RD −0.04 (−0.08 to 0.01)	0	0.15	1 Level 2 1 Level 3

DMEK, Descemet's membrane endothelial keratoplasty; MD, mean difference; RD, risk difference.

TABLE 2 | Summary of meta-analysis result of each surgical outcomes in the non-comparative studies.

Surgical outcomes	Number of studies, *n*	DMEK Alone or "triple" DMEK	Number of eyes included *n*	Overall effect (95% CI)	I^2, %
Postoperative re-bubbling rate	6	DMEK Alone	950	3.9% (1.9–5.8)	43
Complete graft detachment	4	DMEK Alone	1,085	8.3% (4.2–12.4)	84
Partial graft detachment	5	DMEK Alone	1,152	8.3 (5.1–11.5)	73
Best corrected visual acuity, LogMAR at 3-month	3	DMEK Alone	107	0.15 (0.10–0.20)	54
Best corrected visual acuity, LogMAR at 6- month	4	DMEK Alone	838	0.15 (0.09–0.22)	97
Best corrected visual acuity, LogMAR at 1-month	3	"Triple" DMEK	123	0.20 (0.12–0.29)	95
Best corrected visual acuity, LogMAR at 3-month	4	"Triple" DMEK	275	0.15 (0.11–0.19)	87
Endothelial cell loss at 6- month	2	DMEK Alone	549	33.1 (24.89–41.25)	92
Cataract development postoperative	7	DMEK Alone	465	13.5% (5.4–21.7)	91

DMEK, Descemet's membrane endothelial keratoplasty.

Best Corrected Visual Acuity

Five comparative studies ($n = 822$ eyes) reported BCVA at 1–6 months postoperatively (21, 35, 42–44). "Triple DMEK" was shown to have a better BCVA compared to DMEK at 1 month postoperative (MD 0.10 logMAR; 95% CI: 0.07–0.13; $I^2 = 0\%$; $p < 0.001$; **Figure 5A**). Whilst the MD of BCVA between "triple DMEK" and DMEK at 3–6 months was insignificant, we however found that the result was highly heterogenous (MD 0.07 logMAR; 95% CI: −0.01 to 0.15; $I^2 = 88\%$; $p = 0.08$; **Figure 5B**).

A total of seven DMEK studies ($n = 692$ eyes) (49, 54, 56, 60, 62, 68), and three "triple DMEK" studies ($n = 275$ eyes) reported BCVA at 1–6 months postoperative (64, 65, 67). The mean BCVA following DMEK was 0.50 logMAR (reported by one study), 0.14 (95% CI: 0.10–0.20) logMAR, and 0.07 (95% CI: 0.09–0.22) logMAR at 1-, 3-, and 6-month postoperative, respectively (**Figures 5C,D**), whereas the mean BCVA following "triple DMEK" was 0.19 (95% CI: 0.12–0.29) logMAR, 0.15 (95% CI: 0.11–0.19) logMAR, and 0.19 logMAR (reported by one study) at 1, 3, and 6 months postoperative, respectively (**Figures 5E,F**).

Endothelial Cell Loss

Three non-randomized studies ($n = 394$ eyes), which included 191 DMEK eyes and 203 "triple DMEK" eyes, reported the ECL at 3–6 months postoperative (35, 42, 43). Based on non-randomized studies, the rate of ECL was similar between DMEK and "triple DMEK" at 3 months postoperative (MD −3.24%; 95% CI: −9.30 to 2.81; $I^2 = 78\%$; $p = 0.29$) and at 6 months postoperative (MD 2.93%; 95% CI: −3.94 to 9.79; $I^2 = 49\%$; $p = 0.40$; **Figures 6A,B**).

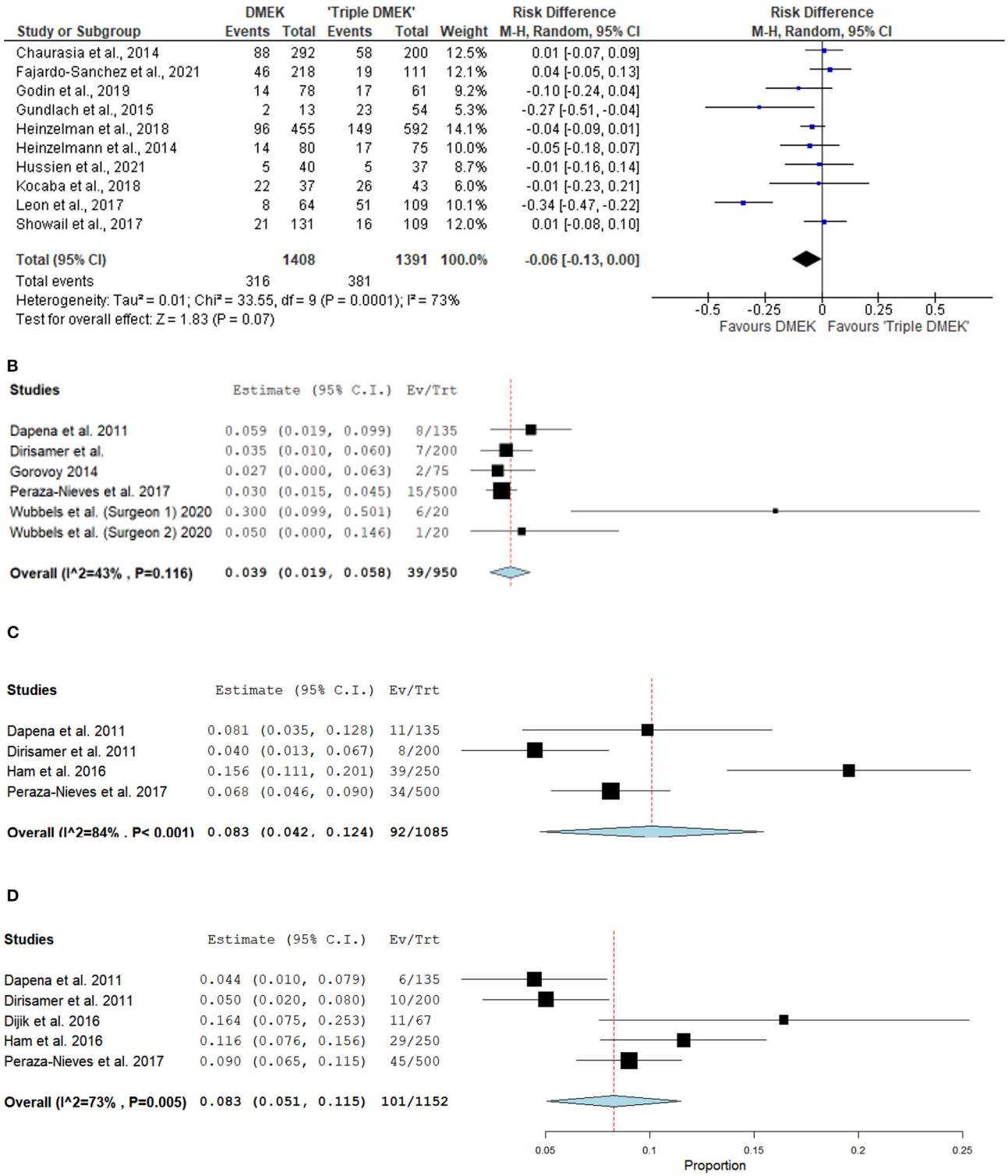

FIGURE 4 | Forest plot of **(A,B)** re-bubbling rates and **(C,D)** graft detachments (complete and partial) in comparative Descemet's membrane endothelial keratoplasty (DMEK) vs. "Triple DMEK" studies (comparative meta-analysis), and non-comparative DMEK alone studies (single-arm meta-analysis).

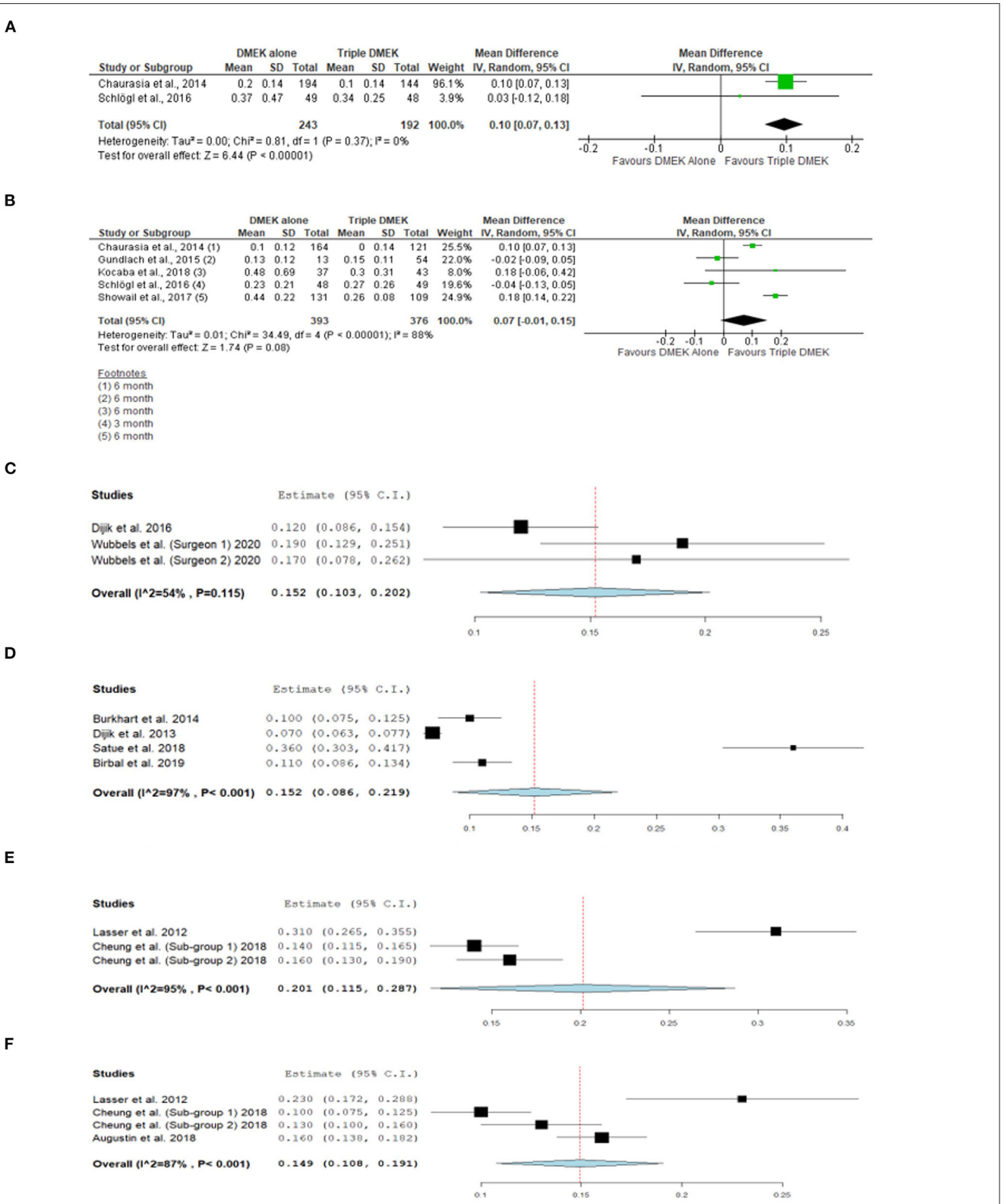

FIGURE 5 | Forest plot of **(A)** 1-month and **(B)** 3–6 month visual outcomes in comparative Descemet's membrane endothelial keratoplasty (DMEK) vs. "Triple DMEK" studies (comparative meta-analysis), and **(C)** 3-month and **(D)** 6-month visual outcomes in non-comparative DMEK, and **(E)** 1-month and **(F)** 3-month visual outcomes "Triple DMEK" studies (single-arm meta-analysis).

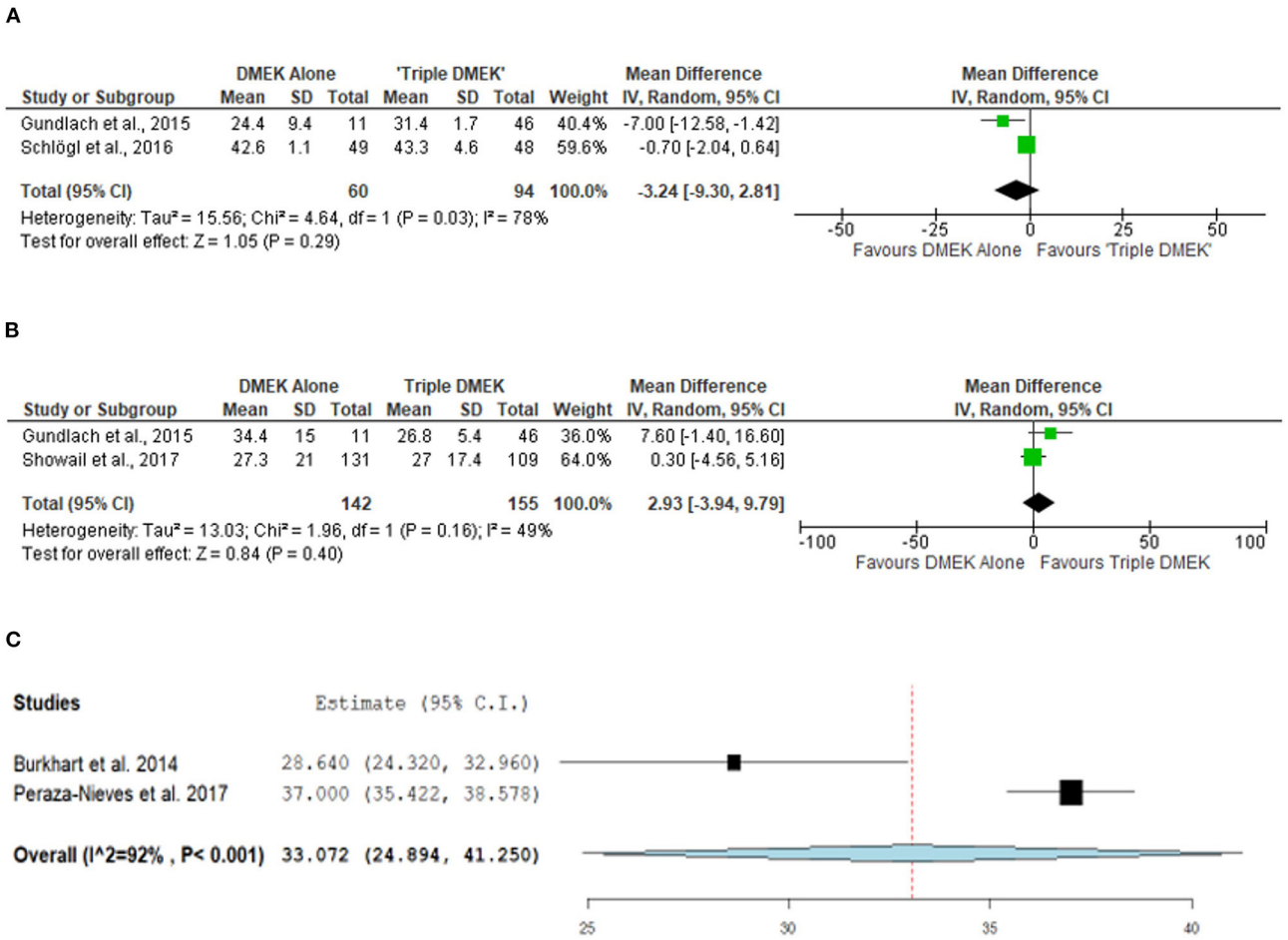

FIGURE 6 | Forest plot of **(A)** 3-month, **(B)** 6-month mean endothelial cell loss (ECL) in comparative Descemet's membrane endothelial keratoplasty (DMEK) vs. "Triple DMEK" studies (comparative meta-analysis), and **(C)** 6-month mean ECL in non-comparative DMEK studies (single-arm meta-analysis).

A total of three DMEK studies (n = 572 eyes) reported the postoperative ECL at 1–6 months postoperative (49, 51, 58). The mean ECL following DMEK was 37% (reported by one study) and 33.1% (95% CI: 24.9–41.3) at 1 and 6 months postoperative, respectively (**Figure 6C**). Data regarding mean ECL was not available in the non-comparative "triple DMEK" studies.

Primary Graft Failure

Seven non-randomized studies (n = 1,414 eyes) reported the primary graft failure rate, which was similar between DMEK and "triple DMEK" (RD 0.01; 95% CI: −0.02 to 0.05; I^2 = 34%; p = 0.44; **Figure 7A**) (21, 34, 35, 43–45, 48). There was no data available regarding primary graft failures among non-comparative DMEK and "triple DMEK" studies.

Cystoid Macular Edema

Five non-randomized studies reported the development of CME postoperatively (21, 36, 44, 46, 48). The risk of CME was similar between DMEK and "triple DMEK" (RD = −0.00; 95% CI: −0.02 to 0.01; I^2 = 0%; p = 0.70; **Figure 7B**). Data regarding CME was not available in the non-comparative DMEK and "triple DMEK" studies.

Other Complications

Amongst the non-randomized studies, two studies reported the development of posterior capsular rupture (PCR) intraoperatively (36, 44). The risk of PCR was similar between DMEK and "triple DMEK" (RD = −0.03; 95% CI = −0.08 to −0.01; I^2 = 0%; p = 0.15; **Figure 7C**). One study with 11 phakic DMEK eyes and 46 "triple DMEK" eyes reported elevated intraocular pressures in 18.2 and 8.7% of the eyes, respectively (35). In addition, 18.2% of the phakic DMEK eyes developed cataracts by 6 months' postoperative (35). Hyphaema were reported in 31% of the DMEK eyes and 49.8% of the "triple DMEK" eyes, with triple DMEK eyes having a 1.5 times (95% CI = 1.2–1.9) higher risk of developing hyphema (38).

For non-comparative DMEK studies, seven studies (n = 465) phakic eyes reported 68 eyes developed cataracts postoperatively (47, 50–52, 58, 59, 68). The overall risk of cataract development

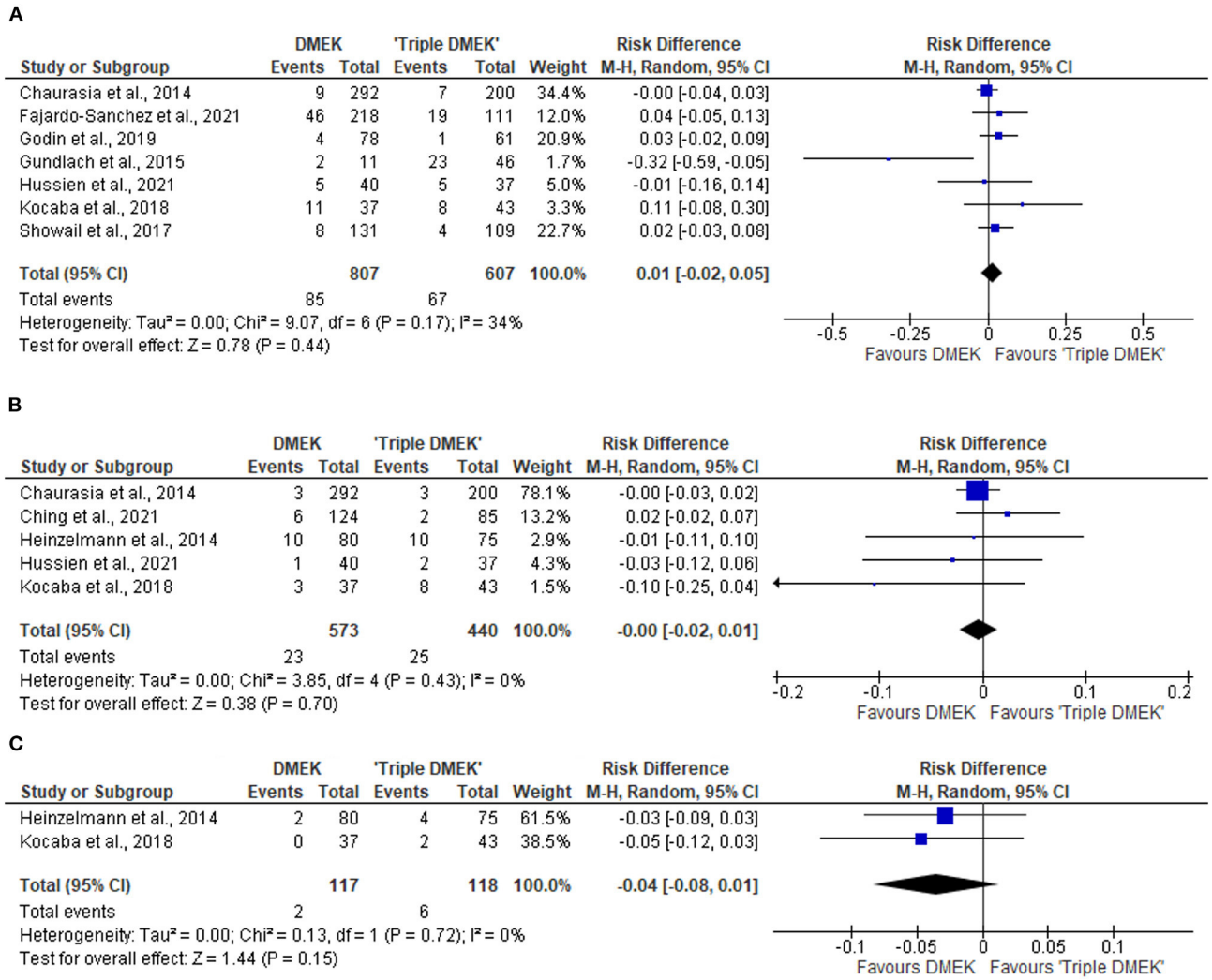

FIGURE 7 | Forest plot of other complications—**(A)** primary graft failures, **(B)** cystoid macular edema (CME), and **(C)** posterior capsular rupture (PCR) in comparative Descemet's membrane endothelial keratoplasty (DMEK) vs. "Triple DMEK" studies (comparative meta-analysis).

was 13.5% (95% CI = 5.4–21.7; **Figure 8A**). Specifically, four studies ($n = 170$ eyes) reported 20 eyes developed cataracts post-operatively within the first year, with an overall risk of 10.0% (95% CI = 0.01–0.20; **Figure 8B**) (49, 50, 52, 59), two studies ($n = 186$) reported 27 at 2 years follow-up with an overall risk of 20.5% in developing cataracts postoperatively (95% CI = −0.174 to 0.584; **Figure 8C**) (47, 58), and one study ($n = 124$) reported 21 at 5-year follow-up (68).

DISCUSSION

In this systematic review, we aimed to compare the surgical outcomes and safety between DMEK alone and "triple DMEK", with 36 studies and 11,401 eyes being included in this review. "Triple DMEK" demonstrated a better BCVA at 1-month postoperative (0.10 logMAR better) than DMEK, albeit non-significant at 3–6 months (0.07 logMAR better, $p = 0.08$). There was no significant difference in the rate of ECL and other postoperative complications such as re-bubbling rate, primary graft failure, CME, and PCR.

Our meta-analysis suggested that DMEK has a comparable rate of postoperative re-bubbling to "triple DMEK" (RD = −0.06; 95% CI: −0.13 to 0.00; $p = 0.07$). Whilst the difference in re-bubbling rate was statistically insignificant, it is important to highlight that there was a substantial heterogeneity ($I^2 = 73\%$) among the included studies. The heterogeneity is likely ascribed to multiple confounding factors such as patient factors (e.g., age, lens status, depth of anterior chamber, and compliance to postoperative management like posturing), indication, surgeon's experience, surgical technique, choice of tamponade agent, and criteria for re-bubbling, amongst others. For instance, Dapena et al. (52) demonstrated that the graft detachment rate of DMEK reduced from 20% in the first 45 cases to 4.4% in the 91–135 cases. In addition, the use of 20% SF_6 for intraocular tamponade

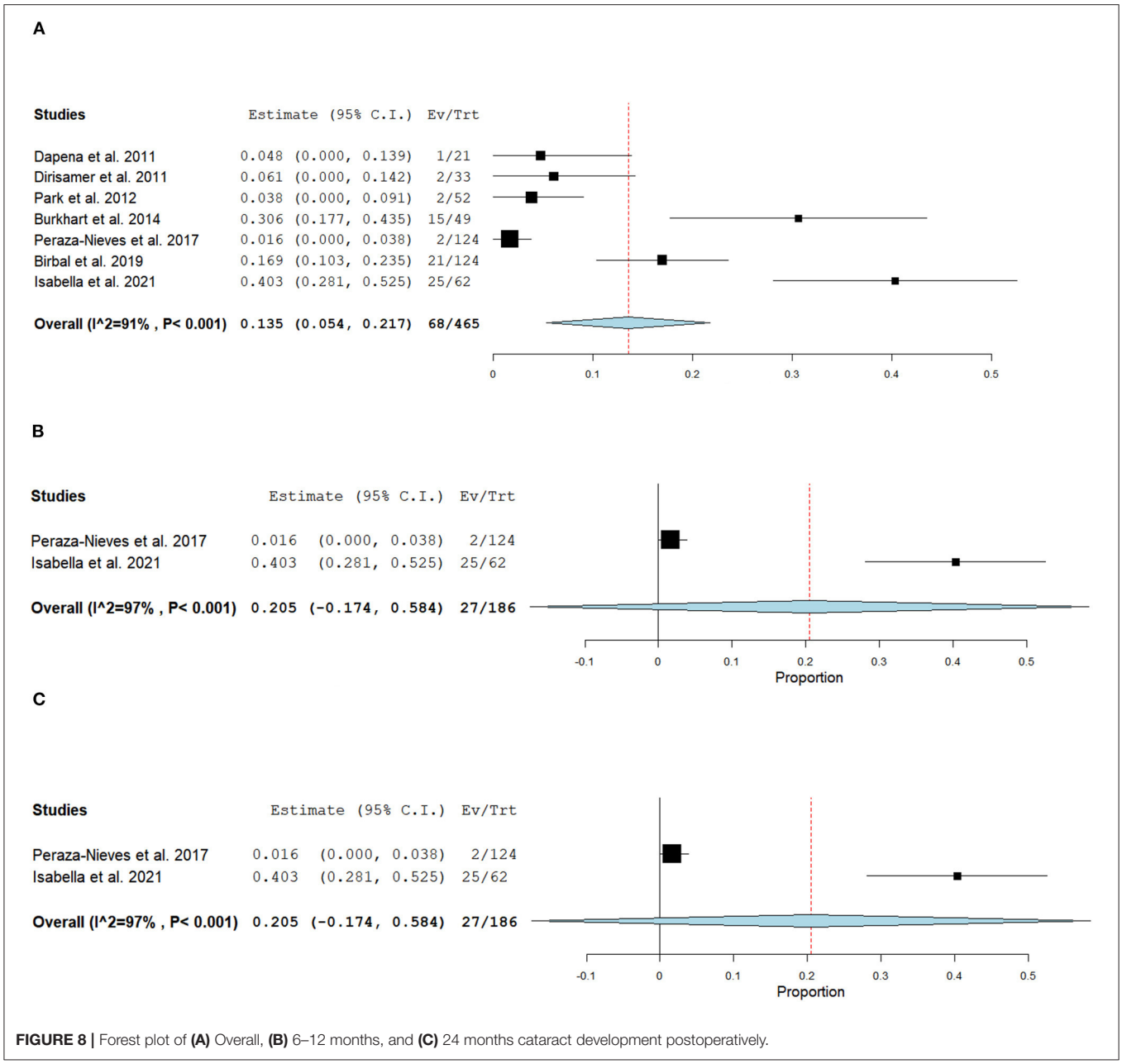

FIGURE 8 | Forest plot of **(A)** Overall, **(B)** 6–12 months, and **(C)** 24 months cataract development postoperatively.

in DMEK has been reported to reduce the rate of partial graft detachment significantly when compared with air (69).

As direct comparative studies were lacking, we performed a meta-analysis of non-comparative DMEK studies to examine the difference in reported graft detachment comparing combined cataract surgery with DMEK and standalone DMEK. We found that in DMEK alone, the overall total and partial graft detachment rates were both 8.2%. Showail et al. reported no significant difference in graft detachment between both approaches (p = 0.78) (43) and similar observations were made by other studies (34, 39, 41). Contrary to that, Leon et al. (22) and Gundlach et al. (35) have identified triple DMEK as an independent risk factor for early graft detachment. These studies, however, do demonstrate significant heterogeneity with various confounders, e.g., age, surgeons' techniques, indications for DMEK and pre-operative lens status (phakic vs. pseudophakic) which may have led to varying outcomes of the studies. Our meta-analyses are also affected by several outliers which may reflect the learning curve of DMEK—e.g. surgeon 1 from Wubbels et al. (62) demonstrated a much higher rate of re-bubbling compared to other studies as the aim of the study was to establish the learning curve from the first 40 consecutive cases of DMEK performed.

In terms of visual outcome, our meta-analysis of existing literature suggests that "triple DMEK" offered better visual outcomes at 1 month postoperative, though non-statistically

significant at 3–6 months postoperative. It is, however, important to note that the visual outcome at 1 month postoperative was based on only two studies, with significant weightage (96%) placed on one study (21). Chaurasia et al. (21) observed that "triple DMEK" resulted in a better BCVA (0.10 logMAR better) than DMEK at 1–6 months postoperative; however their finding was confounded by the higher rate of ocular co-morbidities and non-FECD cases in the latter group. Whilst there was limited long-term BCVA data available, a study by Schlogl et al. (42) evaluated the long-term outcomes of 250 eyes and found no significant difference between both approaches up to 5 years postoperatively. On the other hand, the ECL was shown to be comparable (0.8% difference) between the two approaches at 6 months postoperative, and the similarity was maintained at 5 years postoperative according to one study (42).

It is important to note that of the 17 studies that compared both approaches, four studies did not specify the preoperative lens status of DMEK eyes (39, 41–43), two studies reported a mix of pseudophakic and phakic DMEK surgeries but did not analyze them separately (37, 40). Similarly, Godin et al. (34) have reported a mix of pseudophakic and phakic DMEK surgeries and the group analyzed them independently. Four studies compared "triple DMEK" directly with pseudophakic DMEK surgeries (21, 36, 38, 44), whilst one study compared "triple DMEK" with phakic DMEK (35). These studies concluded that the surgical outcomes are comparable regardless of preoperative lens status and approaches, except for Crew et al. (38) who reported intraoperative hyphema was more common in "triple DMEK" compared to pseudophakic DMEK. Between approaches, both shared similar complication rates in terms of primary graft failure, CME and PCR.

One sequala to phakic DMEK is accelerated cataract progression, which may be secondary to surgical manipulation, air injection and postoperative topical steroid use (35). It was observed that cataract progression occurred in 72% of the phakic eyes post-DMEK and patients above the age of 50 have a higher risk of cataract progression when compared to younger patients (83 vs. 40%) (49). This differs from our meta-analysis where we observed a considerably lower (but highly variable) risk of cataract development in phakic eyes post-DMEK (mean 9.3%, ranged 0.4–72%) (49, 50, 52, 58, 59, 68). This could be attributed to several factors such as patient cohort and follow-up duration. The mean age of included studies reported cataract progression ranged from 50 to 68 years old, and the youngest patient included was 20 years old, whereas the oldest was 96 years old. Furthermore, follow-up duration was highly heterogeneous amongst studies as well, ranging from 6 to 60 months. These factors combined could lead to variable detection rates of cataract post-DMEK. Whilst doing a staged "DMEK followed by cataract surgery" offers several advantages such as more accurate biometry and potential ability to use a wider variety of intraocular lenses, anecdotally, staged "DMEK then cataract surgery" is less commonly performed due to the potential of damaging the *in-situ* DMEK (70, 71).

We have also attempted to further compare phakic DMEK (i.e., DMEK in phakic eyes) vs. "triple DMEK", and pseudophakic DMEK (i.e., DMEK in pseudophakic eyes) vs. "triple DMEK". However, this was not possible due to the lack of data and the heterogeneity in study design. Whilst we did not quantitatively evaluate the accommodation and refractive outcomes of either approach, Gundlach et al. (35) have suggested that phakic DMEK (i.e., DMEK in phakic eyes) may be beneficial in younger patients as accommodation power can be preserved. In addition, a hyperopic shift may occur following triple DMEK (65, 66), and this can be potentially avoided if cataract surgery is performed after DMEK. Given the low incidence of cataract development post-DMEK, the decision to conduct a targeted DMEK surgery or triple/sequential DMEK should consider the patient's age, preferences, refractive need, and social circumstances.

This review has several limitations. There was no RCT available in the literature that directly compared the outcome of DMEK alone and triple DMEK. In addition, the level and quality of the available evidence were mostly level 3 or 4, and low respectively, with a significant number of studies judged as having moderate to high risks of bias (**Figures 2**, **3**). Furthermore, significant heterogeneity existed in the studies, such as study design, study population, surgical techniques, outcome measures, methods of reporting, and duration of follow-up; and we could not study other factors or important complications such as glaucoma (72), which was not routinely reported. Risk of bias is high as the indication for DMEK included not only FECD but also other causes of corneal endothelial dysfunction such as PBK, complex eyes and re-grafts (73), which have been shown to have a prognostic impact on the surgical outcome (21). There were also inadequate longitudinal studies that compared DMEK alone and triple DMEK, hence making it difficult to provide a meaningful comparison regarding the long-term clinical outcomes of both approaches. With the reasons cited above, whilst meta-analysis could be done with the limited literature available at this juncture, it is hard to make a conclusive assessment on these two approaches.

Overall, our review showed that "triple DMEK" and DMEK alone surgeries are largely comparable in surgical outcomes, sharing similar ECL and complication rates, except for re possible graft detachment rates (lower in DMEK only eyes), which are important clinical points that should be discussed with patients prior to surgery. Looking at the existing evidences, sequential DMEK surgery (cataract surgery followed by DMEK) in patients with endothelial disease who are above the age of 50 years old or have concurrent cataracts could potentially avoid graft detachment. Targeted DMEK alone may be considered in younger patients with no evidence of cataract formation. The decision should, however, be guided by other factors such as patient's preference, social circumstances, surgeon's experience, and availability of operating theaters. Finally, there exists gap in current literature and further adequately powered, randomized controlled trials specifically looking at the long-term outcomes of combined and staged DMEK (with cataract surgery) are warranted for a definitive comparison of the two approaches.

DATA AVAILABILITY STATEMENT

The original contributions presented in the study are included in the article/**Supplementary Material**, further inquiries can be directed to the corresponding author/s.

AUTHOR CONTRIBUTIONS

JM and MA conceptualized and supervised the study. KT, ST, and MA conducted the literature review and curated the data. KT, ST, DT, and MA conducted the formal analysis of the data. All authors wrote, reviewed, edited and approved the manuscript.

SUPPLEMENTARY MATERIAL

The Supplementary Material for this article can be found online at: https://www.frontiersin.org/articles/10.3389/fmed.2022.857200/full#supplementary-material

REFERENCES

1. Allen Foster. Vision 2020: the cataract challenge. *Comm Eye Health.* (2000) 13:17–9.
2. Price MO, Mehta JS, Jurkunas UV, Price FW Jr. Corneal endothelial dysfunction: Evolving understanding and treatment options. *Prog Retin Eye Res.* (2020) 100904. doi: 10.1016/j.preteyeres.2020.100904
3. Park CY, Lee JK, Gore PK, Lim CY, Chuck RS. Keratoplasty in the United States: A 10-Year Review from 2005 through 2014. *Ophthalmology.* (2015) 122:2432–42. doi: 10.1016/j.ophtha.2015.08.017
4. Ting DS, Sau CY, Srinivasan S, Ramaesh K, Mantry S, Roberts F. Changing trends in keratoplasty in the West of Scotland: a 10-year review. *Br J Ophthalmol.* (2012) 96:405–8. doi: 10.1136/bjophthalmol-2011-300244
5. Nanda GG, Alone DP. REVIEW: Current understanding of the pathogenesis of Fuchs' endothelial corneal dystrophy. *Mol Vis.* (2019) 25:295–310.
6. Vedana G, Villarreal G Jr, Jun AS. Fuchs endothelial corneal dystrophy: current perspectives. *Clin Ophthalmol.* (2016) 10:321–30. doi: 10.2147/OPTH.S83467
7. Tan D, Ang M, Arundhati A, Khor WB. Development of Selective Lamellar Keratoplasty within an Asian Corneal Transplant Program: The Singapore Corneal Transplant Study (An American Ophthalmological Society Thesis). *Trans Am Ophthalmol Soc.* (2015) 113:T10.
8. Price FW Jr, Price MO. Combined Cataract/DSEK/DMEK: Changing Expectations. *Asia Pac J Ophthalmol.* (2017) 6:388–92. doi: 10.22608/APO.2017127
9. Bose S, Ang M, Mehta JS, Tan DT, Finkelstein E. Cost-effectiveness of Descemet's stripping endothelial keratoplasty versus penetrating keratoplasty. *Ophthalmology.* (2013) 120:464–70. doi: 10.1016/j.ophtha.2012.08.024
10. Ang M, Soh Y, Htoon HM, Mehta JS, Tan D. Five-year graft survival comparing Descemet stripping automated endothelial keratoplasty and penetrating keratoplasty. *Ophthalmology.* (2016) 123:1646–52. doi: 10.1016/j.ophtha.2016.04.049
11. Melles GRJ, Lander F, Rietveld FJR. Transplantation of DESCEMET's membrane carrying viable endothelium through a small scleral incision. *Cornea.* (2002) 21:415–8. doi: 10.1097/00003226-200205000-00016
12. Melles GRJ, Ong TS, Ververs B, van der Wees J. Descemet membrane endothelial keratoplasty (DMEK). *Cornea.* (2006) 25:987–90. doi: 10.1097/01.ico.0000248385.16896.34
13. Ang M, Mehta JS, Newman SD, Han SB, Chai J, Tan D. Descemet membrane endothelial keratoplasty: preliminary results of a donor insertion pull-through technique using a donor mat device. *Am J Ophthalmol.* (2016) 171:27–34. doi: 10.1016/j.ajo.2016.08.023
14. Marques RE, Guerra PS, Sousa DC, Gonçalves AI, Quintas AM, Rodrigues W. DMEK versus DSAEK for Fuchs' endothelial dystrophy: a meta-analysis. *Eur J Ophthalmol.* (2019) 29:15–22. doi: 10.1177/1120672118757431
15. Deng SX, Lee WB, Hammersmith KM, Kuo AN, Li JY, Shen JF, et al. Descemet membrane endothelial keratoplasty: safety and outcomes: a report by the American Academy of Ophthalmology. *Ophthalmology.* (2018) 125:295–310. doi: 10.1016/j.ophtha.2017.08.015
16. Stuart AJ, Romano V, Virgili G, Shortt AJ. Descemet's membrane endothelial keratoplasty (DMEK) versus Descemet's stripping automated endothelial keratoplasty (DSAEK) for corneal endothelial failure. *Cochr Database Syst Rev.* (2018) 6. doi: 10.1002/14651858.CD012097.pub2
17. Woo JH, Ang M, Htoon HM, Tan D. Descemet membrane endothelial keratoplasty versus Descemet stripping automated endothelial keratoplasty and penetrating keratoplasty. *Am J Ophthalmol.* (2019) 207:288–303. doi: 10.1016/j.ajo.2019.06.012
18. Ang M, Wilkins MR, Mehta JS, Tan D. Descemet membrane endothelial keratoplasty. *Br J Ophthalmol.* (2016) 100:15–21. doi: 10.1136/bjophthalmol-2015-306837
19. Tan TE, Devarajan K, Seah XY, Lin SJ, Peh GSL, Cajucom-Uy HY, et al. Lamellar dissection technique for Descemet membrane endothelial keratoplasty graft preparation. *Cornea.* (2020) 39:23–9. doi: 10.1097/ICO.0000000000002090
20. Tan TE, Devarajan K, Seah XY, Lin SJ, Peh GSL, Cajucom-Uy HY, et al. Descemet membrane endothelial keratoplasty with a pull-through insertion device: surgical technique, endothelial cell loss, and early clinical results. *Cornea.* (2020) 39:558–65. doi: 10.1097/ICO.0000000000002268
21. Chaurasia S, Price FW, Jr., Gunderson L, Price MO. Descemet's membrane endothelial keratoplasty: clinical results of single versus triple procedures (combined with cataract surgery). *Ophthalmology.* (2014) 121:454–8. doi: 10.1016/j.ophtha.2013.09.032
22. Leon P, Parekh M, Nahum Y, Mimouni M, Giannaccare G, Sapigni L, et al. Factors associated with early graft detachment in primary Descemet membrane endothelial keratoplasty. *Am J Ophthalmol.* (2018) 187:117–24. doi: 10.1016/j.ajo.2017.12.014
23. Deshmukh R, Nair S, Ting DSJ, Agarwal T, Beltz J, Vajpayee RB. Graft detachments in endothelial keratoplasty. *Br J Ophthalmol.* (2021) 106:1–13. doi: 10.1136/bjophthalmol-2020-318092
24. Ang M, Ting DSJ, Kumar A, May KO, Htoon HM, Mehta JS. Descemet membrane endothelial keratoplasty in asian eyes: intraoperative and postoperative complications. *Cornea.* (2020) 39:940–5. doi: 10.1097/ICO.0000000000002302
25. Hwang HB, Lyu B, Yim HB, Lee NY. Endothelial cell loss after phacoemulsification according to different anterior chamber depths. *J Ophthalmol.* (2015) 2015:210716. doi: 10.1155/2015/210716
26. Tiew S, Lim C, Sivagnanasithiyar T. Using an excel spreadsheet to convert Snellen visual acuity to LogMAR visual acuity. *Eye.* (2020) 34:2148–49. doi: 10.1038/s41433-020-0783-6
27. Luo D, Wan X, Liu J, Tong T. Optimally estimating the sample mean from the sample size, median, mid-range, and/or mid-quartile range. *Stat Methods Med Res.* (2018) 27:1785–805. doi: 10.1177/0962280216669183
28. Wan X, Wang W, Liu J, Tong T. Estimating the sample mean and standard deviation from the sample size, median, range and/or interquartile range. *BMC Med Res Methodol.* (2014) 14:135. doi: 10.1186/1471-2288-14-135
29. Higgins JP, Savović J, Page MJ, Elbers RG, Sterne JA. Chapter 8: assessing risk of bias in a randomized trial. In: Higgins JP, Thomas J, Chandler J, Cumpston M, Li T, Page MJ, editors. *Cochrane Handbook for Systematic Reviews of Interventions version 60.* 6th ed. Chichester: Cochrane (2019) 82.
30. Sterne JA, Hernán MA, Reeves BC, Savović J, Berkman ND, Viswanathan M, et al. ROBINS-I: a tool for assessing risk of bias in non-randomised studies of interventions. *BMJ.* (2016) 355:i4919. doi: 10.1136/bmj.i4919
31. CEBM. *Oxford Centre for Evidence-based Medicine – Levels of Evidence.* (2009). Available from: https://www.cebm.net/2009/06/oxford-centre-evidence-based-medicine-levels-evidence-march-2009/ (accessed January 1, 2022).

32. Guyatt GH, Oxman AD, Vist GE, Kunz R, Falck-Ytter Y, Alonso-Coello P, et al. GRADE: an emerging consensus on rating quality of evidence and strength of recommendations. *BMJ.* (2008) 336:924–6. doi: 10.1136/bmj.39489.470347.AD
33. Higgins JPT, Thomas J, Chandler J, Cumpston M, Page MJ. Identifying and Measuring Heterogeneity. In: Deeks JJ, Higgins JPT, Altman DG, on behalf of the Cochrane Statistical Methods Group editors. *Cochrane Handbook for Systematic Reviews of Interventions Cochrane*. Chichester: Cochrane (2020).
34. Godin MR, Boehlke CS, Kim T, Gupta PK. Influence of lens status on outcomes of Descemet membrane endothelial keratoplasty. *Cornea.* (2019) 38:409–12. doi: 10.1097/ICO.0000000000001872
35. Gundlach E, Maier A-KB, Tsangaridou M-A, Riechardt AI, Brockmann T, Bertelmann E, et al. DMEK in phakic eyes: targeted therapy or highway to cataract surgery? *Graefes Arch Clin Exp Ophthalmol.* (2015) 253:909–14. doi: 10.1007/s00417-015-2956-8
36. Heinzelmann S, Maier P, Böhringer D, Hüther S, Eberwein P, Reinhard T. Cystoid macular oedema following Descemet membrane endothelial keratoplasty. *Br J Ophthalmol.* (2015) 99:98–102. doi: 10.1136/bjophthalmol-2014-305124
37. Singh SK, Sitaula S. Visual outcome of Descemet membrane endothelial keratoplasty during the learning curve in initial fifty cases. *J Ophthalmol.* (2019) 2019:5921846. doi: 10.1155/2019/5921846
38. Crews JW, Price MO, Lautert J, Feng MT, Price FW Jr. Intraoperative hyphema in Descemet membrane endothelial keratoplasty alone or combined with phacoemulsification. *J Cataract Refract Surg.* (2018) 44:198–201. doi: 10.1016/j.jcrs.2017.11.015
39. Heinzelmann S, Bohringer D, Haverkamp C, Lapp T, Eberwein P, Reinhard T, et al. Influence of postoperative intraocular pressure on graft detachment after Descemet membrane endothelial keratoplasty. *Cornea.* (2018) 37:1347–50. doi: 10.1097/ICO.0000000000001677
40. Schrittenlocher S, Bachmann B, Tiurbe AM, Tuac O, Velten K, Schmidt D, et al. Impact of preoperative visual acuity on Descemet Membrane Endothelial Keratoplasty (DMEK) outcome. *Graefes Arch Clin Exp Ophthalmol.* (2019) 257:321–9. doi: 10.1007/s00417-018-4193-4
41. Oellerich S, Baydoun L, Peraza-Nieves J, Ilyas A, Frank L, Binder PS, et al. Multicenter study of 6-month clinical outcomes after Descemet membrane endothelial keratoplasty. *Cornea.* (2017) 36:1467–76. doi: 10.1097/ICO.0000000000001374
42. Schlogl A, Tourtas T, Kruse FE, Weller JM. Long-term clinical outcome after Descemet membrane endothelial keratoplasty. *Am J Ophthalmol.* (2016) 169:218–26. doi: 10.1016/j.ajo.2016.07.002
43. Showail M, Obthani MA, Sorkin N, Einan-Lifshitz A, Boutin T, Borovik A, et al. Outcomes of the first 250 eyes of Descemet membrane endothelial keratoplasty: Canadian centre experience. *Can J Ophthalmol.* (2018) 53:510–7. doi: 10.1016/j.jcjo.2017.11.017
44. Kocaba V, Mouchel R, Fleury J, Marty A-S, Janin-Manificat H, Maucort-Boulch D, et al. Incidence of cystoid macular edema after Descemet membrane endothelial keratoplasty. *Cornea.* (2018) 37:277–82. doi: 10.1097/ICO.0000000000001501
45. Fajardo-Sanchez J, de Benito-Llopis L. Clinical outcomes of Descemet membrane endothelial keratoplasty in pseudophakic eyes compared with triple-DMEK at 1-year follow-up. *Cornea.* (2021) 40:420–4. doi: 10.1097/ICO.0000000000002636
46. Ching G, Covello AT, Bae SS, Holland S, McCarthy M, Ritenour R, et al. Incidence and outcomes of cystoid macular edema after Descemet membrane endothelial keratoplasty (DMEK) and DMEK combined with cataract surgery. *Curr Eye Res.* (2021) 46:678–82. doi: 10.1080/02713683.2020.1818260
47. Moshiri I, Karimi-Golkar D, Schrittenlocher S, Cursiefen C, Bachmann B. Outcomes of pseudophakic, phakic, and triple DMEK. *Cornea.* (2021) 40:1253–7. doi: 10.1097/ICO.0000000000002723
48. Hussien A, Elmassry A, Ghaith AA, Goweida MBB. Descemet's membrane endothelial keratoplasty and phacoemulsification: combined versus sequential surgery. *J Curr Ophthalmol.* (2021) 33:277–84. doi: 10.4103/joco.joco_188_20
49. Burkhart ZN, Feng MT, Price FW, Jr., Price MO. One-year outcomes in eyes remaining phakic after Descemet membrane endothelial keratoplasty. *J Cataract Refract Surg.* (2014) 40:430–4. doi: 10.1016/j.jcrs.2013.08.047
50. Parker J, Dirisamer M, Naveiras M, Tse WH, van Dijk K, Frank LE, et al. Outcomes of Descemet membrane endothelial keratoplasty in phakic eyes. *J Cataract Refract Surg.* (2012) 38:871–7. doi: 10.1016/j.jcrs.2011.11.038
51. Birbal RS, Tong CM, Dapena I, Parker JS, Parker JS, Oellerich S, et al. Clinical outcomes of Descemet membrane endothelial keratoplasty in eyes with a glaucoma drainage device. *Am J Ophthalmol.* (2019) 199:150–8. doi: 10.1016/j.ajo.2018.11.014
52. Dapena I, Ham L, Droutsas K, van Dijk K, Moutsouris K, Melles GR. Learning curve in Descemet's membrane endothelial keratoplasty: first series of 135 consecutive cases. *Ophthalmology.* (2011) 118:2147–54. doi: 10.1016/j.ophtha.2011.03.037
53. Ham L, Dapena I, Moutsouris K, Balachandran C, Frank LE, van Dijk K, et al. Refractive change and stability after Descemet membrane endothelial keratoplasty: effect of corneal dehydration-induced hyperopic shift on intraocular lens power calculation. *J Catar Refract Surg.* (2011) 37:1455–64. doi: 10.1016/j.jcrs.2011.02.033
54. Satue M, Idoipe M, Gavin A, Romero-Sanz M, Liarakos VS, Mateo A, et al. Early changes in visual quality and corneal structure after DMEK: does DMEK approach optical quality of a healthy cornea? *J Ophthalmol.* (2018) 2018:2012560. doi: 10.1155/2018/2012560
55. Gorovoy MS. DMEK complications. *Cornea.* (2014) 33:101–4. doi: 10.1097/ICO.0000000000000023
56. van Dijk K, Parker J, Liarakos VS, Ham L, Frank LE, Melles GR. Incidence of irregular astigmatism eligible for contact lens fitting after Descemet membrane endothelial keratoplasty. *J Cataract Refract Surg.* (2013) 39:1036–46. doi: 10.1016/j.jcrs.2013.02.051
57. Baydoun L, Ham L, Borderie V, Dapena I, Hou J, Frank LE, et al. Endothelial survival after Descemet membrane endothelial keratoplasty: effect of surgical indication and graft adherence status. *JAMA Ophthalmol.* (2015) 133:1277–85. doi: 10.1001/jamaophthalmol.2015.3064
58. Peraza-Nieves J, Baydoun L, Dapena I, Ilyas A, Frank LE, Luceri S, et al. Two-year clinical outcome of 500 consecutive cases undergoing Descemet membrane endothelial keratoplasty. *Cornea.* (2017) 36:655–60. doi: 10.1097/ICO.0000000000001176
59. Dirisamer M, Ham L, Dapena I, Moutsouris K, Droutsas K, van Dijk K, et al. Efficacy of Descemet membrane endothelial keratoplasty: clinical outcome of 200 consecutive cases after a learning curve of 25 cases. *Arch Ophthalmol.* (2011) 129:1435–43. doi: 10.1001/archophthalmol.2011.195
60. van Dijk K, Rodriguez-Calvo-de-Mora M, van Esch H, Frank L, Dapena I, Baydoun L, et al. Two-year refractive outcomes after Descemet membrane endothelial keratoplasty. *Cornea.* (2016) 35:1548–55. doi: 10.1097/ICO.0000000000001022
61. Ham L, Dapena I, Liarakos VS, Baydoun L, van Dijk K, Ilyas A, et al. Midterm results of Descemet membrane endothelial keratoplasty: 4 to 7 years clinical outcome. *Am J Ophthalmol.* (2016) 171:113–21. doi: 10.1016/j.ajo.2016.08.038
62. Wubbels RJ, Remeijer L, Engel A, van Rooij J. The learning curve for Descemet membrane endothelial keratoplasty performed by two experienced corneal surgeons: a consecutive series of 40 cases. *Acta Ophthalmol.* (2020) 98:74–9. doi: 10.1111/aos.14152
63. Schoenberg ED, Price FW, Jr., Miller J, McKee Y, Price MO. Refractive outcomes of Descemet membrane endothelial keratoplasty triple procedures (combined with cataract surgery). *J Cataract Refract Surg.* (2015) 41:1182–9. doi: 10.1016/j.jcrs.2014.09.042
64. Laaser K, Bachmann BO, Horn FK, Cursiefen C, Kruse FE. Descemet membrane endothelial keratoplasty combined with phacoemulsification and intraocular lens implantation: advanced triple procedure. *Am J Ophthalmol.* (2012) 154:47–55.e2. doi: 10.1016/j.ajo.2012.01.020
65. Cheung AY, Chachare DY, Eslani M, Schneider J, Nordlund ML. Tomographic changes in eyes with hyperopic shift after triple Descemet membrane endothelial keratoplasty. *J Cataract Refract Surg.* (2018) 44:738–44. doi: 10.1016/j.jcrs.2018.04.040
66. Fritz M, Grewing V, Böhringer D, Lapp T, Maier P, Reinhard T, et al. Avoiding hyperopic surprises after Descemet membrane endothelial keratoplasty in fuchs dystrophy eyes by assessing corneal shape. *Am J Ophthalmol.* (2019) 197:1–6. doi: 10.1016/j.ajo.2018.08.052

67. Augustin VA, Weller JM, Kruse FE, Tourtas T. Can we predict the refractive outcome after triple Descemet membrane endothelial keratoplasty? *Eur J Ophthalmol.* (2019) 29:165–70. doi: 10.1177/1120672118785282
68. Birbal RS, Ni Dhubhghaill S, Bourgonje VJA, Hanko J, Ham L, Jager MJ, et al. Five-year graft survival and clinical outcomes of 500 consecutive cases after Descemet membrane endothelial keratoplasty. *Cornea.* (2020) 39:290–7. doi: 10.1097/ICO.0000000000002120
69. Botsford B, Vedana G, Cope L, Yiu SC, Jun AS. Comparison of 20% sulfur hexafluoride with air for intraocular tamponade in Descemet membrane endothelial keratoplasty (DMEK). *Arq Bras Oftalmol.* (2016) 79:299–302. doi: 10.5935/0004-2749.20160086
70. Bailey TC, Zaidman GW, Mirochnik B, Naadimuthu R. The incidence of cataract extraction following corneal transplantation in young and middle-aged patients. *Invest Ophthalmol Vis Sci.* (2009) 50:2207.
71. Chaurasia S, Ramappa M, Sangwan V. Cataract surgery after Descemet stripping endothelial keratoplasty. *Indian J Ophthalmol.* (2012) 60:572–4. doi: 10.4103/0301-4738.103803
72. Ang M, Sng CCA. Descemet membrane endothelial keratoplasty and glaucoma. *Curr Opin Ophthalmol.* (2018) 29:178–84. doi: 10.1097/ICU.0000000000000454
73. Ang M, Tan D. Anterior segment reconstruction with artificial iris and Descemet membrane endothelial keratoplasty: a staged surgical approach. *Br J Ophthalmol.* (2021). doi: 10.1136/bjophthalmol-2020-317906

Conflict of Interest: The authors declare that the research was conducted in the absence of any commercial or financial relationships that could be construed as a potential conflict of interest.

Publisher's Note: All claims expressed in this article are solely those of the authors and do not necessarily represent those of their affiliated organizations, or those of the publisher, the editors and the reviewers. Any product that may be evaluated in this article, or claim that may be made by its manufacturer, is not guaranteed or endorsed by the publisher.

frontiers | Frontiers in Medicine

CASE REPORT
published: 27 April 2022
doi: 10.3389/fmed.2022.836873

Case Report: Use of Amniotic Membrane for Tectonic Repair of Peripheral Ulcerative Keratitis With Corneal Perforation

Maryam Eslami[1]*, *Blanca Benito-Pascual*[2,3], *Saadiah Goolam*[2,3], *Tanya Trinh*[2,3,4] and *Greg Moloney*[1,2,3,4]

[1] Department of Ophthalmology and Visual Sciences, University of British Columbia, Vancouver, BC, Canada, [2] Sydney Eye Hospital, Sydney, NSW, Australia, [3] Save Sight Institute, University of Sydney, Sydney, NSW, Australia, [4] Mosman Eye Centre and Narellan Eye Specialists, Sydney, NSW, Australia

OPEN ACCESS

Edited by:
Jorge L. Alió Del Barrio,
Miguel Hernández University of Elche, Spain

Reviewed by:
Kendrick Co Shih,
The University of Hong Kong, Hong Kong SAR, China
Katarzyna Krysik,
Wojewódzki Szpital Specjalistyczny nr 5 Sosnowiec, Poland
Mo Ziaei,
The University of Auckland, New Zealand
Arzu Taskiran Comez,
Çanakkale Onsekiz Mart University, Turkey

***Correspondence:**
Maryam Eslami
maryam.eslami@alumni.ubc.ca

Specialty section:
This article was submitted to Ophthalmology, a section of the journal Frontiers in Medicine

Received: 16 December 2021
Accepted: 28 March 2022
Published: 27 April 2022

Citation:
Eslami M, Benito-Pascual B, Goolam S, Trinh T and Moloney G (2022) Case Report: Use of Amniotic Membrane for Tectonic Repair of Peripheral Ulcerative Keratitis With Corneal Perforation. Front. Med. 9:836873. doi: 10.3389/fmed.2022.836873

Purpose: To provide a perspective and surgical video demonstration of peripheral corneal ulceration and perforation managed with multilayered amniotic membrane transplantation.

Case Reports: Case 1 describes a 48-year-old female with progressive redness and pain, and an inferonasal corneal thinning and perforation in the left eye from peripheral ulcerative keratitis. She underwent conjunctival recession with amniotic membrane inlay and onlay (Sandwich technique) transplantation. The amniotic membrane integrated well, and her Snellen visual acuity improved from 6/21 preoperatively to 6/9 at 3 months post op. Case 2 describes a 78-year-old male with redness and pain with temporal corneal thinning bilaterally and perforation in the right eye from peripheral ulcerative keratitis. Both eyes underwent similar surgical intervention with smooth integration of the amniotic membrane in the cornea and improvement in the visual acuity. Both patients were also started on systemic immunosuppression in collaboration with the rheumatology team.

Conclusion: We report successful use of multilayered amniotic membrane transplantation for the treatment of corneal ulceration and perforation. The authors believe the simplicity of the surgical technique, easier access to amniotic membrane tissue, and lower induced post-operative astigmatism all provide advantages over alternative treatment modalities.

Keywords: amniotic membrane transplantation, corneal perforation, peripheral ulcerative keratitis, corneal ulceration, tectonic graft repair

INTRODUCTION

Various corneal pathologies can lead to corneal perforation, including infectious keratitis (bacterial, viral, fungal or parasitic), inflammatory keratitis (Mooren's ulcer, rheumatoid arthritis, systemic lupus erythematosus), neurotrophic keratitis, peripheral corneal thinning (pellucid marginal degeneration, Terrien's marginal degeneration), trauma, and chemical injuries (1–3).

The management of corneal perforation varies from non-surgical treatments such as bandage contact lenses or tissue adhesives, to surgical modalities like corneal suturing, conjunctival flaps, amniotic membrane (AM) transplantation and ultimately tectonic corneal patch graft (2, 3). The treatment chosen often depends on the size, location, and etiology of the corneal perforation, as well as the surgeon's experience and availability of donor tissues (amniotic membrane or donor cornea) (3, 4).

AM may be used as a graft (inlay), patch (onlay) or both for the management of corneal ulcers and perforations (5). It is not immunogenic, prevents apoptosis and has antimicrobial, antifibrotic, anti-inflammatory and antiangiogenic properties (3, 6). AM enhances epithelialisation by facilitating migration and differentiation of epithelial cells, reinforcing adhesion of basal epithelial cells, and regulating proliferation of normal corneal, conjunctival, and limbal fibroblasts (3).

In this paper, we present two cases of corneal perforation secondary to peripheral ulcerative keratitis managed with a sandwich technique of AM transplantation demonstrated in the **Supplementary Video**. Informed consent was obtained from both patients for publication of this case report.

FIGURE 1 | Inferonasal corneal ulceration with adjacent inflammation of the left eye.

CASE 1

A 48-year-old female presented with progressive pain, redness, and foreign body sensation in the left eye (LE) over the past 6 months. She had a history of peripheral ulcerative keratitis in the right eye (RE) requiring systemic immunosuppression and tectonic lamellar keratoplasty to reconstruct the area of the corneal thinning 15 years ago. Her systemic workup (complete cell blood count, electrolytes, urea, creatinine, liver function test, thyroid function test, C reactive protein (CRP), erythrocyte sedimentation rate (ESR), rheumatoid factor, antinuclear antibodies (ANA), antineutrophil cytoplasmic antibodies (ANCA), extractable nuclear antigens, anti-citrullinated protein antibody, syphilis, herpetic and hepatitis serologies) was negative 15 years prior. Her systems review at that point revealed a chronically inflamed elbow; therefore, she was started on oral cyclosporine up to 100 mg oral BID and Felodipine 2.5 mg oral daily for presumed seronegative rheumatoid arthritis. This systemic management was successfully tapered off 4 years ago with no recurrence of symptoms in the eye or the elbow joint.

On examination, she had uncorrected Snellen visual acuity of 6/30 on the right and 6/21 on the left. RE revealed an uninflamed tectonic lamellar keratoplasty. The LE was acutely inflamed inferonasally adjacent to an area of peripheral corneal ulceration without perforation. The anterior chamber was deep and quiet bilaterally at this point. She had trace nuclear sclerosis in both eyes.

She was commenced on oral ascorbic acid, topical moxifloxacin QID andprednisolone acetate 1% QID in the LE, and advised to use an eye shield at night. The rheumatology team was consulted again, and she was started on oral prednisone 60 mg daily as well as oral mycophenolate mofetil 1 g BID. On repeat assessment a week later, she had not yet started systemic treatment and had not been using her eye shield. She was found to have a perforation within the area of thinning with a flat anterior chamber (**Figure 1**).

A bandage contact lens was put on the LE as a temporizing measure before surgical management. She was continued on topical moxifloxacin and prednisolone acetate in the LE. Two days later, a conjunctival recession, amniotic membrane transplant and a temporary tarsorrhaphy was performed under retrobulbar anesthesia. A single piece of folded, multi-layered, fresh frozen amniotic membrane was packed and sutured into the LE corneal defect and held in place using fibrin glue. An overlying large single layer of amniotic membrane with the epithelial side down was sutured with interrupted sutures of 10.0 nylon with tension over the temporal ocular surface in a bandage fashion (**Supplementary Video**). A medial temporary tarsorrhaphy was carried out using bolsters and 6-0 nylon. Subconjunctival antibiotics of cefazolin and dexamethasone were injected at the end of the procedure. Postoperatively the patient was commenced on moxifloxacin eye drops QID, prednisolone acetate 1% QID and preservative-free lubricants 2-hourly.

The patient had an uneventful post-operative course without further episodes of ulceration, melt or inflammation. The AM patch integrated well into the corneal stroma at the 1-month postoperative visit with Snellen visual acuity of 6/15 and a quiet ocular surface (**Figure 2A**). Her uncorrected Snellen visual acuity improved to 6/9 at 3-months post op (**Figure 2B**).

CASE 2

A 78-year-old male from rural New South Wales presented to the Sydney Eye Hospital emergency department with a RE corneal perforation following a 4-day history of severe right ocular pain.

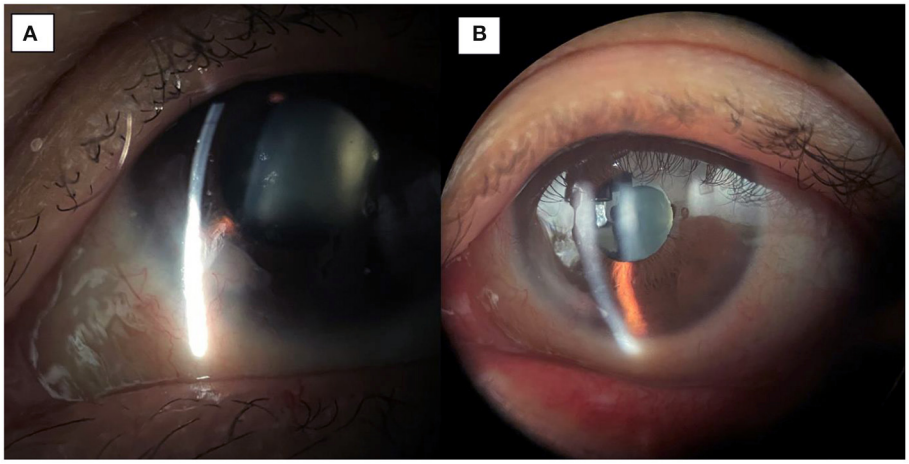

FIGURE 2 | (A) 1-month post-op image showing integration of the amniotic membrane patch in the inferonasal corneal stroma. **(B)** 3-month post-op image demonstrating smooth integration and an uninflamed left eye.

Past ocular history included LE pseudophakia and bilateral pterygium excision several years ago as well as bilateral dry age-related macular degeneration. He had a medical history of hypertension and ischemic heart disease with no other systemic complaints.

Examination on presentation revealed Snellen visual acuities of 6/38 in the RE and 6/24 in the LE. Intraocular pressure (IOP) was 13 and 11 mmHg in the right and left eye, respectively. Conjunctiva were bilaterally injected without any scleritic foci or evidence of scleromalacia. Corneas bilaterally were found to have temporal peripheral ulcerative keratitis (PUK) (6.5 mm in the RE and 7 mm in the LE), with RE corneal perforation of 2 mm with iris prolapse and LE thinning of ∼80–90% within the area of ulceration (**Figures 3A,B**). RE Anterior chamber was almost flat with 3+ cells and a fibrinous reaction. LE anterior chamber was deep with 2+ cells. Other examination findings included pseudoexfoliative cataract in the RE and pseudophakia in the LE.

A cautious corneal scrape and swab of the RE ulcer bed excluded a superimposed microbial keratitis. Blood tests mentioned above, quantiferon gold test and a chest X-Ray were ordered to exclude infective and inflammatory/autoimmune causes of peripheral ulcerative keratitis. Blood tests were positive for a raised ESR (18 mm/h) and ANA (1:320 speckled); the remaining blood tests were unremarkable.

The patient was admitted on an initial treatment regimen of fortified topical antibiotics (gentamicin 0.9% and Cefazolin 5%) hourly in the RE and QID in the LE, topical prednisolone sodium phosphate preservative free 0.5% twice a day in both eyes, oral anti-collagenolytic agents (ascorbic acid 2 grams daily, doxycycline 100 mg twice a day), oral prednisolone 60 mg daily, oral ciprofloxacin 750 mg twice a day and valacyclovir 500 mg three times a day.

Gluing of the corneal perforation as a temporizing measure was not possible due to the significant area of perforation and degree of iris prolapse. For the RE, a conjunctival recession, amniotic membrane transplants and tarsorrhaphy was performed. A single piece of folded, multi-layered, fresh frozen amniotic membrane was packed and sutured into the RE corneal defect and an overlying large single layer of amniotic membrane with the epithelial side down was sutured with tension over the temporal ocular surface with interrupted sutures of 10.0 nylon. A nasal paracentesis was used to reform the anterior chamber and reposit the iris. A second layer of amniotic membrane was then applied to the entire ocular surface with a purse-string suture.

The LE had conjunctival recession and 3 glue patches applied to the area of melt before a layer of amniotic membrane was glued over the area of thinning incorporating the area of conjunctival recession. Subconjunctival antibiotics of cefazolin and dexamethasone were injected bilaterally at the end of the procedures.

Postoperatively the patient was commenced on preservative-free chloramphenicol 0.5% drops QID, cyclosporine 1% BID and preservative-free lubricants 2-hourly. Topical steroids and fortified antibiotics were ceased. The rheumatology team was consulted as part of the multidisciplinary management of this patient's idiopathic immune-mediated corneal disease. 3 cycles of intravenous methyl prednisolone 500 mg and intravenous cyclophosphamide 650 mg were administered, followed by a tapering dose of the oral prednisone and initiation of long-term immunosuppression with oral mycophenolate 360 mg twice daily.

The patient had an uneventful post-operative course without further episodes of ulceration, melt or inflammation. Snellen visual acuity at the 1-month postoperative visit was 6/90 in RE (with cataract) and 6/9 in LE with normal intraocular pressures and a quiet ocular surface (**Figures 4A,B**).

Topical and systemic immunosuppressants were reduced as the patient continued on a stable postoperative course. At the 4-month post-operative visit the patient had similar visual acuity, and was maintained on topical preservative free lubricants and Mycophenolate 500 mg BD (**Figures 4C,D**).

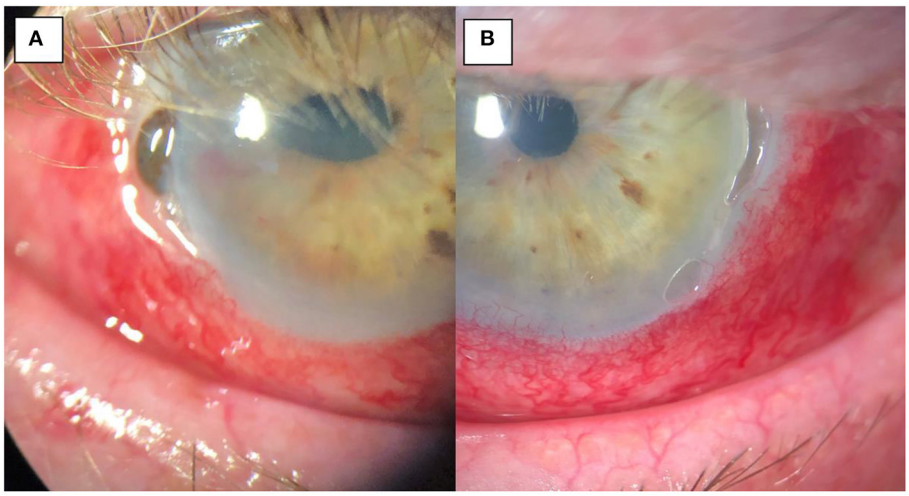

FIGURE 3 | (A) Pre-operative image of the right eye with temporal thinning and perforation, iris prolapse and surrounding inflammation. **(B)** pre-operative image of the left eye with temporal thinning and surrounding inflammation but no corneal perforation.

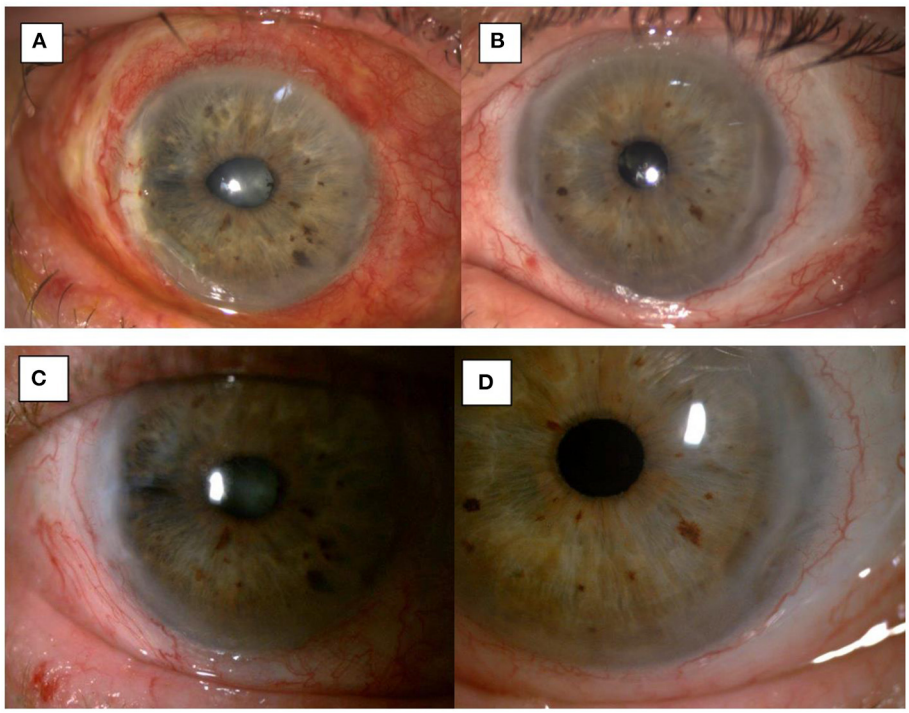

FIGURE 4 | 1-month post-op image showing integration of the amniotic membrane patch in the temporal corneal stroma of the right eye **(A)** and the left eye **(B)**. 3-month post-op image showing uninflamed eyes and a smooth integration of the amniotic membrane patch in the temporal corneal stroma of the right eye **(C)** and the left eye **(D)**.

DISCUSSION

In this article, we present two cases of peripheral ulcerative keratitis (3 eyes) with corneal perforation treated with multi-layered amniotic membrane transplantation using cigar technique demonstrated in the **Supplementary Video**. We found the AM integrated well into the host cornea in all 3 eyes with rapid visual recovery in all eyes but one, in which the reduced vision was attributed to cataract formation.

To replace the corneal tissue defect and fill in the corneal ulceration, the main options are fibrin glue, conjunctival and tenons tissue, donor corneal tissue, and AM (6–8). Fibrin glue,

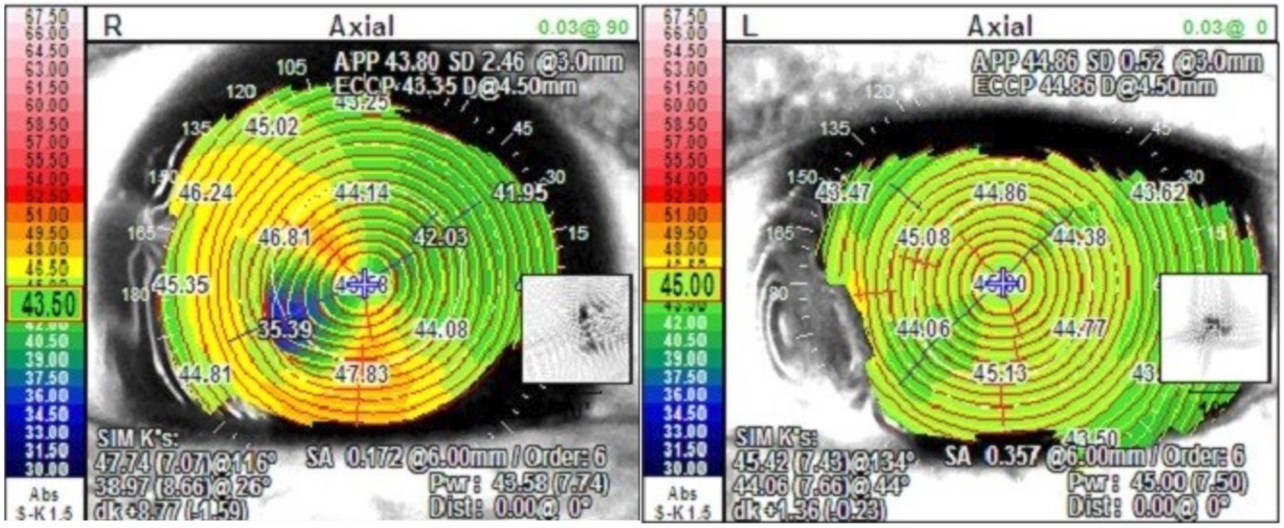

FIGURE 5 | Topographic map of Case 1 post operatively with tectonic corneal graft in the right eye and AM transplantation in the left eye.

TABLE 1 | A comparison of advantages and preferred utilization of AM transplantation and tectonic corneal graft.

	AM transplantation	Tectonic corneal graft
Advantages:	• Rapid recovery • Relative availability and ease of access • Relative simplicity of surgical technique • Less induced astigmatism • Less risk of rejection and ongoing melt	• Transparent tissue • Superior structural integrity with less potential for dislodgement
The technique may be preferred in:	• Peripheral corneal melt • Large areas of thinning with small or medium-sized perforation • Inflamed eye • Rheumatic etiology of corneal melt	• Large-sized perforation • Central disease • Intraocular tissue involvement

although a valuable tool in small perforations, is often ineffective on its own in filling the entire depth of corneal ulceration in large defects and may prolong wound healing and closure of epithelial defect (7). Conjunctival tissue often leads to neovascularization, scarring and conjunctivilization of the epithelium (7). Donor corneal tissue is often in short supply or may not be immediately available for the treatment of corneal perforation (7). It also has an increased risk of rejection and ongoing melt due to the inflamed host cornea and the underlying rheumatic disease (8). Many studies have reported on the successful use of AM in the treatment of corneal perforation (1–4, 6, 7). Some authors believe AM transplantation to be superior to alternatives due to AM's antifibrotic, anti-inflammatory and antiangiogenic properties that not only fills the defect and restores the globe's integrity, but also prevents further tissue loss (3, 6, 7). This technique does require a tightly "packed" scroll of AM into a "cigar" shape—we find that this contour lends itself well to simultaneously filling in the central "bulk" for the largest portion of the defect alongside tapered "ends" and each pole of the "cigar", allowing for a gradual filling of crescenteric defects at superior and inferior ends. The initial placement of sutures from the host-AM-host requires replacing with tighter tension as the walls of the crevice become more and more closely apposed.

In our cases, we found the rapid visual rehabilitation and low induced astigmatism to be superior to tectonic corneal graft as well. The first case previously required a tectonic lamellar keratoplasty in the right eye for the same indication with an induced astigmatism of 6.5 diopters, while the left eye of the same patient treated with AM transplantation described above had a cylinder of 0.75 diopters at 3 months (**Figure 5**). This is consistent with prior studies with some authors reporting declining astigmatism with time as the AM continues to integrate into the host cornea (1, 3).

Lastly, the simplicity of the surgical technique (**Supplementary Video**) and the relative ease of availability of AM compared to donor cornea makes this an attractive choice for the management of corneal ulcers and perforations. This was also highlighted in a study by Ngan and Chau (9) on Mooren ulcers in Vietnam where systemic immunosuppressive medications are not readily available. Indeed, the management of corneal melting and perforation can be complex, and the treatment modality chosen may vary significantly depending on the clinical picture, other ocular comorbidities, and the size, location, and etiology of corneal thinning (**Table 1**). The authors agree that AM transplantation may not be suitable as the sole treatment of central corneal ulceration, as it leads to corneal opacity once healed and may degrade visual acuity. However, it may be an appropriate temporizing measure to allow for an uninflamed and quiet eye prior to donor corneal graft transplantation, thereby increasing success for

visual rehabilitation. Additionally, while there is no absolute perforation size cut-off for the use of AM transplantation, it may be difficult to pack and close large perforation defects and restore the globe's integrity. However, its successful use in large or 360 degrees of corneal thinning has been previously reported (9).

CONCLUSION

Multi-layered amniotic membrane transplantation may be an effective surgical modality in the treatment of corneal ulceration and small to mid-sized perforation from peripheral ulcerative keratitis. The surgical technique is simple and leads to relatively rapid visual recovery with low induced astigmatism.

ETHICS STATEMENT

Ethical review and approval was not required for the study on human participants in accordance with the local legislation and institutional requirements. The patients/participants provided their written informed consent to participate in this study. Written informed consent was obtained from the individual(s) for the publication of any potentially identifiable images or data included in this article.

AUTHOR CONTRIBUTIONS

ME, BB-P, and SG drafted the manuscript and the two cases. TT and GM were supervisors, performed the surgeries, and edited the manuscript and the surgical video. All authors contributed to the article and approved the submitted version.

SUPPLEMENTARY MATERIAL

The Supplementary Material for this article can be found online at: https://1drv.ms/v/s!Al8oT3NYnmDhhJhibB2ulm_ViljONQ?e=ppBLa2

REFERENCES

1. Namba H, Narumi M, Nishi K, Goto S, Hayashi S, Yamashita H. "Pleats fold" technique of amniotic membrane transplantation for management of corneal perforations. *Cornea*. (2014) 33:653–7. doi: 10.1097/ICO.0000000000000128
2. Yokogawa H, Kobayashi A, Yamazaki N, Masaki T, Sugiyama K. Surgical therapies for corneal perforations: 10 years of cases in a tertiary referral hospital. *Clin Ophthalmol.* (2014) 8:2165–70. doi: 10.2147/OPTH.S71102
3. Krysik K, Dobrowolski D, Wylegala E, Lyssek-Boron A. Amniotic membrane as a main component in treatments supporting healing and patch grafts in corneal melting and perforations. *J Ophthalmol.* (2020) 2020:4238919–7. doi: 10.1155/2020/4238919
4. Chan E, Shah AN, O'Brart DPS. "Swiss roll" amniotic membrane technique for the management of corneal perforations. *Cornea*. (2011) 30:838–41. doi: 10.1097/ICO.0b013e31820ce80f
5. Meller D, Pauklin M, Thomasen H, Westekemper H, Steuhl KP. Amniotic membrane transplantation in the human eye. *Dtsch Arztebl Int.* (2011) 108:243–48. doi: 10.3238/arztebl.2011.0243
6. Malhotra C, Jain AK. Human amniotic membrane transplantation: different modalities of its use in ophthalmology. *World J Transplant*. (2014) 4:111–21. doi: 10.5500/wjt.v4.i2.111
7. Hanada K, Shimazaki J, Shimmura S, Tsubota K. Multilayered amniotic membrane transplantation for severe ulceration of the cornea and sclera. *Am J Ophthalmol.* (2001) 131:324–31. doi: 10.1016/S0002-9394(00)00825-4
8. Solomon A, Meller D, Prabhasawat P, John T, Espana EM, Steuhl KP, et al. Amniotic membrane grafts for nontraumatic corneal perforations, descemetoceles, and deep ulcers. *Ophthalmology*. (2002) 109:694–703. doi: 10.1016/S0161-6420(01)01032-6
9. Ngan ND, Chau HT. Amniotic membrane transplantation for Mooren's ulcer: amniotic membrane for Mooren's ulcer. *Clin Exp Ophthalmol.* (2011) 39:386–92. doi: 10.1111/j.1442-9071.2010.02479.x

Conflict of Interest: The authors declare that the research was conducted in the absence of any commercial or financial relationships that could be construed as a potential conflict of interest.

frontiers | Frontiers in Medicine

REVIEW
published: 25 May 2022
doi: 10.3389/fmed.2022.836009

A Review of the Diagnosis and Treatment of Limbal Stem Cell Deficiency

Anahita Kate[1] *and Sayan Basu*[2,3]*

[1] The Cornea Institute, KVC Campus, LV Prasad Eye Institute, Vijayawada, India, [2] The Cornea Institute, KAR Campus, LV Prasad Eye Institute, Hyderabad, India, [3] Prof. Brien Holden Eye Research Centre (BHERC), LV Prasad Eye Institute, Hyderabad, Telangana, India

Limbal stem cell deficiency (LSCD) can cause significant corneal vascularization and scarring and often results in serious visual morbidity. An early and accurate diagnosis can help prevent the same with a timely and appropriate intervention. This review aims to provide an understanding of the different diagnostic tools and presents an algorithmic approach to the management based on a comprehensive clinical examination. Although the diagnosis of LSCD usually relies on the clinical findings, they can be subjective and non-specific. In such cases, using an investigative modality offers an objective method of confirming the diagnosis. Several diagnostic tools have been described in literature, each having its own advantages and limitations. Impression cytology and *in vivo* confocal microscopy (IVCM) aid in the diagnosis of LSCD by detecting the presence of goblet cells. With immunohistochemistry, impression cytology can help in confirming the corneal or conjunctival source of epithelium. Both IVCM and anterior segment optical coherence tomography can help supplement the diagnosis of LSCD by characterizing the corneal and limbal epithelial changes. Once the diagnosis is established, one of various surgical techniques can be adopted for the treatment of LSCD. These surgeries aim to provide a new source of corneal epithelial stem cells and help in restoring the stability of the ocular surface. The choice of procedure depends on several factors including the involvement of the ocular adnexa, presence of systemic co-morbidities, status of the fellow eye and the comfort level of the surgeon. In LSCD with wet ocular surfaces, autologous and allogeneic limbal stem cell transplantation is preferred in unilateral and bilateral cases, respectively. Another approach in bilateral LSCD with wet ocular surfaces is the use of an autologous stem cell source of a different epithelial lineage, like oral or nasal mucosa. In eyes with bilateral LSCD with significant adnexal issues, a keratoprosthesis is the only viable option. This review provides an overview on the diagnosis and treatment of LSCD, which will help the clinician choose the best option amongst all the therapeutic modalities currently available and gives a clinical perspective on customizing the treatment for each individual case.

Keywords: Limbal stem cell deficiency (LSCD), simple limbal epithelial transplantation (SLET), limbal stem cell transplantation (LSCT), Keratoprosthesis (KPro), Anterior segment optical coherence tomography (AS-OCT), impression cytology (IC), confocal microscopy, cultivated limbal epithelial transplantation (CLET)

OPEN ACCESS

Edited by:
Jorge L. Alió Del Barrio, Miguel Hernández University of Elche, Spain

Reviewed by:
Yousef Ahmed Fouad, Ain Shams University, Egypt
Mee Kum Kim, Seoul National University, South Korea

***Correspondence:**
Sayan Basu
sayanbasu@lvpei.org

Specialty section:
This article was submitted to Ophthalmology, a section of the journal Frontiers in Medicine

Received: *15 December 2021*
Accepted: *03 May 2022*
Published: *25 May 2022*

Citation:
Kate A and Basu S (2022) A Review of the Diagnosis and Treatment of Limbal Stem Cell Deficiency. Front. Med. 9:836009. doi: 10.3389/fmed.2022.836009

INTRODUCTION

The corneal epithelium is essential for the maintenance of the anatomic integrity and physiological functioning of the transparent cornea. The maintenance of the corneal surface is ensured by the constant turnover of the corneal epithelium from the limbal epithelial stem cells (LESC) (1, 2). These LESC straddle the junction between the cornea and the conjunctiva and reside in the basal epithelial layer of the limbus. The microenvironment surrounding the LESC within the palisades of Vogt, is responsible for ensuring the viability and efficacy of the stem cells. The LESC prevent the migration of the conjunctival epithelial cells over the corneal surface and in the presence of a dysfunction of the LESC themselves or the surrounding niche, there occurs conjunctivalization of the cornea.

Limbal stem cell deficiency (LSCD) can stem from numerous etiologies, resulting in serious visual morbidity (3, 4). And so, early diagnosis of this entity is essential in order to institute the appropriate therapy in a timely manner. Also, the need for diagnosing LSCD is even more essential when a keratoplasty is planned as the graft is unlikely to fair well if the LSCD is not corrected in advance. Although the diagnosis of LSCD is still primarily a clinical one, there are several diseases that can mimic its clinical picture (5, 6). In such scenarios, the clinician can choose from an array of diagnostic tests aimed at detecting LSCD. Similarly, numerous therapeutic options are available in management of LSCD and the choice of one intervention over the other depends upon the severity of ocular and adnexal involvement. This review aims to provide an understanding of the various tools in the diagnostic armamentarium of LSCD in the context of their advantages and limitations. It also endeavors to crystallize the clinical approach to a case of LSCD based on the laterality, severity, and resources available.

ETIOLOGY

Pathologies that affect the LESC or their supporting niche can cause LSCD (3). These can be classified as per **Table 1**. Understanding the underlying primary disease process often provides an added perspective into the management of LSCD. Several conditions such as chemical or thermal ocular burns, Stevens-Johnson syndrome (SJS), etc. are one-time insults and usually the treatment approaches are limited to the sequalae that ensue (7). On the other hand, in autoimmune disorders such as mucous membrane pemphigoid (MMP), there is a constant disruption of the systemic and ocular milieu occurring via inflammatory mediators (8). In such cases, addressing the LSCD in isolation invariably has very poor outcomes and so it must be done in conjunction with the management of the systemic pathology. Furthermore, in case of congenital causes of LSCD, treatment options include specific gene targeted therapy which is possible only if a particular type of limbal stem cell transplant (LSCT) is performed. Therefore, it is essential for the treating physician to know the primary disease process in order to make an informed decision and choose the appropriate therapeutic modality on a case-to-case basis.

TABLE 1 | Causes of limbal stem cell deficiency.

Congenital
Congenital aniridia
Multiple endocrine deficiency
Ectodermal dysplasia
Epidermolysis bullosa
Xeroderma pigmentosum
Traumatic/Acquired
Ocular burns (Chemical/thermal)
Post-surgical
Contact lens wear
Radiation
Drug Induced
Autoimmune
Stevens-Johnson syndrome
Mucous membrane pemphigoid
Sjogren's syndrome (Primary and Secondary)
Vernal keratoconjunctivitis
Graft-vs. host disease
Idiopathic

CLINICAL FEATURES

Symptoms

Patients with LSCD present with non-specific symptoms such as ocular redness, discomfort, pain, watering, and photophobia. When the disease is severe enough to involve the visual axis, the complaints extend to blurring or decreased vision (2, 7).

Signs

The diagnosis of LSCD is primarily clinical but needs to be confirmed by one or more objective methods. The clinical findings vary depending upon the severity of the disease. In early cases of LSCD, there may be focal areas of the corneal epithelium which take up the characteristic stippled staining pattern (7). There is loss of clarity within the epithelium, creating a lackluster appearance. The limbal palisades of Vogt, which are usually most easily visible superiorly and inferiorly, may be difficult to discern or may become flattened (**Figure 1**). With the progression of the disease there occurs conjunctivalization of the cornea and superficial corneal vascularization (**Figure 2**) (7, 8). Due to patches of irregular epithelial thinning, a whorl pattern is noted which is better picked up as areas of pooling up of fluorescein(**Figure 3**). These zones also exhibit late staining (7, 8). A sharp demarcation between the abnormal and normal corneal epithelium may also be seen in cases of sectoral involvement (7–9). Epithelial instability is a hallmark of the disease process which manifests as repeated breakdown of the epithelium and in advanced cases this can progress to form a persistent epithelial defect (PED) (7). Recurrent episodes of PEDs can affect the underlying stroma leading to scarring or sterile melts in non-resolving cases (7).

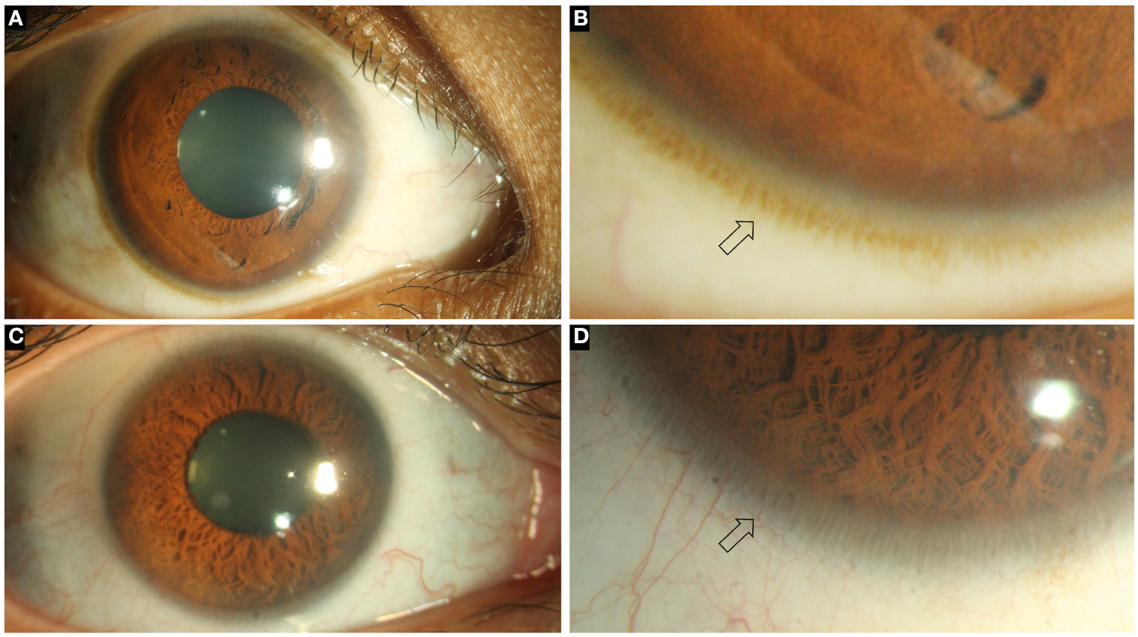

FIGURE 1 | Collage of images depicting the normal ocular surface and limbus (arrows) in pigmented **(A, B)** and hypopigmented **(C, D)** eyes.

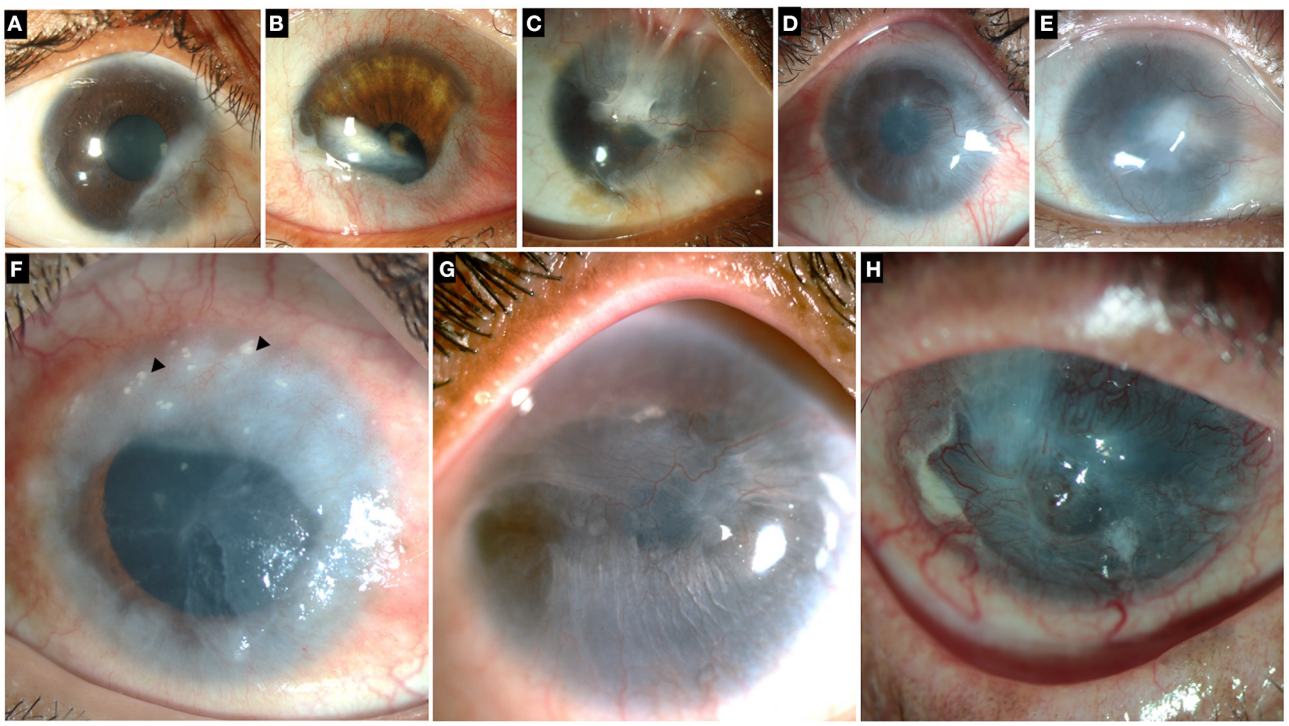

FIGURE 2 | Collage of images illustrating different grades and etiologies of limbal stem cell deficiency (LSCD). Top row: LSCD due to chemical injury which is partial and sparing the visual axis **(A)**, involving the visual axis **(B,C)**. **(D,E)** Total LSCD in chemical injury. **(F)** LSCD in chronic vernal keratoconjunctivitis. Superior cornea shows Horner-Trantas dots (black arrowheads). **(G)** LSCD in Epidermolysis Bullosa **(H)** LSCD in mucous membrane pemphigoid.

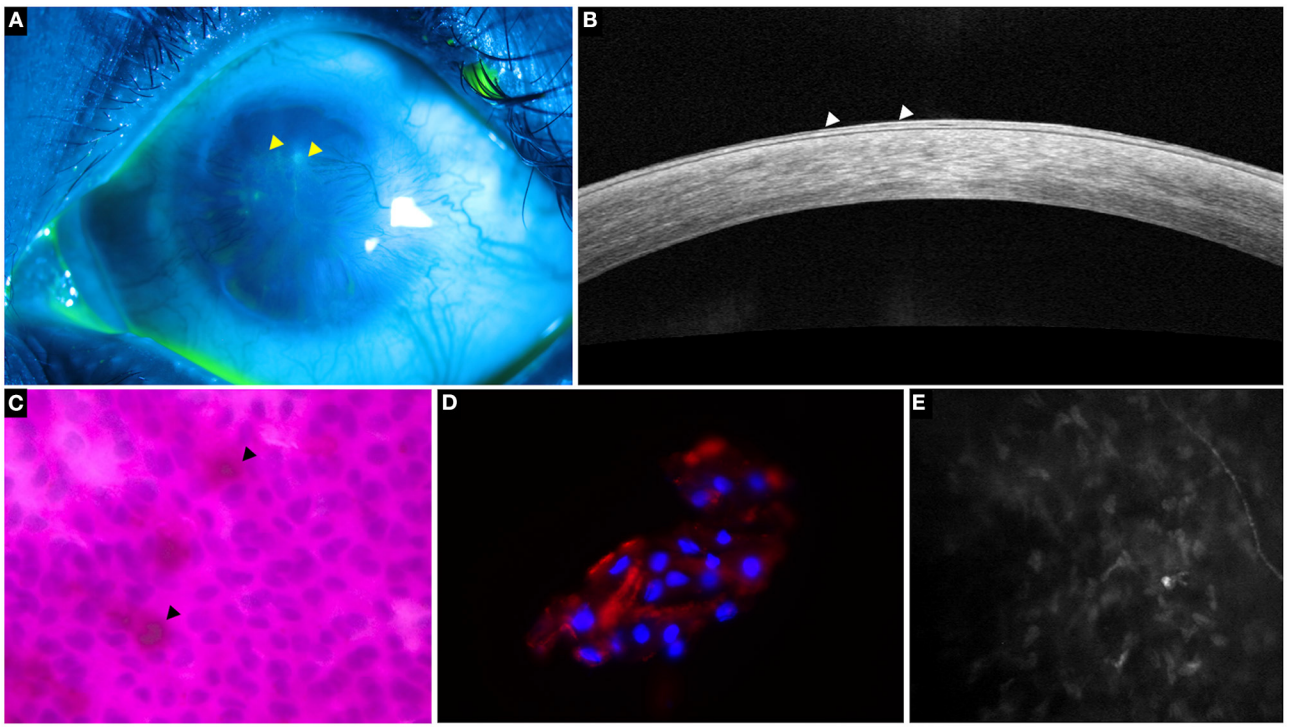

FIGURE 3 | A representative collage of various diagnostic modalities in limbal stem cell deficiency (LSCD). **(A)** Fluorescein-stained image showing characteristic stippled staining (yellow arrowheads). **(B)** Optical coherence tomography line scan showing hyperreflective epithelium indicative of LSCD (white arrowheads). **(C)** Impression cytology depicting Periodic acid-Schiff positive goblet cells (black arrowheads) and CK19 positive cells on immunohistochemistry **(D,E)** *in vivo* confocal microscopy showing decreased sub-basal nerve density.

DIAGNOSTIC INVESTIGATIONS

In cases of severe ocular burns or advanced cicatricial conjunctivitis following SJS, the diagnosis of LSCD can be straightforward. However, in several cases the clinical presentation is subtle and establishing the diagnosis may be challenging. In such cases the ancillary tests mentioned below help supplementing the diagnosis. In addition to confirming the diagnosis, these tests may facilitate the quantification of the disease and provide an understanding of its progression. They also help to confirm the epithelial phenotype following a stem cell transplant and in monitoring the postoperative recovery (10–13).

Impression Cytology

This test involves sampling of the superficial epithelial cells of the ocular surface and subjecting them to histopathological and immunohistochemistry tests. The sample can be obtained from the cornea or the conjunctiva and is usually acquired using a nitrocellulose or cellulose acetate filter paper (14). Although the test typically acquires the superficial corneal and conjunctival cells, repeated sampling in a particular area will facilitate access to the deeper layers as well (14). Following a standardized sampling technique is recommended as this will affect the quantity and quality of tissue obtained (7, 9, 14). Ensuring that the ocular surface is not too wet and that the pore size of the paper is adequate to collect the epithelial cells will also help in improving the yield (9, 15).

Histopathology

The cytology specimen procured undergoes histopathological processing with various stains such as hematoxylin and eosin (H&E), Giemsa, Periodic acid-Schiff, etc (14). These stains detect the presence of goblets cells which indicates the invasion of conjunctival epithelial cells over the surface of the cornea (14). Although the detection of goblet cells is considered the sine qua non of LSCD (**Figure 3**), its absence does not imply a healthy limbus. Also, there may be a decrease in the concentration of goblet cells due to the underlying disease process itself as is the case in SJS (16, 17). As mentioned earlier the sensitivity of the test is largely dependent on the sampling procedure. And so, assessment of the epithelial cells which are also concurrently sampled can enhance the detection rate of LSCD. However, the differentiation of corneal from conjunctival epithelial cells is not possible with the routine stains used and requires immunohistochemistry.

Immunohistochemistry

Several markers have been investigated and of these cytokeratin 12 has been found to be specific for the mature corneal epithelium (7, 18). Although cytokeratin 3 was also considered to be cornea specific, recent studies have found this marker in the conjunctiva

also (19, 20). Cytokeratin 7, 13 and 19 are markers which are specifically expressed in conjunctival epithelial cells while mucin 5AC(MUC5AC) is used for the detection of goblet cells (**Figure 3**) (18, 20–22). However, negative MUC5AC staining has been noted despite positive conjunctival marker staining, signifying the low sensitivity of this marker (18). This fallacy has been subverted with the use of reverse transcriptase polymerase chain reaction test for the detection of MUC5AC which increases the test sensitivity to 98% (23).

Obtaining normal corneal cells through impression cytology is challenging because of the inherent adherence of the cells to each other and the underlying basement membrane. This is in contrast to the conjunctival cells which freely desquamate and so, the presence of an abundance of cellularity can itself indicate the presence of conjunctival cells (18, 20) Since conjunctivalization of the cornea is considered a hallmark of LSCD, the confirmation of conjunctival epithelial cells from a corneal cytology specimen has been deemed sufficient to diagnosis LSCD (**Figure 3**) (20). The subsequent presence of the cytokeratin 12 marker is used to quantify the disease which is considered mild or partial if the corneal marker can still be detected (20). The degree of the fluorescence exhibited by these markers has also been used to quantify the severity of the disease (19, 24).

In-Vivo Confocal Microscopy (IVCM)

IVCM is a non-invasive tool that provides an *in vivo* picture of the microstructures within the cornea. Of the various parameters measured by the device, presence of goblet cells, the basal epithelial measurements of the cornea and limbus along with the changes of the sub-basal nerve plexus are used in the diagnosis of LSCD (**Figure 3**).

Goblet Cells

The presence of goblet cells in a corneal IVCM scan is confirmatory of the diagnosis of LSCD. The detection rate of goblet cells with IVCM closely correlates with that of impression cytology (25). However, as mentioned previously, several factors may affect the detection of goblet cells in a case of LSCD and with an IVCM this is further confounded by the small area that is scanned. Also, the described morphology of a goblet cell is variable with descriptions of both a hypo and hyper-reflective cytoplasm (26–28). Thus, although the detection of goblet cells is feasible with an IVCM, the test has low sensitivity.

Corneal and Limbal Epithelial Changes

A decrease in basal cell density (BCD) with an increase in the size of the cells is noted in patients with LSCD (29–31). This decrease corresponds with the severity of the disease and in advanced cases, there is significant alteration in the morphology of the cells with an increased number of visible hyperreflective cell nuclei (31, 32). Deng et al. found that a BCD value of $<$7930 cells/mm^2 for basal cell density diagnosed LSCD with a 95.5% sensitivity and 100% specificity (31). In cases of partial LSCD, the epithelium in the clinically normal areas maintains the normal pattern on IVCM although there is often an increase in the number of dendritic cells in the underlying stroma (25, 33, 34). A clear demarcation is noted at the junction between the corneal and conjunctival epithelial cells as the two have very distinct morphological features on IVCM (33). Corneal basal cells have a dark cytoplasm with well-defined borders and are much smaller than the conjunctival cells. Intraepithelial cystic lesions with surrounding goblet cells have also been described in cases of LSCD (33). Overall thinning of the epithelium is seen in LSCD (35). A similar pattern of change is noted in the limbal epithelium as well with a decreased BCD which correlates with disease severity (34–36). In cases of partial LSCD, the clinically unaffected areas also exhibit the same changes indicating a pre-clinical method of detection of LSCD (34, 36).

Corneal Nerves Changes

A progressive decrease in the density of the sub-basal plexus of nerves is noted with increasing severity of the disease until a complete nerve drop out occurs (**Figure 3**) (29, 34, 37). Additionally, several other changes have also been reported which include decreased branch length, increased angulation of branching, increased tortuosity, etc (31, 37). A cut off for sub-basal nerve density of 53 nerves/mm^2 resulted in an 87% sensitivity and 91.7% specificity for the diagnosis of LSCD (31). Caro-Magdaleno et al. found that the sub basal nerve density had an inverse association with conjunctivalization and a value of $<$17,215 μm/mm^2 diagnosed LSCD with a 95.5% sensitivity and specificity of 90.6% (38).

Anterior Segment Optical Coherence Tomography (AS-OCT)

AS-OCT is a non-invasive imaging tool that has low operator dependence and yields repeatable results. It has been used to augment the diagnosis of LSCD with its corneal and limbal epithelial measurements. Additionally, with the help of image processing software, the reflectivity from these measurements have been quantified. The role of the angiography feature of OCT for detecting LSCD has also been investigated.

Epithelial Changes

Similar to the IVCM findings, a decrease in both the corneal and limbal epithelial thickness has been observed with AS-OCT in eyes with LSCD (**Figure 3**) (30, 39). Although epithelial thinning is not specific to LSCD and is seen in disease entities such as keratoconus, dry eye, etc.; the degree to which the thinning occurs is different. A 20–30% thinning has been reported in eyes with LSCD, while in other disorders the thinning is $<$10% (35, 39, 40). Liang et al. proposed a new parameter measured as a mean of the central epithelial thickness and thickness measured at two points, 1 mm on either side of the central thickness (39). Values $<$46.6 μm for this parameter were considered diagnostic for LSCD with a sensitivity and specificity of 61.7% and 100% respectively (39).

In addition to measuring the limbal epithelium, the OCT can also provide an *in vivo* visualization of the palisades of Vogt. This is possible even in eyes where the palisades are not visualized clinically (41). Although the IVCM can also image the palisades, the image procurement takes time and requires a skilled and experienced operator whereas the process is much simpler in case of an OCT. Also, as seen with IVCM, in eyes with partial LSCD

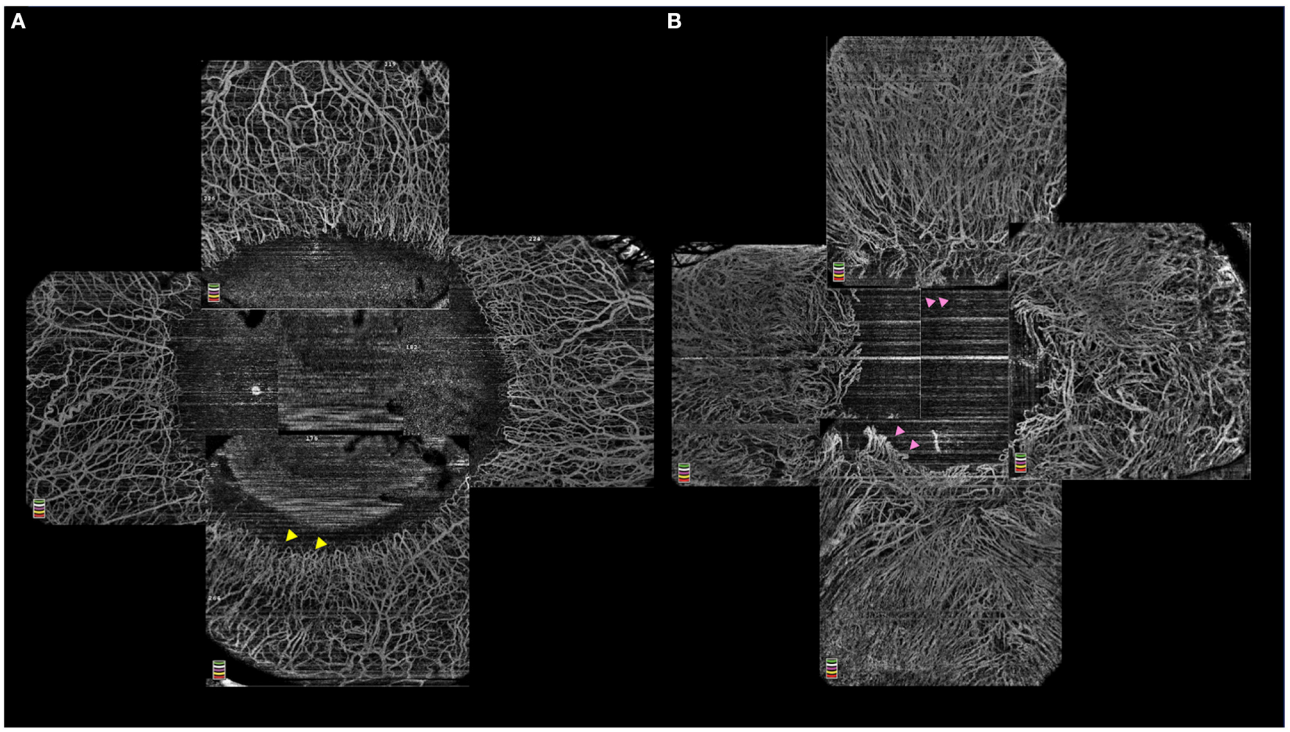

FIGURE 4 | (A) Optical coherence tomography-angiography (OCT-A) illustrating a normal limbal vasculature with hairpin looped limbal vessels (yellow arrowheads) and surrounding normal perilimbal conjunctival and episcleral vessels. **(B)** OCT-A in in limbal stem cell deficiency with vascular invasion of the peripheral corneal and distortion of the annular ring of hairpin looped limbal vessels (pink arrowheads).

the thinning of the limbal epithelium is similar in the affected and unaffected areas (39). This epithelial thickness correlates with the presence of the palisades with significant thinning manifesting when the palisades are absent (42). Volumetric scans of the limbus provide a three dimensional image which can further help quantify the severity of LSCD (43, 44).

Scans from an AS-OCT can be subjected to image processing and thus the epithelial and stromal reflectivity is derived. Varma et al. found the epithelial reflectivity value to be a better indicator of the presence of LSCD than stromal reflectivity (45). They also studied the ratio of these two reflectivities (ES ratio) and proposed a cut off 1.29 to be diagnostic of LSCD with good sensitivity and specificity. Furthermore, a reversal of this ratio following SLET was noted by Kate et al. (12). However the values at the end of one year follow up did not reach the ES ratio seen in normal eyes (12).

OCT Angiography (OCT-A)

The use of the angiography feature of the OCT has been explored in quantifying the changes seen in the limbal vasculature as well as in corneal neovascularization (**Figure 4**) (46, 47). A progressive increase in the density of vascularization and its extent into the cornea has been reported with increasing severity of LSCD (48). Also, OCT-A has been used to differentiate true LSCD from its mimickers which also have corneal vascularization. A significant reduction in vascular density is noted after segmentation of the superficial layers in non-LSCD cases as in these eyes the vessels are usually located within the deep stromal layers (45). When this superficial vascular density values are >0.38, the diagnosis of LSCD can be confirmed with a sensitivity and specificity of 97.9% and 73.8% respectively (45).

CLASSIFICATION

Several classifications have been proposed to grade the severity of LSCD (1, 2, 31, 49). These are based on corneal epithelial thinning, fluorescein staining patterns, presence of neovascularization, fibrovascular pannus, etc. The grading proposed by the Limbal Stem Cell Working Group has divided the corneal involvement into three groups depending on involvement of the central 5 mm of the cornea and these groups have further been subcategorized based on the percentage of limbal involvement (7). These gradations which are based on corneal findings help understand disease severity and assess progression. This is particularly helpful for uniform and standardized documentation for research and monitoring progression or response to therapy. However, the classification does not include adnexal involvement, and this is vital in the decision-making process for the management of these eyes. Hence, classification systems that incorporate the eyelid and conjunctival changes in addition to the corneal ones may better

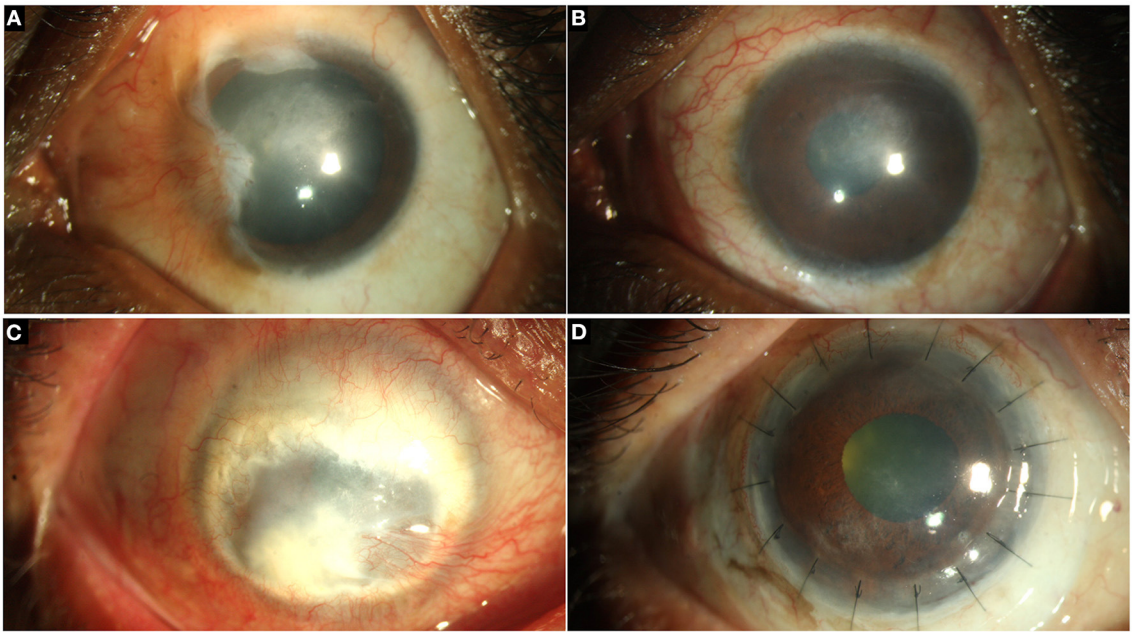

FIGURE 5 | (A) Partial limbal stem cell deficiency (LSCD) following chemical injury managed with conjunctival limbal autograft (CLAu). **(B)** Restoration of a stable ocular surface is noted. **(C)** Total LSCD with leucomatous corneal scarring. **(D)** Reestablishment of an optically clear visual axis and a stable corneal epithelium with deep anterior lamellar keratoplasty and CLAu.

help in delivering appropriate therapy based on the composite disease severity (50).

MANAGEMENT

The management of LSCD includes several surgical and non-surgical options and for each patient the treatment plan has to be tailored to suit the involved eye. However, LSCD rarely occurs in isolation and so the concurrent management of the systemic and ocular comorbidities is vital and often has to precede the surgical management of the disease. This includes systemic immunosuppression in cases of MMP, ocular anti-inflammatory therapy in cases of vernal keratoconjunctivitis, SJS, etc. A component of aqueous deficiency dry eye (ADDE) is usually present in most of these eyes and addressing the same with preservative free lubricants, punctal occlusion, etc. will aid in stabilizing the tear film prior to the surgical intervention.

Several of the comorbidities present with LSCD also require surgical intervention and the sequence of these surgeries often determines the final functional outcome. Ideally, lid and other adnexal issues are addressed prior to the stem cell deficiency. In the presence of significant corneal scarring there is often need for a keratoplasty for visual rehabilitation (**Figure 5**). Although LSCT contributes to stromal remodeling and eventually a decrease in the density of the scar is noted, the degree to which this happens may vary. And so, several of these cases ultimately require a partial or full thickness corneal transplantation to restore an optically clear visual axis.

The management of LSCD can be surgical or non-surgical depending upon the severity of damage to the LESC and the underlying pathology. Based on the clinical presentation, an algorithmic approach can be considered in most of the cases of LSCD (**Figure 6**).

Partial LSCD

In cases of partial LSCD, the decision of surgical intervention is dictated by the involvement of the visual axis (**Figures 2A-C**). If the visual axis is affected, a surgical therapy is required is most cases. However, if the axis is clear, the patient can be followed up at regular intervals to determine if the disease is progressive or stationary. In case of the former, again the eye will require a surgical procedure while in case of the latter the same can be deferred.

Non-surgical Intervention

Eyes with partial LSCD with sparing of the visual axis and documented non-progression of the disease can be observed with regular follow ups. These cases can be visually rehabilitated with glasses or with rigid contact lenses when significant irregular astigmatism is present. Scleral lenses with large vaults are particularly beneficial in such eyes as they provide a fluid layer which addresses the dry eye component in addition to improving the visual acuity (51–53). Lenses which vault over the limbus are preferred as mechanical compression and trauma to the limbal epithelium is prevented (53). Optimizing the fit of the lenses in eyes with LSCD is vital as the resultant hypoxia in eyes with a compromised fit can exacerbate the severity of the LSCD (54).

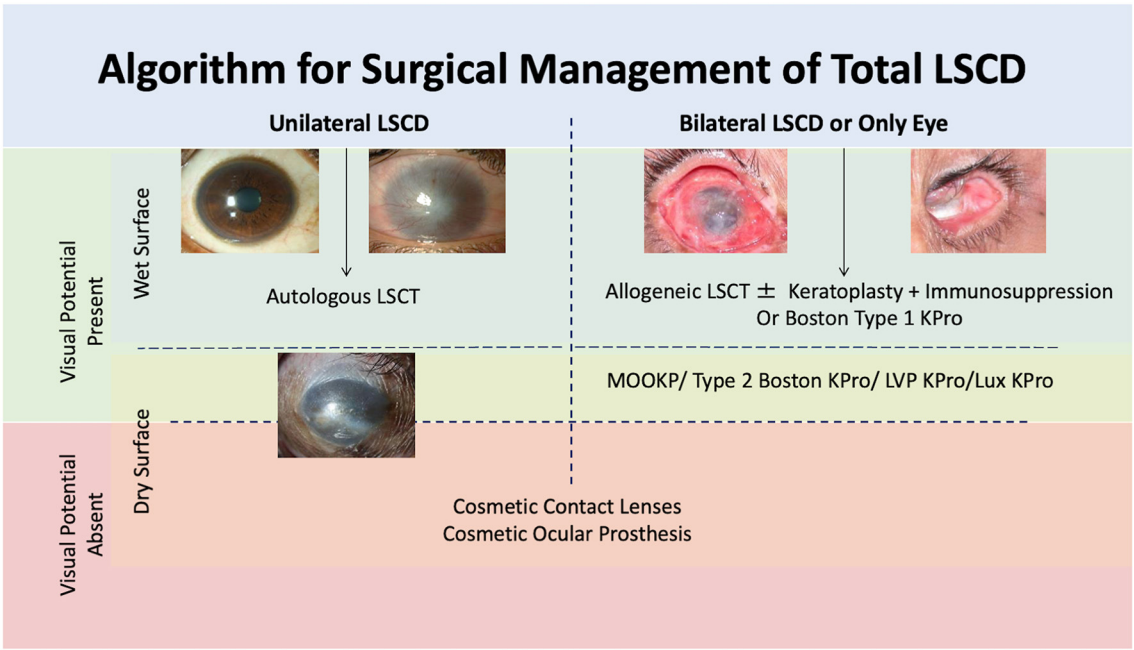

FIGURE 6 | Algorithmic approach of management of limbal stem cell deficiency (LSCD). LSCT: limbal stem cell transplantation, KPro: keratoprosthesis, MOOKP: modified osteo-odontokeratoprosthesis.

Surgical Intervention

When partial LSCD is progressive or involving the visual axis, a surgical procedure is usually carried out to correct the same. The choice of procedure depends upon the involvement of the fellow eye. In unilateral cases an autologous LSCT is preferred where the LESC can be harvested from the contralateral eye or from the uninvolved areas of the same eye. In a comparative series with 70 patients, the outcome in eyes where the LESC were harvested from the same eye was similar to the outcome of eyes with stem cells from the contralateral eye (55). In bilateral cases also an autologous LSCT can be considered if the involved areas are limited to 3-4 clock hours in both eyes (56). Several studies have described the use of an amniotic membrane (AM) alone in the treatment of partial LSCD (57–62). Most of these reports have combined a superficial keratectomy to remove the conjunctival epithelium prior to placing the AM. Although the initial corneal epithelialization rates are good, the ability of the AM to maintain a stable epithelial surface in the long run is poor (58–61, 63). And so, an AM can be used for the temporary restoration of the ocular surface, until a LSCT can be performed. The use of only conjunctival autografts (CAG) has also been described in the treatment of partial LSCD. Shanbhag et al. found a better anatomical success rate with CAG when compared to LSCT in eyes with partial unilateral LSCD (64). Following the treatment of the LSCD, these patients may eventually require rigid contact lenses for visual rehabilitation.

Total LSCD

In eyes with total LSCD, the initial step to determine the therapeutic approach would be to assess the presence of visual potential (**Figure 6**). In eyes with no visual potential, no further intervention is carried out unless there is a need to restore cosmesis in which case a contact lens trial is given, or an ocular prosthesis is implanted. In the presence of visual potential, the status of the fellow eye determines the next course of treatment.

Unilateral Total LSCD

In unilateral cases, if the surrounding adnexa is relatively uninvolved and the ocular surface is wet with a fairly clear corneal stroma, an autologous LSCT is performed. If there are significant cicatricial changes of the conjunctiva, a combined or staged procedure with a conjunctival autograft (in unilateral cases) or mucous membrane graft (in bilateral cases) can be planned (65). Similarly if a lamellar or penetrating keratoplasty (LK or PK) is planned for visual rehabilitation, it can carried out as a one or two step procedure (66–69). Although the grafts maintain clarity in the initial postoperative period after a combined procedure, the rate of rejection is usually higher in these cases and so a staged procedure is preferred (67–70). Whenever possible a LK is favored over a PK as the former lacks a transplanted endothelium and so is associated with lower rates of rejection.

Bilateral Total LSCD

The treatment algorithm for bilateral cases is similar to that of unilateral cases (71). If no dry eye is detected and the conjunctiva and lids are relatively uninvolved, then an allogeneic LSCT is the chosen procedure. In the presence of significant symblephara with adnexal pathologies the choice of LSCT over keratoprosthesis (KPro) depends upon the surgeon's preference.

The former will require multiple procedures to correct the co-morbid pathologies before the LSCD is addressed. Systemic immunosuppression will also be necessary in view of the allogeneic nature of the transplant. A keratoprosthesis will circumvent these issues and offers a one-step procedure with early visual rehabilitation (72). Nevertheless, this technique is associated with several serious sight threatening complications such as glaucoma, retinal detachment, implant extrusion,

TABLE 2 | Brief description of various KPros employed in the management of limbal stem cell deficiency.

	Type of Keratoprosthesis	Structure
Biocompatible KPro	Boston KPro 1 (77)	PMMA optical cylinder fitted with a titanium back plate. Complex is secured with a titanium locking ring
	Boston KPro 2 (78)	Similar to Boston KPro 1-has an additional anterior PPMA segment which projects through the lids
	Auro KPro (79)	Similar to Boston KPro 1 but with a PMMA backplate
	LUX (80)	PMMA optic, titanium backplate and a titanium sleeve
	LVP KPro (81)	Similar to Boston KPro 1 but with a longer optical cylinder which allows tucking of MMG beneath the front plate
	S-KPro (82, 83)	PMMA optic with a polyurethane and polypropylene skirt.
	Lucia KPro (84)	Boston KPro with reduced manufacturing cost by altering the design of the backplate
	Filatov KPro (85)	Titanium frame with two flanges with a PMMA cylinder
	Fyodorov–Zuev KPro (86)	Similar to MICOF KPro but implanted in a single sitting
	MICOF KPro (87)	Titanium frame with two flanges within which a PMMA cylinder is threaded. Auricular cartilage is also used to supplement the implant
Bio-integrable KPro	Pintucci KPro (88)	Central PMMA optic with a peripheral Dacron skirt
	AlphaCor (Chirila KPro) (89)	Made of poly-2-hydroxyethyl methacrylate with different water content in the central clear optical zone and peripheral bio-integrable skirt
	Legeais BioKPro-III	Polytetrafluoroethylene skirt and polyvinylpyrrolidone-coated polydimethylsiloxane optic
Biological KPro	MOOKP (90)	Optical cylinder is embedded in the canine tooth and implanted in a bed of MMG over the ocular surface
	Osteo-KPro (91)	Similar to MOOKP-tibia is used instead of a tooth

KPro, keratoprosthesis; MOOKP, Modified osteo-odonto keratoprosthesis; S-KPro, Seoul keratoprosthesis; MICOF, Moscow Eye Microsurgery Complex in Russia; LVP KPro, LV Prasad Keratoprosthesis.

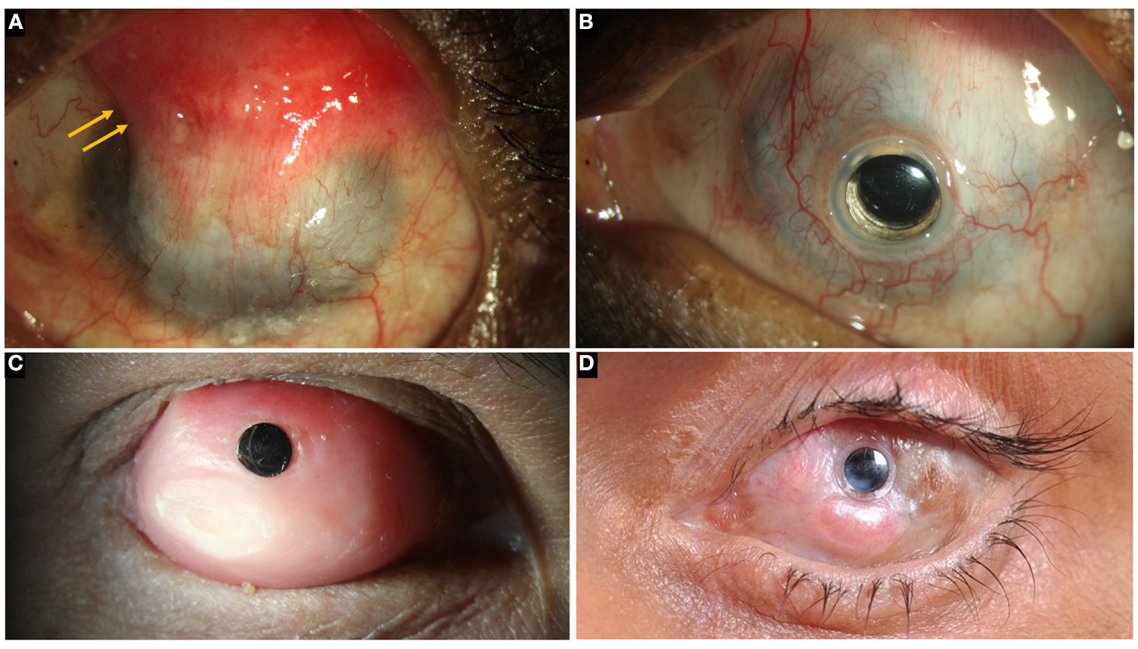

FIGURE 7 | (A) Left eye in a case of bilateral total limbal stem cell deficiency (LSCD) with a wet surface due to Stevens-Johnson syndrome (SJS). A superior conjunctival hooding (yellow arrows) was carried out previously for microbial keratitis with a corneal perforation. **(B)** A Boston keratoprosthesis in the same eye. **(C)** Modified osteo-odontokeratoprosthesis in an eye with total LSCD and a dry ocular surface. **(D)** LVP KPro in an eye with SJS.

TABLE 3 | Comparison of the most commonly used keratoprosthesis in the management of limbal stem cell deficiency.

KPro	Prerequisite*	Number of surgeries required	Outcomes**		
			Follow up years	*Retention rate %*	*Visual Recovery %*
Boston KPro Type 1 (95)	Wet ocular surface	1	5	74	51
AuroKPro (96)	Wet ocular surface	1	5	43	35
Boston KPro Type 2 (78)	Intact lids	1	5.9	50	38
LVP KPro (100)	-	2	2.5	76	36
MOOKP (99, 101)	Adults, healthy oral cavity	2	1	96–100	45–83#

*Prerequisites in addition to being suitable for a KPro.
**Visual recovery is proportion of eyes with vision better than 20/200.
#Proportion of eyes with vision better than 20/60.
KPro, keratoprosthesis.

endophthalmitis, etc (73–75). Thus, KPros are usually reserved for eyes with end stage corneal pathologies or in eyes where prior LSCTs have failed (76).

There are different types of KPros and the choice of one KPro over the other is determined by the presence or absence of ADDE. **Table 2** lists different types of KPros that have been utilized in the management of LSCD. If the surface is wet, a Boston KPro type 1 or Aurolab KPro (auroKPro) is carried out and if the eye has ADDE, then a Boston KPro type 2, LV Prasad KPro (LVP KPro) or modified osteo-odontokeratoprosthesis (MOOKP) is performed (**Figure 7**). The Boston KPro type 1 is the most commonly used prosthesis and has an optical cylinder with a skirt of donor cornea (**Figures 7A,B**). It has good visual outcomes and retention rates especially in eyes with non-autoimmune underlying diseases (74, 75, 77, 92–94) Since the cost of the device is a major inhibitory factor for its use, the auroKPro, its cheaper alternative is a more viable option in low resource settings. Both prosthesis have similar outcomes in terms of visual function, retention rates, and other secondary complications (95, 96).

In case of dry eyes or dermalised ocular surfaces with lid changes, both Boston KPro type 2 and the MOOKP have good functional and anatomical outcomes (90, 97–99). The former is similar to its type 1 counterpart and has a longer cylinder which is exteriorized through lid while the latter has a cylinder embedded in an osteo-dental lamina (**Figure 7C**). However, the surgical procedure for both devices is cumbersome, time consuming and has a steep learning curve. The LVP KPro, which is similar to the Boston KPro with a longer optical cylinder, is implanted as a two staged procedure under a mucous membrane graft used to reconstruct the ocular surface (**Figure 7D**) (78, 100). Its anatomical outcomes are better than those of Boston KPro type 2 but they are not superior than those of MOOKP (78). **Table 3** compares the outcomes of the most commonly used KPros in LSCD.

Transplantation of cultivated oral mucosal epithelium (COMET) is another alternative in eyes with bilateral LSCD where labial or buccal epithelial cells are cultured on an AM and transplanted over the cornea. Studies have reported a stable ocular surface following the procedure however there is a higher risk of persistent epithelial defects, corneal neovascularization and graft rejection when compared to LSCT (81, 102–104). And so, an allogeneic LSCT is considered superior to and is favored over COMET despite the latter being an autologous transplant with no requirement for systemic immunosuppression (104). In a series comparing the outcomes of cell based therapies (CLET, CLAL, COMET) vs. Boston KPro type 1 in cases of bilateral LSCD without ADDE, the KPro group was found to have the best functional outcome at the end of five years (68, 71). However, a recent meta-analysis revealed that in patients undergoing LSCT, nearly 61% maintained a vision of at least 20/200 at end of 2.5 years which is similar to the 64% of patients who had the same vision in the KPro group (105).

Various modifications of the COMET procedure have been proposed which alter the type of carriers used to transfer the cultivated cells. These include the AM, fibrin glue and temperature sensitive polymers. In case of the latter, the polymer is stable at 37°C, however when the temperature drops to 30°C, the cultivated epithelial sheet detaches spontaneously (106, 107). This is in contrast to traditional methods where a carrier or enzymatic detachment is required. Furthermore, biomaterial free sheets have also been used, wherein the cultivated sheet is directly transplanted from the culture plate onto the eye without a carrier for the cells (108, 109). Establishment of a well epithelialized surface have been reported with the use of the same and these outcomes were found to be better than those of COMET with the use of AM as a substrate (108, 109).

As an alternative to cultivation of oral mucosal epithelial cells, which requires the necessary infrastructure, direct transplantation of the oral mucosa has also been described for the management of LSCD (110, 111). The graft is transplanted directly over the limbal area and can re-establish a stable surface and cause regression of neovascularization (110, 111). An additional benefit that the mucosal graft has over conventional LSCT is that adnexal pathologies such as lid margin keratinization or symblephara can be addressed with the same harvested tissue. As the procedure is autologous, no systemic immunosuppression is required. A similar approach has also been reported with the use of nasal mucosal grafts which primarily aim to replenish the goblet cells in the ocular surface (112).

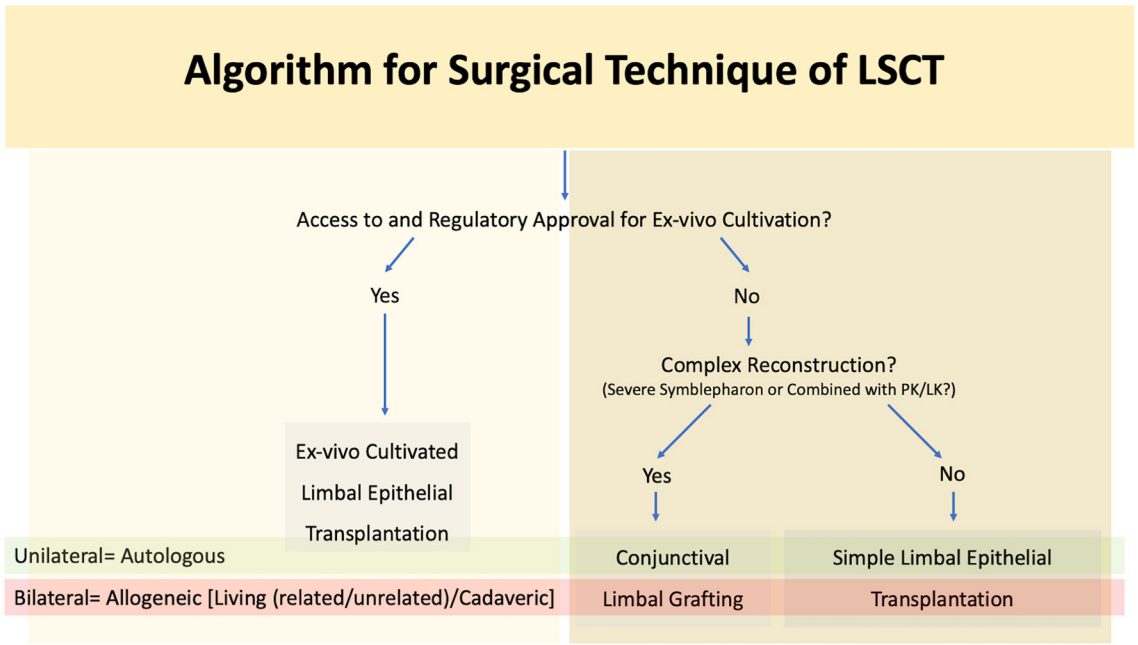

FIGURE 8 | Algorithm for surgical technique of limbal stem cell transplantation (LSCT) PK, penetrating keratoplasty; LK, lamellar keratoplasty.

Technique of LSCT

Types

There are two chief types of LSCT: allogeneic and autologous. These can be further divided into different types based on the anatomical source of the graft which includes conjunctival limbal auto or allograft (CLAu and CLAL), allogeneic keratolimbal allograft (KLAL) or pure limbal tissues as in cases of auto and allogeneic cultivated or simple limbal epithelial transplants (CLET and SLET). In cases of allogeneic LSCT, the donor can be a cadaveric or a living related donor. In pure limbal transplants, once the limbal lenticule is harvested it can be directly transplanted as in SLET where the proliferation of epithelial cells occurs *in vivo* over the corneal surface. Alternatively, the biopsied tissue can be cultivated *in vitro* and then transplanted as a sheet of epithelium as in case of CLET.

Choice of Procedure

As mentioned previously autologous procedures are performed in unilateral cases while allogeneic transplants are reserved for bilateral LSCD (**Figure 8**). The major difference between the two lies in the need for long term systemic immunosuppression for allogeneic LSCT. A combination of corticosteroids and steroid sparing agents are usually given initially, and the patients are then maintained only on the steroid sparing immunosuppressive agent (113, 114) Most of these medications are both expensive and associated with a side effect profile necessitating regular systemic monitoring (113, 114).

The choice of procedure is often determined by the extent of involvement of the surrounding adnexa. A limbal transplant (SLET/CLET for autologous cases, SLET/CLET/KLAL for allogeneic cases) is preferred for LSCD in wet eyes without significant adnexal involvement (**Figure 9**). Access to a laboratory facility with regulatory approval is required for the practice of cultivated stem cells. CLAu or CLAL is preferred in cases where concurrent correction of cicatricial conjunctival changes is also required as seen in eyes with significant symblephara adjacent to a partial LSCD (**Figure 5**). The graft can be harvested from the same eye or fellow eye, depending upon the amount of healthy residual limbus. In the traditional CLAu, a large limbal graft is usually harvested (4-6 clock hours) which can result in an iatrogenic LSCD. To avoid this complication, a mini-CLAu with only 1-2 clock hours of limbal tissue is a viable substitute (66, 115). Alternatively conjunctival tissue can be harvested separately as a CAG along with a pure limbal transplant (CLET/SLET). This combination is usually adopted in eyes with total LSCD and symblephara. **Tables 4**, **5** detail the relative advantages and disadvantages of each of the LSCT procedures.

Comparison of Outcomes

In a systematic review of 1023 eyes, SLET and CLAu were found to have better outcomes than CLET in cases of unilateral LSCD (116). A similar result was seen in a recent meta-analysis where SLET was found to have better functional outcomes when compared to CLET (117). The overall performance of autologous procedures has been deemed to be better than that of allogeneic procedures with the latter having a failure rate of up to 40% (105). The former group of procedures also have a higher percentage of patients with a 2 line improvement in visual acuity following surgery (105).

Ganger et al. found CLET and KLAL to have similar anatomical outcomes, but KLAL fared better than CLET in terms of functional outcomes (117). The cumulative success of KLAL

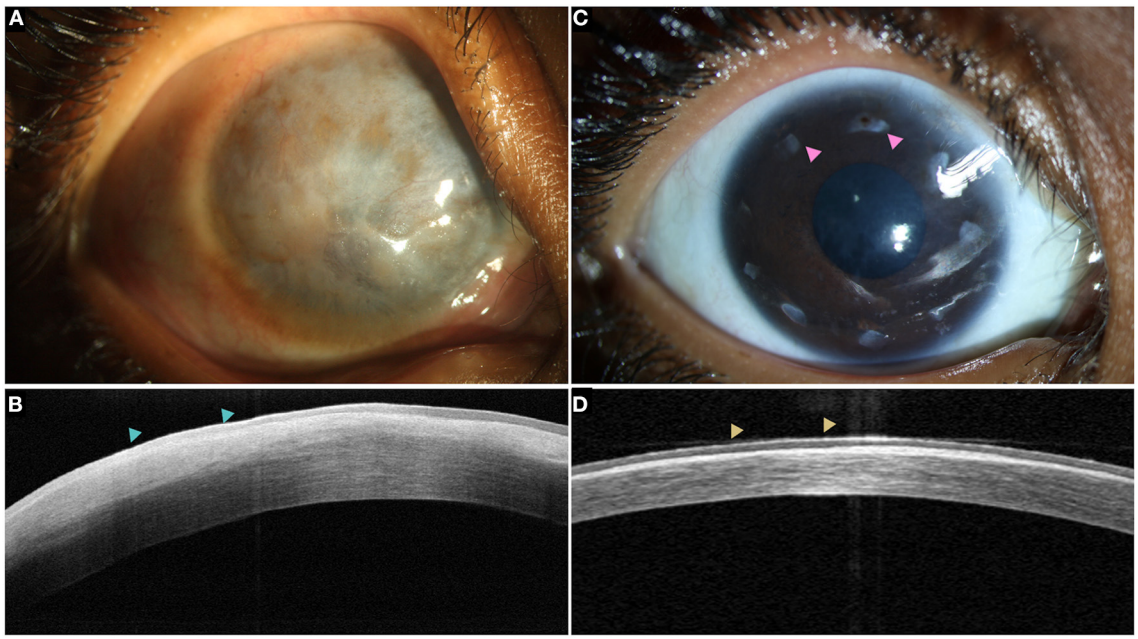

FIGURE 9 | (A) Total LSCD with a thick pannus in a case of chronic vernal keratoconjunctivitis with hyperreflective epithelium (blue arrowheads) on the optical coherence tomography (OCT) line scan **(B)**. **(C)** A stable ocular surface is observed following allogeneic simple epithelial limbal transplantation. The intact limbal tissues are also visible (pink arrowheads). **(D)** Restoration of epithelium with a normal reflectivity is noted on the OCT scan (yellow arrowheads).

TABLE 4 | Comparison of different autologous Limbal stem cell transplantation procedures.

Procedure	Regulatory approval	Laboratory set up	Risk of iatrogenic LSCD in donor eye	Feasibility of a repeat procedure	Number of procedures required
SLET	Not required	Not required	No	Yes	1
CLET	Required	Required	No	Yes	2
CLAu	Not required	Not required	Yes	No	1
Mini-CLAu	Not required	Not required	No	Yes	1

TABLE 5 | Comparison of different allogeneic Limbal stem cell transplantation procedures.

Procedure	Regulatory approval	Laboratory set up	Need for immunosuppression	Feasibility of a repeat procedure	Number of procedures required
SLET	Not required	Not required	Yes	Yes	1
CLET	Required	Required	Yes	Yes	2
CLAL	Not required	Not required	Yes	No	2
KLAL	Not required	Not required	Yes	Yes	1

SLET, simple limbal epithelial transplant; CLET, cultivated limbal epithelial transplant; CLAu, conjunctival limbal autograft; CLAL, conjunctival limbal allograft; KLAL, keratolimbal allograft.

from a systematic review was found to be 63% with 69% of cases having vision better than 20/200 (118). A recent series on allogeneic SLET reported a success rate of 83% and more than 60% of the cases had an improvement in vision which was >20/60 (119). And so, in the context of the expensive nature of CLET with its need for a laboratory set up, KLAL and allogeneic SLET are perhaps the more feasible options in cases of bilateral LSCD. However more studies are required on the long-term outcomes of allogeneic SLET to determine its benefits over other allogeneic procedures. **Table 6** compares the outcomes of different modalities of stem cell transplants.

Recent Advances

The search for new therapies for LSCD is always ongoing because of the need for treatment modalities that do not have the risk of rejection, require immunosuppression, etc. And the epitome of such endeavors would be to arrive at a medical therapy for LSCD. One such intervention was identified serendipitously

TABLE 6 | Comparison of indications and outcomes of different surgical modalities of management of limbal stem cell deficiency.

Surgical Procedure	Tissue transplanted	Indication	Outcomes*	
			Anatomical %	*Functional %*
SLET (120)	LESC	Autologous, Allogeneic LSCD	78, 83	69, 60
CLAu (117)	Conjunctiva+LESC	Autologous LSCD	81	74.4
CLAL/KLAL (118)	Conjunctiva+LESC	Allogeneic LSCD	68	51
CLET (106)	Limbus	Autologous, Allogeneic LSCD	71, 52	65, 65
COMET (102)	Oral mucosal epithelium	Allogeneic LSCD	71	64
Oral mucosa transplantation (112)	Oral mucosa	Allogeneic LSCD	86	71
Nasal mucosa transplantation (113)	Nasal mucosa	Allogeneic LSCD	NA	18

SLET, simple limbal epithelial transplantation; CLET, Cultivated epithelial limbal transplantation; COMET, Cultivated oral mucosal epithelial transplantation; LSCD, limbal stem cell deficiency.

**Anatomical outcomes: defined as a stable, avascular surface.*

Functional outcome: proportion of eyes with vision better than 20/200.

during the treatment of patients with ocular surface neoplasia with interferon α-2b and retinoic acid (120). These cases had partial LSCD which responded to the topical medications. The rationale proposed for the same was that retinoic acid improves corneal wound healing and promotes proliferation of transient amplifying cells while interferon α-2b mediates the healing through its anti-inflammatory function, specifically on macrophages (120).

Another novel technique in the treatment of total LSCD is the amnion-assisted conjunctival epithelial redirection (ACER) which involves the placement of an amniotic membrane over the cornea and limbal explants. The edges of the membrane are tucked under the free edges of the recessed conjunctiva and as a result of this, the conjunctival cells migrate over the membrane (121). This allows the limbal explants under the membrane to proliferate over the surface of the cornea unhindered. Establishment of a stable ocular surface has been reported following this procedure. The use of a modified version of this procedure has also been described for partial LSCD with good outcomes (122).

Novel prosthetic devices such as the Lux and CorNeat keratoprosthesis are being developed as alternatives to LSCT. The former is similar to a traditional Boston KPro with a polymethylmethacrylate cylinder and a titanium backplate (123). This prothesis does not rely on the presence of intact lids which is required for Boston KPro type 2 and has better cosmesis than a MOOKP. Thus the Lux KPro is a viable option for eyes with dry ocular surfaces and LSCD, with good functional vision and retention rates (123). The long term outcomes with this device are awaited. The CorNeat is a true corneal prosthetic device and is structurally different from other KPros. This synthetic cornea has a central PMMA optic and a surrounding porous skirt made of polyurethane fibers (80). The skirt is implanted beneath the conjunctiva where it integrates with the surrounding tissue. Animal models with the CorNeat KPro have shown good retention of the implant while results of human trials are awaited (80).

The use of stems cells obtained from sources other than the LESC is another interesting avenue being explored in the management of LSCD. Of these, limbal mesenchymal stem cells have been best studied and have an established role in corneal wound healing, scar remodeling and angiogenesis (124–127). Its role as a therapeutic option for LSCD is being investigated with a recent clinical trial suggesting that they are as efficacious as CLET in restoring a stable ocular surface (128). Other stem cells that are being studied include those from hair follicles, dental pulp, embryonic stem cells, etc (129–133). Their exact utility and efficacy in LSCD is yet to be determined.

SUMMARY

This review presents an overview of the different diagnostic tests and management modalities in LSCD in order to provide a clinical perspective which will help the physician determine the best course of therapy in cases with LSCD. An in-depth write-up on the pathophysiology of stem cell deficiency is beyond the scope of this review. The diagnosis of limbal stem cell deficiency is often made based on clinical features but can be supplemented by several investigative tools especially when faced with challenging case scenarios. Although both impression cytology and IVCM can confirm the diagnosis of LSCD the expense of the equipment involved, and the skilled personnel required often restrict their use. AS-OCT is a more commonly available device and has several measurable parameters which can be used in the diagnosis of LSCD. However more studies are required to determine the exact diagnostic cut offs. The interpretation of the results of any of these tests must be made in the context of the clinical picture to arrive at the correct diagnosis. Additionally, these investigative modalities have also been used to monitor the response to LSCT and to confirm the restoration of a corneal epithelial phenotype (10, 134–136). Using a combination of clinical and one or more diagnostic tests, a standardized method of validating the outcomes of LSCT can be established.

A comprehensive approach is usually required for the management of LSCD with simultaneous treatment of comorbid ocular and systemic pathologies. Autologous LSCT for unilateral LSCD and allogeneic LSCT for bilateral cases, in the absence of dry eye, are the preferred modalities of therapy which render a stable ocular surface and good visual outcomes. A KPro is favored in more complex cases and provides a rapid visual recovery. The exact choice of procedure is ultimately dependent upon the status of the adnexa, the resources available and the expertise of the surgeon.

AUTHOR CONTRIBUTIONS

AK contributed to the collection of resources, original draft preparation, and revisions of the manuscript. SB contributed to the conceptualization, methodology, supervision, revision, and editing of the manuscript. Both authors contributed to the article and approved the submitted version.

FUNDING

Hyderabad Eye Research Foundation.

REFERENCES

1. Dua HS, Joseph A, Shanmuganathan VA, Jones RE. Stem cell differentiation and the effects of deficiency. *Eye (Lond).* (2003) 17:877–85. doi: 10.1038/sj.eye.6700573
2. Sacchetti M, Lambiase A, Cortes M, Sgrulletta R, Bonini S, Merlo D, et al. Clinical and cytological findings in limbal stem cell deficiency. *Graefes Arch Clin Exp Ophthalmol.* (2005) 243:870–6. doi: 10.1007/s00417-005-1159-0
3. Vazirani J, Nair D, Shanbhag S, Wurity S, Ranjan A, Sangwan V. Limbal stem cell deficiency-demography and underlying causes. *Am J Ophthalmol.* (2018) 188:99–103. doi: 10.1016/j.ajo.2018.01.020
4. Rama P, Matuska S, Paganoni G, Spinelli A, De Luca M, Pellegrini G. Limbal stem-cell therapy and long-term corneal regeneration. *N Engl J Med.* (2010) 363:147–55. doi: 10.1056/NEJMoa0905955
5. Le Q, Samson CM, Deng SX. A case of corneal neovascularization misdiagnosed as total limbal stem cell deficiency. *Cornea.* (2018) 37:1067–70. doi: 10.1097/ICO.0000000000001631
6. Chan E, Le Q, Codriansky A, Hong J, Xu J, Deng SX. Existence of normal limbal epithelium in eyes with clinical signs of total limbal stem cell deficiency. *Cornea.* (2016) 35:1483–7. doi: 10.1097/ICO.0000000000000914
7. Deng SX, Borderie V, Chan CC, Dana R, Figueiredo FC, Gomes JAP, et al. Global consensus on the definition, classification, diagnosis and staging of limbal stem cell deficiency. *Cornea.* (2019) 38:364–75. doi: 10.1097/ICO.0000000000001820
8. Taurone S, Spoletini M, Ralli M, Gobbi P, Artico M, Imre L, et al. Ocular mucous membrane pemphigoid: a review. *Immunol Res.* (2019) 67:280–9. doi: 10.1007/s12026-019-09087-7
9. Sejpal K, Bakhtiari P, Deng SX. Presentation, diagnosis and management of limbal stem cell deficiency. *Middle East Afr J Ophthalmol.* (2013) 20:5–10. doi: 10.4103/0974-9233.106381
10. Le Q, Xu J, Deng SX. The diagnosis of limbal stem cell deficiency. *Ocul Surf.* (2018) 16:58–69. doi: 10.1016/j.jtos.2017.11.002
11. Prabhasawat P, Chirapapaisan C, Ngowyutagon P, Ekpo P, Tangpagasit W, Lekhanont K, et al. Efficacy and outcome of simple limbal epithelial transplantation for limbal stem cell deficiency verified by epithelial phenotypes integrated with clinical evaluation. *Ocul Surf.* (2021) 22:27–37. doi: 10.1016/j.jtos.2021.06.012
12. Pauklin M, Kakkassery V, Steuhl K-P, Meller D. Expression of membrane-associated mucins in limbal stem cell deficiency and after transplantation of cultivated limbal epithelium. *Curr Eye Res.* (2009) 34:221–30. doi: 10.1080/02713680802699408
13. Kate A, Mudgil T, Basu S. Longitudinal changes in corneal epithelial thickness and reflectivity following simple limbal epithelial transplantation: an optical coherence tomography-based study. *Curr Eye Res.* (2022) 47:336–42. doi: 10.1080/02713683.2021.1988985
14. Pauklin M, Steuhl K-P, Meller D. Characterization of the corneal surface in limbal stem cell deficiency and after transplantation of cultivated limbal epithelium. *Ophthalmology.* (2009) 116:1048–56. doi: 10.1016/j.ophtha.2009.01.005
15. Singh R, Joseph A, Umapathy T, Tint NL, Dua HS. Impression cytology of the ocular surface. *Br J Ophthalmol.* (2005) 89:1655–9. doi: 10.1136/bjo.2005.073916
16. Vadrevu VL, Fullard RJ. Enhancements to the conjunctival impression cytology technique and examples of applications in a clinico-biochemical study of dry eye. *CLAO J.* (1994) 20:59–63.
17. Kinoshita S, Kiorpes TC, Friend J, Thoft RA. Goblet cell density in ocular surface disease. a better indicator than tear mucin. *Arch Ophthalmol.* (1983) 101:1284–7. doi: 10.1001/archopht.1983.01040020286025
18. Rivas L, Oroza MA, Perez-Esteban A. Murube-del-Castillo J. Morphological changes in ocular surface in dry eyes and other disorders by impression cytology. *Graefes Arch Clin Exp Ophthalmol.* (1992) 230:329–34. doi: 10.1007/BF00165940
19. Poli M, Burillon C, Auxenfans C, Rovere M-R, Damour O. Immunocytochemical diagnosis of limbal stem cell deficiency: comparative analysis of current corneal and conjunctival biomarkers. *Cornea.* (2015) 34:817–23. doi: 10.1097/ICO.0000000000000457
20. Barbaro V, Ferrari S, Fasolo A, Pedrotti E, Marchini G, Sbabo A, et al. Evaluation of ocular surface disorders: a new diagnostic tool based on impression cytology and confocal laser scanning microscopy. *Br J Ophthalmol.* (2010) 94:926–32. doi: 10.1136/bjo.2009.164152
21. Poli M, Janin H, Justin V, Auxenfans C, Burillon C, Damour O. Keratin 13 immunostaining in corneal impression cytology for the diagnosis of limbal stem cell deficiency. *Invest Ophthalmol Vis Sci.* (2011) 52:9411–5. doi: 10.1167/iovs.10-7049
22. Ramirez-Miranda A, Nakatsu MN, Zarei-Ghanavati S, Nguyen CV, Deng SX. Keratin 13 is a more specific marker of conjunctival epithelium than keratin 19. *Mol Vis.* (2011) 17:1652–61.
23. Liang Q, Le Q, Wang L, Cordova D, Baclagon E, Garrido SG, et al. Cytokeratin 13 is a new biomarker for the diagnosis of limbal stem cell deficiency. *Cornea.* (in press) doi: 10.1097/ICO.0000000000002903
24. García I, Etxebarria J, Merayo-Lloves J, Torras J. Boto-de-Los-Bueis A, Díaz-Valle D, et al. Novel molecular diagnostic system of limbal stem cell deficiency based on MUC5AC transcript detection in corneal epithelium by PCR-reverse dot blot. *Invest Ophthalmol Vis Sci.* (2013) 54:5643–52. doi: 10.1167/iovs.13-11933
25. Pisella PJ, Brignole F, Debbasch C, Lozato PA, Creuzot-Garcher C, Bara J, et al. Flow cytometric analysis of conjunctival epithelium in ocular rosacea and keratoconjunctivitis sicca. *Ophthalmology.* (2000) 107:1841–9. doi: 10.1016/s0161-6420(00)00347-x
26. Araújo AL de, Ricardo JR da S, Sakai VN, Barros JN de, Gomes JÁP. Impression cytology and *in vivo* confocal microscopy in corneas with total limbal stem cell deficiency. *Arq Bras Oftalmol.* (2013) 76:305–8. doi: 10.1590/s0004-27492013000500011
27. Efron N, Al-Dossari M, Pritchard N. *In vivo* confocal microscopy of the bulbar conjunctiva. *Clin Exp Ophthalmol.* (2009) 37:335–44. doi: 10.1111/j.1442-9071.2009.02065.x
28. Hong J, Zhu W, Zhuang H, Xu J, Sun X, Le Q, et al. *In vivo* confocal microscopy of conjunctival goblet cells in patients with Sjogren's syndrome dry eye. *Br J Ophthalmol.* (2010) 94:1454–8. doi: 10.1136/bjo.2009.161059
29. Zhu W, Hong J, Zheng T, Le Q, Xu J, Sun X. Age-Related changes of human conjunctiva on in vivo confocal microscopy. *Br J Ophthalmol.* (2010) 94:1448–53. doi: 10.1136/bjo.2008.155820

30. Bhattacharya P, Edwards K, Harkin D, Schmid KL. Central corneal basal cell density and nerve parameters in ocular surface disease and limbal stem cell deficiency: a review and meta-analysis. *Br J Ophthalmol.* (2020) 104:1633–9. doi: 10.1136/bjophthalmol-2019-315231
31. Banayan N, Georgeon C, Grieve K, Ghoubay D, Baudouin F, Borderie V. *In vivo* confocal microscopy and optical coherence tomography as innovative tools for the diagnosis of limbal stem cell deficiency. *J Fr Ophtalmol.* (2018) 41:e395–406. doi: 10.1016/j.jfo.2018.09.003
32. Deng SX, Sejpal KD, Tang Q, Aldave AJ, Lee OL Yu F. Characterization of limbal stem cell deficiency by *in vivo* laser scanning confocal microscopy: a microstructural approach. *Arch Ophthalmol.* (2012) 130:440–5. doi: 10.1001/archophthalmol.2011.378
33. Nubile M, Lanzini M, Miri A, Pocobelli A, Calienno R, Curcio C, et al. *In vivo* confocal microscopy in diagnosis of limbal stem cell deficiency. *Am J Ophthalmol.* (2013) 155:220–32. doi: 10.1016/j.ajo.2012.08.017
34. Miri A, Alomar T, Nubile M, Al-Aqaba M, Lanzini M, Fares U, et al. *In vivo* confocal microscopic findings in patients with limbal stem cell deficiency. *Br J Ophthalmol.* (2012) 96:523–9. doi: 10.1136/bjophthalmol-2011-300551
35. Chidambaranathan GP, Mathews S, Panigrahi AK, Mascarenhas J, Prajna NV, Muthukkaruppan V. *In vivo* confocal microscopic analysis of limbal stroma in patients with limbal stem cell Ddficiency. *Cornea.* (2015) 34:1478–86. doi: 10.1097/ICO.0000000000000593
36. Chan EH, Chen L, Yu F, Deng SX. Epithelial thinning in limbal stem cell deficiency. *Am J Ophthalmol.* (2015) 160:669–77.e4. doi: 10.1016/j.ajo.2015.06.029
37. Chan EH, Chen L, Rao JY, Yu F, Deng SX. Limbal basal cell density decreases in limbal stem cell deficiency. *Am J Ophthalmol.* (2015) 160:678-684.e4. doi: 10.1016/j.ajo.2015.06.026
38. Chuephanich P, Supiyaphun C, Aravena C, Bozkurt TK Yu F, Deng SX. Characterization of corneal subbasal nerve plexus in limbal stem cell deficiency. *Cornea.* (2017) 36:347–52. doi: 10.1097/ICO.0000000000001092
39. Caro-Magdaleno M, Alfaro-Juárez A, Montero-Iruzubieta J, Fernández-Palacín A, Muñoz-Morales A, Castilla-Martino MA, et al. *In vivo* confocal microscopy indicates an inverse relationship between the sub-basal corneal plexus and the conjunctivalisation in patients with limbal stem cell deficiency. *Br J Ophthalmol.* (2019) 103:327–31. doi: 10.1136/bjophthalmol-2017-311693
40. Liang Q, Le Q, Cordova DW, Tseng C-H, Deng SX. Corneal epithelial thickness measured using AS-OCT as a diagnostic parameter for limbal stem cell deficiency. *Am J Ophthalmol.* (2020) 216:132–9. doi: 10.1016/j.ajo.2020.04.006
41. Mehtani A, Agarwal MC, Sharma S, Chaudhary S. Diagnosis of limbal stem cell deficiency based on corneal epithelial thickness measured on anterior segment optical coherence tomography. *Indian J Ophthalmol.* (2017) 65:1120–6. doi: 10.4103/ijo.IJO_218_17
42. Haagdorens M, Behaegel J, Rozema J, Van Gerwen V, Michiels S, Ní Dhubhghaill S, et al. method for quantifying limbal stem cell niches using OCT imaging. *Br J Ophthalmol.* (2017) 101:1250–5. doi: 10.1136/bjophthalmol-2016-309549
43. Le Q, Yang Y, Deng SX, Xu J. Correlation between the existence of the palisades of Vogt and limbal epithelial thickness in limbal stem cell deficiency. *Clin Exp Ophthalmol.* (2017) 45:224–31. doi: 10.1111/ceo.12832
44. Grieve K, Ghoubay D, Georgeon C, Thouvenin O, Bouheraoua N, Paques M, et al. Three-Dimensional structure of the mammalian limbal stem cell niche. *Exp Eye Res.* (2015) 140:75–84. doi: 10.1016/j.exer.2015.08.003
45. Bizheva K, Hutchings N, Sorbara L, Moayed AA, Simpson T. *In vivo* volumetric imaging of the human corneo-scleral limbus with spectral domain OCT. *Biomed Opt Express.* (2011) 2:1794–1702. doi: 10.1364/BOE.2.001794
46. Varma S, Shanbhag SS, Donthineni PR, Mishra DK, Singh V, Basu S. High-Resolution optical coherence tomography angiography characteristics of limbal stem cell deficiency. *Diagnostics (Basel).* (2021) 11:1130. doi: 10.3390/diagnostics11061130
47. Patel CN, Antony AK, Kommula H, Shah S, Singh V, Basu S. Optical coherence tomography angiography of perilimbal vasculature: validation of a standardised imaging algorithm. *Br J Ophthalmol.* (2020) 104:404–9. doi: 10.1136/bjophthalmol-2019-314030
48. Oie Y, Nishida K. Evaluation of corneal neovascularization using optical coherence tomography angiography in patients with limbal stem cell deficiency. *Cornea.* (2017) 36 Suppl 1:S72–5. doi: 10.1097/ICO.0000000000001382
49. Binotti WW, Nosé RM, Koseoglu ND, Dieckmann GM, Kenyon K, Hamrah P. The utility of anterior segment optical coherence tomography angiography for the assessment of limbal stem cell deficiency. *Ocul Surf.* (2021) 19:94–103. doi: 10.1016/j.jtos.2020.04.007
50. Shortt AJ, Bunce C, Levis HJ, Blows P, Doré CJ, Vernon A, et al. Three-year outcomes of cultured limbal epithelial allografts in aniridia and Stevens-Johnson syndrome evaluated using the clinical outcome assessment in surgical trials assessment tool. *Stem Cells Transl Med.* (2014) 3:265–75. doi: 10.5966/sctm.2013-0025
51. Sotozono C, Ang LPK, Koizumi N, Higashihara H, Ueta M, Inatomi T, et al. New grading system for the evaluation of chronic ocular manifestations in patients with Stevens-Johnson syndrome. *Ophthalmology.* (2007) 114:1294–302. doi: 10.1016/j.ophtha.2006.10.029
52. Parra AS, Roth BM, Nguyen TM, Wang L, Pflugfelder SC, Al-Mohtaseb Z. Assessment of the Prosthetic Replacement of Ocular Surface Ecosystem (PROSE) scleral lens on visual acuity for corneal irregularity and ocular surface disease. *Ocul Surf.* (2018) 16:254–8. doi: 10.1016/j.jtos.2018.01.003
53. Wong BM, Garg A, Trinh T, Mimouni M, Ramdass S, Liao J, et al. Diagnoses and outcomes of prosthetic replacement of the ocular surface ecosystem treatment-a Canadian experience. *Eye Contact Lens.* (2021) 47:394–400. doi: 10.1097/ICL.0000000000000779
54. Harthan JS, Shorter E. Therapeutic uses of scleral contact lenses for ocular surface disease: patient selection and special considerations. *OPTO.* (2018) 10:65–74. doi: 10.2147/OPTO.S144357
55. Bonnet C, Lee A, Shibayama VP, Tseng C-H, Deng SX. Clinical outcomes and complications of fluid-filled scleral lens devices for the management of limbal stem cell deficiency. *Cont Lens Anterior Eye.* (in press) 101528. doi: 10.1016/j.clae.2021.101528
56. Vazirani J, Basu S, Kenia H, Ali MH, Kacham S, Mariappan I, et al. Unilateral partial limbal stem cell deficiency: contralateral versus ipsilateral autologous cultivated limbal epithelial transplantation. *Am J Ophthalmol.* (2014) 157:584–90.e1–2. doi: 10.1016/j.ajo.2013.11.011
57. Sangwan VS, Vemuganti GK, Iftekhar G, Bansal AK, Rao GN. Use of autologous cultured limbal and conjunctival epithelium in a patient with severe bilateral ocular surface disease induced by acid injury: a case report of unique application. *Cornea.* (2003) 22:478–81. doi: 10.1097/00003226-200307000-00016
58. Anderson DF, Ellies P, Pires RT, Tseng SC. Amniotic membrane transplantation for partial limbal stem cell deficiency. *Br J Ophthalmol.* (2001) 85:567–75. doi: 10.1136/bjo.85.5.567
59. Gomes JAP, dos Santos MS, Cunha MC, Mascaro VLD, Barros J de N, de Sousa LB. Amniotic membrane transplantation for partial and total limbal stem cell deficiency secondary to chemical burn. *Ophthalmology.* (2003) 110:466–73. doi: 10.1016/s0161-6420(02)01888-2
60. Kheirkhah A, Casas V, Raju VK, Tseng SCG. Sutureless amniotic membrane transplantation for partial limbal stem cell deficiency. *Am J Ophthalmol.* (2008) 145:787–94. doi: 10.1016/j.ajo.2008.01.009
61. Konomi K, Satake Y, Shimmura S, Tsubota K, Shimazaki J. Long-Term results of amniotic membrane transplantation for partial limbal deficiency. *Cornea.* (2013) 32:1110–5. doi: 10.1097/ICO.0b013e31828d06d2
62. Le Q, Deng SX. The application of human amniotic membrane in the surgical management of limbal stem cell deficiency. *Ocul Surf.* (2019) 17:221–9. doi: 10.1016/j.jtos.2019.01.003
63. Sangwan VS, Matalia HP, Vemuganti GK, Rao GN. Amniotic membrane transplantation for reconstruction of corneal epithelial surface in cases of partial limbal stem cell deficiency. *Indian J Ophthalmol.* (2004) 52:281–5.
64. Sharma N, Mohanty S, Jhanji V, Vajpayee RB. Amniotic membrane transplantation with or without autologous cultivated limbal stem cell transplantation for the management of partial limbal stem cell deficiency. *Clin Ophthalmol.* (2018) 12:2103–6. doi: 10.2147/OPTH.S181035

65. Shanbhag SS, Chanda S, Donthineni PR, Basu S. Surgical management of unilateral partial limbal stem cell deficiency: conjunctival autografts vs. simple limbal epithelial transplantation. *Clin Ophthalmol.* (2021) 15:4389–97. doi: 10.2147/OPTH.S338894
66. Shanbhag SS, Tarini S, Kunapuli A, Basu S. Simultaneous surgical management of unilateral limbal stem cell deficiency and symblepharon post chemical burn. *BMJ Case Rep.* (2020) 13:e237234. doi: 10.1136/bcr-2020-237234
67. Kate A, Basu S. Mini-conjunctival autograft combined with deep anterior lamellar keratoplasty for chronic sequelae of severe unilateral chemical burn: a case report. *Int J Surg Case Rep.* (2021) 88:106508. doi: 10.1016/j.ijscr.2021.106508
68. Fogla R, Padmanabhan P. Deep anterior lamellar keratoplasty combined with autologous limbal stem cell transplantation in unilateral severe chemical injury. *Cornea.* (2005) 24:421–5. doi: 10.1097/01.ico.0000151550.51556.2d
69. Deng SX, Kruse F, Gomes JAP, Chan CC, Daya S, Dana R, et al. Global consensus on the management of limbal stem cell deficiency. *Cornea.* (2020) 39:1291–302. doi: 10.1097/ICO.0000000000002358
70. Omoto M, Shimmura S, Hatou S, Ichihashi Y, Kawakita T, Tsubota K. Simultaneous deep anterior lamellar keratoplasty and limbal allograft in bilateral limbal stem cell deficiency. *Jpn J Ophthalmol.* (2010) 54:537–43. doi: 10.1007/s10384-010-0879-9
71. Basu S, Mohamed A, Chaurasia S, Sejpal K, Vemuganti GK, Sangwan VS. Clinical outcomes of penetrating keratoplasty after autologous cultivated limbal epithelial transplantation for ocular surface burns. *Am J Ophthalmol.* (2011) 152:917–24.e1. doi: 10.1016/j.ajo.2011.05.019
72. Vazirani J, Mariappan I, Ramamurthy S, Fatima S, Basu S, Sangwan VS. Surgical management of bilateral limbal stem cell deficiency. *Ocul Surf.* (2016) 14:350–64. doi: 10.1016/j.jtos.2016.02.006
73. Atallah MR, Palioura S, Perez VL, Amescua G. Limbal stem cell transplantation: current perspectives. *Clin Ophthalmol.* (2016) 10:593–602. doi: 10.2147/OPTH.S83676
74. Goldman DR, Hubschman J-P, Aldave AJ, Chiang A, Huang JS, Bourges J-L, et al. Postoperative posterior segment complications in eyes treated with the Boston type I keratoprosthesis. *Retina.* (2013) 33:532–41. doi: 10.1097/IAE.0b013e3182641848
75. Lee WB, Shtein RM, Kaufman SC, Deng SX, Rosenblatt MI. Boston keratoprosthesis: outcomes and complications: a report by the American academy of ophthalmology. *Ophthalmology.* (2015) 122:1504–11. doi: 10.1016/j.ophtha.2015.03.025
76. Greiner MA Li JY, Mannis MJ. Longer-term vision outcomes and complications with the Boston type 1 keratoprosthesis at the university of California, Davis. *Ophthalmology.* (2011) 118:1543–50. doi: 10.1016/j.ophtha.2010.12.032
77. Shanbhag SS, Saeed HN, Paschalis EI, Chodosh J. Boston keratoprosthesis type 1 for limbal stem cell deficiency after severe chemical corneal injury: a systematic review. *Ocul Surf.* (2018) 16:272–81. doi: 10.1016/j.jtos.2018.03.007
78. Lee R, Khoueir Z, Tsikata E, Chodosh J, Dohlman CH, Chen TC. Long-Term visual outcomes and complications of Boston keratoprosthesis type II implantation. *Ophthalmology.* (2017) 124:27–35. doi: 10.1016/j.ophtha.2016.07.011
79. Sharma N, Falera R, Arora T, Agarwal T, Bandivadekar P, Vajpayee RB. Evaluation of a low-cost design keratoprosthesis in end-stage corneal disease: a preliminary study. *Br J Ophthalmol.* (2016) 100:323–7. doi: 10.1136/bjophthalmol-2015-306982
80. Bakshi SK, Graney J, Paschalis EI, Agarwal S, Basu S, Iyer G, et al. Design and outcomes of a novel keratoprosthesis: addressing unmet needs in end-stage cicatricial corneal blindness. *Cornea.* (2020) 39:484–90. doi: 10.1097/ICO.0000000000002207
81. Basu S, Sureka S, Shukla R, Sangwan V. Boston type 1 based keratoprosthesis (Auro Kpro) and its modification (LVP Kpro) in chronic Stevens Johnson syndrome. *BMJ Case Rep.* (2014) 2014:bcr2013202756. doi: 10.1136/bcr-2013-202756
82. Lee JH, Wee WR, Chung ES, Kim HY, Park SH, Kim YH. Development of a newly designed double-fixed Seoul-type keratoprosthesis. *Arch Ophthalmol.* (2000) 118:1673–8. doi: 10.1001/archopht.118.12.1673
83. Kim MK, Lee SM, Lee JL, Chung TY, Kim YH, Wee WR, et al. Long-Term outcome in ocular intractable surface disease with Seoul-type keratoprosthesis. *Cornea.* (2007) 26:546–51. doi: 10.1097/ICO.0b013e3180415d35
84. Bakshi SK, Paschalis EI, Graney J, Chodosh J. Lucia and beyond: development of an Affordable Keratoprosthesis. *Cornea.* (2019) 38:492–7. doi: 10.1097/ICO.0000000000001880
85. Iakymenko S. Forty-five years of keratoprosthesis study and application at the Filatov Institute: a retrospective analysis of 1 060 cases. *Int J Ophthalmol.* (2013) 6:375–80. doi: 10.3980/j.issn.2222-3959.2013.03.22
86. Ghaffariyeh A, Honarpisheh N, Karkhaneh A, Abudi R, Moroz ZI, Peyman A, et al. Fyodorov-Zuev keratoprosthesis implantation: long-term results in patients with multiple failed corneal grafts. *Graefes Arch Clin Exp Ophthalmol.* (2011) 249:93–101. doi: 10.1007/s00417-010-1493-8
87. Huang Y, Yu J, Liu L, Du G, Song J, Guo H. Moscow eye microsurgery complex in Russia keratoprosthesis in Beijing. *Ophthalmology.* (2011) 118:41–6. doi: 10.1016/j.ophtha.2010.05.019
88. Pintucci S, Pintucci F, Cecconi M, Caiazza S. New dacron tissue colonisable keratoprosthesis: clinical experience. *Br J Ophthalmol.* (1995) 79:825–9. doi: 10.1136/bjo.79.9.825
89. Hicks CR, Crawford GJ, Dart JKG, Grabner G, Holland EJ, Stulting RD, et al. AlphaCor: clinical outcomes. *Cornea.* (2006) 25:1034–42. doi: 10.1097/01.ico.0000229982.23334.6b
90. Falcinelli G, Falsini B, Taloni M, Colliardo P, Falcinelli G. Modified osteo-odonto-keratoprosthesis for treatment of corneal blindness: long-term anatomical and functional outcomes in 181 cases. *Arch Ophthalmol.* (2005) 123:1319–29. doi: 10.1001/archopht.123.10.1319
91. Iyer G, Srinivasan B, Agarwal S, Talele D, Rishi E, Rishi P, et al. Keratoprosthesis: current global scenario and a broad Indian perspective. *Indian J Ophthalmol.* (2018) 66:620–9. doi: 10.4103/ijo.IJO_22_18
92. Hou JH. de la Cruz J, Djalilian AR. Outcomes of Boston keratoprosthesis implantation for failed keratoplasty after keratolimbal allograft. *Cornea.* (2012) 31:1432–5. doi: 10.1097/ICO.0b013e31823e2ac6
93. Ciolino JB, Belin MW, Todani A, Al-Arfaj K, Rudnisky CJ. Boston keratoprosthesis type 1 study group. *retention of the Boston keratoprosthesis type 1: multicenter study results. Ophthalmology.* (2013) 120:1195–200. doi: 10.1016/j.ophtha.2012.11.025
94. Sejpal K, Yu F, Aldave AJ. The Boston keratoprosthesis in the management of corneal limbal stem cell deficiency. *Cornea.* (2011) 30:1187–94. doi: 10.1097/ICO.0b013e3182114467
95. Priddy J, Bardan AS, Tawfik HS, Liu C. Systematic review and meta-analysis of the medium- and long-term outcomes of the boston type 1 keratoprosthesis. *Cornea.* (2019) 38:1465–73. doi: 10.1097/ICO.0000000000002098
96. Shanbhag SS, Senthil S, Mohamed A, Basu S. Outcomes of the Boston type 1 and the aurolab keratoprosthesis in eyes with limbal stem cell deficiency. *Br J Ophthalmol.* (2021) 105:473–8. doi: 10.1136/bjophthalmol-2020-316369
97. Basu S, Serna-Ojeda JC, Senthil S, Pappuru RR, Bagga B, Sangwan V. The aurolab Keratoprosthesis (KPro) vs. the Boston type I Kpro: 5-year clinical outcomes in 134 cases of bilateral corneal blindness. *Am J Ophthalmol.* (2019) 205:175–83. doi: 10.1016/j.ajo.2019.03.016
98. Pujari S, Siddique SS, Dohlman CH, Chodosh J. The Boston keratoprosthesis type II: the Massachusetts eye and ear infirmary experience. *Cornea.* (2011) 30:1298–303. doi: 10.1097/ICO.0b013e318215207c
99. Iyer G, Pillai VS, Srinivasan B, Falcinelli G, Padmanabhan P, Guruswami S, et al. Modified osteo-odonto keratoprosthesis–the Indian experience–results of the first 50 cases. *Cornea.* (2010) 29:771–6. doi: 10.1097/ICO.0b013e3181ca31fc
100. Basu S, Nagpal R, Serna-Ojeda JC, Bhalekar S, Bagga B, Sangwan V. LVP keratoprosthesis: anatomical and functional outcomes in bilateral end-stage corneal blindness. *Br J Ophthalmol.* (2018) 103:592–98. doi: 10.1136/bjophthalmol-2017-311649
101. Basu S, Pillai VS, Sangwan VS. Mucosal complications of modified osteo-odonto keratoprosthesis in chronic Stevens-Johnson syndrome.

Am J Ophthalmol. (2013) 156:867–73.e2. doi: 10.1016/j.ajo.2013.06.012
102. Cabral JV, Jackson CJ, Utheim TP, Jirsova K. *Ex vivo* cultivated oral mucosal epithelial cell transplantation for limbal stem cell deficiency: a review. *Stem Cell Res Ther.* (2020) 11:301. doi: 10.1186/s13287-020-01783-8
103. Satake Y, Dogru M, Yamane G-Y, Kinoshita S, Tsubota K, Shimazaki J. Barrier function and cytologic features of the ocular surface epithelium after autologous cultivated oral mucosal epithelial transplantation. *Arch Ophthalmol.* (2008) 126:23–8. doi: 10.1001/archopht.126.1.23
104. Ma DH-K, Kuo M-T, Tsai Y-J, Chen H-CJ, Chen X-L, Wang S-F, et al. Transplantation of cultivated oral mucosal epithelial cells for severe corneal burn. *Eye (Lond).* (2009) 23:1442–50. doi: 10.1038/eye.2009.60
105. Wang J, Qi X, Dong Y, Cheng J, Zhai H, Zhou Q, et al. Comparison of the efficacy of different cell sources for transplantation in total limbal stem cell deficiency. *Graefes Arch Clin Exp Ophthalmol.* (2019) 257:1253–63. doi: 10.1007/s00417-019-04316-z
106. Le Q, Chauhan T, Yung M, Tseng C-H, Deng SX. Outcomes of limbal stem cell transplant: a meta-analysis. *JAMA Ophthalmol.* (2020) 138:660–70. doi: 10.1001/jamaophthalmol.2020.1120
107. Nishida K, Yamato M, Hayashida Y, Watanabe K, Yamamoto K, Adachi E, et al. Corneal reconstruction with tissue-engineered cell sheets composed of autologous oral mucosal epithelium. *N Engl J Med.* (2004) 351:1187–96. doi: 10.1056/NEJMoa040455
108. Burillon C, Huot L, Justin V, Nataf S, Chapuis F, Decullier E, et al. Cultured autologous oral mucosal epithelial cell sheet (CAOMECS) transplantation for the treatment of corneal limbal epithelial stem cell deficiency. *Invest Ophthalmol Vis Sci.* (2012) 53:1325–31. doi: 10.1167/iovs.11-7744
109. Kim YJ, Lee HJ Ryu JS, Kim YH, Jeon S, Oh JY, Choung HK, et al. Prospective clinical trial of corneal reconstruction with biomaterial-free cultured oral mucosal epithelial cell sheets. *Cornea.* (2018) 37:76–83. doi: 10.1097/ICO.0000000000001409
110. Hirayama M, Satake Y, Higa K, Yamaguchi T, Shimazaki J. Transplantation of cultivated oral mucosal epithelium prepared in fibrin-coated culture dishes. *Invest Ophthalmol Vis Sci.* (2012) 53:1602–9. doi: 10.1167/iovs.11-7847
111. Liu J, Sheha H, Fu Y, Giegengack M, Tseng SC. Oral mucosal graft with amniotic membrane transplantation for total limbal stem cell deficiency. *Am J Ophthalmol.* (2011) 152:739-47.e1. doi: 10.1016/j.ajo.2011.03.037
112. Choe HR, Yoon CH, Kim MK. Ocular surface reconstruction using circumferentially trephined autologous oral mucosal graft transplantation in limbal stem cell deficiency. *Korean J Ophthalmol.* (2019) 33:16–25. doi: 10.3341/kjo.2018.0111
113. Wenkel H, Rummelt V, Naumann GOH. Long term results after autologous nasal mucosal transplantation in severe mucus deficiency syndromes. *Br J Ophthalmol.* (2000) 84:279–84. doi: 10.1136/bjo.84.3.279
114. Kate A, Basu S. Systemic immunosuppression in Cornea and ocular surface disorders: a ready reckoner for ophthalmologists. *Semin Ophthalmol.* (2022) 37:330–44. doi: 10.1080/08820538.2021.1966059
115. Serna-Ojeda JC, Basu S, Vazirani J, Garfias Y, Sangwan VS. Systemic immunosuppression for limbal allograft and allogenic limbal epithelial cell transplantation. *Med Hypothesis Discov Innov Ophthalmol.* (2020) 9:23–32.
116. Kheirkhah A, Raju VK, Tseng SCG. Minimal conjunctival limbal autograft for total limbal stem cell deficiency. *Cornea.* (2008) 27:730–3. doi: 10.1097/QAI.0b013e31815cea8b
117. Shanbhag SS, Nikpoor N, Rao Donthineni P, Singh V, Chodosh J, Basu S. Autologous limbal stem cell transplantation: a systematic review of clinical outcomes with different surgical techniques. *Br J Ophthalmol.* (2020) 104:247–53. doi: 10.1136/bjophthalmol-2019-314081
118. Ganger A, Singh A, Kalaivani M, Gupta N, Vanathi M, Mohanty S, et al. Outcomes of surgical interventions for the treatment of limbal stem cell deficiency. *Indian J Med Res.* (2021) 154:51–61. doi: 10.4103/ijmr.IJMR_1139_18
119. Shanbhag SS, Saeed HN, Paschalis EI, Chodosh J. Keratolimbal allograft for limbal stem cell deficiency after severe corneal chemical injury: a systematic review. *Br J Ophthalmol.* (2018) 102:1114–21. doi: 10.1136/bjophthalmol-2017-311249
120. Shanbhag SS, Patel CN, Goyal R, Donthineni PR, Singh V, Basu S. Simple limbal epithelial transplantation (SLET): review of indications, surgical technique, mechanism, outcomes, limitations, and impact. *Indian J Ophthalmol.* (2019) 67:1265–77. doi: 10.4103/ijo.IJO_117_19
121. Tan JC, Tat LT, Coroneo MT. Treatment of partial limbal stem cell deficiency with topical interferon α-2b and retinoic acid. *Br J Ophthalmol.* (2016) 100:944–8. doi: 10.1136/bjophthalmol-2015-307411
122. Dua HS, Miri A, Elalfy MS, Lencova A, Said DG. Amnion-Assisted conjunctival epithelial redirection in limbal stem cell grafting. *Br J Ophthalmol.* (2017) 101:913–9. doi: 10.1136/bjophthalmol-2015-307935
123. Han SB, Ibrahim FNIM, Liu Y-C, Mehta JS. Efficacy of modified Amnion-Assisted Conjunctival Epithelial Redirection (ACER) for partial limbal stem cell deficiency. *Medicina (Kaunas).* (2021) 57:369. doi: 10.3390/medicina57040369
124. Litvin G, Klein I, Litvin Y, Klaiman G, Nyska A. CorNeat KPro: ocular implantation study in rabbits. *Cornea.* (2021) 40:1165–74. doi: 10.1097/ICO.0000000000002798
125. Al-Jaibaji O, Swioklo S, Connon CJ. Mesenchymal stromal cells for ocular surface repair. *Expert Opin Biol Ther.* (2019) 19:643–53. doi: 10.1080/14712598.2019.1607836
126. Demirayak B, Yüksel N, Çelik OS, Subaşi C, Duruksu G, Unal ZS, et al. Effect of bone marrow and adipose tissue-derived mesenchymal stem cells on the natural course of corneal scarring after penetrating injury. *Exp Eye Res.* (2016) 151:227–35. doi: 10.1016/j.exer.2016.08.011
127. Basu S, Hertsenberg AJ, Funderburgh ML, Burrow MK, Mann MM, Du Y, et al. Human limbal biopsy–derived stromal stem cells prevent corneal scarring. *Sci Transl Med.* (2014) 6:266ra172. doi: 10.1126/scitranslmed.3009644
128. Alio del Barrio JL, Chiesa M, Garagorri N, Garcia-Urquia N, Fernandez-Delgado J, Bataille L, et al. Acellular human corneal matrix sheets seeded with human adipose-derived mesenchymal stem cells integrate functionally in an experimental animal model. *Exp Eye Res.* (2015) 132:91–100. doi: 10.1016/j.exer.2015.01.020
129. Calonge M, Pérez I, Galindo S, Nieto-Miguel T, López-Paniagua M, Fernández I, et al. proof-of-concept clinical trial using mesenchymal stem cells for the treatment of corneal epithelial stem cell deficiency. *Transl Res.* (2019) 206:18–40. doi: 10.1016/j.trsl.2018.11.003
130. Meyer-Blazejewska EA, Call MK, Yamanaka O, Liu H, Schlötzer-Schrehardt U, Kruse FE, et al. From hair to cornea: toward the therapeutic use of hair follicle-derived stem cells in the treatment of limbal stem cell deficiency. *Stem Cells.* (2011) 29:57–66. doi: 10.1002/stem.550
131. Gomes JAP, Geraldes Monteiro B, Melo GB, Smith RL, Cavenaghi Pereira da. Silva M, et al. Corneal reconstruction with tissue-engineered cell sheets composed of human immature dental pulp stem cells. *Invest Ophthalmol Vis Sci.* (2010) 51:1408–14. doi: 10.1167/iovs.09-4029
132. Kushnerev E, Shawcross SG, Sothirachagan S, Carley F, Brahma A, Yates JM, et al. Regeneration of corneal epithelium with dental pulp stem cells using a contact lens delivery system. *Invest Ophthalmol Vis Sci.* (2016) 57:5192–9. doi: 10.1167/iovs.15-17953
133. Kumagai Y, Kurokawa MS, Ueno H, Kayama M, Tsubota K, Nakatsuji N, et al. Induction of corneal epithelium-like cells from cynomolgus monkey embryonic stem cells and their experimental transplantation to damaged cornea. *Cornea.* (2010) 29:432–8. doi: 10.1097/ICO.0b013e3181b9ffcc
134. Ueno H, Kurokawa MS, Kayama M, Homma R, Kumagai Y, Masuda C, et al. Experimental transplantation of corneal epithelium-like cells induced by Pax6 gene transfection of mouse embryonic stem cells. *Cornea.* (2007) 26:1220–7. doi: 10.1097/ICO.0b013e31814fa814
135. Prabhasawat P, Chirapapaisan C, Jiravarnsirikul A, Ekpo P, Uiprasertkul M, Thamphithak R, et al. Phenotypic characterization of corneal epithelium in long-term follow-up of patients post-autologous cultivated oral mucosal epithelial transplantation. *Cornea.* (2021) 40:842–50. doi: 10.1097/ICO.0000000000002498
136. Prabhasawat P, Luangaram A, Ekpo P, Lekhanont K, Tangpagasit W, Boonwong C, et al. Epithelial analysis of simple limbal epithelial transplantation in limbal stem cell deficiency by in vivo confocal

microscopy and impression cytology. *Cell Tissue Bank.* (2019) 20:95–108. doi: 10.1007/s10561-018-09746-3

Conflict of Interest: The authors declare that the research was conducted in the absence of any commercial or financial relationships that could be construed as a potential conflict of interest.

Publisher's Note: All claims expressed in this article are solely those of the authors and do not necessarily represent those of their affiliated organizations, or those of the publisher, the editors and the reviewers. Any product that may be evaluated in this article, or claim that may be made by its manufacturer, is not guaranteed or endorsed by the publisher.

frontiers | Frontiers in Medicine

ORIGINAL RESEARCH
published: 02 June 2022
doi: 10.3389/fmed.2022.831352

Machine Learning to Analyze Factors Associated With Ten-Year Graft Survival of Keratoplasty for Cornea Endothelial Disease

Marcus Ang[1,2,3], Feng He[2], Stephanie Lang[1], Charumathi Sabanayagam[2,3], Ching-Yu Cheng[2,3], Anshu Arundhati[1,2,3] and Jodhbir S. Mehta[1,2,3]*

[1] Singapore National Eye Centre, Singapore, Singapore, [2] Singapore Eye Research Institute, Singapore, Singapore, [3] Department of Ophthalmology and Visual Sciences, Duke-NUS Medical School, Singapore, Singapore

Purpose: Machine learning analysis of factors associated with 10-year graft survival of Descemet stripping automated endothelial keratoplasty (DSAEK) and penetrating keratoplasty (PK) in Asian eyes.

Methods: Prospective study of donor characteristics, clinical outcomes and complications from consecutive patients (n = 1,335) who underwent DSAEK (946 eyes) or PK (389 eyes) for Fuchs' endothelial dystrophy (FED) or bullous keratopathy (BK) were analyzed. Random survival forests (RSF) analysis using the highest variable importance (VIMP) factors were determined to develop the optimal Cox proportional hazards regression model. Main outcome measure was 10-year graft survival with RSF analysis of factors associated with graft failure.

Results: Mean age was 68 ± 11 years, 47.6% male, in our predominantly Chinese (76.6%) Asian cohort, with more BK compared to FED (62.2 vs. 37.8%, $P < 0.001$). Overall 10-year survival for DSAEK was superior to PK (73.6 vs. 50.9%, log-rank $P < 0.001$). RSF based on VIMP (best Harrell C statistic: 0.701) with multivariable modeling revealed that BK (HR:2.84, 95%CI:1.89–4.26; $P < 0.001$), PK (HR: 1.64, 95%CI:1.19–2.27; $P = 0.002$), male recipients (HR:1.75, 95%CI:1.31–2.34; $P < 0.001$) and poor pre-operative visual acuity (HR: 1.60, 95%CI:1.15–2.22, $P = 0.005$) were associated with graft failure. Ten-year cumulative incidence of complications such as immune-mediated graft rejection ($P < 0.001$), epitheliopathy ($P < 0.001$), and wound dehiscence ($P = 0.002$) were greater in the PK compared to the DSAEK group.

OPEN ACCESS

Edited by:
Eray Atalay, Eskişehir Osmangazi University, Turkey

Reviewed by:
Darren Shu Jeng Ting, University of Nottingham, United Kingdom
Laura Gutierrez, Singapore Eye Research Institute (SERI), Singapore
Ali Riza Cenk Celebi, Acıbadem University, Turkey

***Correspondence:**
Marcus Ang
marcus.ang@snec.com.sg

Specialty section:
This article was submitted to Ophthalmology, a section of the journal Frontiers in Medicine

Received: *08 December 2021*
Accepted: *28 April 2022*
Published: *02 June 2022*

Citation:
Ang M, He F, Lang S, Sabanayagam C, Cheng C-Y, Arundhati A and Mehta JS (2022) Machine Learning to Analyze Factors Associated With Ten-Year Graft Survival of Keratoplasty for Cornea Endothelial Disease. Front. Med. 9:831352. doi: 10.3389/fmed.2022.831352

Conclusion: In our study, RSF combined with Cox regression was superior to traditional regression techniques alone in analyzing a large number of high-dimensional factors associated with 10-year corneal graft survival in Asian eyes with cornea endothelial disease.

Keywords: machine learning, keratoplasty, graft survival, endothelial (dys)function, penetrating keratoplasty

INTRODUCTION

Corneal transplantation is currently the most frequently performed type of transplant worldwide (1), with corneal endothelial diseases as the leading surgical indication (2). Today, endothelial keratoplasty (EK) has replaced penetrating keratoplasty (PK) as the corneal transplantation of choice for endothelial disease in the United States (3), and increasingly in the rest of the world (4). Currently, Descemet stripping automated endothelial keratoplasty (DSAEK) is the most popular EK technique, supported by eye banks providing pre-cut donor tissue (5). The short-term advantages of DSAEK over PK are related to its minimally invasive approach—avoiding a full-thickness wound that requires sutures, thereby reducing the risk of intraoperative sight-threatening complications, suture-related problems, graft rejection and potential wound dehiscence (6). Thus, faster visual rehabilitation can be achieved, with reduced post-operative corneal astigmatism and potentially superior visual outcomes (7).

However, long-term outcomes of DSAEK compared to the traditional PK in terms of graft survival and complications such as graft rejection still vary in the published literature. Long-term studies from the Asia-Pacific (8, 9) and Europe (10) support the advantages of DSAEK over PK, but national registries in the United Kingdom (11) and Australia (12), have suggested poorer survival outcomes for DSAEK compared to PK for the same indications. While registries reflect "real-world" data from multiple centers with varying surgical techniques and surgeon experience (12), outcomes from such studies are often confounded by differences in donor characteristics or recipient populations, which may be not well delineated (13). Thus, there is an unmet need for long-term studies that directly compare DSAEK and PK outcomes from a variety of populations (14).

A randomized controlled trial is not always feasible to compare DSAEK and PK, and outcomes from registry studies are valuable in providing representative results by including a large number of cases performed by several surgeons (14). However, cornea graft registries often collect a large number of variables generating enormous datasets over time, which can be difficult to analyze using traditional statistical techniques such as Kaplan-Meier survival and Cox proportional hazards regression analyses. Random forests is a machine-learning technique that is gaining popularity to analyze large datasets with less restrictive assumptions, and random survival forests (RSF) can be used to analyze high-dimensional graft survival data (15, 16). This potentially allows us to study a larger number of factors that influence graft survival outcomes with comparable or even better prediction measures. Thus, we used this machine learning method to examine the large database of outcomes prospectively collected from the Singapore Cornea Transplant Registry over 10 years, to examine factors associated with graft failure comparing PK and DSAEK for corneal endothelial diseases.

MATERIALS AND METHODS

We collated all the data from our ongoing prospective Singapore Corneal Transplant Study (SCTS) cohort, which tracks all patients who have underwent a cornea transplant through an annual audit (17). Our inclusion and exclusion criteria have been previously described (18), and in this study we included all consecutive patients with either FED or BK who underwent either a primary DSAEK or PK for optical indications, excluding re-grafts and patients requiring systemic immunosuppresion (19). All corneal surgeons from the Singapore National Eye Center performed all surgeries over the same time period (1999–2011), which included cases performed or partially performed by numerous local or international corneal fellows in training under direct supervision. All data collected in this registry audit include patient demographics, diagnosis, details of surgeries including intra-operative complications, pre- and post-operative best-corrected LogMar visual acuity (BCVA), clinical outcomes and post-operative complications (18).

Our main outcome measure was graft survival, where graft failure was defined as irreversible loss of optical clarity, sufficient to compromise vision for a minimum of three consecutive months (20). Complications were monitored and recorded such as primary graft failure, graft rejection, and graft-related infections as previously defined (21). Graft rejection was defined as presence of an endothelial rejection line or inflammation (keratic precipitates, cells in the stroma, or an increase in aqueous cells from a previous visit, with or without any clinically apparent change in recipient stromal thickness or clarity) in the absence of an endothelial rejection line in a previously clear graft. Endothelial cell counts were performed by certified ophthalmic technicians using a non-contact specular microscope (Konan Medical Corp, Hyogo, Japan) as previously decribed (22). Our study followed the principles of the Declaration of Helsinki, with ethics approval obtained from our local Institutional Review Board (SingHealth Centralized IRB, R847/42/2011).

Surgical Technique

Essentially, PK surgeries were performed using a standard technique previously described (18), with a Hanna vacuum trephine system (Moria Inc, Antony, France). Briefly, the recipient cornea was first excised using the Hanna trephine system. A 0.25- to 0.50-mm oversized donor cornea then was punched out endothelial side up and sutured on to

TABLE 1 | Baseline characteristics of study cohort comparing penetrating keratoplasty (PK) and Descemet stripping automated endothelial keratoplasty (DSAEK) from the Singapore Cornea Transplant Registry.

Characteristics		Corneal Graft		*P* value*
	Total (*n* = 1,335)	PK (*n* = 389)	DSAEK (*n* = 946)	
Mean age, years (± SD)	68.3 ± 11.4	67.4 ± 12.0	68.7 ± 11.1	0.212
Gender (%)				
Male	635 (47.6)	191 (49.1)	444 (46.9)	0.509
Female	700 (52.4)	198 (50.9)	502 (53.1)	
Race (%)				
Chinese	1,023 (76.6)	306 (78.7)	717 (75.8)	0.515
Malay	63 (4.7)	20 (5.1)	43 (4.5)	
Indian	70 (5.2)	18 (4.6)	52 (5.5)	
Others	179 (13.4)	45 (11.6)	134 (14.2)	
Surgical indication				
Fuchs Dystrophy (FED)	504 (37.8)	93 (23.9)	411 (43.4)	<0.001
Bullous Keratopathy (BK)	831 (62.2)	296 (76.1)	535 (56.6)	
Baseline/preoperative				
Visual Acuity (logMAR) (mean, SD)	1.24 ± 0.58	1.57 ± 0.45	1.10 ± 0.57	<0.001
Endothelial cell counts (cells/mm^2, SD)	2,819 ± 281	2,704 ± 340	2,865 ± 237	<0.001

PK, penetrating keratoplasty; DSAEK, Descemet's stripping automated endothelial keratoplasty; SD, standard deviation.
**P value from Mann–Whitney test or chi-square test as appropriate.*

the recipient with 10-0 nylon, using either 8-bite, 10-0 nylon double continuous running suture or a combination of a single 8-bite 10-0 nylon continuous and 8 interrupted sutures. All DSAEK surgeries were performed using pull-through techniques as previously described (23). Donors were prepared by the surgeon or eye bank technician using an automated lamellar therapeutic keratoplasty system (ALTK, Moria SA, Antony, France). Essentially, after recipient Descemets membrane stripping, insertion of anterior chamber (AC) maintainer and preplaced venting incisions, a DSAEK forceps (ASICO, IL, United States) was used to pull the donor cornea through the scleral incision using a sheets glide (BD Visitec) (23), or a donor inserter device (Endoglide, Network Medical Products, North Yorkshire, United Kingdom) (24). An inferior peripheral iridectomy was performed through a limbal stab incision. Wounds were secured with 10/0 nylon interrupted sutures, and a full air tamponade under slight compression was achieved with a large bubble in the AC for varying periods of time, ranging from 2 to 8 min, while removing interface fluid from the venting incisions. For both PK and DSAEK surgeries a bandage contact lens was placed at the end, and dexamethasone (0.1%) (Merck & Co Inc, Rahway, NJ, United States), gentamicin (14 mg/ml, Schering AG, Berlin-Wedding, Germany), and cefazolin (50 mg/ml, GlaxoSmithKline, NC, United States) was injected subconjunctivally after all surgeries. All PK and DSAEK patients received a standard post-operative regime: topical antibiotic (levofloxacin 0.5%, Santen, Osaka, Japan) and topical prednisolone acetate ophthalmic suspension 1% (Allergan, Marlow, United Kingdom) three hourly for a month, four times daily for 2 months, which was tapered by one drop per 3 month down to 1 drop per day dosing by one year, and thereafter continued indefinitely.

Statistical Analysis

For the current study, 49 variables from SCTS audit were identified by literature review for their potential relevance to the graft failure, including donor and recipient demographics, clinical data (visual acuity, ocular findings, etc.), and operative data (primary procedure, secondary procedure, donor/recipient sizes, surgical complications, etc.) (**Supplementary Table 1**). We used a RSF machine learning algorithm for multivariate survival analysis to detect important linear, non-linear, and interaction effects among variables (25). These variables were fed into a RSF model consisting of 10,000 trees, where each tree was grown using the log-rank splitting rule on a random sample of 63.2% of the original population by default, with additional RSF parameters (e.g., node size, number of variables to try at each potential split) tuned using a greedy approach to minimize the out-of-bag (OOB) error rate, that is, the error rate using the remaining data not used for model training (25). We then ranked top variables and pair-wise interactions according to their VIMP scores (larger VIMP indicates greater importance for a successful prediction model). Based on VIMP ranking, we then analyzed a sequence of nested Cox regression models using the top 15 variables, among which the model using best variables that achieved the best OOB Harrell C statistic (OOB C-index) will be used. Simply, the OOB C-index is a validation score that estimates the prediction error of random forests (25). Multivariate Cox proportional hazards regression analysis based on this model was used to describe the factors associated with graft failure represented using hazard ratios (HR) and its relative 95% confidence interval (95% CI). Proportional hazard assumption was validated using both individual and global Schoenfeld Test. We used penalized splines from R package survival to assess non-linearity for all continuous variables in the nested Cox regression models. Kaplan–Meier (KM) survival analysis was conducted to compare 10-year survival probabilities of PK and DSAEK groups. Complications were recorded prospectively in our Singapore Cornea Transplant Registry database and represented as a cumulative incidence rate during the follow-up period of 10 years (17). A P-value <0.05 was considered statistically significant. The analysis was conducted using R, version 4.0.2 (R Foundation for Statistical Computing) with the *randomForestSRC* package (26, 27).

RESULTS

We analyzed 1,335 consecutive patients who underwent either PK (389 eyes) or DSAEK (946 eyes) based on our inclusion criteria. Overall mean age was 68 ± 11 years, 47.6% male, in our predominantly Chinese (76.6%) Asian cohort with no significant

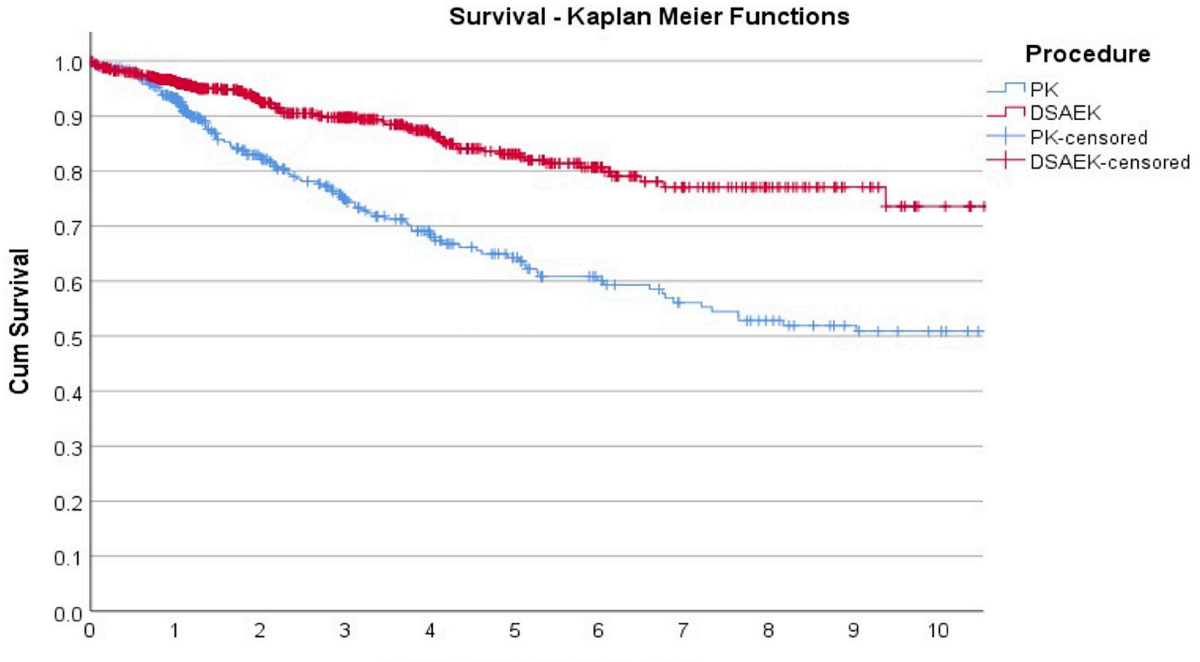

	PK		DSAEK	
Year	N	%	N	%
1	374	93.2%	920	96.2%
2	296	82.5%	700	92.4%
3	199	74.8%	412	89.7%
4	152	68.5%	323	87.0%
5	121	64.3%	224	83.1%
10	51	50.9%	27	73.6%

Kaplan Meier Survival comparing penetrating keratoplasty (PK) with Descemet stripping automated endothelial keratoplasty (DSAEK) log-rank P<0.001

FIGURE 1 | Kaplan–Meier graft survival curves demonstrated superior 5- and 10-year graft survival comparing Descemet stropping automated endothelial keratoplasty (DSAEK) to penetrating keratoplasty (PK), N = number of grafts analyzed (log-rank *P*-value < 0.001).

differences in these baseline demographics in our PK and DSAEK groups (**Table 1**). We had a higher proportion of patients with BK compared to FED (62.2 vs. 37.8%, $P < 0.001$) in our study cohort (**Supplementary Table 2**). Five-year cumulative graft survival was superior for DSAEK compared to PK (83.1 vs. 64.3%)—log-rank *P* value < 0.001; while 10-year cumulative graft survival was superior for DSAEK compared to PK (73.6 vs. 50.9%)—log-rank *P* value < 0.001 in the remaining surviving grafts ($n = 78$) (**Figure 1**). Sub-group analysis also revealed significantly superior 10-year survival comparing DSAEK to PK in the BK (57.5 vs. 43.1%, $P < 0.001$) and FED (89.2 vs. 68.1%, $P < 0.001$) groups (**Figure 2**).

We ranked top variables and pair-wise interactions according to their VIMP scores (**Figure 3**) to develop a sequence of nested Cox regression models using the top 15 variables, among which we chose the model with the best variables (diagnosis, procedure, gender, pre-operative visual acuity, and donor endothelial cell count) that achieved the highest OOB C-index of 0.701 on 3,000 bootstrap samples. Using likelihood-ratio tests for nested models, no significant improvement was observed on the model performance after including additional variables (**Supplementary Figure 1**). Multivariate Cox proportional hazards regression was performed for the top VIMP factors identified by the RSF model that achieved the best OOB Harrell C statistic, i.e., diagnosis (surgical indication, i.e., BK or FED), procedure (surgical technique, i.e., PK or DSAEK), gender, pre-operative visual acuity and donor endothelial cell count was performed (**Table 2**). We found that BK was a significant factor associated with graft failure (HR: 2.84 95%CI 1.89–4.26; $P < 0.001$) compared to FED and PK was a significant factor associated with graft failure more likely to fail compared to DSAEK (HR: 1.64 95%CI 1.19–2.27; $P = 0.002$).

Overall, we observed a greater 10-year cumulative incidence of complications in the PK compared to DSAEK group (**Table 3**). Five-year endothelial cell loss was greater in PK compared to DSAEK (67.6 ± 10.7% vs. 53.3 ± 21.0%, $P = 0.011$), as our study was not adequately powered to compare 10-year endothelial cell loss between groups. Complications such as graft rejection

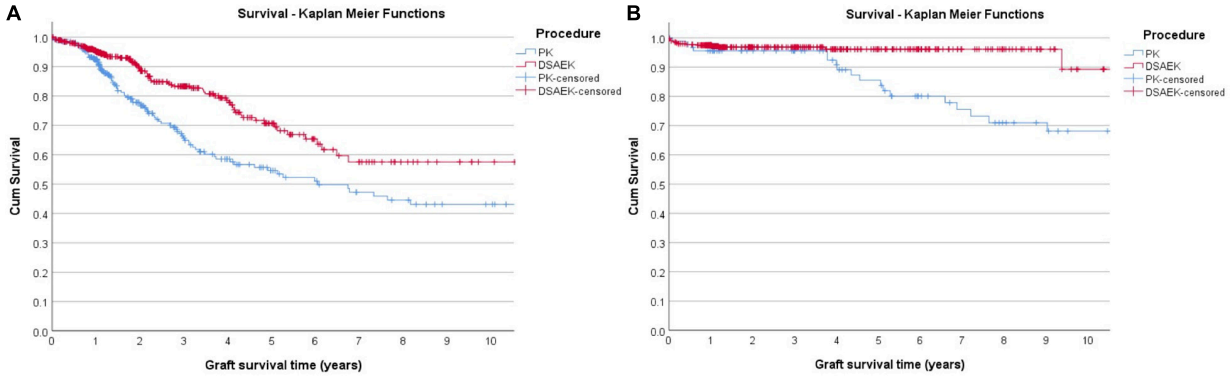

A. BK	PK		DSAEK	
Year	N	%	N	%
1	282	92.4%	518	95.2%
2	214	77.2%	376	88.5%
3	128	65.6%	207	83.3%
4	87	58.5%	153	78.5%
5	65	54.6%	100	70.7%
10	26	43.1%	10	57.5%

Bullous keratopathy (BK) comparing penetrating keratoplasty (PK) and Descemet stripping automated endothelial keratoplasty (DSAEK) log-rank P<0.001

B. FED	PK		DSAEK	
Year	N	%	N	%
1	92	95.6%	402	97.5%
2	82	95.6%	324	96.8%
3	71	95.6%	205	96.8%
4	65	90.8%	170	96.1%
5	56	85.5%	124	96.1%
10	25	68.1%	17	89.2%

Fuchs endothelial dystrophy (FED) comparing penetrating keratoplasty (PK) and Descemet stripping automated endothelial keratoplasty (DSAEK) log-rank P<0.001

FIGURE 2 | Kaplan Meier graft survival curves demonstrated superior 10-year graft survival comparing Descemet stropping automated endothelial keratoplasty (DSAEK) to penetrating keratoplasty (PK) in eyes (N = number of grafts analyzed) with **(A)** bullous keratopathy (BK, log-rank P < 0.001) and **(B)** Fuchs endothelial dystrophy (FED, log-rank $P < 0.001$).

(9.5 vs. 4.2%, $P < 0.001$) and corneal epitheliopathy (11.6 vs. 2.5%, $P < 0.001$) were significantly greater in PK compared to DSAEK. There was a greater incidence of transient intraocular pressure (IOP) elevation (as previously defined, i.e., short-term IOP readings > 21 mmHg with ≤ 3 months use of anti-glaucoma medications) comparing PK and DSAEK (26.0 vs. 20.8%, $P = 0.04$). Complications such as wound dehiscence was unique to PK ($P < 0.001$) and graft detachment was unique to DSAEK ($P < 0.001$).

DISCUSSION

The Singapore Cornea Transplant Registry prospectively collects a large database of variables and outcomes as an audit of multiple surgeons of various surgical experience, practicing with standardized surgical techniques and post-operative management (28). Traditionally, we have used statistical methods such as Kaplan-Meier survival with the log-rank test to analyze graft outcomes, which is only able to examine only one variable at a time (29). While Cox proportional hazards regression analysis can analyze multiple factors associated with graft survival, the various stepwise (e.g., backward or forward) variable selection methods often lead to well-described limitations (30). Random forests is gaining popularity as a machine learning technique that is able to handle big data with more flexibility in modeling non-linear effects with interactions, for regression and prediction tasks (15, 16). In this current study, we used a RSF model that enabled us to analyze a large number of variables to determine high-importance values, and derive a model with improved prediction performance (OOB C-index of 0.701, compared to traditional Cox regression modeling OOB C-index of 0.576–0.686) (**Supplementary Figure 1**). However, the advantages of using a machine learning model may come at a cost when it comes to clinical interpretation, due to the complexity of the ensemble tree learning methods. Thus, we presented our results combining features of the robust decision tree ensemble from the random forest, with elements of a Cox proportional hazards regression to explain the factors associated with graft failure in our study (31).

Based on this RSF technique, we found that PK was almost twice as more likely to fail in 10 years compared to DSAEK in the treatment of corneal endothelial diseases, i.e., bullous keratopathy (BK) and Fuchs dystrophy (FED) in our study cohort. Similar to previous studies (32, 33), our 10-year graft survival was superior in DSAEK compared to PK in eyes with BK (57.5 vs. 43.1%, $P < 0.001$) and FED (89.2 vs. 68.1%, $P < 0.001$). These long-term graft survival results reflect the higher proportion of BK compared in FED in our Asian population, as BK was almost three times more likely to be associated with graft failure compared to FED, and BK has been shown to have poorer outcomes in both PK (34–36) and DSAEK (37–39). Another advantage of using the RSF is the ability to examine non-linear associations between various factors and graft failure. A Cox proportional hazards regression analysis assumes a linear relationship between any continuous predictors and an outcome, i.e., graft failure, and thus donor endothelial cell count was not a significant factor (HR: 1.0, $P = 0.171$) after adjusting for other variables. However, the RSF describes a closely associated but non-linear relationship between the donor endothelial cell count and 10-year graft survival in both PK and DSAEK (**Supplementary Figure 2**).

The RSF analysis also identified recipient gender as an important factor, with the multivariate Cox regression

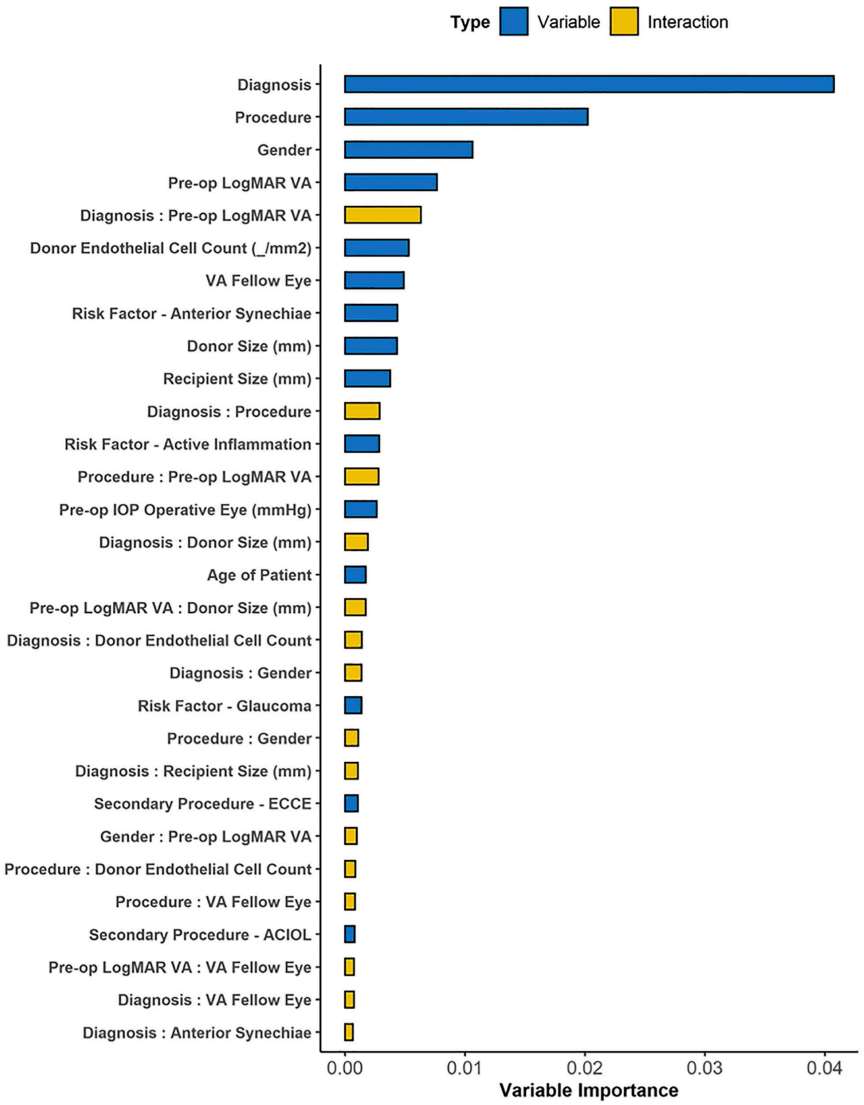

FIGURE 3 | The variable importance (VIMP) plot showing the top 30 variables and interactions for predicting graft failure using Random Survival Forest (RSF) machine learning algorithm. The VIMP score for each candidate variable calculates the difference between the original OOB error rate and the rate after permuting variable values, while VIMP for pair-wise interaction measures the difference between the sum of paired VIMP scores and the VIMP permuting two variables simultaneously. Top-ranked interactions highlight the association between variable pairs that is important for successful prediction in the model.

demonstrating that male recipients and those with poorer pre-operative visual acuity are associated with graft failure. A sub-group multivariate Cox regression analysis of our study cohort comparing gender-recipient matched and unmatched subjects revealed a higher risk of 10-year graft failure amongst the gender unmatched (HR: 1.57 95%CI 1.06–2.33, $P = 0.024$) in the PK group but not in the DSAEK group (HR: 0.82 95%CI 0.53–1.276, $P = 0.382$) (**Supplementary Table 3**). While this observation is consistent with previous large studies on gender matching in penetrating keratoplasty (40), we found male recipients to be still an independent factor associated with 10-year graft failure in the multivariate model, which requires further study. A poor pre-operative visual acuity may suggest presence of more severe corneal decompensation with edema, or underlying factors such as glaucoma or inflammation that could lead to a higher risk of graft failure (41). Our RSF machine learning technique took into account these possible confounders to suggest that poor pre-operative visual acuity was an important, independent factor associated with graft failure. This has useful clinical implications as we may use this as a potential surrogate to counsel patients for risk of graft failure based on their pre-morbid visual acuity and ocular condition.

There are currently few studies that have reported 10-year outcomes of DSAEK, and to our knowledge, no reports that directly compare 10-year outcomes and complication rates of DSAEK to PK from the same study cohort. Moreover,

TABLE 2 | Hazard ratios for factors associated with 10-year graft failure using random survival forest to determine optimal multivariate regression model.

Factors	*N** (*n* = 1,283)	Hazard ratio	*P* > | z|	95% CI	
				Lower	Upper
Diagnosis/Surgical indication					
BK	791	2.838	< 0.001	1.892	4.259
FED	492				
Procedure/surgical technique					
PK	368	1.643	0.002	1.192	2.265
DSAEK	915				
Gender					
Male	608	1.751	< 0.001	1.308	2.344
Female	675				
Pre-operative visual acuity (logMAR)**	1,283	1.601	0.005	1.154	2.220
Donor endothelial cell count**	1,283	1.000	0.171	0.999	1.000

**N = 1283 after excluding 52 subjects who did not have pre-operative visual acuity data available.*
***For continuous variables, but linear and non-linear associations were also assessed using penalized splines.*
BK, bullous keratopathy; FED, Fuchs endothelial dystrophy; PK, penetrating keratoplasty; DSAEK, Descemet stripping automated endothelial keratoplasty.

TABLE 3 | Ten-year cumulative incidence of complications comparing Descemet stripping automated endothelial keratoplasty (DSAEK) and penetrating keratoplasty (PK) in our study cohort.

*Complications	Cumulative incidence (%) ± 95%CI		*P* value
	PK	DSAEK	
Transient elevated IOP (>21 mmHg)	26.0 (21.7–30.6)	20.8 (18.3–23.6)	0.040
Late graft failure	12.3 (9.2–16.0)	4.5 (3.3–6.1)	< 0.001
Epithelial problems	11.6 (8.6–15.2)	2.5 (1.6–3.8)	< 0.001
Graft rejection episode	9.5 (6.8–12.9)	4.2 (3.0–5.7)	< 0.001
Primary graft failure	2.3 (1.1–4.3)	1.8 (1.1–2.9)	0.535
Anterior synechiae	2.3 (1.1–4.3)	1.4 (0.7–2.3)	0.221
Microbial keratitis	2.1 (0.9–4.0)	1.3 (0.7–2.2)	0.281
Wound dehiscence	2.1 (0.9–4.0)	0 (0–0.4)	< 0.001
Cytomegalovirus infection	1.3 (0.4–3.0)	1.4 (0.7–2.3)	0.898
Herpes simplex virus infection	1.0 (0.3–2.6)	0.8 (0.4–1.7)	0.754
Endophthalmitis	0.5 (0.1–1.8)	0.2 (0–0.8)	0.585
Graft detachment	0 (0–0.9)	3.5 (2.4–4.9)	< 0.001

PK, penetrating keratoplasty; DSAEK, Descemet's stripping automated endothelial keratoplasty; SD, standard deviation; IOP, intraocular pressure.
**Complications as recorded in our prospective Singapore Corneal Transplant Registry database.*

our study used a relatively novel machine learning analysis technique to study a large number of variables while accounting for interactions and non-linear associations with a better prediction compared to traditional model development methods. Another strength is the availability of long-term graft outcomes from registry data, which can vary according to surgeon versus center experience as surgical outcomes are improved by using standardized techniques and post-operative management protocols (42). Compared to a *post hoc* re-analysis of the Cornea Preservation Time Study to specifically examined intra-operative complications, it was reported that surgeon and eye bank factors were the top 2 factors found to be important predictor of graft failure (16). In our study, we found that surgeon experience and surgery performed from earlier years (based on year performed) were not significant factors associated with graft failure on multivariate analysis. Our study also supports the advantages of DSAEK over PK in terms of a lower incidence of complications over a 10-year follow-up, such as epitheliopathy ($P < 0.001$), graft rejection ($P < 0.001$), and as such, less incidence of raised IOP from steroid response as the need for post-operative steroids may be reduced in DSAEK ($P = 0.04$).

However, we recognize the limitations of our study which included the transition of surgical techniques from PK to DSAEK that was introduced in 2006 onward, and the reduction in number of follow-ups at 10 years. We discussed the effect of surgical experience and patient selection in our previous studies, which was mitigated by our standardized protocols and surgical techniques. Thus, we only selected primary grafts for specific corneal endothelial diseases, i.e., Fuchs dystrophy or bullous keratopathy, and previously detailed the transition of proportion of PK toward DSAEK in our study cohort (8). We also acknowledge the differences in our study demographics compared to other reports, in our predominantly Asian population with shallow anterior chambers and a higher proportion of BK compared to FED (5). Despite these limitations common to most registry studies, we believe that our results provide additional evidence to support the trend toward selective lamellar keratoplasty for endothelial diseases. We also recognize the limitations of the RSF analysis used in our study—for example, potentially favoring continuous variables that have more split points (43). Nonetheless, our RSF model selected categorical variables, which further validated these factors' significance to graft failure. The use of other algorithms such as conditional inference forest may help generate more accurate VIMP scores (43); however, we highlight that the RSF analysis merely serves as a complementary technique to the traditional Cox regression model.

In summary, our study provides long-term graft survival outcomes and cumulative incidence of complications, highlighting the advantages of DSAEK over PK in the treatment of end-stage corneal endothelial decompensation in Asian eyes. We used machine learning techniques to analyze the large registry database collected over a 10-year audit to determine the most important factors associated with graft failure, and used these factors to derive the optimal model for multivariate analysis, which was superior to traditional techniques. A combination of predictive (machine learning) and explanatory (regression) modeling may be a useful way of analyzing large registry datasets to examine cornea graft survival and factors associated with graft failure in future studies, which may then be used to develop a risk prediction model.

DATA AVAILABILITY STATEMENT

The data analyzed in this study is subject to the following licenses/restrictions: Anonmyized data collected as prospective audit. Requests to access these datasets should be directed to MA, marcus.ang@snec.com.sg.

ETHICS STATEMENT

The studies involving human participants were reviewed and approved by Institutional Review Board (SingHealth Centralized IRB, R847/42/2011). The patients/participants provided their written informed consent to participate in this study.

AUTHOR CONTRIBUTIONS

All authors contributed significantly to the development of the study, analysis, and manuscript preparation.

FUNDING

This work was supported by NMRC Transition Award (TA21jun-0003).

SUPPLEMENTARY MATERIAL

The Supplementary Material for this article can be found online at: https://www.frontiersin.org/articles/10.3389/fmed.2022.831352/full#supplementary-material

Supplementary Figure 1 | Boxplot showing the out of bag (OOB) Harrell C Statistic (C-index) of nested models using top variables identified by VIMP. Forward and backward step-wise multivariate Cox regression modeling only achieved OOB C-index of 0.576–0.686 (based on age, gender, race, diagnosis, surgery, glaucoma, donor age).

Supplementary Figure 2 | Partial dependence plot showing the adjusted non-linear association between donor endothelial cell count and 10-year graft survival comparing Descemet stripping automated endothelial keratoplasty (DSAEK) and penetrating keratoplasty (PK).

REFERENCES

1. Gain P, Jullienne R, He Z, Aldossary M, Acquart S, Cognasse F, et al. Global survey of corneal transplantation and eye banking. *JAMA Ophthalmol.* (2016) 134:167–73. doi: 10.1001/jamaophthalmol.2015.4776
2. Ong HS, Ang M, Mehta JS. Evolution of therapies for the corneal endothelium: past, present and future approaches. *Br J Ophthalmol.* (2020) 105:454–67. doi: 10.1136/bjophthalmol-2020-316149
3. Park CY, Lee JK, Gore PK, Lim CY, Chuck RS. Keratoplasty in the United States: a 10-year review from 2005 through 2014. *Ophthalmology.* (2015) 122:2432–42. doi: 10.1016/j.ophtha.2015.08.017
4. Mathews PM, Lindsley K, Aldave AJ, Akpek EK. Etiology of global corneal blindness and current practices of corneal transplantation: a focused review. *Cornea.* (2018) 37:1198–203. doi: 10.1097/ICO.0000000000001666
5. Bose S, Ang M, Mehta JS, Tan DT, Finkelstein E. Cost-effectiveness of Descemet's stripping endothelial keratoplasty versus penetrating keratoplasty. *Ophthalmology.* (2013) 120:464–70. doi: 10.1016/j.ophtha.2012.08.024
6. Lee WB, Jacobs DS, Musch DC, Kaufman SC, Reinhart WJ, Shtein RM. Descemet's stripping endothelial keratoplasty: safety and outcomes: a report by the American academy of ophthalmology. *Ophthalmology.* (2009) 116:1818–30. doi: 10.1016/j.ophtha.2009.06.021
7. Ang M, Lim F, Htoon HM, Tan D, Mehta JS. Visual acuity and contrast sensitivity following Descemet stripping automated endothelial keratoplasty. *Br J Ophthalmol.* (2016) 100:307–11. doi: 10.1136/bjophthalmol-2015-306975
8. Tan D, Ang M, Arundhati A, Khor WB. Development of selective lamellar keratoplasty within an Asian corneal transplant program: the Singapore corneal transplant study (an American ophthalmological society thesis). *Trans Am Ophthalmol Soc.* (2015) 113:T10.
9. Williams K, Keane M, Galettis R, Jones V, Mills R, Coster D. *The Australian Corneal Graft Registry – 2015 Report*. Adelaide, SA: Flinders University (2015).
10. Dickman MM, Peeters JM, van den Biggelaar FJ, Ambergen TA, van Dongen MC, Kruit PJ, et al. Changing practice patterns and long-term outcomes of endothelial versus penetrating keratoplasty: a prospective dutch registry study. *Am J Ophthalmol.* (2016) 170:133–42. doi: 10.1016/j.ajo.2016.07.024
11. Greenrod EB, Jones MN, Kaye S, Larkin DF, National Health Service Blood and Transplant Ocular Tissue Advisory Group and Contributing Ophthalmologists (Ocular Tissue Advisory Group Audit Study 16). Center and surgeon effect on outcomes of endothelial keratoplasty versus penetrating keratoplasty in the United Kingdom. *Am J Ophthalmol.* (2014) 158:957–66.
12. Coster DJ, Lowe MT, Keane MC, Williams KA, Australian Corneal Graft Registry Contributors. A comparison of lamellar and penetrating keratoplasty outcomes: a registry study. *Ophthalmology.* (2014) 121:979–87.
13. Fajgenbaum MA, Hollick EJ. Center and surgeon effect on outcomes of endothelial keratoplasty versus penetrating keratoplasty in the United Kingdom. *Am J Ophthalmol.* (2015) 160:392–3.
14. Patel SV, Armitage WJ, Claesson M. Keratoplasty outcomes: are we making advances? *Ophthalmology.* (2014) 121:977–8. doi: 10.1016/j.ophtha.2014.01.029
15. Hallak JA. A machine learning Model with survival statistics to identify predictors of Descemet stripping automated endothelial keratoplasty graft failure. *JAMA Ophthalmol.* (2021) 139:198–9. doi: 10.1001/jamaophthalmol.2020.5741
16. O'Brien RC, Ishwaran H, Szczotka-Flynn LB, Lass JH, Cornea Preservation Time Study (CPTS) Group. Random survival forests analysis of intraoperative complications as predictors of Descemet stripping automated endothelial keratoplasty graft failure in the cornea preservation time study. *JAMA Ophthalmol.* (2021) 139:191–7. doi: 10.1001/jamaophthalmol.2020.5743
17. Tan DT, Janardhanan P, Zhou H, Chan YH, Htoon HM, Ang LP, et al. Penetrating keratoplasty in Asian eyes: the Singapore corneal transplant study. *Ophthalmology.* (2008) 115:975–82.e1. doi: 10.1016/j.ophtha.2007.08.049
18. Ang M, Mehta JS, Lim F, Bose S, Htoon HM, Tan D. Endothelial cell loss and graft survival after Descemet's stripping automated endothelial keratoplasty and penetrating keratoplasty. *Ophthalmology.* (2012) 119:2239–44. doi: 10.1016/j.ophtha.2012.06.012
19. Ang M, Ho H, Wong C, Htoon HM, Mehta JS, Tan D. Endothelial keratoplasty after failed penetrating keratoplasty: an alternative to repeat penetrating keratoplasty. *Am J Ophthalmol.* (2014) 158:1221–7.e1. doi: 10.1016/j.ajo.2014.08.024
20. Ang M, Mehta JS, Sng CC, Htoon HM, Tan DT. Indications, outcomes, and risk factors for failure in tectonic keratoplasty. *Ophthalmology.* (2012) 119:1311–9. doi: 10.1016/j.ophtha.2012.01.021
21. Ang M, Htoon HM, Cajucom-Uy HY, Tan D, Mehta JS. Donor and surgical risk factors for primary graft failure following Descemet's stripping automated endothelial keratoplasty in Asian eyes. *Clin Ophthalmol.* (2011) 5:1503–8. doi: 10.2147/OPTH.S25973
22. Ang M, Mehta JS, Anshu A, Wong HK, Htoon HM, Tan D. Endothelial cell counts after Descemet's stripping automated endothelial keratoplasty versus penetrating keratoplasty in Asian eyes. *Clin Ophthalmol.* (2012) 6:537–44. doi: 10.2147/OPTH.S26343
23. Ang M, Saroj L, Htoon HM, Kiew S, Mehta JS, Tan D. Comparison of a donor insertion device to sheets glide in Descemet stripping endothelial keratoplasty: 3-year outcomes. *Am J Ophthalmol.* (2014) 157:1163–9.e3. doi: 10.1016/j.ajo.2014.02.049

24. Khor WB, Han SB, Mehta JS, Tan DT. Descemet stripping automated endothelial keratoplasty with a donor insertion device: clinical results and complications in 100 eyes. *Am J Ophthalmol.* (2013) 156:773–9. doi: 10.1016/j.ajo.2013.05.012
25. Ishwaran H, Kogalur UB, Blackstone EH, Lauer MS. Random survival forests. *Ann Appl Stat.* (2008) 2:841–60.
26. R Core Team. *R: A Language and Environment for Statistical Computing*. Vienna: R Foundation for Statistical Computing (2013).
27. Ishwaran H, Kogalur UB, Kogalur MUB. *Package 'randomForestSRC'*. (2021).
28. Woo JH, Ang M, Htoon HM, Tan D. Descemet membrane endothelial keratoplasty versus Descemet stripping automated endothelial keratoplasty and penetrating keratoplasty. *Am J Ophthalmol.* (2019) 207:288–303. doi: 10.1016/j.ajo.2019.06.012
29. Ang M, Soh Y, Htoon HM, Mehta JS, Tan D. Five-year graft survival comparing Descemet stripping automated endothelial keratoplasty and penetrating keratoplasty. *Ophthalmology.* (2016) 123:1646–52. doi: 10.1016/j.ophtha.2016.04.049
30. Wiegand RE. Performance of using multiple stepwise algorithms for variable selection. *Stat Med.* (2010) 29:1647–59.
31. Ishwaran H, Kogalur UB. Consistency of random survival forests. *Stat Probab Lett.* (2010) 80:1056–64. doi: 10.1016/j.spl.2010.02.020
32. Price MO, Fairchild KM, Price DA, Price FW Jr. Descemet's stripping endothelial keratoplasty five-year graft survival and endothelial cell loss. *Ophthalmology.* (2011) 118:725–9. doi: 10.1016/j.ophtha.2010.08.012
33. Writing Committee for the Cornea Donor Study Research Group, Mannis MJ, Holland EJ, Gal RL, Dontchev M, Kollman C, et al. The effect of donor age on penetrating keratoplasty for endothelial disease: graft survival after 10 years in the cornea donor study. *Ophthalmology.* (2013) 120:2419–27. doi: 10.1016/j.ophtha.2013.08.026
34. Writing Committee for the Cornea Donor Study Research Group, Sugar A, Gal RL, Kollman C, Raghinaru D, Dontchev M, et al. Factors associated with corneal graft survival in the cornea donor study. *JAMA Ophthalmol.* (2015) 133:246–54. doi: 10.1001/jamaophthalmol.2014.3923
35. Dandona L, Naduvilath TJ, Janarthanan M, Ragu K, Rao GN. Survival analysis and visual outcome in a large series of corneal transplants in India. *Br J Ophthalmol.* (1997) 81:726–31. doi: 10.1136/bjo.81.9.726
36. Anshu A, Li L, Htoon HM, de Benito-Llopis L, Shuang LS, Singh MJ, et al. Long-term review of penetrating keratoplasty: a 20-year review in Asian eyes. *Am J Ophthalmol.* (2021) 224:254–66. doi: 10.1016/j.ajo.2020.10.014
37. Price DA, Kelley M, Price FW Jr, Price MO. Five-year graft survival of Descemet membrane endothelial keratoplasty (EK) versus Descemet stripping EK and the effect of donor sex matching. *Ophthalmology.* (2018) 125:1508–14. doi: 10.1016/j.ophtha.2018.03.050
38. Wacker K, Baratz KH, Maguire LJ, McLaren JW, Patel SV. Descemet stripping endothelial keratoplasty for fuchs' endothelial corneal dystrophy: five-year results of a prospective study. *Ophthalmology.* (2016) 123:154–60. doi: 10.1016/j.ophtha.2015.09.023
39. Fajgenbaum MA, Hollick EJ. Modeling endothelial cell loss after Descemet stripping endothelial keratoplasty: data from 5 years of follow-up. *Cornea.* (2017) 36:553–60. doi: 10.1097/ICO.0000000000001177
40. Hopkinson CL, Romano V, Kaye RA, Steger B, Stewart RM, Tsagkataki M, et al. The influence of donor and recipient gender incompatibility on corneal transplant rejection and failure. *Am J Transplant.* (2017) 17:210–7. doi: 10.1111/ajt.13926
41. Fuest M, Ang M, Htoon HM, Tan D, Mehta JS. Long-term visual outcomes comparing Descemet stripping automated endothelial keratoplasty and penetrating keratoplasty. *Am J Ophthalmol.* (2017) 182:62–71. doi: 10.1016/j.ajo.2017.07.014
42. Baydoun L, Liarakos VS, Dapena I, Melles GR. Re: Coster et al.: a comparison of lamellar and penetrating keratoplasty outcomes (Ophthalmology 2014;121:979-87). *Ophthalmology.* (2014) 121:e61–2. doi: 10.1016/j.ophtha.2013.12.017
43. Nasejje JB, Mwambi H, Dheda K, Lesosky M. A comparison of the conditional inference survival forest model to random survival forests based on a simulation study as well as on two applications with time-to-event data. *BMC Med Res Methodol.* (2017) 17:115. doi: 10.1186/s12874-017-0383-8

Conflict of Interest: The authors declare that the research was conducted in the absence of any commercial or financial relationships that could be construed as a potential conflict of interest.

Publisher's Note: All claims expressed in this article are solely those of the authors and do not necessarily represent those of their affiliated organizations, or those of the publisher, the editors and the reviewers. Any product that may be evaluated in this article, or claim that may be made by its manufacturer, is not guaranteed or endorsed by the publisher.

frontiers | Frontiers in Medicine

ORIGINAL RESEARCH
published: 14 June 2022
doi: 10.3389/fmed.2022.868533

"Endothelium-Out" and "Endothelium-In" Descemet Membrane Endothelial Keratoplasty (DMEK) Graft Insertion Techniques: A Systematic Review With Meta-Analysis

Hon Shing Ong[1,2,3], Hla M. Htoon[2,3], Marcus Ang[1,2,3] and Jodhbir S. Mehta[1,2,3,4]**

[1] Department of Corneal & External Eye Diseases, Singapore National Eye Centre, Singapore, Singapore, [2] Singapore Eye Research Institute, Singapore, Singapore, [3] Duke-NUS Medical School, Singapore, Singapore, [4] School of Materials Science and Engineering, Nanyang Technological University, Singapore, Singapore

OPEN ACCESS

Edited by:
Mohit Parekh,
University College London,
United Kingdom

Reviewed by:
Vito Romano,
University of Brescia, Italy
Hannah Levis,
University of Liverpool,
United Kingdom

***Correspondence:**
Jodhbir S. Mehta
jodmehta@gmail.com
Hon Shing Ong
honshing@gmail.com

Specialty section:
This article was submitted to Ophthalmology, a section of the journal Frontiers in Medicine

Received: *02 February 2022*
Accepted: *10 May 2022*
Published: *14 June 2022*

Citation:
Ong HS, Htoon HM, Ang M and Mehta JS (2022) "Endothelium-Out" and "Endothelium-In" Descemet Membrane Endothelial Keratoplasty (DMEK) Graft Insertion Techniques: A Systematic Review With Meta-Analysis. Front. Med. 9:868533. doi: 10.3389/fmed.2022.868533

Background: We evaluated the visual outcomes and complications of "endothelium-out" and "endothelium-in" Descemet membrane endothelial keratoplasty (DMEK) graft insertion techniques.

Materials and Methods: Electronic searches were conducted in CENTRAL, Cochrane databases, PubMed, EMBASE, ClinicalTrials.gov. Study designs included clinical trials, comparative observational studies, and large case series (≥25 eyes). PRISMA guidelines were used for abstracting data and synthesis. Random-effects models were employed for meta-analyses.

Results: 21,323 eyes (95 studies) were included. Eighty-six studies reported on "endothelium-out" techniques; eight studies reported on "endothelium-in" techniques. One study compared "endothelium-out" to "endothelium-in" techniques. Eighteen "endothelium-out" studies reported that 42.5–85% of eyes achieved best-corrected visual acuity (BCVA) ≥20/25 at 6 months; pooled proportion of eyes achieving BCVA ≥20/25 at 6 months was 58.7% (95% CI 49.4–67.7%,15 studies). Three "endothelium-in" studies reported that 44.7–87.5% of eyes achieved BCVA of ≥20/25 at 6 months; pooled proportion of eyes achieving BCVA ≥20/25 at 6 months was 62.4% (95% CI 33.9–86.9%). Pooled mean endothelial cell loss was lower in the *"endothelium-in"* studies (28.1 ± 1.3%, 7 studies) compared to *"endothelium-out"* studies (36.3 ± 6.9%,10 studies) at 6 months (p = 0.018). Graft re-bubbling rates were higher in the "endothelium-out" studies (26.2%, 95% CI 21.9–30.9%, 74 studies) compared to "endothelium-in" studies (16.5%, 95% CI 8.5–26.4%, 6 studies), although statistical significance was not reached (p = 0.440). Primary graft failure rates were comparable between the two groups (p = 0.552). Quality of evidence was considered low and significant heterogeneity existed amongst the studies.

Conclusion: Reported rates of endothelial cell loss were lower in "endothelium-in" DMEK studies at 6 months compared to "endothelium-out" studies. Outcomes of "endothelium-in" techniques were otherwise comparable to those reported in "endothelium-out" studies. Given the technical challenges encountered in "endothelium-out" procedures, surgeons may consider "endothelium-in" techniques designed for easier intra-operative DMEK graft unfolding. "Endothelium-in" studies evaluating outcomes at longer time points are required before conclusive comparisons between the two techniques can be drawn.

Keywords: endothelial keratoplasty, Descemet's membrane endothelial keratoplasty, DMEK, bullous keratopathy, cornea, corneal transplants, outcomes, surgical techniques

INTRODUCTION

Background

Loss of vision from diseases of the corneal endothelium is the predominant indication for corneal transplantations (1, 2). Over the past 20 years, selective replacement of damaged corneal endothelium using lamellar keratoplasty procedures has significantly changed the management of endothelial diseases (3–5). The first posterior lamellar keratoplasty procedure was described in the late 1990s (6). In this report, the surgeon only partially replaced the recipient's diseased corneal endothelium, avoiding full-thickness or penetrating keratoplasty (PK). Ensuing developments to the procedure have resulted in more advanced techniques of endothelial keratoplasty (EK), which are associated with better visual outcomes, lower graft rejection risks, and improved graft survival rates (5, 7–9). Unlike PK, these EK techniques avoid full-thickness corneal trephination and intra-operative "open sky" situations associated the risks of severe blinding complications such as suprachoroidal hemorrhage. Endothelial keratoplasties also maintain corneal biomechanics and the overall strength of the globe, important in protecting the eye from external trauma. Data from national corneal graft registries have reported that EK procedures have now overtaken full-thickness PK as the leading procedure for treating corneal endothelial diseases in several countries (1, 2, 10).

Currently, there are two predominant techniques of EK performed worldwide: Descemet's stripping automated endothelial keratoplasty (DSAEK) and Descemet membrane endothelial keratoplasty (DMEK) (3, 4, 11). In DSAEK, the transplanted corneal grafts are comprised of donor endothelium, Descemet's membrane (DM), and some posterior stroma. Advancement of the DSAEK technique, such as the development of devices for graft insertion and techniques to cut thinner grafts, has greatly simplified DSAEK (12–15). With more predictable visual outcomes and faster visual recovery compared to PK (8, 16, 17), many corneal surgeons are now performing DSAEK as the primary technique to treat end-stage corneal endothelial diseases (18, 19).

Descemet membrane endothelial keratoplasty is the more recent advancement in EK surgery (20). In DMEK, only the DM and the corneal endothelium are harvested from donor corneal tissues and transplanted, rendering them anatomically more accurate. As corneal stroma is not transplanted, changes in corneal profiles are avoided. Faster visual recovery and improved visual outcomes compared to DSAEK can thus be achieved (21–25). Lower rates of graft rejection have also been reported in DMEK compared to DSAEK (26).

Rationale for This Review

Current methods of DMEK graft transfer into the anterior chamber involve inserting the graft through a small clear corneal wound. Different surgical instruments have been described for the insertion of DMEK grafts. Examples of such instruments include glass injectors (27, 28) and intraocular lens cartridges (29, 30). All these instruments are designed to shield the DMEK graft scroll from the surgical wound. Nevertheless, the majority of techniques reported in published literature involves the loading and insertion of the DMEK graft with the endothelium on the outer surface ("endothelium-out"). Thus, the grafts are potentially at risk of endothelial cell loss due to endothelial contact with the walls of the injection devices. Furthermore, "endothelium-out" DMEK techniques all involve the injection of the entire scrolled graft into the anterior chamber. The unscrolling of the free floating graft, following its insertion, can be difficult and unpredictable (31, 32). Such challenges have hindered corneal surgeons from adopting DMEK as a primary treatment for corneal endothelial failure (2, 3). In a recent eye banking report, DSAEK still accounted for over 55% of EK procedures performed in the United States (2).

"Endothelium-in" DMEK graft insertion techniques have been described more recently (33–37) (**Figure 1**). In these techniques, the harvested DM is folded and prevented from adopting its natural scroll with its endothelium on the outside. By maintaining the orientation of the DMEK graft during graft insertion, these "endothelium-in" techniques aim to provide more control in graft unscrolling following insertion into the eye. Nevertheless, the differences in surgical outcomes of either technique for DMEK graft insertion, "endothelium-in" or "endothelium-out," remains unclear.

Objectives of This Review

This review aims to evaluate the published literature reporting the visual outcomes and complications of both "endothelium-out" and "endothelium-in" graft insertion techniques for DMEK.

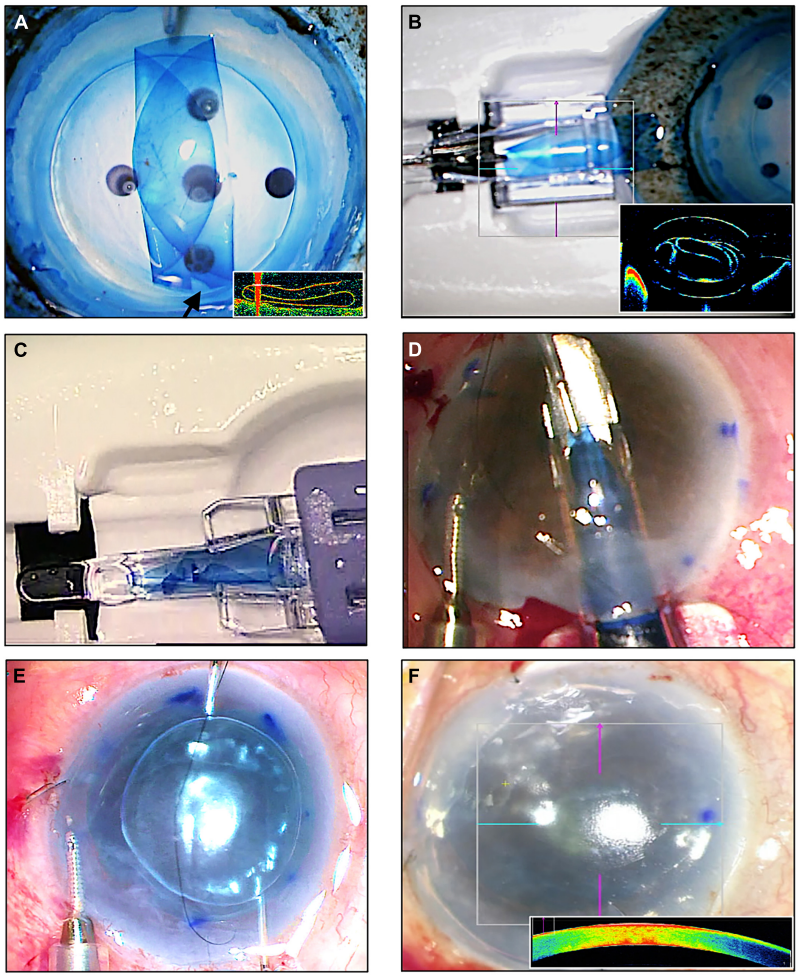

FIGURE 1 | An "endothelium-in" surgical technique of Descemet membrane endothelial keratoplasty (DMEK) using the using the DMEK EndoGlide (Network Medical Products, United Kingdom). **(A)** DMEK graft is folded into a tri-fold with its endothelium in its inner surface; note the asymmetrical orientation marker (arrow); (inset) intraoperative optical coherence tomography (OCT) image of the tri-folded graft – note that the leaves of the tri-fold do not touch. **(B)** Graft is pulled and loaded into the EndoGlide; (inset) OCT image showing the tri-folded graft within the DMEK EndoGlide – note that the leaves of the tri-fold do not touch. **(C)** Customized clip fixed to the back of the EndoGlide; this creates a "closed system" after graft insertion maintaining anterior chamber stability. **(D)** Graft is drawn into the anterior chamber with micro-forceps with its endothelium facing down. **(E)** Unfolding of the graft with its orientation maintained whilst air is injected for tamponade. **(F)** Full air-gas tamponade of graft; (inset) intraoperative OCT showing a fully attached DMEK graft.

MATERIALS AND METHODS

This review was submitted to PROSPERO International prospective register of systematic reviews (reference ID: 160657)[1]. A study protocol for this systematic review is available in **Supplementary Appendix 1**.

Criteria for Considering Studies for This Review

Types of Intervention

We included publications in which the visual outcomes and complications of DMEK performed for the treatment of endothelial dysfunction were reported.

[1]https://www.crd.york.ac.uk/PROSPERO

Types of Studies

Study designs included controlled clinical trials, prospective or retrospective comparative observational studies, and large case series (≥25 eyes). Small case series (<25 eyes), letters, reviews, published abstracts, and laboratory-based studies were excluded.

Types of Participants (Study Population)

Studies reporting only surgical outcomes of DMEK performed for graft failure (including repeat DMEK surgery) or specific high-risk disease groups (e.g., glaucoma, cytomegalovirus endotheliitis, herpes simplex) were also excluded. To avoid duplicate reporting of similar study populations, where the same group of investigators published several studies, earlier smaller studies were excluded if more recent larger studies reporting the same outcome measures were available.

Information Sources

Information sources included all applicable electronic databases, all relevant articles in the reference list of any relevant articles, and all relevant articles which cite any relevant articles.

Search Methods for Identification of Studies

Electronic literature searches were conducted in the following databases: CENTRAL, Cochrane Library databases[2], PubMed, EMBASE, ClinicalTrials.gov.[3] No date or language restrictions were set in our electronic searches. Key search terms were the MeSH headings Descemet's membrane endothelial keratoplasty, Descemet membrane endothelial keratoplasty, and DMEK. The last electronic database search was performed on 30 June 2021. The search strategies for the relevant databases can be found in **Supplementary Appendix 2**.

Data Collection and Analysis

Selection of Studies

Citations and abstracts obtained from electronic searches were examined. Replicated studies and evidently irrelevant studies were removed. Full text prints of relevant studies were retrieved; they were assessed against our inclusion criteria for this review.

Data Extraction and Management

Only data from eyes that had received DMEK surgeries were included. Where studies reported on the outcomes of eyes that had undergone surgeries other than DMEK, these eyes were excluded from the review. The following details of each study were extracted for this review: study participants' characteristics, study design, DMEK graft insertion techniques, and surgical outcome measures.

Assessment of Risks of Bias in Included Studies

The study design of each article was assessed and rated according to its level of evidence. A rating scale adapted from the Oxford Centre for Evidence-Based Medicine was used (38) (**Table 1**).

Studies meeting the inclusion criteria were also assessed for risk of bias using Chapter 8 of the *Cochrane Handbook for Systematic Reviews of Intervention* (39). The following domains for potential risk of bias were considered: (a) *selection bias* – random sequence generation, (b) *selection bias* – allocation concealment, (c) *performance/detection bias* – masking of outcome examiners and participants (to determine whether knowledge of the allocated intervention was adequately prevented during the study), (d) *attrition bias* incomplete outcome data, and (e) *reporting bias* – selective outcome reporting. Each study was graded as "low risk" of bias, "high risk" of bias, or "unclear risk." Any differences between the authors were resolved by discussion.

Outcome Measures

Data on the following surgical outcome measures were obtained: visual outcomes, endothelial cell loss, and complications including graft detachment/re-bubbling, graft rejection, and graft failure. For direct comparison of visual outcomes, measures of visual acuities in Snellen were converted to the respective logarithm of the minimum angle of resolution (LogMAR) equivalents. The proportion of eyes that achieved a best-corrected visual acuity (BCVA) of 20/25 or better at a specific time points were also evaluated.

Measures of Treatment Effect

All outcome measures (proportion of eyes achieving ≥20/25 BCVA, re-bubbling rates for graft detachments, graft rejection rates, and graft failure rates) were discrete data, except mean endothelial cell loss where outcome measures were continuous data. Outcomes for eyes rather than individuals were used as the unit of analysis. Studies where both eyes received the same treatment were included.

Managing Missing Data

All relevant data were extracted from the published studies. These included the details of studies and their quantitative results, without having to request these data from the original investigators.

Data Synthesis

Data analyses were performed according to Chapter 9 of the Cochrane Handbook for Systematic Reviews of Interventions (39). As published studies were performed in different institutions at various times, it is likely that variations exist amongst the patient populations included in this review. We therefore employed a random-effects model for our meta-analyses as the true effect size might differ between studies. Where we could not perform a meta-analysis, narrative syntheses describing the directions, magnitude, and consistencies of effects across the studies has been presented. MedCalc software was used for providing the meta-analyses results (MedCalc®

TABLE 1 | Level of evidence used to rate the design of each study (adapted from the Oxford Centre for Evidence-Based Medicine March) (38).

Level of evidence	Study design
1	Well-designed and conducted RCT
2	Cohort studies and low quality RCT (e.g., <80% follow-up)
3	Case-control studies
4	Case-series and poor quality† cohort studies or case-control studies

RCT, randomized controlled trials.

†Poor quality cohort study indicate one that failed to clearly define comparison groups and/or failed to measure exposures and outcomes in the same (preferably blinded), objective way in both exposed and non-exposed individuals and/or failed to identify or appropriately control known confounders and/or failed to carry out a sufficiently long and complete follow-up of patients; poor quality case-control study indicate one that failed to clearly define comparison groups and/or failed to measure exposures and outcomes in the same (preferably blinded), objective way in both cases and controls and/or failed to identify or appropriately control known confounders.

[2]www.thecochranelibrary.com

[3]www.clinicaltrials.gov

Statistical Software version 20.014; MedCalc Software Ltd., Ostend, Belgium; 2021).[4]

Assessment of Heterogeneity

We identified dissimilarities between published studies which are expected to introduce heterogeneities. As some degree of heterogeneity would always exist due to the diversities in methodologies of studies, where appropriate, we employed the Chi^2 test and I^2 statistic to quantify heterogeneities across reports. Significant heterogeneity was defined as an I^2 statistic of $\geq$50% and a Chi^2 test p-value of $<$0.1. If all the effects of an outcome measure were in a similar direction, then we considered data-pooling to be acceptable even in the existence of heterogeneities.

RESULTS

Results of Search

Electronic searches generated a total of 1,603 citations. Publications not relevant to the review were removed. After removal of duplicated publications, abstracts of 579 records were screened and a further 463 records were removed. Full text copies of 116 articles were obtained and reviewed. We included 95 studies in this review; 21 studies that failed to meet the inclusion criteria were excluded. The PRISMA flow diagram is illustrated in **Figure 2**.

Characteristics of Included Studies

Studies included in this review are summarized in **Supplementary Table 1**. A total of 21,323 eyes in 95 studies that had undergone DMEK were included. Eighty-six studies (19,945 eyes) reported on "endothelium-out" insertion techniques; eight studies (624 eyes) reported on "endothelium-in" insertion techniques, respectively. Only one study (36) compared "endothelium-out" to "endothelium-in" DMEK graft insertion techniques; this study was a large comparative series of 754 eyes (36).

Levels of Evidence and the Risks of Bias in Included Studies

Using the Oxford Centre for Evidence-Based Medicine rating (38) of the "endothelium-out" studies included, 4/86 (4.7%) were rated level I, 17/86 (19.8%) were rated level II, 22/86 (25.6%) were rated level III, and 43/86 (50.0%) were rated level IV evidence. Of the eight "endothelium-in" studies included, 5/8 (62.5%) were rated level III evidence and 3/8 (37.5%) were rated level IV evidence. The study that included both "endothelium-out" and "endothelium-in" techniques was rated level III evidence.

Figure 3 summarizes the judgments of each risk of bias domain of all studies included. Five of 95 included studies (5.3%) were assessed as "low risk" and 90/95 (94.7%) as "high risk" of random sequence generation (selection bias). Four of 95 studies (4.2%) were assessed as "low risk" and 91/95 (95.8%) as "high risk" of allocation concealment (selection bias). Two of 95 studies (2.1%) and two studies (2.1%) were assessed as "low risk" of performance bias and detection bias, respectively. Fifty-six of 95 studies (58.9%), 28/95 (29.5%), and 11/76 (11.6%) were assessed as "low risk," "high risk," and "unclear risk" of attrition bias, respectively. When assessing selective reporting (reporting bias), it was noted that all included studies reported results on some of the pre-specified outcome measures for this review. No study reported results for every outcome measure. All included studies did not state whether the published methods used in the analysis of outcomes were pre-specified in a protocol. Thus, 55/95 (57.9%) and 40/95 (42.1%) of studies were assessed as "high risk" or "unclear risk" for selective reporting, respectively. The authors' judgments of each risk of bias item for each included study is found in **Supplementary Appendix 3**.

Visual Outcomes and Complications Reported in Studies

The visual outcomes and complications reported in studies included are summarized in **Supplementary Table 1**.

Follow-Up

The reported mean length of follow-up of all studies ranged from 0 to 60 months (mean 12.8 $\pm$ 12.2 months).

Visual Outcomes

"Endothelium-out" studies: Thirty-four of the 87 studies (39.1%) reported the mean BCVA at 6 months after DMEK surgery; BCVA ranged from 0.0 to 0.49 LogMAR.

Fifteen studies (17.2%) reported that 42.5–85% of eyes achieved a BCVA of 20/25 or better at 6 months. The random pooled proportion of eyes achieving BCVA of 20/25 or better at 6 months was 58.7% (95% CI 49.4–67.7%) (15 studies).

"Endothelium-in" studies: Two of the nine studies (22.2%) reported the mean BCVA at 6 months after DMEK surgery; BCVA ranged from 0.09 to 0.10 LogMAR. Three studies (33.3%) reported that 44.7–87.5% of eyes achieved a BCVA of 20/25 or better at 6 months. The random pooled proportion of eyes achieving BCVA of 20/25 or better at 6 months was 62.4% (95% CI 33.9–86.9%) (3 studies).

Endothelial Cell Loss

"Endothelium-out" studies: 67/87 (77.0%) studies reported data on percentage endothelial cell loss following DMEK surgery at various time points. The mean endothelial cell loss ranged from 19 to 53%. One study (40), reported a rate of 5.6–6.4% endothelial cell loss per year. The random pooled mean endothelial cell loss was 36.3 $\pm$ 6.4% at 6 months (27 studies) and 38.7 $\pm$ 7.2% at 12 months (12 studies).

"Endothelium-in" studies: Percentage endothelial cells loss data following DMEK surgery were reported in eight out of the nine studies (88.9%) at various time points. The reported mean endothelial cell loss range from 26.6 to 56.0%. The random pooled mean endothelial cell loss was 28.1 $\pm$ 1.3% at 6 months (7 studies) and 29.6 $\pm$ 1.2% at 12 months (1 studies).

Comparing outcomes of *"endothelium-out"* to *"endothelium-in"* techniques, pooled mean endothelial cell loss was lower in the *"endothelium-in"* group, compared to *"endothelium-out"* group

[4]https://www.medcalc.org

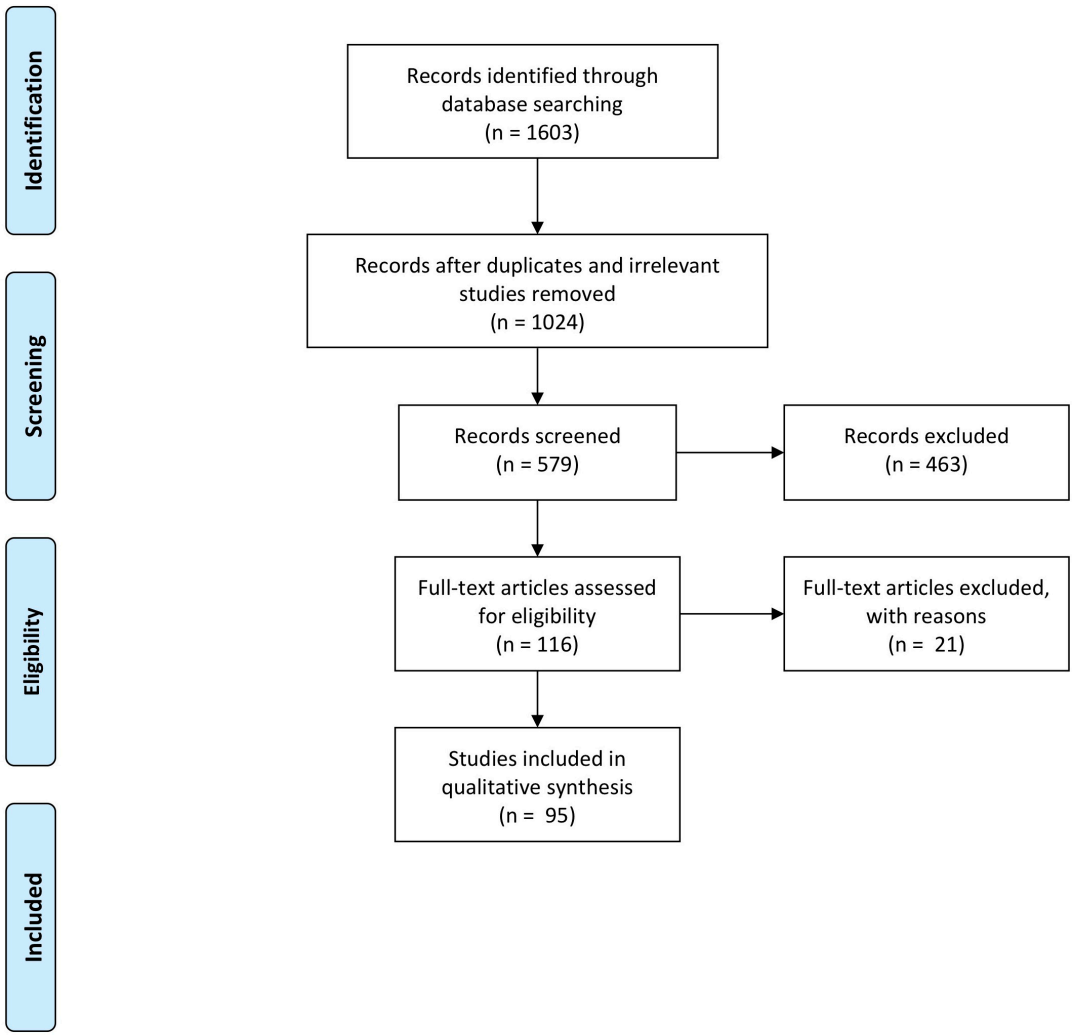

FIGURE 2 | The PRISMA flow diagram.

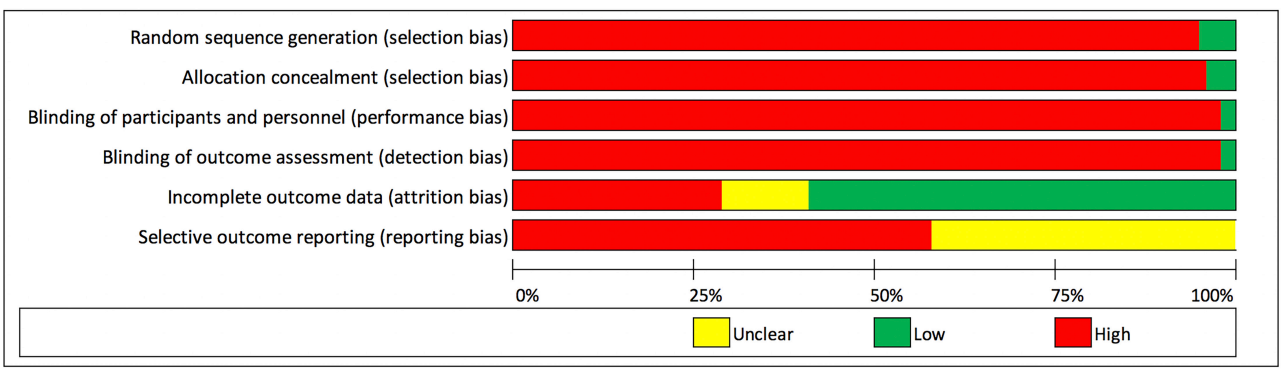

FIGURE 3 | Risk of bias graph: review authors' judgments about each risk of bias domain presented as percentages across all included studies.

at 6 months (p = 0.018). However, this was not statistically computable at 12 months as there was only 1 study for the "*endothelium in*" group.

Rates of Complications

"Endothelium-out" studies: Re-bubbling rates to treat DMEK graft detachments were reported in 77/87 (88.5%) studies and ranged

from 0 to 82%. Fifty-eight (66.7%) studies reported primary graft failure rates which ranged from 0 to 21.0%. Thirty-five (40.2%) studies reported secondary graft failure rates which ranged from 0 to 7.0% at 15.3 ± 13.9 months. Fifty (57.5%) studies reported graft rejection rates; rates ranged from 0 to 7.0%.

"Endothelium-in" studies: Re-bubbling rates to treat DMEK graft detachments were reported in all nine studies and ranged from 4.7 to 45.7%. Six of the nine studies (66.7%) reported primary graft failure rates which ranged from 0 to 3.0%. Three of the nine studies (33.3%) reported on secondary graft failures rates which ranged from 0 to 6.5%.

The random pooled graft re-bubbling rates for *"endothelium-out"* and *"endothelium-in"* techniques were 26.2% (95% CI 21.9–30.9%) (74 studies) and 16.5% (95% CI 8.5–26.4%) (6 studies), respectively. Comparing outcomes of *"endothelium-out"* to *"endothelium-in"* techniques, graft re-bubbling rates were not statistically significant in the "endothelium-out" group ($p = 0.440$). The random pooled primary graft failure rates for *"endothelium-out"* and *"endothelium-in"* techniques were 2.9% (95% CI 2.03–4.02%) (58 studies) and 1.5% (95% CI 0.6–2.7%) (5 studies), respectively. Comparing outcomes of *"endothelium-out"* to *"endothelium-in"* techniques, there was no significant difference in primary graft failure rates between the two groups ($p = 0.552$).

DISCUSSION

Although DMEK offers the advantages of faster visual rehabilitation, better visual and refractive outcomes (21–25), and lower risks of graft rejection compared to DSAEK (26), many transplant surgeons have been slow to adopt DMEK as procedure of choice for the management of endothelial diseases (2, 3). Indeed, DSAEK still accounts for approximately 57% of EK surgeries performed in the United States (2). This has been ascribed to: the technical difficulties in DMEK donor preparation and surgical technique, with the reported higher risks of early complications, namely graft detachment and iatrogenic graft failure due to inadvertent up-side-down graft (25, 26, 31, 41–45) (**Figure 4**). The insertion and un-scrolling of the DMEK graft, once inside the anterior chamber, are indeed the most demanding steps in DMEK. The challenges occur as the DM, once detached from the cornea stromal surface, has an intrinsic propensity to adopt a scrolled configuration with the endothelial surface on its outside (46, 47). This is particularly the case for DMEK grafts harvested from young donors (46). Unlike conventional DSAEK, an alternative surgical skill set is needed by the corneal surgeon (42). The surgeon should understand the different described techniques to unscroll the DMEK graft once in the eye (48–50). Such techniques include methodological approaches to unfolding a double scrolled graft by tapping the cornea in a shallow anterior chamber, and the use of air bubbles to assist in tight or single scrolls (49, 50). In situations, for example tight scrolls or deep anterior chambers, the unscrolling of the graft can be technically demanding (46). Consequently, many corneal surgeons still reserve DMEK for more straightforward cases of endothelial diseases and DSAEK for more challenging cases (e.g., advanced bullous keratopathy, aphakia, large iris defects, vitrectomized eyes, previous glaucoma filtration surgery) (51–54).

In current clinical practice, the vast majority of DMEK surgeries performed are "endothelium-out" techniques. This was reflected in this systematic review. Of the 21,323 included eyes that underwent DMEK, 19,945 (93.5%) received their grafts through various "endothelium-out" insertion techniques. In these techniques, the DMEK graft is loaded into an injector and inserted into the anterior chamber as a scroll, with the endothelium on its outer surface. Injectors used included modified intraocular lens cartridges, implantable contact lens cartridges, intravenous tubing, or glass injectors (**Supplementary Table 1**). Direct contact of the endothelium of the DMEK graft to the walls of the injectors can potentially cause endothelial cell damage and loss. Studies have indicated that plastic graft injectors are associated with higher rates of post-operative graft detachments, compared to glass devices (55, 56). Such observations have been explained by more damage to the corneal endothelium with plastic materials, and intra-operative alterations in the morphologies of the grafts during insertion and un-scrolling, which may be caused by electro-static forces produced by plastic (55). Nonetheless, not all reports have found similar effects (57).

Moreover, in "endothelium-out" techniques, there is often no control of the scrolled graft during insertion. Despite the use of intraoperative imaging (58), orientation markers such as S-stamps (59) or other asymmetrical indicators (60), determining the orientation of the graft in the anterior chamber can sometimes be difficult. Especially in cases of prolonged surgery, DMEK grafts in the eye can lose their pre-stained trypan blue stains, making visualization of graft orientation even more difficult. This is especially so in patients with dark irides (**Figure 5**).

The unfolding of a scrolled DMEK graft and its central positioning on the recipient's posterior stromal surface can also be problematic and time-consuming. To unfold the DMEK scroll after insertion into the anterior chamber, numerous approaches such as using air bubbles or jets of balanced salt solution in the presence of a shallow anterior chamber and the stroking of the corneal surface have been described (48). To overcome these difficulties of intracameral DMEK graft unfolding, different groups have investigated various alternative techniques. An example of such alternative techniques is the transplantation of DMEK tissue of various shapes (61). Authors have showed that certain DMEK graft shapes, such as the Maltese cross graft design, may be less prone to tight scrolling.

The concept of "endothelium-in" DMEK insertion techniques have been recently introduced (33–37, 44, 45). The grafts are folded, usually in a trifold, with the endothelium on the inside. These "endothelium-in" techniques prevent the DMEK grafts from adopting their natural scrolls with the endothelium on the outside. These "endothelium-in" techniques are believed to have the benefits of minimizing endothelial cell damage from the mechanical stress of the endothelial cells on the walls of the injectors. Moreover, in "endothelium-in" techniques, the grafts are pulled into the eyes with the endothelium facing downward. Once in the eye, the graft begins to unfold to acquire

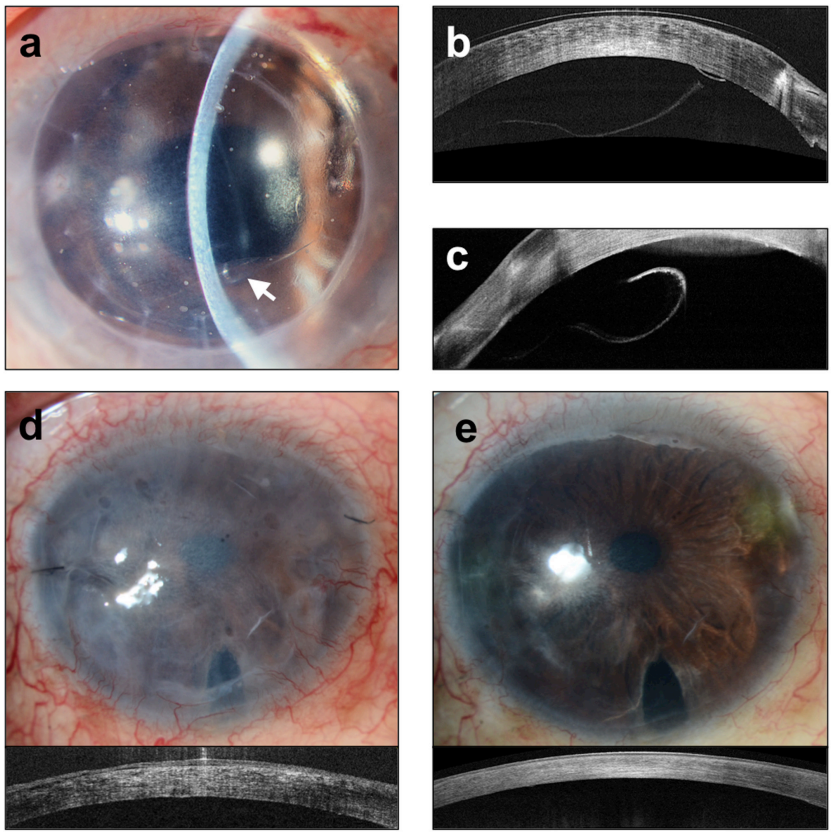

FIGURE 4 | Complications of Descemet membrane endothelial keratoplasty (DMEK). **(a)** Slit lamp image of graft detachment (arrow) at post-operative day 7 and corresponding anterior segment optical coherence tomography (ASOCT) (Optovue, Oculus, CA, United States). Images **(b,c)** showing detached graft. **(d)** Iatrogenic graft failure likely a result of inadvertent graft eversion showing a hazy and thick cornea. **(e)** Repeated DMEK surgery with correct graft orientation showing rapid clearance of cornea and reduction in corneal thickness.

its physiological "endothelium-out" configuration, effectively "aiding" the surgeon in graft unfolding. Pre-clinical laboratory studies have also reported significantly shorter graft unfolding times for "endothelium-in" compared to "endothelium-out" techniques (62). These factors in "endothelium-in" techniques reduce the technical difficulties of intracameral graft orientation and unscrolling, making DMEK procedures more controlled and predictable. Some of these "endothelium-in" techniques also use devices created to mimic DSAEK techniques, which many corneal surgeons are accustomed to (33, 44, 45). Various laboratory studies have reported no significant differences in endothelial cell loss when DMEK grafts were loaded "endothelium-in" and pulled-through or loaded "endothelium-out" and injected-through different graft insertion devices (62–64). In this review, the surgical outcomes of both "endothelium-out" and "endothelium-in" techniques were evaluated.

Summary of Evidence

This review included a total of 95 studies (**Supplementary Table 1**). Eighty-six studies using "endothelium-out" insertion techniques, eight studies using "endothelium-in" insertion techniques, and one study comparing "endothelium-out" to "endothelium-in" techniques. The majority of studies, 73/95 (76.8%), were rated as level III or level IV evidence. Only 4/95 (4.2%) studies were rated as level I evidence.

Evaluating the outcomes of "endothelium-out" techniques, the mean BCVA at 6 months after DMEK surgery ranged from 0.0 to 0.49 LogMAR (34 studies); 42.5–85% of eyes (15 studies) achieved a best-corrected visual acuity (BCVA) of 20/25 or better at 6 months. The mean endothelial cell loss ranged from 19 to 53%. The random pooled mean endothelial cell loss was 36.3 ± 6.4% at 6 months (27 studies) and 38.7 ± 7.2% at 12 months (12 studies). Rates of re-bubbling for graft detachments, primary graft failure rates, secondary graft failure rates, and graft rejection rates ranged from 0 to 82%, 0 to 21.0%, 0 to 7.0%, and 0 to 7.0%, respectively. The random pooled graft re-bubbling rates for "*endothelium-out*" techniques were 26.2% (95% CI 21.9–30.9%) (74 studies). The random pooled primary graft failure rates for "*endothelium-out*" techniques was 2.9% (95% CI 2.03–4.02%) (58 studies).

Of the eight "endothelium-in" studies reporting visual acuity data, the mean BCVA at 6 months after DMEK surgery ranged from 0.09 to 0.10 LogMAR (2 studies); 44.7–87.5% of eyes (3 studies) achieved a best-corrected visual acuity (BCVA) of 20/25 or better at 6 months. The mean endothelial cell loss ranged from 26.6 to 56.0% (7 studies). The random pooled mean endothelial cell loss was 28.1 ± 1.3% at 6 months (7 studies) and 29.6 ± 1.2%

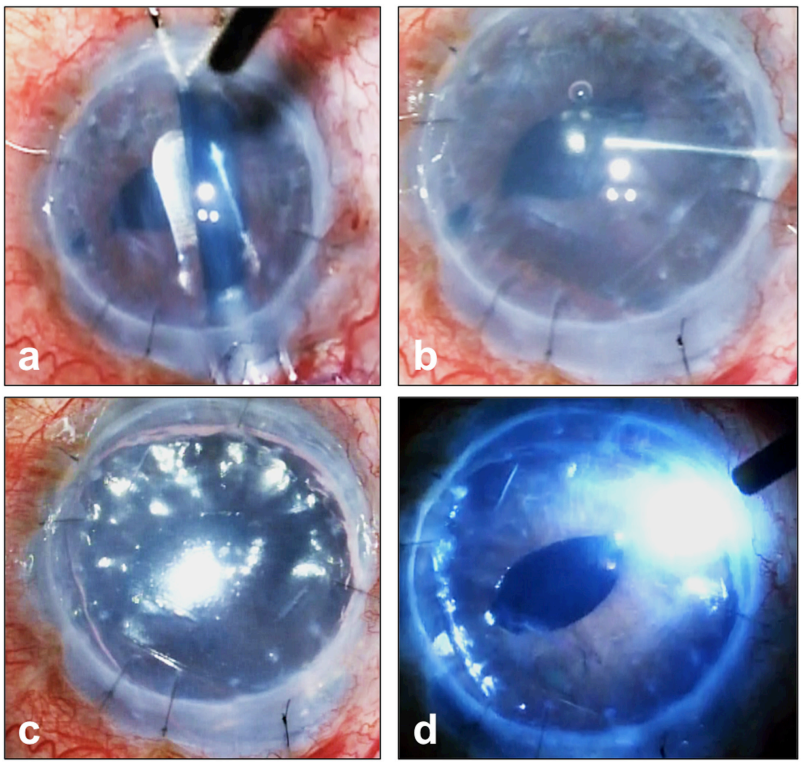

FIGURE 5 | Complex Descemet membrane endothelial keratoplasty (DMEK) surgery performed in an eye with previously failed penetrating keratoplasty graft and iridocorneal endothelial (ICE) syndrome. **(a)** DMEK graft pre-stained with Membrane Blue Dual (D.O.R.C., Netherlands) and inserted into the eye. **(b)** Prolonged surgery has resulted in the loss of the blue stain making visualization of graft orientation and attachment difficult; **(c)** this is made more difficult given the patient's dark iris **(d)** full air-gas tamponade of graft and the use of an external light pipe to assist the surgeon in graft orientation and attachment.

at 12 months (1 study). Graft detachment re-bubbling rates and primary graft failure rates ranged from 4.7 to 45.7% (nine studies) and 0 to 3.0% (six studies), respectively. Only one study reported on secondary graft failure rates in which there were none. None of the studies reporting on "endothelium-in" techniques reported the graft rejection rates. The random pooled graft re-bubbling rates for *"endothelium-in"* techniques was 16.5% (95% CI 8.5–26.4%) (6 studies). The random pooled primary graft failure rates for *"endothelium-in"* techniques was 1.5% (95% CI 0.6–2.7%) (six studies).

Comparing outcomes of *"endothelium-out"* to *"endothelium-in"* techniques, pooled mean endothelial cell loss was lower in the *"endothelium-in"* studies compared to *"endothelium-out"* studies at 6 months ($p = 0.018$); this was not statistically computable at 12 months as there was only 1 study for "*endothelium in"* group. Although re-bubbling rates for graft detachments were higher in the "endothelium-out" studies compared to "endothelium-in" studies, statistical significance was not achieved ($p = 0.440$). There was no significant difference in primary graft failure rates between the two groups ($p = 0.552$).

Limitations of This Review

This review has several limitations. The quality of available evidence was considered low (grade III and IV) with a significant number of studies judged as having high risks of bias (**Figure 3** and **Supplementary Appendix 3**). Significant heterogeneity existed in the studies, such as study designs, study population, surgical techniques, surgeon experience, outcome measures, and duration of follow-up. Studies published after the date of the pre-defined search strategy have also not been included. Furthermore, there was a smaller number of studies that reported on outcomes using "endothelium-in" DMEK surgeries that met the inclusion criteria for this review. This makes it difficult to provide any definitive conclusions through a comparative meta-analysis, especially in longer post-operative time points. Thus, the evidence to compare "endothelium-out" to "endothelium-in" techniques cannot be considered complete with this review.

CONCLUSION

The rates of endothelial cell loss were reported to be significantly lower in "endothelium-in" DMEK surgeries at 6 months following surgery compared to "endothelium-out" surgeries. Despite the above-mentioned limitations, visual outcomes and rates of complications of "endothelium-in" techniques from the small number of studies were noted to be comparable to those reported in "endothelium-out" studies. Given the intra-operative challenges following graft insertion encountered using "endothelium-out" techniques, surgeons may consider "endothelium-in" techniques designed for easier intra-operative DMEK graft unfolding after graft insertion. However, further well-conducted, adequately powered,

randomized controlled trials and studies with longer duration of follow-up are needed before conclusive comparisons between the two techniques can be made.

DATA AVAILABILITY STATEMENT

The original contributions presented in this study are included in the article/**Supplementary Material**, further inquiries can be directed to the corresponding authors.

AUTHOR CONTRIBUTIONS

HO and JM: conceptualization and supervision. HO and HH: data curation. HO, HH, MA, and JM: formal analysis, investigation, methodology, writing draft, and review and editing. All authors approved the manuscript.

FUNDING

The costs of publication of this article was funded by a grant from SingHealth Fund-SNEC (SHF-SNEC).

SUPPLEMENTARY MATERIAL

The Supplementary Material for this article can be found online at: https://www.frontiersin.org/articles/10.3389/fmed.2022.868533/full#supplementary-material

REFERENCES

1. Australian Corneal Graft Registry. *The Australian Graft Registry 2018 Report*. Adelaide, SA: Flinders University South Australian Health and Medical Research Institute (2018).
2. EBAA. *Eye Banking Statistical Report 2019*. Washington, DC: Eye Bank Association of America (2020).
3. Park CY, Lee JK, Gore PK, Lim CY, Chuck RS. Keratoplasty in the United States: a 10-year review from 2005 through 2014. *Ophthalmology.* (2015) 122:2432–42. doi: 10.1016/j.ophtha.2015.08.017
4. Tan DT, Dart JK, Holland EJ, Kinoshita S. Corneal transplantation. *Lancet.* (2012) 379:1749–61.
5. Ong HS, Ang M, Mehta JS. Evolution of therapies for the corneal endothelium: past, present and future approaches. *Br J Ophthalmol.* (2020) 105:454–67. doi: 10.1136/bjophthalmol-2020-316149
6. Melles GR, Eggink FA, Lander F, Pels E, Rietveld FJ, Beekhuis WH, et al. A surgical technique for posterior lamellar keratoplasty. *Cornea.* (1998) 17:618–26.
7. Koenig SB, Covert DJ, Dupps WJ Jr, Meisler DM. Visual acuity, refractive error, and endothelial cell density six months after Descemet stripping and automated endothelial keratoplasty (DSAEK). *Cornea.* (2007) 26:670–4. doi: 10.1097/ICO.0b013e3180544902
8. Aung TT, Yam JK, Lin S, Salleh SM, Givskov M, Liu S, et al. Biofilms of pathogenic nontuberculous mycobacteria targeted by new therapeutic approaches. *Antimicrob Agents Chemother.* (2016) 60:24–35. doi: 10.1128/AAC.01509-15
9. Woo JH, Ang M, Htoon HM, Tan DT. Descemet membrane endothelial keratoplasty versus Descemet stripping automated endothelial keratoplasty and penetrating keratoplasty. *Am J Ophthalmol.* (2019) 207:288–303. doi: 10.1016/j.ajo.2019.06.012
10. Guell JL, El Husseiny MA, Manero F, Gris O, Elies D. Historical review and update of surgical treatment for corneal endothelial diseases. *Ophthalmol Ther.* (2014) 3:1–15. doi: 10.1007/s40123-014-0022-y
11. Price FW Jr, Feng MT, Price MO. Evolution of endothelial keratoplasty: where are we headed? *Cornea.* (2015) 34:S41–7. doi: 10.1097/ICO.0000000000000505
12. Ang M, Saroj L, Htoon HM, Kiew S, Mehta JS, Tan D. Comparison of a donor insertion device to sheets glide in Descemet stripping endothelial keratoplasty: 3-year outcomes. *Am J Ophthalmol.* (2014) 157:1163–1169.e3. doi: 10.1016/j.ajo.2014.02.049
13. Ang M, Htoon HM, Cajucom-Uy HY, Tan D, Mehta JS. Donor and surgical risk factors for primary graft failure following Descemet's stripping automated endothelial keratoplasty in Asian eyes. *Clin Ophthalmol.* (2011) 5:1503–8. doi: 10.2147/OPTH.S25973
14. Ang M, Mehta JS, Anshu A, Wong HK, Htoon HM, Tan D. Endothelial cell counts after Descemet's stripping automated endothelial keratoplasty versus penetrating keratoplasty in Asian eyes. *Clin Ophthalmol.* (2012) 6:537–44. doi: 10.2147/OPTH.S26343
15. Ang M, Mehta JS, Lim F, Bose S, Htoon HM, Tan D. Endothelial cell loss and graft survival after Descemet's stripping automated endothelial keratoplasty and penetrating keratoplasty. *Ophthalmology.* (2012) 119:2239–44. doi: 10.1016/j.ophtha.2012.06.012
16. Ang M, Lim F, Htoon HM, Tan D, Mehta JS. Visual acuity and contrast sensitivity following Descemet stripping automated endothelial keratoplasty. *Br J Ophthalmol.* (2016) 100:307–11. doi: 10.1136/bjophthalmol-2015-306975
17. Fuest M, Ang M, Htoon HM, Tan D, Mehta JS. Long-term visual outcomes comparing Descemet stripping automated endothelial keratoplasty and penetrating keratoplasty. *Am J Ophthalmol.* (2017) 182:62–71. doi: 10.1016/j.ajo.2017.07.014
18. Bose S, Ang M, Mehta JS, Tan DT, Finkelstein E. Cost-effectiveness of Descemet's stripping endothelial keratoplasty versus penetrating keratoplasty. *Ophthalmology.* (2013) 120:464–70. doi: 10.1016/j.ophtha.2012.08.024
19. Tan D, Htoon HM, Ang M. Descemet's stripping automated endothelial keratoplasty with anterior chamber intraocular lenses. *Br J Ophthalmol.* (2014) 98:1462.
20. Melles GR, Ong TS, Ververs B, van der Wees J. Descemet membrane endothelial keratoplasty (DMEK). *Cornea.* (2006) 25:987–90.
21. Singh A, Zarei-Ghanavati M, Avadhanam V, Liu C. Systematic review and meta-analysis of clinical outcomes of Descemet membrane endothelial keratoplasty versus Descemet stripping endothelial keratoplasty/Descemet stripping automated endothelial keratoplasty. *Cornea.* (2017) 36:1437–43. doi: 10.1097/ICO.0000000000001320
22. Droutsas K, Lazaridis A, Papaconstantinou D, Brouzas D, Moschos MM, Schulze S, et al. Visual outcomes after Descemet membrane endothelial keratoplasty versus Descemet stripping automated endothelial keratoplasty-comparison of specific matched Pairs. *Cornea.* (2016) 35:765–71. doi: 10.1097/ICO.0000000000000822
23. Tourtas T, Laaser K, Bachmann BO, Cursiefen C, Kruse FE. Descemet membrane endothelial keratoplasty versus descemet stripping automated endothelial keratoplasty. *Am J Ophthalmol.* (2012) 153:1082–90.e2.
24. Guerra FP, Anshu A, Price MO, Price FW. Endothelial keratoplasty: fellow eyes comparison of Descemet stripping automated endothelial keratoplasty and Descemet membrane endothelial keratoplasty. *Cornea.* (2011) 30:1382–6. doi: 10.1097/ICO.0b013e31821ddd25
25. Stuart AJ, Romano V, Virgili G, Shortt AJ. Descemet's membrane endothelial keratoplasty (DMEK) versus Descemet's stripping automated endothelial keratoplasty (DSAEK) for corneal endothelial failure. *Cochrane Database Syst Rev.* (2018) 6:CD012097. doi: 10.1002/14651858.CD012097.pub2
26. Marques RE, Guerra PS, Sousa DC, Goncalves AI, Quintas AM, Rodrigues W. DMEK versus DSAEK for Fuchs' endothelial dystrophy: a meta-analysis. *Eur J Ophthalmol.* (2018) 29:15–22. doi: 10.1177/1120672118757431
27. Dapena I, Moutsouris K, Droutsas K, Ham L, van Dijk K, Melles GR. Standardized "no-touch" technique for Descemet membrane endothelial keratoplasty. *Arch Ophthalmol.* (2011) 129:88–94.

28. Arnalich-Montiel F, Munoz-Negrete FJ, De Miguel MP. Double port injector device to reduce endothelial damage in DMEK. *Eye (Lond).* (2014) 28:748–51. doi: 10.1038/eye.2014.67
29. Kruse FE, Laaser K, Cursiefen C, Heindl LM, Schlotzer-Schrehardt U, Riss S, et al. A stepwise approach to donor preparation and insertion increases safety and outcome of Descemet membrane endothelial keratoplasty. *Cornea.* (2011) 30:580–7. doi: 10.1097/ico.0b013e3182000e2e
30. Kim EC, Bonfadini G, Todd L, Zhu A, Jun AS. Simple, inexpensive, and effective injector for descemet membrane endothelial keratoplasty. *Cornea.* (2014) 33:649–52. doi: 10.1097/ICO.0000000000000121
31. Maier AK, Gundlach E, Schroeter J, Klamann MK, Gonnermann J, Riechardt AI, et al. Influence of the difficulty of graft unfolding and attachment on the outcome in Descemet membrane endothelial keratoplasty. *Graefes Arch Clin Exp Ophthalmol.* (2015) 253:895–900. doi: 10.1007/s00417-015-2939-9
32. Ang M, Ting DSJ, Kumar A, May KO, Htoon HM, Mehta JS. Descemet membrane endothelial keratoplasty in Asian eyes: intraoperative and postoperative complications. *Cornea.* (2020) 39:940–5. doi: 10.1097/ICO.0000000000002302
33. Ang M, Mehta JS, Newman SD, Han SB, Chai J, Tan D. Descemet membrane endothelial keratoplasty: preliminary results of a donor insertion pull-through technique using a donor mat device. *Am J Ophthalmol.* (2016) 171:27–34. doi: 10.1016/j.ajo.2016.08.023
34. Busin M, Leon P, D'Angelo S, Ruzza A, Ferrari S, Ponzin D, et al. Clinical outcomes of preloaded Descemet membrane endothelial keratoplasty grafts with endothelium tri-folded inwards. *Am J Ophthalmol.* (2018) 193:106–13. doi: 10.1016/j.ajo.2018.06.013
35. Leon P, Parekh M, Nahum Y, Mimouni M, Giannaccare G, Sapigni L, et al. Factors associated with early graft detachment in primary Descemet membrane endothelial keratoplasty. *Am J Ophthalmol.* (2018) 187:117–24.
36. Price MO, Lisek M, Kelley M, Feng MT, Price FW Jr. Endothelium-in versus endothelium-out insertion with Descemet membrane endothelial keratoplasty. *Cornea.* (2018) 37:1098–101. doi: 10.1097/ICO.0000000000001650
37. Ong HS, Mehta JS. Descemet's membrane endothelial keratoplasty (DMEK)—why Surgeons should consider adopting endothelium-in techniques. *US Ophthalmic Rev.* (2019) 12:65–8.
38. CEBM. *Oxford Centre for Evidence-Based Medicine – Levels of Evidence.* Oxford: CEBM (2009).
39. Higgins JPT, Altman DG, Sterne JAC. Chapter 8: assessing risk of bias in included studies. In: Higgins JPT, Green S editors. *Cochrane Handbook for Systematic Reviews of Interventions Version 5.1.0.* (London: The Cochrane Collaboration) (2011).
40. Price MO, Scanameo A, Feng MT, Price FW Jr. Descemet's membrane endothelial keratoplasty: risk of immunologic rejection episodes after discontinuing topical corticosteroids. *Ophthalmology.* (2016) 12:1232–6. doi: 10.1016/j.ophtha.2016.02.001
41. Hamzaoglu EC, Straiko MD, Mayko ZM, Sales CS, Terry MA. The first 100 eyes of standardized Descemet stripping automated endothelial keratoplasty versus standardized Descemet membrane endothelial keratoplasty. *Ophthalmology.* (2015) 122:2193–9. doi: 10.1016/j.ophtha.2015.07.003
42. Phillips PM, Phillips LJ, Muthappan V, Maloney CM, Carver CN. Experienced DSAEK Surgeon's transition to DMEK: outcomes comparing the last 100 DSAEK surgeries with the first 100 DMEK surgeries exclusively using previously published techniques. *Cornea.* (2017) 36:275–9. doi: 10.1097/ICO.0000000000001069
43. Rose-Nussbaumer J, Alloju S, Chamberlain W. Clinical outcomes of Descemet membrane endothelial keratoplasty during the Surgeon learning curve versus Descemet stripping endothelial keratoplasty performed at the same time. *J Clin Exp Ophthalmol.* (2016) 7:599. doi: 10.4172/2155-9570.1000599
44. Romano V, Kazaili A, Pagano L, Gadhvi KA, Titley M, Steger B, et al. Eye bank versus Surgeon prepared DMEK tissues: influence on adhesion and re-bubbling rate. *Br J Ophthalmol.* (2022) 106:177–83. doi: 10.1136/bjophthalmol-2020-317608
45. Parekh M, Pedrotti E, Viola P, Leon P, Neri E, Bosio L, et al. Factors affecting the success rate of pre-loaded DMEK with endothelium-inwards technique: a multi-centre clinical study. *Am J Ophthalmol.* (2022). doi: 10.1016/j.ajo.2022.03.009 [Epub ahead of print].
46. Heinzelmann S, Bohringer D, Haverkamp C, Lapp T, Eberwein P, Reinhard T, et al. Influence of postoperative intraocular pressure on graft detachment after Descemet membrane endothelial keratoplasty. *Cornea.* (2018) 37:1347–50.
47. Tan TE, Devarajan K, Seah XY, Lin SJ, Peh GSL, Cajucom-Uy HY, et al. Lamellar dissection technique for Descemet membrane endothelial keratoplasty graft preparation. *Cornea.* (2019) 39:23–9. doi: 10.1097/ICO.0000000000002090
48. Ang M, Wilkins MR, Mehta JS, Tan D. Descemet membrane endothelial keratoplasty. *Br J Ophthalmol.* (2016) 100:15–21.
49. Liarakos VS, Dapena I, Ham L, van Dijk K, Melles GR. Intraocular graft unfolding techniques in Descemet membrane endothelial keratoplasty. *JAMA Ophthalmol.* (2013) 131:29–35. doi: 10.1001/2013.jamaophthalmol.4
50. Yoeruek E, Bayyoud T, Hofmann J, Bartz-Schmidt KU. Novel maneuver facilitating Descemet membrane unfolding in the anterior chamber. *Cornea.* (2013) 32:370–3. doi: 10.1097/ICO.0b013e318254fa06
51. Ang M, Ho H, Wong C, Htoon HM, Mehta JS, Tan D. Endothelial keratoplasty after failed penetrating keratoplasty: an alternative to repeat penetrating keratoplasty. *Am J Ophthalmol.* (2014) 158:1221–1227.e1. doi: 10.1016/j.ajo.2014.08.024
52. Ang M, Li L, Chua D, Wong C, Htoon HM, Mehta JS, et al. Descemet's stripping automated endothelial keratoplasty with anterior chamber intraocular lenses: complications and 3-year outcomes. *Br J Ophthalmol.* (2014) 98:1028–32.
53. Ang M, Sng CCA. Descemet membrane endothelial keratoplasty and glaucoma. *Curr Opin Ophthalmol.* (2018) 29:178–84. doi: 10.1097/ICU.0000000000000454
54. Ang M, Sng CC. Descemet membrane endothelial keratoplasty developing spontaneous 'malignant glaucoma' secondary to gas misdirection. *Clin Exp Ophthalmol.* (2018) 46:811–3. doi: 10.1111/ceo.13150
55. Monnereau C, Quilendrino R, Dapena I, Liarakos VS, Alfonso JF, Arnalich-Montiel F, et al. Multicenter study of descemet membrane endothelial keratoplasty: first case series of 18 Surgeons. *JAMA Ophthalmol.* (2014) 132:1192–8. doi: 10.1001/jamaophthalmol.2014.1710
56. Dirisamer M, van Dijk K, Dapena I, Ham L, Oganes O, Frank LE, et al. Prevention and management of graft detachment in descemet membrane endothelial keratoplasty. *Arch Ophthalmol.* (2012) 130:280–91. doi: 10.1001/archophthalmol.2011.343
57. Oellerich S, Baydoun L, Peraza-Nieves J, Ilyas A, Frank L, Binder PS, et al. Multicenter study of 6-month clinical outcomes after Descemet membrane endothelial keratoplasty. *Cornea.* (2017) 36:1467–76. doi: 10.1097/ICO.0000000000001374
58. Ang M, Dubis AM, Wilkins MR. Descemet membrane endothelial keratoplasty: intraoperative and postoperative imaging spectral-domain optical coherence tomography. *Case Rep Ophthalmol Med.* (2015) 2015:506251. doi: 10.1155/2015/506251
59. Veldman PB, Dye PK, Holiman JD, Mayko ZM, Sales CS, Straiko MD, et al. The S-stamp in Descemet membrane endothelial keratoplasty safely eliminates upside-down graft implantation. *Ophthalmology.* (2016) 123:161–4. doi: 10.1016/j.ophtha.2015.08.044
60. Bhogal M, Maurino V, Allan BD. Use of a single peripheral triangular mark to ensure correct graft orientation in Descemet membrane endothelial keratoplasty. *J Cataract Refract Surg.* (2015) 41:2022–4. doi: 10.1016/j.jcrs.2015.08.005
61. Modabber M, Talajic JC, Mabon M, Mercier M, Jabbour S, Choremis J. The role of novel DMEK graft shapes in facilitating intraoperative unscrolling. *Graefes Arch Clin Exp Ophthalmol.* (2018) 256:2385–90. doi: 10.1007/s00417-018-4145-z
62. Parekh M, Ruzza A, Ferrari S, Ahmad S, Kaye S, Ponzin D, et al. Endothelium-in versus endothelium-out for Descemet membrane endothelial keratoplasty graft preparation and implantation. *Acta Ophthalmol.* (2017) 95:194–8. doi: 10.1111/aos.13162
63. Barnes K, Chiang E, Chen C, Lohmeier J, Christy J, Chaurasia A, et al. Comparison of tri-folded and scroll-based graft viability in preloaded Descemet membrane endothelial keratoplasty. *Cornea.* (2019) 38:392–6. doi: 10.1097/ICO.0000000000001831
64. Romano V, Ruzza A, Kaye S, Parekh M. Pull-through technique for delivery of a larger diameter DMEK graft using endothelium-in method. *Can J Ophthalmol.* (2017) 52:e155–6. doi: 10.1016/j.jcjo.2017.03.006

65. Price MO, Price FW Jr, Kruse FE, Bachmann BO, Tourtas T. Randomized comparison of topical prednisolone acetate 1% versus fluorometholone 0.1% in the first year after Descemet membrane endothelial keratoplasty. *Cornea.* (2014) 33:880–6. doi: 10.1097/ICO.0000000000000206
66. Price MO, Feng MT, Scanameo A, Price FW Jr. Loteprednol etabonate 0.5% Gel Vs. prednisolone acetate 1% solution after Descemet membrane endothelial keratoplasty: prospective randomized trial. *Cornea.* (2015) 34:853–8. doi: 10.1097/ICO.0000000000000475
67. Chamberlain W, Lin CC, Austin A, Schubach N, Clover J, McLeod SD, et al. Descemet endothelial thickness comparison trial: a randomized trial comparing ultrathin Descemet stripping automated endothelial keratoplasty with Descemet membrane endothelial keratoplasty. *Ophthalmology.* (2019) 126:19–26.
68. Dunker SL, Dickman MM, Wisse RPL, Nobacht S, Wijdh RHJ, Bartels MC, et al. Descemet membrane endothelial keratoplasty versus ultrathin Descemet stripping automated endothelial keratoplasty: a multicenter randomized controlled clinical trial. *Ophthalmology.* (2020) 127:1152–9. doi: 10.1016/j.ophtha.2020.02.029
69. Santander-Garcia D, Peraza-Nieves J, Muller TM, Gerber-Hollbach N, Baydoun L, Liarakos VS, et al. Influence of intraoperative air tamponade time on graft adherence in Descemet membrane endothelial keratoplasty. *Cornea.* (2019) 38:166–72. doi: 10.1097/ICO.0000000000001795
70. Price MO, Giebel AW, Fairchild KM, Price FW Jr. Descemet's membrane endothelial keratoplasty: prospective multicenter study of visual and refractive outcomes and endothelial survival. *Ophthalmology.* (2009) 116:2361–8. doi: 10.1016/j.ophtha.2009.07.010
71. Rudolph M, Laaser K, Bachmann BO, Cursiefen C, Epstein D, Kruse FE. Corneal higher-order aberrations after Descemet's membrane endothelial keratoplasty. *Ophthalmology.* (2012) 119:528–35. doi: 10.1016/j.ophtha.2011.08.034
72. Feng MT, Burkhart ZN, Price FW Jr, Price MO. Effect of donor preparation-to-use times on Descemet membrane endothelial keratoplasty outcomes. *Cornea.* (2013) 32:1080–2. doi: 10.1097/ICO.0b013e318292a7e5
73. Chaurasia S, Price FW Jr, Gunderson L, Price MO. Descemet's membrane endothelial keratoplasty: clinical results of single versus triple procedures (combined with cataract surgery). *Ophthalmology.* (2014) 121:454–8. doi: 10.1016/j.ophtha.2013.09.032
74. Cabrerizo J, Livny E, Musa FU, Leeuwenburgh P, van Dijk K, Melles GR. Changes in color vision and contrast sensitivity after descemet membrane endothelial keratoplasty for fuchs endothelial dystrophy. *Cornea.* (2014) 33:1010–5. doi: 10.1097/ICO.0000000000000216
75. Guell JL, Morral M, Gris O, Elies D, Manero F. Comparison of sulfur hexafluoride 20% versus air tamponade in Descemet membrane endothelial keratoplasty. *Ophthalmology.* (2015) 122:1757–64. doi: 10.1016/j.ophtha.2015.05.013
76. Heinzelmann S, Maier P, Bohringer D, Huther S, Eberwein P, Reinhard T. Cystoid macular oedema following Descemet membrane endothelial keratoplasty. *Br J Ophthalmol.* (2015) 99:98–102. doi: 10.1136/bjophthalmol-2014-305124
77. Heinzelmann S, Bohringer D, Eberwein P, Reinhard T, Maier P. Outcomes of Descemet membrane endothelial keratoplasty, Descemet stripping automated endothelial keratoplasty and penetrating keratoplasty from a single centre study. *Graefes Arch Clin Exp Ophthalmol.* (2016) 254:515–22. doi: 10.1007/s00417-015-3248-z
78. Schaub F, Enders P, Snijders K, Schrittenlocher S, Siebelmann S, Heindl LM, et al. One-year outcome after Descemet membrane endothelial keratoplasty (DMEK) comparing sulfur hexafluoride (SF6) 20% versus 100% air for anterior chamber tamponade. *Br J Ophthalmol.* (2017) 101:902–8. doi: 10.1136/bjophthalmol-2016-309653
79. Aravena C, Yu F, Deng SX. Outcomes of Descemet membrane endothelial keratoplasty in patients with previous glaucoma surgery. *Cornea.* (2017) 36:284–9. doi: 10.1097/ICO.0000000000001095
80. Tourtas T, Schlomberg J, Wessel JM, Bachmann BO, Schlotzer-Schrehardt U, Kruse FE. Graft adhesion in descemet membrane endothelial keratoplasty dependent on size of removal of host's descemet membrane. *JAMA Ophthalmol.* (2014) 132:155–61. doi: 10.1001/jamaophthalmol.2013.6222
81. Gundlach E, Maier AK, Tsangaridou MA, Riechardt AI, Brockmann T, Bertelmann E, et al. DMEK in phakic eyes: targeted therapy or highway to cataract surgery? *Graefes Arch Clin Exp Ophthalmol.* (2015) 253:909–14. doi: 10.1007/s00417-015-2956-8
82. Rock T, Bramkamp M, Bartz-Schmidt KU, Rock D, Yoruk E. Causes that influence the detachment rate after Descemet membrane endothelial keratoplasty. *Graefes Arch Clin Exp Ophthalmol.* (2015) 253:2217–22.
83. Hoerster R, Stanzel TP, Bachmann BO, Siebelmann S, Felsch M, Cursiefen C. Intensified topical steroids as prophylaxis for macular Edema after posterior lamellar keratoplasty combined with cataract surgery. *Am J Ophthalmol.* (2016) 163:174–179.e2. doi: 10.1016/j.ajo.2015.12.008
84. Schaub F, Pohl L, Enders P, Adler W, Bachmann BO, Cursiefen C, et al. Impact of corneal donor lens status on two-year course and outcome of Descemet membrane endothelial keratoplasty (DMEK). *Graefes Arch Clin Exp Ophthalmol.* (2017) 255:2407–14. doi: 10.1007/s00417-017-3827-2
85. Regnier M, Auxenfans C, Maucort-Boulch D, Marty AS, Damour O, Burillon C, et al. Eye bank prepared versus Surgeon cut endothelial graft tissue for Descemet membrane endothelial keratoplasty: an observational study. *Medicine (Baltimore).* (2017) 96:e6885. doi: 10.1097/MD.0000000000006885
86. Botsford B, Vedana G, Cope L, Yiu SC, Jun AS. Comparison of 20% sulfur hexafluoride with air for intraocular tamponade in Descemet membrane endothelial keratoplasty (DMEK). *Arq Bras Oftalmol.* (2016) 79:299–302. doi: 10.5935/0004-2749.20160086
87. Rickmann A, Opitz N, Szurman P, Boden KT, Jung S, Wahl S, et al. Clinical comparison of two methods of graft preparation in Descemet membrane endothelial keratoplasty. *Curr Eye Res.* (2018) 43:12–7. doi: 10.1080/02713683.2017.1368086
88. Schrittenlocher S, Bachmann B, Cursiefen C. Impact of donor tissue diameter on postoperative central endothelial cell density in Descemet membrane endothelial keratoplasty. *Acta Ophthalmol.* (2018) 97:e618–22. doi: 10.1111/aos.13943
89. Brockmann T, Brockmann C, Maier AB, Schroeter J, Bertelmann E, Torun N. Primary Descemet's membrane endothelial keratoplasty for fuchs endothelial dystrophy versus bullous keratopathy: histopathology and clinical results. *Curr Eye Res.* (2018) 43:1221–7. doi: 10.1080/02713683.2018.1490773
90. Kocluk Y, Kasim B, Sukgen EA, Burcu A. Descemet membrane endothelial keratoplasty (DMEK): intraoperative and postoperative complications and clinical results. *Arq Bras Oftalmol.* (2018) 81:212–8. doi: 10.5935/0004-2749.20180043
91. Rickmann A, Szurman P, Jung S, Boden KT, Wahl S, Haus A, et al. Impact of 10% SF6 gas compared to 100% air tamponade in descemet's membrane endothelial keratoplasty. *Curr Eye Res.* (2018) 43:482–6. doi: 10.1080/02713683.2018.1431286
92. von Marchtaler PV, Weller JM, Kruse FE, Tourtas T. Air versus sulfur hexafluoride gas tamponade in Descemet membrane endothelial keratoplasty: a fellow eye comparison. *Cornea.* (2018) 37:15–9. doi: 10.1097/ICO.0000000000001413
93. Rickmann A, Wahl S, Hofmann N, Haus A, Michaelis R, Petrich T, et al. Precut DMEK using dextran-containing storage medium is equivalent to conventional DMEK: a prospective pilot study. *Cornea.* (2019) 38:24–9. doi: 10.1097/ICO.0000000000001778
94. Shahnazaryan D, Hajjar Sese A, Hollick EJ. Endothelial cell loss after Descemet's membrane endothelial keratoplasty for Fuchs' endothelial dystrophy: DMEK compared to triple DMEK. *Am J Ophthalmol.* (2020) 218:1–6. doi: 10.1016/j.ajo.2020.05.003
95. Koechel D, Hofmann N, Unterlauft JD, Wiedemann P, Girbardt C. Descemet membrane endothelial keratoplasty (DMEK): clinical results of precut versus Surgeon-cut grafts. *Graefes Arch Clin Exp Ophthalmol.* (2021) 259:113–9. doi: 10.1007/s00417-020-04901-7
96. Potts LB, Bauer AJ, Xu DN, Chen SY, Alqudah AA, Sanchez PJ, et al. The last 200 Surgeon-loaded descemet membrane endothelial keratoplasty tissue versus the first 200 preloaded descemet membrane endothelial keratoplasty tissue. *Cornea.* (2020) 39:1261–6. doi: 10.1097/ICO.0000000000002400
97. Bohm MS, Wylegala A, Leon P, Ong Tone S, Ciolino JB, Jurkunas UV. One-year clinical outcomes of preloaded descemet membrane endothelial keratoplasty versus non-preloaded descemet membrane endothelial keratoplasty. *Cornea.* (2021) 40:311–9. doi: 10.1097/ICO.0000000000002430

98. Zwingelberg SB, Buscher F, Schrittenlocher S, Rokohl AC, Loreck N, Wawer-Matos P, et al. Long-term outcome of descemet membrane endothelial keratoplasty in eyes with fuchs endothelial corneal dystrophy versus pseudophakic bullous keratopathy. *Cornea.* (2021) 41:304–9. doi: 10.1097/ICO.0000000000002737
99. Jansen C, Zetterberg M. Descemet membrane endothelial keratoplasty versus Descemet stripping automated keratoplasty – outcome of one single Surgeon's more than 200 initial consecutive cases. *Clin Ophthalmol.* (2021) 15:909–21. doi: 10.2147/OPTH.S289730
100. Fajardo-Sanchez J, de Benito-Llopis L. Clinical outcomes of descemet membrane endothelial keratoplasty in pseudophakic eyes compared with triple-DMEK at 1-year follow-up. *Cornea.* (2021) 40:420–4. doi: 10.1097/ICO.0000000000002636
101. Guerra FP, Anshu A, Price MO, Giebel AW, Price FW. Descemet's membrane endothelial keratoplasty: prospective study of 1-year visual outcomes, graft survival, and endothelial cell loss. *Ophthalmology.* (2011) 118:2368–73. doi: 10.1016/j.ophtha.2011.06.002
102. Laaser K, Bachmann BO, Horn FK, Cursiefen C, Kruse FE. Descemet membrane endothelial keratoplasty combined with phacoemulsification and intraocular lens implantation: advanced triple procedure. *Am J Ophthalmol.* (2012) 154:47–55e2. doi: 10.1016/j.ajo.2012.01.020
103. Parker J, Dirisamer M, Naveiras M, Tse WH, van Dijk K, Frank LE, et al. Outcomes of Descemet membrane endothelial keratoplasty in phakic eyes. *J Cataract Refract Surg.* (2012) 38:871–7.
104. Anshu A, Price MO, Price FW Jr. Risk of corneal transplant rejection significantly reduced with Descemet's membrane endothelial keratoplasty. *Ophthalmology.* (2012) 119:536–40. doi: 10.1016/j.ophtha.2011.09.019
105. Gorovoy MS. DMEK complications. *Cornea.* (2014) 33:101–4.
106. Burkhart ZN, Feng MT, Price FW Jr, Price MO. One-year outcomes in eyes remaining phakic after Descemet membrane endothelial keratoplasty. *J Cataract Refract Surg.* (2014) 40:430–4. doi: 10.1016/j.jcrs.2013.08.047
107. Maier AK, Wolf T, Gundlach E, Klamann MK, Gonnermann J, Bertelmann E, et al. Intraocular pressure elevation and post-DMEK glaucoma following Descemet membrane endothelial keratoplasty. *Graefes Arch Clin Exp Ophthalmol.* (2014) 252:1947–54. doi: 10.1007/s00417-014-2757-5
108. Feng MT, Price MO, Miller JM, Price FW Jr. Air reinjection and endothelial cell density in Descemet membrane endothelial keratoplasty: five-year follow-up. *J Cataract Refract Surg.* (2014) 40:1116–21. doi: 10.1016/j.jcrs.2014.04.023
109. Deng SX, Sanchez PJ, Chen L. Clinical outcomes of descemet membrane endothelial keratoplasty using eye bank-prepared tissues. *Am J Ophthalmol.* (2015) 159:590–6. doi: 10.1016/j.ajo.2014.12.007
110. Rodriguez-Calvo-de-Mora M, Quilendrino R, Ham L, Liarakos VS, van Dijk K, Baydoun L, et al. Clinical outcome of 500 consecutive cases undergoing Descemet's membrane endothelial keratoplasty. *Ophthalmology.* (2015) 122:464–70. doi: 10.1016/j.ophtha.2014.09.004
111. Bhandari V, Reddy JK, Relekar K, Prabhu V. Descemet's stripping automated endothelial keratoplasty versus descemet's membrane endothelial keratoplasty in the fellow eye for fuchs endothelial dystrophy: a retrospective study. *Biomed Res Int.* (2015) 2015:750567. doi: 10.1155/2015/750567
112. Schoenberg ED, Price FW Jr, Miller J, McKee Y, Price MO. Refractive outcomes of descemet membrane endothelial keratoplasty triple procedures (combined with cataract surgery). *J Cataract Refract Surg.* (2015) 41:1182–9. doi: 10.1016/j.jcrs.2014.09.042
113. Gorovoy IR, Gorovoy MS. Descemet membrane endothelial keratoplasty postoperative year 1 endothelial cell counts. *Am J Ophthalmol.* (2015) 159:597–600e2. doi: 10.1016/j.ajo.2014.12.008
114. Ham L, Dapena I, Liarakos VS, Baydoun L, van Dijk K, Ilyas A, et al. Midterm results of descemet membrane endothelial keratoplasty: 4 to 7 years clinical outcome. *Am J Ophthalmol.* (2016) 171:113–21. doi: 10.1016/j.ajo.2016.08.038
115. Siggel R, Adler W, Stanzel TP, Cursiefen C, Heindl LM. Bilateral descemet membrane endothelial keratoplasty: analysis of clinical outcome in first and fellow eye. *Cornea.* (2016) 35:772–7. doi: 10.1097/ICO.0000000000000811
116. van Dijk K, Rodriguez-Calvo-de-Mora M, van Esch H, Frank L, Dapena I, Baydoun L, et al. Two-year refractive outcomes after descemet membrane endothelial keratoplasty. *Cornea.* (2016) 35:1548–55. doi: 10.1097/ICO.0000000000001022
117. Schlogl A, Tourtas T, Kruse FE, Weller JM. Long-term clinical outcome after descemet membrane endothelial keratoplasty. *Am J Ophthalmol.* (2016) 169:218–26.
118. Bhandari V, Reddy JK, Chougale P. Descemet's membrane endothelial keratoplasty in south Asian population. *J Ophthalmic Vis Res.* (2016) 11:368–71. doi: 10.4103/2008-322X.194072
119. Debellemaniere G, Guilbert E, Courtin R, Panthier C, Sabatier P, Gatinel D, et al. Impact of surgical learning curve in descemet membrane endothelial keratoplasty on visual acuity gain. *Cornea.* (2017) 36:1–6. doi: 10.1097/ICO.0000000000001066
120. Peraza-Nieves J, Baydoun L, Dapena I, Ilyas A, Frank LE, Luceri S, et al. Two-year clinical outcome of 500 consecutive cases undergoing descemet membrane endothelial keratoplasty. *Cornea.* (2017) 36:655–60. doi: 10.1097/ICO.0000000000001176
121. Showail M, Obthani MA, Sorkin N, Einan-Lifshitz A, Boutin T, Borovik A, et al. Outcomes of the first 250 eyes of descemet membrane endothelial keratoplasty: canadian centre experience. *Can J Ophthalmol.* (2018) 53:510–7. doi: 10.1016/j.jcjo.2017.11.017
122. Basak SK, Basak S, Pradhan VR. Outcomes of descemet membrane endothelial keratoplasty (DMEK) using Surgeon's prepared donor DM-roll in consecutive 100 Indian eyes. *Open Ophthalmol J.* (2018) 12:134–42. doi: 10.2174/1874364101812010134
123. Kurji KH, Cheung AY, Eslani M, Rolfes EJ, Chachare DY, Auteri NJ, et al. Comparison of visual acuity outcomes between nanothin descemet stripping automated endothelial keratoplasty and descemet membrane endothelial keratoplasty. *Cornea.* (2018) 37:1226–31. doi: 10.1097/ICO.0000000000001697
124. Fajgenbaum MAP, Kopsachilis N, Hollick EJ. Descemet's membrane endothelial keratoplasty: surgical outcomes and endothelial cell count modelling from a UK centre. *Eye (Lond).* (2018) 32:1629–35. doi: 10.1038/s41433-018-0152-x
125. Newman LR, DeMill DL, Zeidenweber DA, Mayko ZM, Bauer AJ, Tran KD, et al. Preloaded descemet membrane endothelial keratoplasty donor tissue: surgical technique and early clinical results. *Cornea.* (2018) 37:981–6.
126. Price DA, Kelley M, Price FW Jr, Price MO. Five-year graft survival of descemet membrane endothelial keratoplasty (EK) versus descemet stripping EK and the effect of donor sex matching. *Ophthalmology.* (2018) 125:1508–14. doi: 10.1016/j.ophtha.2018.03.050
127. Schrittenlocher S, Schaub F, Hos D, Siebelmann S, Cursiefen C, Bachmann B. Evolution of consecutive descemet membrane endothelial keratoplasty outcomes throughout a 5-year period performed by two experienced Surgeons. *Am J Ophthalmol.* (2018) 190:171–8. doi: 10.1016/j.ajo.2018.03.036
128. Droutsas K, Lazaridis A, Giallouros E, Kymionis G, Chatzistefanou K, Sekundo W. Scheimpflug densitometry after dmek versus dsaek-two-year outcomes. *Cornea.* (2018) 37:455–61. doi: 10.1097/ICO.0000000000001483
129. Godin MR, Boehlke CS, Kim T, Gupta PK. Influence of lens status on outcomes of descemet membrane endothelial keratoplasty. *Cornea.* (2019) 38:409–12.
130. Rickmann A, Wahl S, Katsen-Globa A, Szurman P. Safety analysis and results of a borosilicate glass cartridge for no-touch graft loading and injection in descemet membrane endothelial keratoplasty. *Int Ophthalmol.* (2019) 39:2295–301. doi: 10.1007/s10792-018-01067-4
131. Sarnicola C, Sabatino F, Sarnicola E, Perri P, Cheung AY, Sarnicola V. Cannula-assisted technique to unfold grafts in descemet membrane endothelial keratoplasty. *Cornea.* (2019) 38:275–9. doi: 10.1097/ICO.0000000000001827
132. Brockmann T, Pilger D, Brockmann C, Maier AB, Bertelmann E, Torun N. Predictive factors for clinical outcomes after primary descemet's membrane endothelial keratoplasty for fuchs' endothelial dystrophy. *Curr Eye Res.* (2019) 44:147–53. doi: 10.1080/02713683.2018.1538459
133. Schaub F, Gerber F, Adler W, Enders P, Schrittenlocher S, Heindl LM, et al. Corneal densitometry as a predictive diagnostic tool for visual acuity results after descemet membrane endothelial keratoplasty. *Am J Ophthalmol.* (2019) 198:124–9. doi: 10.1016/j.ajo.2018.10.002

134. Livny E, Bahar I, Levy I, Mimouni M, Nahum Y. "PI-less DMEK": results of DESCEMET'S membrane endothelial keratoplasty (DMEK) without a peripheral iridotomy. *Eye (Lond).* (2019) 33:653–8.
135. Basak SK, Basak S, Gajendragadkar N, Ghatak M. Overall clinical outcomes of descemet membrane endothelial keratoplasty in 600 consecutive eyes: a large retrospective case series. *Indian J Ophthalmol.* (2020) 68:1044–53. doi: 10.4103/ijo.IJO_1563_19
136. Siddharthan KS, Shet V, Agrawal A, Reddy JK. Two-year clinical outcome after descemet membrane endothelial keratoplasty using a standardized protocol. *Indian J Ophthalmol.* (2020) 68:2408–14.
137. Lekhanont K, Pisitpayat P, Cheewaruangroj N, Jongkhajornpong P, Nonpassopon M, Anothaisintawee T. Outcomes of descemet membrane endothelial keratoplasty in Bangkok, Thailand. *Clin Ophthalmol.* (2021) 15:2239–51. doi: 10.2147/OPTH.S310873
138. Marchand M, El-Khoury J, Harissi-Dagher M, Robert MC. Outcomes of first cases of DMEK at a canadian university hospital centre. *Can J Ophthalmol.* (2021) 57:214–5. doi: 10.1016/j.jcjo.2021.05.010
139. Studeny P, Hlozankova K, Krizova D, Netukova M, Veith M, Mojzis P, et al. Long-term results of a combined procedure of cataract surgery and descemet membrane endothelial keratoplasty with stromal rim. *Cornea.* (2021) 40:628–34. doi: 10.1097/ICO.0000000000002574
140. Tan TE, Devarajan K, Seah XY, Lin SJ, Peh GSL, Cajucom-Uy HY, et al. Descemet membrane endothelial keratoplasty with a pull-through insertion device: surgical technique, endothelial cell loss, and early clinical results. *Cornea.* (2020) 39:558–65. doi: 10.1097/ICO.0000000000002268
141. Yu AC, Myerscough J, Spena R, Fusco F, Socea S, Furiosi L, et al. Three-year outcomes of tri-folded endothelium-in descemet membrane endothelial keratoplasty with pull-through technique. *Am J Ophthalmol.* (2020) 219:121–31. doi: 10.1016/j.ajo.2020.07.004
142. Woo JH, Htoon HM, Tan D. Hybrid descemet membrane endothelial keratoplasty (H-DMEK): results of a donor insertion pull-through technique using donor stroma as carrier. *Br J Ophthalmol.* (2020) 104:1358–62. doi: 10.1136/bjophthalmol-2019-314932
143. Ighani M, Dzhaber D, Jain S, De Rojas JO, Eghrari AO. Techniques, outcomes, and complications of preloaded, trifolded descemet membrane endothelial keratoplasty using the DMEK endoglide. *Cornea.* (2021) 40:669–74. doi: 10.1097/ICO.0000000000002648
144. Jabbour S, Jun AS, Shekhawat NS, Woreta FA, Krick TW, Srikumaran D. Descemet membrane endothelial keratoplasty using a pull-through technique with novel infusion forceps. *Cornea.* (2021) 40:387–92. doi: 10.1097/ICO.0000000000002558

Conflict of Interest: JM holds a patent on the EndoGlide and receive royalties.

The remaining authors declare that the research was conducted in the absence of any commercial or financial relationships that could be construed as a potential conflict of interest.

Publisher's Note: All claims expressed in this article are solely those of the authors and do not necessarily represent those of their affiliated organizations, or those of the publisher, the editors and the reviewers. Any product that may be evaluated in this article, or claim that may be made by its manufacturer, is not guaranteed or endorsed by the publisher.

frontiers | Frontiers in Medicine

REVIEW
published: 16 June 2022
doi: 10.3389/fmed.2022.835843

Host Defense Peptides at the Ocular Surface: Roles in Health and Major Diseases, and Therapeutic Potentials

Darren Shu Jeng Ting[1,2,3]*, *Imran Mohammed*[1], *Rajamani Lakshminarayanan*[3], *Roger W. Beuerman*[3] *and Harminder S. Dua*[1,2]

[1] *Academic Ophthalmology, School of Medicine, University of Nottingham, Nottingham, United Kingdom,* [2] *Department of Ophthalmology, Queen's Medical Centre, Nottingham, United Kingdom,* [3] *Anti-Infectives Research Group, Singapore Eye Research Institute, Singapore, Singapore*

Sight is arguably the most important sense in human. Being constantly exposed to the environmental stress, irritants and pathogens, the ocular surface – a specialized functional and anatomical unit composed of tear film, conjunctival and corneal epithelium, lacrimal glands, meibomian glands, and nasolacrimal drainage apparatus – serves as a crucial front-line defense of the eye. Host defense peptides (HDPs), also known as antimicrobial peptides, are evolutionarily conserved molecular components of innate immunity that are found in all classes of life. Since the first discovery of lysozyme in 1922, a wide range of HDPs have been identified at the ocular surface. In addition to their antimicrobial activity, HDPs are increasingly recognized for their wide array of biological functions, including anti-biofilm, immunomodulation, wound healing, and anti-cancer properties. In this review, we provide an updated review on: (1) spectrum and expression of HDPs at the ocular surface; (2) participation of HDPs in ocular surface diseases/conditions such as infectious keratitis, conjunctivitis, dry eye disease, keratoconus, allergic eye disease, rosacea keratitis, and post-ocular surgery; (3) HDPs that are currently in the development pipeline for treatment of ocular diseases and infections; and (4) future potential of HDP-based clinical pharmacotherapy for ocular diseases.

Keywords: antimicrobial peptide, cathelicidin, defensin, dry eye, host defense peptide, infection, keratitis, ocular surface

OPEN ACCESS

Edited by:
Claudia Fabiani,
University of Siena, Italy

Reviewed by:
Hon Shing Ong,
Singapore National Eye Center, Singapore
Melis Palamar,
Ege University, Turkey
Ajay Sharma,
Chapman University, United States
Krishna Mohan Poluri,
Indian Institute of Technology Roorkee, India

***Correspondence:**
Darren Shu Jeng Ting
ting.darren@gmail.com

Specialty section:
This article was submitted to Ophthalmology, a section of the journal Frontiers in Medicine

Received: *15 December 2021*
Accepted: *17 May 2022*
Published: *16 June 2022*

Citation:
Ting DSJ, Mohammed I, Lakshminarayanan R, Beuerman RW and Dua HS (2022) Host Defense Peptides at the Ocular Surface: Roles in Health and Major Diseases, and Therapeutic Potentials. Front. Med. 9:835843. doi: 10.3389/fmed.2022.835843

INTRODUCTION

The ocular surface (OS) is a specialized anatomical and functional system composed of various structures and components, including the tear film, conjunctival and corneal epithelium, lacrimal glands, meibomian glands, and nasolacrimal drainage apparatus. Originating embryologically from the surface ectoderm, all these OS structures are linked anatomically *via* the epithelium and functionally *via* the regulation of neuronal, vascular, endocrinological, and immunological systems (1). Together, they maintain the homeostasis of the OS which has critical roles in the optical quality of the eye to focus light at the retina and serving as the most front-line defense system of the eye against a wide array of pathogens as well as physical and chemical insults (2). In addition, the periocular skin, which is in close vicinity to the eye, has important influences on the health of OS. Inflammatory diseases of the periocular skin such as atopic dermatitis and rosacea often result in the manifestation of OS damage (3–5).

Being constantly exposed to pathogens, environmental irritants and stress, the OS relies on a highly functional innate immunity. Innate immunity mechanisms for the OS are composed of three major components, including the physical barrier (e.g., epithelial layers of conjunctiva and cornea), chemical barriers (e.g., tears), and cellular responses (e.g., macrophages, neutrophils, and others), for which the host defense peptides (HDPs) play important roles in the latter two.

Antimicrobial peptides (AMPs) are a group of evolutionarily conserved molecules of the innate immunity (6). To better capture the increasingly recognized multi-faceted roles of AMPs, a broader term "host defense peptides (HDPs)" has been subsequently introduced (7). They are ubiquitously expressed at epithelial surfaces (e.g., eye, skin, respiratory, gastrointestinal linings, etc.) and secreted by immune cells (e.g., polymorphonuclear leukocytes and macrophages) (8, 9). So far more than 3,000 naturally occurring and synthetic HDPs have been discovered across six life kingdoms (10, 11). These HDPs are usually cationic (due to the relative excess of arginine, lysine and/or histidine residues) and amphiphilic, with 30%−50% hydrophobicity (12). They exhibit high structural plasticity and can exist in the form of alpha-helical, beta-sheet, linear extension or mixed a-helical and beta-sheet structures (**Figure 1**) (13). They have recently shown promise as potential therapeutic agents due to their broad-spectrum antimicrobial properties against a wide array of infection, including drug-resistant bacteria, fungi, acanthamoeba, and viruses, with minimal risk of inducing antimicrobial resistance (11). In principle, HDPs are shown to primarily exert their broad-spectrum and rapid antimicrobial action through three main mechanisms of action, namely the barrel-stave, toroidal pore, and carpet models (**Figure 2**) (14, 15). The positively charged amino acid residues are responsible for the adsorption of AMPs onto the anionic bacterial membrane (*via* electrostatic interaction) and the hydrophobic residues interact with the lipid tail region of the membrane, culminating in membrane permeation, leakage of fluid into the bacterial cytoplasm and subsequent bacterial cell death (14). In addition to the membrane-targeting action, emerging evidence has highlighted that HDPs can kill microorganisms through several non-membrane perturbing mechanisms, such as biosynthesis of disorganized bacterial membranes and direct intercalation into the membrane, interfering with the intracellular DNA and RNA molecules, and others (7). HDPs are also shown to participate in chemotaxis, immunomodulation, wound healing, anti-biofilm and anti-cancer activities (16–19), offering a wide range of potential therapeutic applications.

The history of HDPs (or AMPs) dates back to 1922 when lysozyme was first discovered in various human tissues and body secretions, including the tear fluids (20). Since then, a wide spectrum of human HDPs have been identified and reported at the OS. These include lactoferrin, alpha- and beta-defensins, cathelicidin (LL-37), ribonuclease, psoriasin and dermcidin, amongst others (9, 21, 22). The expressions and actions of HDPs in several OS diseases have been previously summarized by Kolar and McDermott (23). Since then, there is a growing body of evidence underlining the roles and therapeutic potential of HDPs at the OS, ranging from novel observations at the molecular level (e.g., upregulation of defensins and LL-37 in ocular rosacea) (24) to the advancement of designed HDPs toward human clinical trials (e.g., development of Mel4 as an antimicrobial coating for contact lens) (25). In view of the rapid evolution of this field, this review article aimed to provide an up-to-date, focused review of the spectrum and expression of HDPs at the OS, the roles in major OS diseases, and the therapeutic potential for OS diseases.

METHOD OF LITERATURE SEARCH

Electronic databases, including MEDLINE and EMBASE, were searched to identify relevant studies on HDPs at the OS. Only English articles were included in this review article. Key words used were "antimicrobial peptide," "defense peptide," "ocular surface," "tear fluid," "defensins," "cathelicidin," "keratitis," "dry eye," "atopic keratoconjunctivitis/atopic dermatitis," "ocular rosacea." The bibliographies of included articles were manually screened to identify further relevant studies. The final search was last updated in November 2021.

SPECTRUM AND CHARACTERISTICS OF HDPs AT OCULAR SURFACE

A wide array of HDPs have been identified and reported at the OS. In this section, we summarize the sources, characteristics, and functions of important HDPs, including lysozyme, lactoferrin, alpha- and beta-defensins, cathelicidin, ribonucleases, psoriasin, dermcidin, and histatin (**Table 1**).

Lysozyme

In 1922, lysozyme was discovered by Sir Alexander Fleming during the investigation of his patient with acute coryza. The nasal secretion of the patient was found to completely inhibit the growth of *Micrococcus* spp. (a Gram-positive bacteria). This striking observation prompted a series of experiments, which led to the discovery of lysozyme in various human tissues and body secretions, including tear fluids, saliva, blood, semen, respiratory tract linings, and connective tissues, amongst others (20). Interestingly, the antibacterial potency of lysozyme was influenced by the location of the tissues and types of microbes (e.g., lysozyme in tears was very active against micrococci, but was much less effective against other cocci in other parts of the body), highlighting the specific adaptation of the human immune system against specific pathogens at defined sties (20).

Lysozyme is primarily secreted in the tear fluid by the tubuloacinar cells of the main and accessory lacrimal glands (82) and, to a lesser extent, expressed by corneal epithelium and meibomian glands (83). It constitutes around 20%−30% of the total protein in tear fluids (82). Lysozyme exhibits its broad-spectrum antimicrobial activity *via* dual mechanisms of action (26). First, it hydrolyzes the bacterial cell wall by breaking down the β-1,4 glycosidic linkages between the disaccharides, *N*-acetylmuramic acid (NAM) and *N*-acetylglucosamine (NAG), which forms the backbone of peptidoglycan in the bacterial membrane. Second, the cationic property of lysozyme enables pore formation in the anionic bacterial membrane, which is

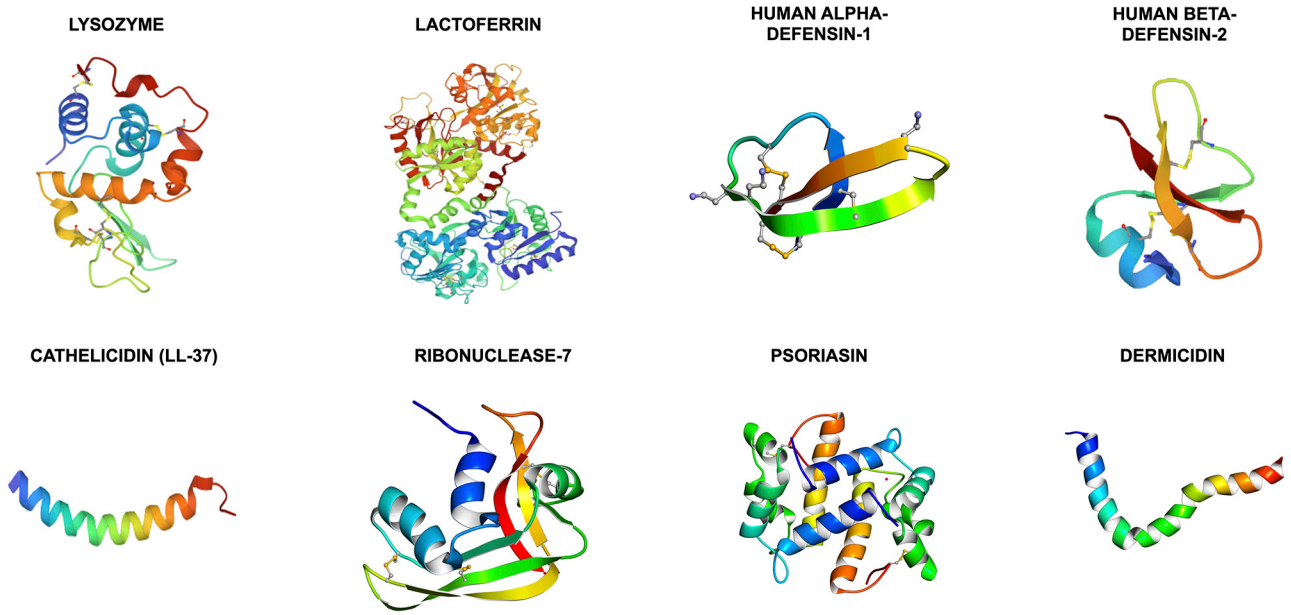

FIGURE 1 | Illustrations of the 3-dimensional secondary structures of the important host defense peptides (HDPs) at the ocular surface. The structures are obtained from the RCSB Protein Data Bank. Cathelicidin, psoriasin, and dermcidin are primarily made of alpha-helical helixes whereas human alpha- and beta-defensins are composed of triple beta-sheets. Lysozyme, lactoferrin and ribonuclease-7 (or RNase-7) are made of mixed alpha-helixes and beta-sheets.

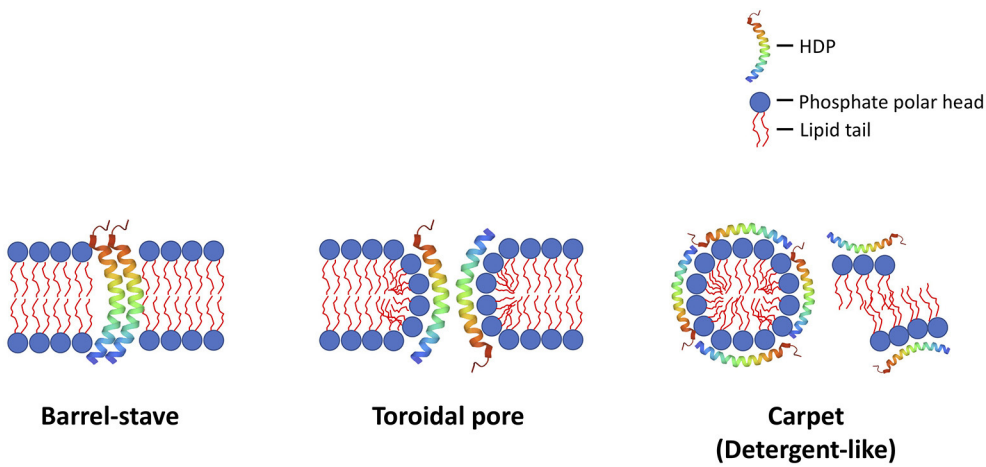

FIGURE 2 | Illustrations of the common membrane-permeabilizing mechanisms of host defense peptides (HDPs) against bacteria (and other microbes), namely: (1) barrel-stave; (2) toroidal pore; and (3) carpet (detergent-like) mechanisms. In the barrel-stave model, the HDPs act as a stave and penetrate vertically into the negatively charged, lipid bilayer bacterial membrane, creating permanent "barrel-shaped" pores. In the toroidal pore model, the HDPs interact with the negatively charged phosphate head groups electrostatically, distort the arrangement of the lipid bilayer, and create a transient membrane pore, with HDPs lining and stabilizing the internal part of the pore. In the carpet (detergent-like) model, the HDPs interact with the bacterial membrane electrostatically, and, upon reaching the critical concentration on the bacterial membrane, they result in membrane fragmentation / aggregation. These mechanisms result in destabilization of the membrane integrity, which leads to influx of fluid and efflux of intracellular content, culminating in cell lysis. Although less common (not shown in this figure), HDPs may also exert their antimicrobial action *via* binding to microbial intracellular targets (i.e., non-membrane-permeabilizing mechanisms), inhibiting DNA/RNA synthesis, protein synthesis and protein folding).

responsible for its rapid and broad-spectrum antimicrobial activity against a wide range of organisms.

In addition to its antimicrobial activity, lysozyme plays an important immunomodulatory role in host defense. Particularly, it activates lysozyme-dependent degradation of the engulfed bacteria within the phagolysosomes of macrophages and releases pathogen associated molecular patterns (PAMPs) from the lysed bacteria, resulting in a pro-inflammatory response *via* interaction with various pattern recognition receptors (PRRs) such as Toll-like receptors (TLRs), nucleotide-binding oligomerization

TABLE 1 | Characteristics and functions of common HDPs at the ocular surface (OS).

Type	Source	Functions
Lysozyme	- Tear fluid (secreted by tubuloacinar cells of lacrimal glands) - Corneal epithelium - Meibomian glands	- Antimicrobial property (*via* hydrolysis and pore formation of cell wall) (20, 26) - Immunomodulatory function *via* interaction with various pattern recognition receptors (26, 27)
Lactoferrin	- Tear fluid (secreted by acinar cells of lacrimal glands) - Conjunctival epithelium - Corneal epithelium - Meibomian glands	- Antimicrobial activity (*via* binding to free iron and membrane permeabilization) (28–30) and anti-biofilm (31) - Immunomodulatory function (anti- and pro-inflammatory) (32, 33) - Antioxidant (*via* inhibition of iron-dependent formation of hydroxyl radicals) (34) - Wound healing (32, 33)
Human alpha-defensins (or HNP)-1 to−4	- Azurophil granules of neutrophils	- All: antimicrobial activity (*via* membrane perturbation) (35) - HNP-1 to−3: immunomodulatory (Pro-inflammatory and anti-inflammatory) (36–38) - HNP-1 to−3: anti-cancer (39, 40)
Human beta-defensins (HBD)-1 to−3	- Conjunctival and corneal epithelium	- All: antimicrobial activity (*via* membrane perturbation) (41, 42) - All: immunomodulatory function (pro-inflammatory and anti-inflammatory) (42, 43) - HBD-3: wound healing (44) - All: anti-cancer (45, 46)
Cathelicidin	- Conjunctival epithelium - Corneal epithelium	- Antimicrobial activity (*via* membrane perturbation) (47–52) and anti-biofilm (47, 53) - Immunomodulatory function (pro-inflammatory and anti-inflammatory) (54, 55) - Wound healing (48, 56) - Anti-cancer (40, 57)
Ribonucleases - (RNases)	- RNase-5: Tear fluid and corneal endothelium - RNase-7: Corneal epithelium and stroma	- Antimicrobial activity (*via* binding to bacterial membrane lipoprotein and membrane perturbation) (58–66) - Immunomodulatory function (activates adaptive immunity) (67, 68) - Angiogenic and neurogenic (69, 70) - Wound healing (71)
Psoriasin	- Conjunctiva - Cornea - Lacrimal gland - Nasolacrimal duct	- Antimicrobial activity (*via* zinc-dependent mechanism) (72, 73) - Immunomodulatory function (chemotaxis, activates adaptive immune system *via* $CD4^+$) (74, 75)
Dermcidin	- Corneal epithelium - Tear fluid	- Antimicrobial activity (*via* zinc-dependent mechanism) (76)
Histatin	- Tear fluid	- Antimicrobial activity (*via* membrane perturbation) (77, 78) - Anti-inflammatory function (79) - Wound healing property (80, 81)

HNP, human neutrophil peptide/human alpha-defensin; HBD, human beta-defensins.

domain-like receptors (NLRs), and inflammasomes (26). Lysozyme may decrease systemic inflammation by restricting bacterial growth (27). In view of the ubiquitous presence and inherent antimicrobial and immunomodulatory activities of host lysozyme, bacteria have evolved several ingenious resistant mechanisms to survive against lysozyme. These include modification of membrane peptidoglycan, alteration of the membrane charges, and production of protein inhibitors against lysozyme (26). The understanding of the mechanisms of antimicrobial resistance (AMR) related to lysozyme (and potentially other naturally occurring HDPs) is unequivocally pivotal for development of the next generation of synthetic peptide-based therapeutics for tackling AMR.

Lactoferrin

Lactoferrin, belongs to the transferrin family, is an 80 kDa iron-sequestering HDP. It consists of a polypeptide chain that is folded into two highly symmetrical lobes (N- and C-lobes), which are capable of binding a variety of metal ions including ferric and ferrous ions (28). It is found abundantly in milk and in many other body tissues and secretions, including tears, saliva, sweat, nasal secretion, bronchial mucus, hepatic bile and others (84). Similar to lysozyme, lactoferrin is also primarily synthesized by the acinar cells of the main and accessory lacrimal glands (85). Some evidence has suggested the expression of lactoferrin in meibomian glands (83) and epithelium of conjunctiva and cornea (83, 86). It constitutes around 25% of the total protein in tear fluids, with a concentration of ∼2.2 mg/ml (29).

Lactoferrin has been shown to play multi-functional roles in host defense, armed with antimicrobial, anti-biofilm, anti-inflammatory, anti-cancer and anti-complement functions (28, 87). The antimicrobial activity of lactoferrin is attributed to its underlying dual mechanisms of action: (a) binding to free iron, an essential element for microbial growth; and (b) interaction and permeabilization of the anionic bacterial membrane through its positively charged N-terminal, which accounts for its rapid antimicrobial action (28). At the OS, it has been shown to exert broad-spectrum antimicrobial activity against Gram-positive and Gram-negative bacteria, fungi, and viruses (29). It has a strong

affinity toward the lipopolysaccharides (LPS) of the Gram-negative bacterial membrane, resulting in increased permeability. Studies have also shown that lysozyme and lactoferrin work in synergy where lactoferrin binds to the lipotechoic acid (LTA) of staphylococcal membrane and enables a greater access of lysozyme to the peptidoglycan (30). Another recent study by Avery et al. (31) showed that lactoferrin exhibits strong antimicrobial and antibiofilm activities against *Acinetobacter baumannii*, which is an important member of the ESKAPE pathogens commonly responsible for multidrug resistance in clinical setting. Interestingly, lactoferrin is ineffective against *Acanthamoeba trophozoites* and this is attributed to the effect of proteases released by *Acanthamoeba* (88).

Lactoferrin has been shown to play an important role in corneal wound closure where it regulates the anti-inflammatory and pro-inflammatory responses (32, 89). Pattamatta et al. (32, 33) demonstrated that lactoferrin stimulates corneal wound healing *via* upregulation of plate-derived growth factor and IL-6, downregulation of IL-1, and reduction of infiltrating inflammatory cells. Lactoferrin also acts as an antioxidant *via* inhibition of iron-dependent formation of hydroxyl radicals, thereby protecting corneal epithelium from oxidation-mediated tissue injury (34). This may have an implication on the pathogenesis of keratoconus (refer to Section Keratoconus). Furthermore, reduced levels of lactoferrin have been associated with systemic mucosal immunity incompetence. Hanstock et al. (90) observed that patients affected by upper respiratory tract infection had a significantly lower concentration of tear lysozyme and/or lactoferrin compared to healthy volunteers, suggesting that lysozyme and lactoferrin may serve as clinically relevant biomarkers for mucosal immune competence.

Defensins

Defensins are a large family of cysteine-rich HDPs that consist of a predominantly triple-stranded beta-sheet core structure stabilized with three pairs of intramolecular disulfide bridges (91). Depending on the pattern of the disulfide linkage, human defensins can be broadly divided into two groups, namely the alpha- and beta-defensins. Alpha-defensins have a cysteine pairing motif of Cys1–Cys6, Cys2–Cys4, and Cys3–Cys5 whereas beta-defensins form disulfide bridges at Cys1–Cys5, Cys2–Cys4, and Cys3–Cys6 (35, 91). Interestingly, this evolutionarily conserved disulphide bridge motif is similarly observed in defensins found in plants and invertebrates (92, 93).

Human alpha-defensins, also known as human neutrophil peptide (HNP) due to their abundant presence in neutrophils, can be subclassified into 6 main subtypes (HNP-1 to−6). HNP-1 to−4 are found primarily in the azurophil granules of neutrophils (35). HNP-1 to−3 sequences are highly homologous with only difference in a single N-terminal residue; removal of the alanine (the first amino acid of HNP-1 at the N-terminal) gives rise to HNP-2 and substitution of the alanine with aspartic acid yields HNP-3. HNP-5 and−6 are primarily located in the epithelium of Paneth cells of small intestines (35). On the other hand, more than 30 types of human beta-defensins (HBDs) have been described in the literature (94). HBD are mainly synthesized by the epithelial cells, including the conjunctiva, cornea, skin, oral mucosa, lining of respiratory and gastrointestinal tracts, and others (95). As described by McIntosh et al. (96), about 28 novel beta defensins were identified in human genome using the hidden Markov model. Thus far, only few, namely the HBD-1 to−4 and HBD-9 were shown to be involved in host immunity at the OS.

In view of the diverse function of defensins, it is not surprising that a plethora of HNPs and HBDs are abundantly present at a variety of bodily surfaces. At the OS, HNP-1 to−3, but not HNP-4 to−6, have been identified in normal human tears, conjunctival and corneal epithelium, lacrimal gland, and inflamed conjunctiva (in relation to infiltrating polymorphonuclear cells) (22, 97, 98). Similarly, McIntosh et al. (96) discovered an array of HBDs, including HBD-1 to−4, at the corneal and conjunctival epithelium, though the level of HBD-4 was relatively low. Another novel HDP, HBD-9, was discovered at the ocular surface epithelia and corneal stroma by our research group (99, 100). Further studies from our group and others have also shown that the expressions of HBDs are modulated by various PRRs, including TLRs and NLRs (99, 101, 102).

Defensins have been shown to exhibit broad-spectrum antimicrobial activity against bacteria, fungi, enveloped viruses, and parasites (35, 41). Similar to most cationic HDPs, the defensins also perturb the microbial membrane through direct interaction with the anionic and lipid microbial membrane. The antimicrobial efficacy of defensins is likely related to their inherent physicochemical characteristics such as cationicity, hydrophobicity, and amphiphilicity (35). It has been shown that cationicity plays a more important role in Gram-negative infections, whereas increased hydrophobicity enhances the antimicrobial action against Gram-positive infections (103, 104). In addition, synergy between different families of HDPs have been reported; for instance, HBD-2 and LL-37 exhibit synergistic antimicrobial killing of *Staphylococcus aureus*, which is likely accountable for the minimal risk of *S. aureus* infection in inflamed psoriatic skin (105).

In addition to the antimicrobial function, defensins are endowed with a wide range of functions, including immunomodulatory (pro-inflammatory and anti-inflammatory), wound healing, maintenance of skin barrier, and anti-cancer (**Figure 3**) (17, 36, 39–41, 43–46, 106). HBD has been shown to orchestrate the cross-talk between innate and adaptive immunity by recruiting T cells and dendritic cells to the infection site through interaction with chemokine (CCR6) receptor (43). HNP-1 regulates inflammation by inhibiting macrophage mRNA translation and secretion of proinflammatory cytokines and nitric oxide, enabling clearance of pathogen and resolution of inflammation with minimal collateral tissue damage (37, 38). Moreover, HBD-3 has been shown to promote wound closure in *S. aureus* infected diabetic wounds (44).

To gain a better understanding of the structure-activity relationship, many research groups have investigated the functional role of the evolutionarily conserved cysteine disulfide bridge moiety of defensins. Although this moiety is widely observed in vertebrate and invertebrate defensins, Wu et al. (42)

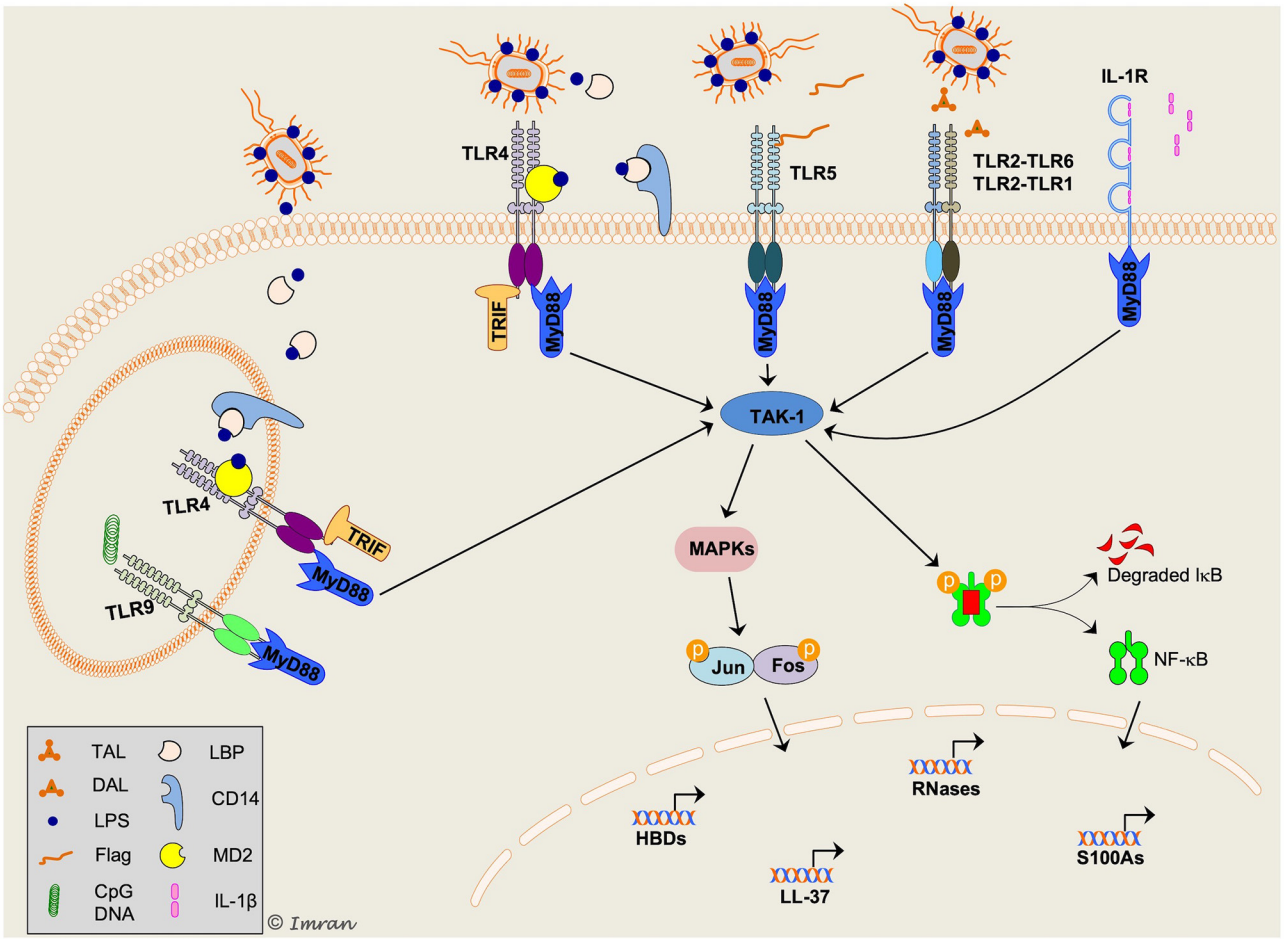

FIGURE 3 | Schematic representation of key signaling mechanisms involved in host defense peptides (HDPs) production in response to bacterial infection. Multiple intracellular signaling pathways are activated downstream of toll-like receptors (TLRs) in response to a variety of pathogen-associated molecular pattern (PAMPs), resulting in production of HDPs and cytokines/chemokines. TLR2/1 and TLR2/6 are shown to recognize diacylated (DAL) and triacylated (TAL) lipopeptides, respectively. TLR4 is present both on cell-surface and intracellularly on endosomes specifically recognizes lipopolysaccharide (LPS). LPS is recognized by LPS binding protein (LBP) and presented to CD14 (present in a soluble form in tear fluid), which transports LPS to myeloid differentiation-2 (MD-2)/TLR4 complex. Flagellin (Flag), a flagellar protein of Gram-negative bacteria, is recognized by TLR5. TLR9 present on endosomes recognizes CpG containing bacterial DNA; however, its role in production of HDPs and associated signaling mechanisms in corneal epithelial cells remain unclear. A pleiotropic cytokine, interleukin-1β (IL-1β) is recognized by IL-1R on cell surface. Activation of toll/IL-1-receptor (TIR) domain of both TLR and IL-1R triggers recruitment of the adaptor molecule myeloid differentiation primary response protein 88 (MyD88). TLR4 signaling can be activated via MyD88 and TIR-domain-containing adaptor protein inducing interferon-β (TRIF). Both MyD88 and TRIF initiate phosphorylation and ubiquitylation of several other molecules (not shown) leading to activation of transforming growth-factor-β activated kinase-1 (TAK1). In the cytosol, TAK-1 triggers activation of mitogen-activated protein kinases (MAPKs) and nuclear-factor-κ-B (NF-κB) pathways. This allows nuclear translocation of NF-κB and activator protein 1 (AP-1; complex of Jun and Fos protein) transcription factors and modulates expression of target HDPs. The scheme was adapted from Mohammed et al. paper (9).

demonstrated that removal of this structure has no influence on their inherent antibacterial activity against *Escherichia coli*. On the other hand, the chemotactic function (e.g., HBD-3) (42), anti-tumor necrosis factor (TNF)-alpha (e.g., HNP-1) (38), and antiviral activity (e.g., HNP-1 to−3) (107) are abolished when this disulfide moiety is destabilized or removed, suggesting that the disulfide bridges play important immunomodulatory and antiviral roles in innate immunity. These observations provide invaluable insight into the design and development of antimicrobial HDPs that are based on cysteine-rich native templates (108).

Cathelicidin

Cathelicidins are a large family of AMPs widely found in vertebrates (93, 109). The hallmark of cathelicidin is the presence of highly conserved cathelin domain, which was first identified in pig leukocytes as a cathepsin-L inhibitor and termed "cathelin" based on this property. Cathelicidin proteins comprised of a conserved 14 kDa cathelin domain flanked by a signal peptide (up to 30 residues) on N-terminus and an antimicrobial peptide region on its C-terminus. hCAP18, an 18 kDa preprotein, is the lone member of cathelicidin found in humans (110, 111). Its derivative, hCAP18(104–140), was shown to neutralize

lipopolysaccharide (LPS) activity both *in vitro* and *in vivo* (112). Proteinase-3, a proteolytic enzyme in human neutrophils can cleave hCAP18 into an active 37 amino-acid AMP, known as LL-37 (110, 113, 114). Moreover, another serum protease, gastricsin, at low vaginal pH was shown to cleave hCAP18 into a slightly longer active peptide, termed ALL-38 (115).

Since its first discovery in 1988 (116), cathelicidin is the most studied cationic HDP due to its wide-spectrum of activity, including anti-infective, anti-biofilm, anti-cancer, immunomodulatory, chemotactic, and wound healing properties (47, 53, 54, 57, 104, 117–120). The protective function of LL-37 against OS has been widely established (48, 49, 121, 122). LL-37 is constitutively expressed in OS epithelial specimens from healthy living patients and donor cadaveric tissues, including conjunctival and corneal epithelium (96, 123). It has been shown to play an important role in corneal wound healing and protection against various types of microbes at the OS (48, 123). In addition to its antimicrobial activity, Torres-Juarez et al. (55) demonstrated the immunomodulatory effects of LL-37 during mycobacterial infection, including reduction of tumor necrosis factor (TNF)-alpha and IL-17, and promoting the production of transforming growth factor (TGF-beta) and anti-inflammatory IL-10. Furthermore, LL-37 promotes wound healing *via* keratinocyte migration, which occurs *via* epidermal growth factor receptor transactivation (56).

Biochemical studies have elegantly demonstrated that smaller synthetic fragments derived from the parent LL-37 sequence were as effective as the full-length LL-37 (124–128). Studies have revealed that the middle region of LL-37_{17-29} (i.e., FK13) and/or LL-37_{18-29} (i.e., KR12) is largely responsible for the antimicrobial activity of LL-37 and has the ability to form amphipathic helix rich in positive charge, which enables effective interaction with the anionic membrane and subsequent microbial killing (126, 127, 129). In view of its therapeutic promise, a variety of strategies have been adopted to enhance the safety and efficacy of LL-37 and its derivatives (104, 130). Similar to LL-37, its smaller derivatives have shown considerable activity against a range of pathogens, including ESKAPE bacteria, fungi and viruses (47, 50–52). Our group has recently demonstrated that LL-37_{17-32} (FK16 peptide with free N- and C-termini) could also be utilized to improve the activity of conventional antibiotics such as vancomycin against *Pseudomonas aeruginosa*, as a strategy to repurpose the antibiotics and tackle AMR (131).

Ribonucleases (RNases)

Human ribonucleases (RNases) have an inherent ability to hydrolyze polymeric RNA and share a unique structural similarity to bovine pancreatic RNase A, therefore, also referred to as RNase A superfamily (132, 133). Similar to defensins, members of RNase A superfamily are comprised of six to eight conserved cysteine residues forming disulfide bridges. Genes encoding for human RNases 1 to 13 are clustered on chromosome 14q11.2 (133, 134). RNases are highly cationic and exhibit strong cytotoxic and microbicidal properties. Human RNase-2 (eosinophil derived neurotoxin) and RNase-3 (eosinophil cationic protein) are the first members of RNase A superfamily to show a strong role in host defense against an RNA virus, respiratory syncytial virus (RSV) (58, 59). Further studies have demonstrated that RNase-2 and−3 also have an ability to activate adaptive immunity (67, 68) and possess potent bactericidal and anti-helminthic properties (60–63). RNase-4 and−5 are shown to display potent angiogenic and neurogenic properties (69, 70). RNase-5, also known as angiogenin, has been widely studied due to its immunomodulatory properties. It is shown to be produced by skin keratinocytes and mast cells and has been detected in lacrimal secretions. RNase-5 has been shown to promote corneal endothelial wound healing *via* activation of PI3-kinase/Akt pathway (71), highlighting its therapeutic potential for corneal endothelial diseases. RNase-6 is ubiquitously expressed in immune cells including neutrophils and monocytes. Similar to RNase-3, it also exhibits bactericidal effect through agglutination and membrane disruption (64). Against *Mycobacterium* spp., it has been shown to induce autophagy in the infected macrophages leading to intracellular growth inhibition (135).

RNase-7 and−8 despite being structurally similar, their expression in different bodily tissues is greatly varied. On the OS, RNase-7 is constitutively expressed in healthy corneal epithelium and stroma (65). Further studies have demonstrated elevated levels of RNase-7 in samples collected from patients with bacterial, viral and Acanthamoeba keratitis as well as in CECs treated with cytokines, live bacteria and different pathogenic proteins that activates innate immune receptor signaling (65, 66). Specifically, the signaling mechanisms that are involved in elevation of RNase-7 levels in CECs in response to activation of interleukin 1β (IL-1β)/IL-1 receptor (IL-1R) axis was mapped by our group (65). Notably, the canonical nuclear factor κB (NFκB) transcription factor which mediates transcription of most HDPs in OS epithelium was found to be non-redundant in regulation of RNase-7. It was shown that IL-1b/IL-1R triggered mitogen activated protein kinases (MAPKs) signaling was responsible for RNase-7 regulation in CECs. Further analysis showed that the transcription factors, c-JUN and ATF, are involved in transcription of RNase-7 in CECs. This suggested that a biomarker or protein that directly activates these transcription factors could elicit HDPs in CECs during infection.

Psoriasin

Psoriasin, or S100A7, represents one of the main members of the S100 family of calcium-binding proteins (136). It is a low molecular weight protein (∼11 kDa) which consists of five alpha-helices and the structure relies on the binding of calcium (137). The term "psoriasin" was first coined in 1991 by Madsen et al. (138), who observed the upregulation of this novel HDP in psoriatic skin. Subsequently, its immunomodulatory role in psoriasis was shown to be related to the downstream stimulation of interleukin-1a (IL-1a) expression in human epidermal keratinocytes *via* the receptor for advanced glycation endproducts (RAGE)-p38 MAPK and calpain-1 pathways (139). At the OS, psoriasin was also found to be constitutively present various structures, including the conjunctiva, cornea, lacrimal gland and nasolacrimal ducts (72, 140), highlighting its protective role at the OS.

Psoriasin has been shown to exhibit strong antimicrobial activity against *E. coli* and *S. aureus*, likely *via* a zinc-dependent mechanism (72, 73). The upregulation of psoriasin against *E. coli* was found to be mediated *via* TLR5 (141). Interestingly, studies have shown that the antibacterial efficacy of psoriasin is likely conferred by the central region of the protein (amino acids at 35–80) (73). In addition to its antimicrobial activity, psoriasin has been shown to play essential important immunomodulatory roles, including chemotaxis for $CD4^+$ and neutrophils, production of cytokines and chemokines by neutrophils, generation of reactive oxygen species, and release of HNP-1 to−3 (74, 75).

Dermcidin

Dermcidin (DCD) is an important 110-residue HDP that is constitutively present in the golgi complex and the secretory granules of eccrine sweat. After being proteolytically processed, it is secreted into the sweat and transported onto the epidermal surface of skin as DCD-1L (which constitutes the N-terminal 48 residues of DCD) (76, 142, 143). It has been shown to adopt a unique high-conductance transmembrane hexameric channel architecture comprising trimers of antiparallel helical pairs, which is responsible for its membrane-disruptive antimicrobial mechanism (144).

The presence of DCD was first discovered in 2001 by Schittek et al. (145) and was found to possess broad-spectrum antimicrobial activity that is maintained over a broad pH range and in high salt concentrations, which resembles the human sweat. At the OS, McIntosh et al. (96) observed that dermcidin may be present at the corneal epithelium but this was only detected in one of the nine corneal samples. The presence of dermcidin in tear fluid was further confirmed by You et al. (146). Unlike most HDPs (which are cationic and kill bacteria *via* pore formation), dermcidin is an anionic peptide (147). It exerts its antimicrobial killing through interaction with the anionic bacterial phospholipids with subsequent zinc-dependent formation of oligomeric complexes in the bacterial membrane, resulting in formation of ion channels, membrane depolarization and cell death (76).

Histatin

Histatin belongs to a family of histidine-rich, cationic HDPs that are produced by the salivary gland into the saliva. They were first identified in 1988 by Oppenheim et al. (77) in human parotid secretion. Within the family, histatin-1,−3 and−5 are the major and most widely studied members and have been shown to exhibit antibacterial, antifungal and wound healing properties (77, 78). Histatin-1 and−3 are encoded by HTN1 and HTN3 genes, respectively, and histatin-5 is a proteolytic product of histatin-3 (148).

The first evidence of the presence of histatin at the ocular surface was demonstrated by Kalmodia et al. (149) in 2019. Histatin-1 was found to be present in normal human tears and reduced in aqueous-deficient dry eye disease by around 10-fold, suggesting the potential diagnostic value in evaluating dry eye disease. Based on *in vitro* studies, histatin-1 has been shown to enhance human corneal epithelial wound healing (80). In addition, histatin-1 can significantly reduce lipopolysaccharide-induced inflammatory signaling and production of nitric oxide and inflammatory cytokines *via* the JNK and NF-kB pathways in RAW264.7 macrophages (79). The multi-faceted properties of histatin, including antimicrobial, anti-inflammatory and wound healing properties, are particularly attractive for ocular surface diseases, especially infectious keratitis where inflammation overdrive and persistent epithelial wound are common sequelae of the infection (81, 150, 151).

ROLES OF HDPs IN MAJOR OCULAR SURFACE DISEASES

It is evident that HDPs play important roles in innate immunity and crosstalk between innate and adaptive immunity. In this section, we aim to provide a concise overview of the roles of HDPs in major OS diseases.

Infectious Keratitis

Infectious keratitis (IK) represents a major cause of corneal blindness worldwide (152). It has been estimated to cause 1.5–2 million new cases of monocular blindness every year, highlighting its significant burden on human health, healthcare resources and economy (152–154). Subject to geographical, temporal and seasonal variations, bacteria and fungi are the most common culprits for IK globally (150, 155–161). Broad-spectrum topical antimicrobials are currently the mainstay of treatment for IK but adjuvant therapy such as amniotic membrane transplant, therapeutic corneal cross-linking treatment (i.e., PACK-CXL) and therapeutic keratoplasty are often required to manage refractory cases of IK (162–166).

The pivotal roles of HDPs in IK are supported by a number of *in vitro* and *in vivo* observations and experiments (9). McIntosh et al. (96) investigated differential gene expression of HDPs in non-infected and infected eyes and demonstrated that some HDPs, notably HBD-3 and LL-37, were significantly elevated during OS infection. In addition, HBD-2 and−3, LL-37, MIP-3α, and thymosin β-4 were shown to exhibit moderate to strong *in vitro* antimicrobial activity against a range of ocular pathogens, including *S. aureus*, *P. aeruginosa*, adenovirus and HSV-1 (49, 123). Furthermore, cathelicidin-deficient/knockout mice were found to be more susceptible to *P. aeruginosa* corneal infection when compared to the wild type mice, underlining the antimicrobial function of cathelicidin at the OS (122). Synergistic antimicrobial action among different HDPs has also been reported in several studies (167, 168). For instance, Chen et al. (167) demonstrated that various combinations of HDPs, including HBD-1 to−3, LL-37 and lysozyme, exhibited synergistic or additive antimicrobial effect against *S. aureus* and *E. coli*.

The role of HDPs has also been implicated in other types of IK such as fungal and Acanthamoeba keratitis (9). Our recent study demonstrated that a range of HDPs, including HBD-1,−2,−3 and−9, LL-37 and S100A7, were upregulated during the active phase of fungal keratitis and returned to the baseline level upon resolution of the infection (169). Interestingly, there was

a preferential increase in mRNA expression of different types of HDPs, with HBD-1 and−2 being most commonly upregulated (90% of the cases) and LL-37 being least commonly upregulated (35% of the cases), highlighting the pathogen-specificity of HDPs. Similarly in Acanthamoeba keratitis, a wide range of HDPs such as HBD-2 and−3, LL-37, LEAP-1 and−2, and RNase-7 (but not HBD-1), were shown to be upregulated (66). Interestingly, HBD-1 and HBD-9 were significantly downregulated in Acanthamoeba keratitis (66, 170). Taken together, it is evident that HDPs serve as an integral component of the innate immunity of the OS, *via* their broad-spectrum and rapid antimicrobial activity against a wide range of ocular pathogens. These unique characteristics also render HDPs (usually those that are membrane-active) an attractive class of antimicrobial agent for managing IK, particularly in the face of polymicrobial keratitis and emerging antimicrobial resistance (152, 158, 171, 172).

Dry Eye Disease and Sjogren's Syndrome

Dry eye disease (DED) is one of the most common ocular surface morbidities with severe impact on vision and quality of life of affected individuals (173, 174). According to the recent TFOS DEWS II report, DED is defined as "a multifactorial disease of the ocular surface characterized by a loss of homeostasis of the tear film, and accompanied by ocular symptoms, in which tear film instability and hyperosmolarity, ocular surface inflammation and damage, and neurosensory abnormalities play etiological roles" (173). Sjogren's syndrome is a systemic autoimmune disease that primarily affects the lacrimal and salivary exocrine glands, leading to dry eyes and dry mouth (175). It is caused by lymphocytic infiltration of the exocrine glands secondary to the abnormal B- and T-cell autoimmune response against the auto-antigens, particularly SSA and SSB (175).

Several studies have demonstrated the dysregulation of HDPs in the DED. A range of HDPs, particularly lysozyme and/or lactoferrin, have been shown to be reduced in various types of DED, including SS and non-SS-related DED (176), evaporative DED (177), graft versus host disease (GvHD)-related DED (178), and others. Furthermore, HBD-2 and HBD-9 are found to be upregulated and downregulated, respectively, whereas HBD-1 and−3 remain unchanged in DED (100, 179). In addition, tear HDPs may also serve as useful biomarkers in DED. Studies have shown that tear lactoferrin was significantly reduced in various types of DED, including SS-related and non-SS-related DED, Steven–Johnson syndrome and evaporative DED secondary to meibomian gland dysfunction (177, 180). Sonobe et al. (176) recently demonstrated an inverse correlation between reduced lactoferrin concentration in tears and increased severity of DED using a novel and innovative microfluidic paper-based analytical device (μPAD). It has been shown that reduced level of lactoferrin serves as a good biomarker for distinguishing SS-related DED from non-SS-related DED (181), and for diagnosing DED in postmenopausal patients (182). The reduction of these tear HDPs in DED, in addition to the breakdown of corneal epithelium and increased bacterial load associated with DED, may potentially account for the increased risk of IK (though lack of strong evidence) (183, 184).

Keratoconus

Keratoconus is a bilateral, non-inflammatory corneal condition characterized by progressive corneal thinning and protrusion with resultant myopia and irregular astigmatism. It is the most common corneal ectatic disorder with an estimated prevalence of 1:2,000 to 1:400 people (185, 186). Depending on the severity and stability of keratoconus, it can be managed with glasses, soft and rigid contact lens, corneal cross-linking, intrastromal corneal ring segments, and corneal transplantation if all other measures fail (187–189). Although uncommon, keratoconus still remains a leading indication for corneal transplantation in many countries (190, 191).

The pathogenesis of keratoconus is likely to be multifactorial, contributed by genetic predisposition, environmental factors, proteolytic degradation of collagen, and mechanical trauma such as eye rubbing (192). Several molecular and proteomics studies (193–196) have also demonstrated the upregulation of certain tear proteins and inflammatory molecules in keratoconus, including interleukin-6, TNF-alpha, matrix metalloproteinases (MMP)-1,−3,−7,−9, and−13, lipocalin-1, neutrophil-defensin 1 precursor, mammaglobulin-B precursor, and keratin types 1 and 2, suggesting that inflammation plays a role in the pathogenesis of keratoconus. A recent proteomic study by Yam et al. (197) demonstrated that the epithelial and stromal proteins in keratoconic corneas were altered. The proteomic changes were primarily related to developmental and metabolic disorders (particularly in relation to mitochondria), cellular assembly, tissue organization and connective tissue disorders (particularly in relation to endoplasmic reticulum protein folding). Interestingly, the changes were not limited to the "cone area" but also involved the peripheral non-cone region of the keratoconic corneas. In addition, patients with keratoconus were found to have a significantly lower level of tear lactoferrin and the amount of reduction correlated with the severity of keratoconus (198). It is postulated that reduced lactoferrin results in accumulation of free iron in the tear fluids and iron deposition on the cornea ("Fleischer's ring"), thereby increasing cytotoxicity to the corneal epithelial cells (199). Based on these observations, Pastori et al. (199) have demonstrated that the oxidative stress induced by the tears in keratoconic patients, due to increased free iron, may be dampened by lactoferrin-loaded contact lens, potentially deterring the progression of keratoconus.

Pterygium

Pterygium is a common inflammatory ocular surface disease that is commonly encountered in tropical countries, with an estimated prevalence of 12% (200). It is characterized by fibrovascular growth of the conjunctiva into the cornea, resulting in ocular surface discomfort, pain, visual disturbance and impairment (if visual axis is encroached upon) (201). The pathogenesis of pterygium is likely attributed to a number of factors, including chronic ultraviolet radiation, human papillomavirus infection, oxidative stress, and genetic predisposition (202). So far, few groups have examined the role of HDPs in patients with pterygium. Ikeda et al. (98) observed the presence of HBD-2 in one of two conjunctival tissues of pterygium but in none of all eight normal conjunctival samples.

In addition, Zhou et al. (203) reported an upregulated expression of HNP-1 to−3, and calcium-binding proteins S100A8 and S100A9 in the tear fluids of eyes affected with pterygium. Another demonstrated the upregulation of HBD-1 and−2 along with a downregulation of HBD-9 in pterygium (204). These observations may be related to the underlying fibrovascular proliferative changes or inflammation. It was also suggested that the dysregulation of these HDPs may play an important contributory role to the pathogenesis of pterygium and may serve as useful biomarkers for predicting the recurrence of pterygium (203).

Post-ocular Surface Surgery and Wound Healing

The integrity of corneal epithelium is of utmost importance for ocular surface defense. Corneal wound healing relies on the regenerative capability of limbal stem cells and involves a complex process of cell death, migration, proliferation, differentiation, and remodeling of extracellular matrix (205). The integral role of HDPs for ocular surface wound healing has been evidently demonstrated in many studies. Zhou et al. (206) observed that the level of HNP-1 to−3 in tear fluids increased significantly after surgical removal of ocular surface neoplasm and returned to the baseline level after complete healing. Moreover, the concentration of HNP-1 and−2 reached a therapeutic level at day 3 postoperative (206). In addition, upregulation of HBD-2 mRNA expression was observed during the phase of corneal re-epithelialization (207).

Similarly, Huang et al. (48) previously demonstrated that LL-37 was increased in injured corneal epithelial cells (CEC), and recombinant LL-37 was capable of increasing the pro-inflammatory cytokines from CECs through the activation of G-protein coupled receptors (i.e., formyl peptide receptor-like 1). Application of vitamin D on wounded mouse corneas was shown to delay the normal wound healing process and increase the production of cathelin-related antimicrobial peptide (CRAMP) (208). However, the cause-effect relationship between CRAMP and corneal wound healing remains unknown but it was suggested that the increase levels of HDPs during epithelial defect would protect the cornea from infection during the healing phase. Recent studies have demonstrated that a deficiency of vitamin D receptors significantly delays the corneal wound healing and decreases the nerve density (209, 210). These findings suggest that HDPs play a crucial role in wound healing and protection against ocular surface infection.

Atopic Dermatitis and Allergic Keratoconjunctivitis

Atopic dermatitis (AD) is the most common inflammatory skin condition characterized by intense pruritus and chronic, relapsing eczematous lesions (211). The lifetime prevalence has been estimated at 20% (211). The pathogenesis of AD is multifactorial, with loss-of-function of the filaggrin gene (which regulates the epidermal barrier function), overgrowth of *S. aureus* (which may be caused by the dysregulation of HBD), IgE-mediated sensitization, and neuroinflammation playing important contributory roles (105, 211). Patients with AD may also suffer concurrently from atopic keratoconjunctivitis (AKC), which is a potentially sight-threatening ocular surface disease. Vernal keratoconjunctivitis (VKC) is another severe form of allergic eye disease that primarily affects the children and young adults (212).

Several studies have implicated the roles of HDPs in AD, AKC and VKC. Both HBD-2 and LL-37 are known to possess good antimicrobial activity against *S. aureus* and they work in synergy (105). Patients with AD are found to have substantially lower expressions of HBD-2 and−3, LL-37, and dermcidin, which may explain their increased susceptibility to staphylococcal skin infection compared to patients with psoriasis (105, 213). Similarly, patients with AKC are at risk of developing staphylococcal and herpetic infectious keratitis (214), which may be linked to the downregulation of mBD-2 mRNA at the ocular surface based on *in vivo* murine allergic eye conjunctivitis studies (215). Hida et al. (216) observed significantly higher levels of HNP-1 to−3 in the tears of patients with AKC complicated by allergic corneal epithelial disease compared to healthy patients or AKC patients with no corneal disease, suggesting a potentially protective role of HDP in corneal complications related to allergic eye disease. In addition, tear lactoferrin is reduced in VKC and the underlying mechanism is likely not related to lacrimal gland dysfunction but other factors since the level of tear lysozyme is unaffected (217).

Rosacea

Rosacea is a chronic, relapsing inflammatory skin disease that affects around 5% of the population (218). The risk of ocular surface involvement may develop in up to 70% of the rosacea patients and may occur with or without concurrent facial/skin rosacea (3). It can result in a wide array of ocular symptoms and signs, ranging from grittiness, visual blurring, and pain to sight-threatening complications such as corneal infection and perforation. The pathogenesis of rosacea remains to be fully elucidated; however dysregulation of the innate immunity (e.g., dysfunctional expression of HDPs) has been implicated, in addition to a number of environmental factors, genetic predisposition, and neurovascular dysregulation (219). The level of LL-37 is significantly increased in the skin epidermis in rosacea, which promotes skin inflammation *via* leukocyte chemotaxis and angiogenesis (220, 221). Gokcinar et al. (24) recently examined the role of HDPs in ocular rosacea and observed that the gene expressions of a wide range of HDPs, including tear HNP-1 to−3 and HBD-2, and conjunctival LL-37, were upregulated. On the other hand, tear lactoferrin was found to be reduced in rosacea (222).

THERAPEUTIC POTENTIALS OF HDPs FOR OCULAR SURFACE DISEASES

Despite their promising potential as effective antimicrobial and immunomodulatory therapies, several issues have impeded the successful translation of HDPs into clinical use. Complex structure-activity relationship, susceptibility to

TABLE 2 | A summary of host defense peptide (HDP)-based molecules that are in the development pipeline for ocular surface diseases.

Molecules (sequence)	Primary sources	Current development stage	Activities
B2088* ([RGRKVVRR]$_2$KK)	HBD-3 (C-terminal)	Pre-clinical stage	- Good activity against PA (108, 226) - Synergism with gatifloxacin and tobramycin (108)
Esculentin1–21(NH2) (GIFSK LAGKK IKNLL ISGLK G-NH_2)	Esculentin (N-terminal)	Pre-clinical stage	- Good activity against SA and PA (227, 228) - Good anti-biofilm activity against PA (228, 229)
RP444 (FAOOF AOOFO OFAOO FAOFA FAF)	Cecropin and magainins	Pre-clinical stage	- Good activity against Gram-positive and Gram-negative bacteria (230)
Melimine/Mel4 (KNKRK RRRRR RGGRR RR)	Melittin and protamine	Pre-clinical stage + phase 3	- Good activity against Gram-positive and Gram-negative bacteria (231, 232) - Reduces risk of CL-related infection (if CL coated with Mel4) (233)
MEL-4** (GIGAV L*K*VLT TGLPA LISWI *K*RKRQ Q)	Melittin (full-length)	Pre-clinical stage	- Good activity against Gram-positive and Gram-negative bacteria and fungi (234)
CaD23 (KRIVQ RIKDW LRKLC KKW)	Cathelicidin and HBD-2	Pre-clinical stage	- Good activity against SA, MRSA and PA (104) - Strong additive effect when used with levofloxacin or amikacin (235)
Histatin-5 (DSHAK RHHGY KRKFH EKHHS HRGY)	Histatin-5	Pre-clinical stage	- Promote corneal wound healing (81)

HBD, human beta-defensin; SA, Staphylococcus aureus; MRSA, methicillin-resistant S. aureus; PA, Pseudomonas aeruginosa; CL, contact lens.
**This is a branched peptide. The duplicating residues are in bracket.*
***The italicized "K" residue refers to epsilon-lysylated lysine residue. This MEL-4 molecule is different from the other Mel4 molecule.*

host/bacterial proteases and physiological conditions, pro-inflammatory properties, discrepancy between *in vitro* and *in vivo* efficacies, and toxicity to the host tissues are the main barriers (14, 23, 223, 224)Furthermore the lack of interest and investment from the pharmaceutical companies, stemming from limited life-span of antimicrobial therapy and low profits, poses another significant hurdle for the development of new antimicrobial agents (225). Herein, we present some of the key HDP-based molecules that have completed *in vivo* animal studies and are in the developmental pipeline for treating ocular surface diseases. These include B2088 branched peptide, Esculentin1–21(NH2), RP444, melimine/Mel4 antimicrobial coating for contact lens, epsilon-lysylated melittin (MEL-4), CaD23, histatin-5, and endogenous LL-37 (**Table 2**).

B2088 Branched Peptide

B2088 is a covalent dimeric peptide that is derived from the C-terminal of HBD-3 [peptide sequence: $(RGRKVVRR)_2KK$] (226). The development of this branched peptide was started in 2007 where Liu et al. (236) demonstrated that the linear form of HBD3 maintained similar antimicrobial efficacy and exhibited lower cytotoxicity and haemolytic activity compared to the native form of HBD3, after refining the hydrophobicity and substituting the cysteine residues with various amino acids. Such properties were postulated to be related to the removal of the disulfide bridges and the loss of secondary structure. Bai et al. (237) further enhanced the antimicrobial activity and reduced the host toxicity of linear HBD3 analogs by shortening the HBD3 to 10 amino acids from the C-terminal end. Taking it further, the antimicrobial efficacy of the truncated HBD3 was further optimized *via* dimerization at the lysine, which yielded the final lead compound of B2088 (108, 226).

B2088 has been shown to demonstrate strong antimicrobial activity against Gram-negative bacteria, particularly *P. aeruginosa* (108, 226). It exerts its bacterial killing through the binding of lipid A and disruption of supramolecular organization of lipopolysaccharides, a major component of the outer membrane of Gram-negative bacteria. In addition, B2088 strong synergism with various antibiotics through time-kill and checkerboard assays. This was further validated in an *in vivo* murine *P. aeruginosa* keratitis study where B2088 0.05%-gatifloxacin 0.15% combination treatment reduced the bacterial burden of corneal infection by an additional 1 LogCFU compared to gatifloxacin 0.3% alone (108).

Esculentin-1a(1–21)NH_2

The skin of amphibians contains a rich source of HDPs (238). Esculentin-1a is a type of frog-derived HDP isolated from the skin of *Rana esculenta*, or now known as *Pelophylax lessonae/ridibundus*. The modified version, Esculentin-1a(1–21)NH_2, is composed of the first 20 amino acids of esculentin-1a with a glycinamide residue at the C-terminal end (peptide sequence: GIFSKLAGKKIKNLLISGLKG-NH_2) (227). It has been shown to demonstrate strong *in vitro* antimicrobial activity against various *P. aeruginosa* laboratory strains (both invasive and cytotoxic strains) and clinical strains (isolated from eyes with keratitis and conjunctivitis), and *Staphylococci species* (with a MIC range of 1–16 μM) (227). In an *in vivo* murine bacterial IK model infected with cytotoxic *P. aeruginosa* strain, topical treatment of esculentin-1a(1–21)NH_2 significantly reduces the bacterial load, clinical severity and recruitment of inflammatory cells to the infected corneas measured by the relative myeloperoxidase activity (227). In addition, it was shown to exhibit anti-biofilm activity against *P. aeruginosa* (228, 229)

and prolong the survival of PAO1-infected mice in both sepsis and pneumonia models (228). The potent activity against both planktonic and sessile forms of *P. aeruginosa* was ascribed to its underlying membrane perturbation activity (228).

RP444

The development of RP444 was inspired by the "freedom from infection" observed in Cecropia moth and African clawed frog, which is attributed to the cecropins and magainins peptides, respectively (113). RP444 is a 23-amino acid designed HDP primarily composed of phenylalanine, alanine and ornithine, which is an unnatural amino acid used to replace lysine residue to enhance antimicrobial activity and proteolytic stability (peptide sequence: FAOOFAOOFOOFAOOFAOFAFAF) (230). This designed HDP possesses a broad-spectrum antimicrobial activity against a range of Gram-positive and Gram-negative bacteria (MIC ranges between 4 and 64 μg/ml) and anti-biofilm efficacy. Similar to other natural and synthetic HDPs, RP444 exhibits rapid bacterial killing within 30–60 min with no risk of developing resistance. Further *in vivo* murine bacterial keratitis study showed that RP444 was able to significantly reduce the bacterial load and clinical severity of *P. aeruginosa* keratitis and reduce inflammatory cell infiltration toward the infected site (230).

Melimine and Mel4 Antimicrobial Coating for Contact Lenses

Melimine is a 29-amino acid cationic synthetic HDP derived from melittin (from honeybee venom) and protamine (from salmon sperm) (239). This hybrid HDP combines the C-terminals of both melittin and protamine, yielding a total cationic charge of +14 (peptide sequence: TLISWIKNKRKQRPRVSRRRRRRGGRRRR). When attached to contact lenses, either through adsorption or covalent binding, melimine demonstrates higher antimicrobial activities against both Gram-positive and Gram-negative bacteria than melittin or protamine alone (239). In addition, the hemolytic activity of melimine is significantly lower than melittin. Furthermore, *in vivo* rabbit models successfully showed that melimine-coated lenses were safe to wear and they prevented bacterial growth on contact lenses, which consequently reduced the rate and severity of adverse reactions such as contact lens-induced acute red eye (CLARE), contact lens-induced peripheral ulcers (CLPUs) and IK (240–242). This suggests that hybridization of two different HDPs serves as a novel strategy to enhance antimicrobial efficacy and reduce toxicity.

However, when the melimine-coated contact lenses were tested in a human clinical trial, these lenses were paradoxically associated with significantly higher corneal staining compared to uncoated lenses at day 1 (241). To overcome this unforeseen corneal toxicity, the same research group has further refined the hybrid HDP, which has led to the creation of Mel4 – a truncated version of melimine with +14 net charge (peptide sequence: KNKRKRRRRRRGGRRRR) (231). This modified HDP exhibits modest antimicrobial activity against a broad range of Gram-positive and Gram-negative bacteria, with good *in vivo* safety demonstrated in rabbit and human trials (231). The mechanism of action of Mel4 against *P. aeruginosa* was found to be related to the neutralization of lipopolysaccharide and disruption of cytoplasmic membrane whereas its action against *S. aureus* was likely attributed to the release of autolysins with resultant cell death instead of pore formation (232, 243). A recent randomized controlled trial demonstrated that Mel4-coated antimicrobial contact lens was able to reduce corneal infiltrative events by at least 50% when compared to uncoated control lens during extended wear over 3 months (233).

Epsilon Lysylated Melittin (MEL-4)

Being as one of the main basic and cationic amino acids, lysine serves as a major constituent of many naturally occurring and synthetic HDPs (244, 245). In addition to the L- and D-form, lysine can also exist in epsilon form (ε-) where the NH_2 group at the side chain of L-lysine is linked to the alpha-carbon. ε-Poly-L-lysine (EPL) is a basic polyamide consisting of 25–30 ε-lysine that is naturally produced by *Streptomycetaceae* and *Ergot* fungi (246). It is commonly used as a food preservative with strong antimicrobial activity (247, 248). Compared to alpha-poly-L-lysine, EPL exhibits enhanced antimicrobial efficacy against a range of Gram-positive and Gram-negative bacteria (248, 249). Employing the similar strategy, Mayandi et al. (234) explored the selective incorporation of ε-lysine in melittin, which is a potent yet toxic HDP that is found in honeybee venom. They showed that ε-lysylation of melittin, in particular MEL-4 (different from the Mel4 described in the above Pterygium Section), improved the cell selectivity of the synthetic HDP toward a range of Gram-positive and Gram-negative bacteria with reduced host cytotoxic and hemolytic activities, whilst maintaining the *in vivo* efficacy of melittin (234). This suggests that ε-lysylation may serve as a novel strategy for improving the cell selectivity in lysine-rich HDPs.

Hybridized LL-37 and HBD-2 (CaD23)

LL-37 and HBDs are major groups of HDP that have been shown to play vital roles in various ocular surface diseases, particularly infectious keratitis. Inspired by these observations, our group recently developed a novel molecule, CaD23, *via* rationale hybridization of LL-37 and HBD-2 (peptide sequence: KRIVQRIKDWLRKLCKKW), and demonstrated good antimicrobial activity against a range of organisms commonly responsible for infectious keratitis, including *S. aureus*, MRSA and *P. aeruginosa* (104). The therapeutic potential of CaD23 was further substantiated by the strong *in vivo* antimicrobial activity against *S. aureus* in a pre-clinical murine model with good safety profile.

In addition, CaD23 demonstrates eight times faster antimicrobial action when compared to amikacin, a commonly used antibiotics for infectious keratitis (104). CaD23 also demonstrates a strong additive effect when used in combination with amikacin and levofloxacin against *S. aureus* and MRSA, underscoring the translational potential of peptide-antibiotic combined therapy in clinic (235). More importantly, when *S. aureus* was exposed to 10 consecutive sub-lethal concentration

of treatment, the bacteria did not develop any antimicrobial resistance against CaD23 whereas it developed significant antimicrobial resistance against amikacin by 32-fold (104). The rapid antimicrobial action (thence low risk of AMR) is likely attributed to its membrane-permeabilizing properties, evidenced by a combination of experimental and computational studies. Moreover, the molecular dynamics (MD) simulations study revealed the importance of alpha-helicity, cationicity, hydrophobicity and amphiphilicity in contributing to the antimicrobial action of CaD23 (235).

Histatin-5

Histatin peptides have been shown to demonstrate antimicrobial activity and wound healing properties. Based on a combination of *in vitro* and *in vivo* murine studies, Shah et al. (81) demonstrated that histatin-5 was able to promote corneal wound healing, and the effect pro-migratory effect was extracellular signal-regulated kinase 1/2 (ERK1/2) dependent. The authors were also able to determine that the C-terminal of histatin-5 (i.e., SHRGY) was the critical functional domain responsible for the wound healing property. These findings highlighting the potential of histatin-5 and/or the SHRGY pentapeptide for further development into clinical therapeutics for ocular surface diseases such as neurotrophic keratopathy or persistent corneal epithelial defect following infection or injury.

Endogenous LL-37 for Atopic Dermatitis

Understanding of the dysregulated expression of HDPs provides a unique opportunity to explore new therapeutic avenue in managing atopic dermatitis and potentially allergic eye diseases. As mentioned, a number of HDPs, including defensins and LL-37, are downregulated in the AD skin lesions (250). It has also been shown that the expression of LL-37 at the skin can be induced by the active 1,25 dihydroxy-vitamin D, which is regulated by the TLR-2 in keratinocytes and monocytes (251). In addition, the severity of AD is inversely proportionate to the level of LL-37 (252). Leveraging on these observations, several research groups have investigated and demonstrated that administration of oral vitamin D may improve the clinical severity of AD (253, 254), accompanied by an increased level of LL-37 (252). Similar strategy can potentially be employed for treating OS diseases, including allergic eye disease.

FUTURE DIRECTIONS

Currently there are a few clinical trials underway investigating the potential translation of HDPs from bench to clinics. Learning from the previous experience of other trials, particularly those that had reached but failed phase 3 trials (255, 256), it is important to select clinical areas and diseases that are likely to benefit from HDP treatment; for instance, comparing the efficacy between HDPs and antibiotic treatment for diseases caused by multi-drug resistant infection instead of routine and mild infection (which can be simply managed by current antibiotic treatment) is more likely to yield significant and clinically relevant results (130). In addition, based on the synergistic effect and benefit of reducing dose-related toxicity and AMR, researchers are exploring the use of HDP as adjuvant therapy in addition to antibiotic instead of monotherapy (108, 235). Furthermore, the increasingly recognized multi-faceted biological functions of HDPs, including anti-biofilm, immunomodulatory, wound healing, and anti-cancer properties, have yet to be fully capitalized in the clinic. For instance, HDPs such as defensins and lactoferricin have been shown to exert strong anti-cancer activity against various types of cancer, including colorectal, bladder, neuroblastoma, melanoma, and cutaneous squamous cell carcinoma (257). Nonetheless, the effect of HDP on OS neoplasia (e.g., squamous cell papilloma / carcinoma) has never been investigated or reported, highlighting a potential area for future research.

As there is no one set rule or principle to predict the efficacy and toxicity of designed HDPs, the infinite chemical space renders the design of HDPs a formidable task (7). With the rapid advancement in bioinformatics study (including molecular dynamic simulation), artificial intelligence and drug delivery technologies, efficient design and development of more effective HDPs are more likely to be achieved (130, 258). Integrating synthetic HDPs with novel delivery systems (e.g., nanoparticles, liposomes) may serve as a useful strategy to enhance the proteolytic stability and reduce toxicity of HDPs in the future (130, 259). Stimulation of the production of endogenous HDP using FDA-approved drugs or supplements, for instance using 4-phenylbutyrate and/or vitamin D to increase the level of LL-37, may also serve as a useful strategy in exploiting the benefits of HDP (251, 260, 261). Such an approach helps overcome the significant hurdles encountered during the bench-to-bedside translational process, including the regulatory barriers, for synthetic HDP-based molecules. In addition, the advancement in proteomics and whole genome sequencing technologies could facilitate the mining of previously unknown and undetected natural gene-encoded HDP sequences (262, 263), which can be utilized for therapeutic use in the future.

AUTHOR CONTRIBUTIONS

Study design and conceptualization: DT. Literature review, data collection, and manuscript drafting: DT and IM. Data interpretation: DT, IM, RL, RB, and HD. Critical revision of manuscript: RL, RB, and HD. Approval of the final version of manuscript. All authors contributed to the article and approved the submitted version.

FUNDING

DT is supported by the Medical Research Council/Fight for Sight (FFS) Clinical Research Fellowship (MR/T001674/1), the FFS/John Lee, Royal College of Ophthalmologists Primer Fellowship (24CO4), and the University of Nottingham International Research Collaboration Fund (A2RRG1). IM acknowledges funding support from the Medical Research Council – Confidence in Concept Scheme (MRC-CIC_2019-028).

REFERENCES

1. Gipson IK. The ocular surface: the challenge to enable and protect vision: the Friedenwald lecture. *Invest Ophthalmol Vis Sci.* (2007) 48:4390; 1–8. doi: 10.1167/iovs.07-0770
2. Ueta M, Kinoshita S. Innate immunity of the ocular surface. *Brain Res Bull.* (2010) 81:219–28. doi: 10.1016/j.brainresbull.2009.10.001
3. Wladis EJ, Adam AP. Treatment of ocular rosacea. *Surv Ophthalmol.* (2018) 63:340–6. doi: 10.1016/j.survophthal.2017.07.005
4. Guglielmetti S, Dart JK, Calder V. Atopic keratoconjunctivitis and atopic dermatitis. *Curr Opin Allergy Clin Immunol.* (2010) 10:478–85. doi: 10.1097/ACI.0b013e32833e16e4
5. Ting DSJ, Bandyopadhyay J, Patel T. Microbial keratitis complicated by acute hydrops following corneal collagen cross-linking for keratoconus. *Clin Exp Optom.* (2019) 102:434–6. doi: 10.1111/cxo.12856
6. Hancock RE, Lehrer R. Cationic peptides: a new source of antibiotics. *Trends Biotechnol.* (1998) 16:82–8. doi: 10.1016/S0167-7799(97)01156-6
7. Haney EF, Straus SK, Hancock REW. Reassessing the host defense peptide landscape. *Front Chem.* (2019) 7:43. doi: 10.3389/fchem.2019.00043
8. Mansour SC, Pena OM, Hancock RE. Host defense peptides: front-line immunomodulators. *Trends Immunol.* (2014) 35:443–50. doi: 10.1016/j.it.2014.07.004
9. Mohammed I, Said DG, Dua HS. Human antimicrobial peptides in ocular surface defense. *Prog Retin Eye Res.* (2017) 61:1–22. doi: 10.1016/j.preteyeres.2017.03.004
10. Zhao X, Wu H, Lu H, Li G, Huang Q, LAMP. A database linking antimicrobial peptides. *PLoS ONE.* (2013) 8:e66557. doi: 10.1371/journal.pone.0066557
11. Wang G, Li X, Wang Z. APD3: the antimicrobial peptide database as a tool for research and education. *Nucleic Acids Res.* (2016) 44:D1087–93. doi: 10.1093/nar/gkv1278
12. Mookherjee N, Anderson MA, Haagsman HP, Davidson DJ. Antimicrobial host defence peptides: functions and clinical potential. *Nat Rev Drug Discov.* (2020) 19:311–32. doi: 10.1038/s41573-019-0058-8
13. Huan Y, Kong Q, Mou H, Yi H. Antimicrobial peptides: classification, design, application and research progress in multiple fields. *Front Microbiol.* (2020) 11:582779. doi: 10.3389/fmicb.2020.582779
14. Li J, Koh JJ, Liu S, Lakshminarayanan R, Verma CS, Beuerman RW. Membrane active antimicrobial peptides: translating mechanistic insights to design. *Front Neurosci.* (2017) 11:73. doi: 10.3389/fnins.2017.00073
15. Bechinger B. Insights into the mechanisms of action of host defence peptides from biophysical and structural investigations. *J Pept Sci.* (2011) 17:306–14. doi: 10.1002/psc.1343
16. Steinstraesser L, Koehler T, Jacobsen F, Daigeler A, Goertz O, Langer S, et al. Host defense peptides in wound healing. *Mol Med.* (2008) 14:528–37. doi: 10.2119/2008-00002.Steinstraesser
17. Hancock RE, Haney EF, Gill EE. The immunology of host defence peptides: beyond antimicrobial activity. *Nat Rev Immunol.* (2016) 16:321–34. doi: 10.1038/nri.2016.29
18. Pletzer D, Coleman SR, Hancock RE. Anti-biofilm peptides as a new weapon in antimicrobial warfare. *Curr Opin Microbiol.* (2016) 33:35–40. doi: 10.1016/j.mib.2016.05.016
19. Riedl S, Zweytick D, Lohner K. Membrane-active host defense peptides–challenges and perspectives for the development of novel anticancer drugs. *Chem Phys Lipids.* (2011) 164:766–81. doi: 10.1016/j.chemphyslip.2011.09.004
20. Fleming A. On a remarkable bacteriolytic element found in tissues and secretions. *Proc R Soc B.* (1922) 93:306–17. doi: 10.1098/rspb.1922.0023
21. Wang G. Human antimicrobial peptides and proteins. *Pharmaceuticals.* (2014) 7:545–94. doi: 10.3390/ph7050545
22. Haynes RJ, Tighe PJ, Dua HS. Innate defence of the eye by antimicrobial defensin peptides. *Lancet.* (1998) 352:451–2. doi: 10.1016/S0140-6736(05)79185-6
23. Kolar SS, McDermott AM. Role of host-defence peptides in eye diseases. *Cell Mol Life Sci.* (2011) 68:2201–13. doi: 10.1007/s00018-011-0713-7
24. Gokcinar NB, Karabulut AA, Onaran Z, Yumusak E, Budak Yildiran FA. Elevated tear human neutrophil peptides 1-3, human beta defensin-2 levels and conjunctival cathelicidin LL-37 Gene expression in ocular rosacea. *Ocul Immunol Inflamm.* (2019) 27:1174–83. doi: 10.1080/09273948.2018.1504971
25. Willcox MD, Chen R, Kalaiselvan P, Yasir M, Rasul R, Kumar N, et al. The development of an antimicrobial contact lens - from the laboratory to the clinic. *Curr Protein Pept Sci.* (2020) 21:357–68. doi: 10.2174/1389203720666190820152508
26. Ragland SA, Criss AK. From bacterial killing to immune modulation: recent insights into the functions of lysozyme. *PLoS Pathog.* (2017) 13:e1006512. doi: 10.1371/journal.ppat.1006512
27. Ganz T, Gabayan V, Liao HI, Liu L, Oren A, Graf T, et al. Increased inflammation in lysozyme M-deficient mice in response to *Micrococcus luteus* and its peptidoglycan. *Blood.* (2003) 101:2388–92. doi: 10.1182/blood-2002-07-2319
28. Garcia-Montoya IA, Cendon TS, Arevalo-Gallegos S, Rascon-Cruz Q. Lactoferrin a multiple bioactive protein: an overview. *Biochim Biophys Acta.* (2012) 1820:226–36. doi: 10.1016/j.bbagen.2011.06.018
29. Flanagan JL, Willcox MD. Role of lactoferrin in the tear film. *Biochimie.* (2009) 91:35–43. doi: 10.1016/j.biochi.2008.07.007
30. Leitch EC, Willcox MD. Elucidation of the antistaphylococcal action of lactoferrin and lysozyme. *J Med Microbiol.* (1999) 48:867–71. doi: 10.1099/00222615-48-9-867
31. Avery TM, Boone RL, Lu J, Spicer SK, Guevara MA, Moore RE, et al. Analysis of antimicrobial and antibiofilm activity of human milk lactoferrin compared to bovine lactoferrin against multidrug resistant and susceptible *Acinetobacter baumannii* clinical isolates. *ACS Infect Dis.* (2021) 7:2116–26. doi: 10.1021/acsinfecdis.1c00087
32. Pattamatta U, Willcox M, Stapleton F, Cole N, Garrett Q. Bovine lactoferrin stimulates human corneal epithelial alkali wound healing *in vitro*. *Invest Ophthalmol Vis Sci.* (2009) 50:1636–43. doi: 10.1167/iovs.08-1882
33. Pattamatta U, Willcox M, Stapleton F, Garrett Q. Bovine lactoferrin promotes corneal wound healing and suppresses IL-1 expression in alkali wounded mouse cornea. *Curr Eye Res.* (2013) 38:1110–7. doi: 10.3109/02713683.2013.811259
34. Kijlstra A. The role of lactoferrin in the nonspecific immune response on the ocular surface. *Reg Immunol.* (1990) 3:193–7.
35. Lehrer RI, Lu W. Alpha-Defensins in human innate immunity. *Immunol Rev.* (2012) 245:84–112. doi: 10.1111/j.1600-065X.2011.01082.x
36. Grigat J, Soruri A, Forssmann U, Riggert J, Zwirner J. Chemoattraction of macrophages, T lymphocytes, and mast cells is evolutionarily conserved within the human alpha-defensin family. *J Immunol.* (2007) 179:3958–65. doi: 10.4049/jimmunol.179.6.3958
37. Brook M, Tomlinson GH, Miles K, Smith RW, Rossi AG, Hiemstra PS, et al. Neutrophil-derived alpha defensins control inflammation by inhibiting macrophage mRNA translation. *Proc Natl Acad Sci USA.* (2016) 113:4350–5. doi: 10.1073/pnas.1601831113
38. Miles K, Clarke DJ, Lu W, Sibinska Z, Beaumont PE, Davidson DJ, et al. Dying and necrotic neutrophils are anti-inflammatory secondary to the release of alpha-defensins. *J Immunol.* (2009) 183:2122–32. doi: 10.4049/jimmunol.0804187
39. Gaspar D, Freire JM, Pacheco TR, Barata JT, Castanho MA. Apoptotic human neutrophil peptide-1 anti-tumor activity revealed by cellular biomechanics. *Biochim Biophys Acta.* (2015) 1853:308–16. doi: 10.1016/j.bbamcr.2014.11.006
40. Ferdowsi S, Pourfathollah AA, Amiri F, Rafiee MH, Aghaei A. Evaluation of anticancer activity of α-defensins purified from neutrophils trapped in leukoreduction filters. *Life Sci.* (2019) 224:249–54. doi: 10.1016/j.lfs.2019.03.072
41. Semple F, Dorin JR. beta-Defensins: multifunctional modulators of infection, inflammation and more? *J Innate Immun.* (2012) 4:337–48. doi: 10.1159/000336619
42. Wu Z, Hoover DM, Yang D, Boulegue C, Santamaria F, Oppenheim JJ, et al. Engineering disulfide bridges to dissect antimicrobial and chemotactic activities of human beta-defensin 3. *Proc Natl Acad Sci USA.* (2003) 100:8880–5. doi: 10.1073/pnas.1533186100
43. Yang D, Chertov O, Bykovskaia SN, Chen Q, Buffo MJ, Shogan J, et al. Beta-defensins: linking innate and adaptive immunity through dendritic and T cell CCR6. *Science.* (1999) 286:525–8. doi: 10.1126/science.286.5439.525

44. Hirsch T, Spielmann M, Zuhaili B, Fossum M, Metzig M, Koehler T, et al. Human beta-defensin-3 promotes wound healing in infected diabetic wounds. *J Gene Med.* (2009) 11:220–8. doi: 10.1002/jgm.1287
45. Hanaoka Y, Yamaguchi Y, Yamamoto H, Ishii M, Nagase T, Kurihara H, et al. *In vitro* and *in vivo* anticancer activity of human β-defensin-3 and its mouse homolog. *Anticancer Res.* (2016) 36:5999–6004. doi: 10.21873/anticanres.11188
46. Ghosh SK, McCormick TS, Weinberg A. Human beta defensins and cancer: contradictions and common ground. *Front Oncol.* (2019) 9:341. doi: 10.3389/fonc.2019.00341
47. Luo Y, McLean DT, Linden GJ, McAuley DF, McMullan R, Lundy FT. The naturally occurring host defense peptide, LL-37, and its truncated mimetics KE-18 and KR-12 have selected biocidal and antibiofilm activities against *Candida albicans*, *Staphylococcus aureus*, and *Escherichia coli in vitro*. *Front Microbiol.* (2017) 8:544. doi: 10.3389/fmicb.2017.00544
48. Huang LC, Petkova TD, Reins RY, Proske RJ, McDermott AM. Multifunctional roles of human cathelicidin (LL-37) at the ocular surface. *Invest Ophthalmol Vis Sci.* (2006) 47:2369–80. doi: 10.1167/iovs.05-1649
49. Huang LC, Jean D, Proske RJ, Reins RY, McDermott AM. Ocular surface expression and *in vitro* activity of antimicrobial peptides. *Curr Eye Res.* (2007) 32:595–609. doi: 10.1080/02713680701446653
50. Yu Y, Cooper CL, Wang G, Morwitzer MJ, Kota K, Tran JP, et al. Engineered human cathelicidin antimicrobial peptides inhibit ebola virus infection. *iScience.* (2020) 23:100999. doi: 10.1016/j.isci.2020.100999
51. Narayana JL, Mishra B, Lushnikova T, Golla RM, Wang G. Modulation of antimicrobial potency of human cathelicidin peptides against the ESKAPE pathogens and *in vivo* efficacy in a murine catheter-associated biofilm model. *Biochim Biophys Acta Biomembr.* (2019) 1861:1592–602. doi: 10.1016/j.bbamem.2019.07.012
52. He M, Zhang H, Li Y, Wang G, Tang B, Zhao J, et al. Cathelicidin-derived antimicrobial peptides inhibit zika virus through direct inactivation and interferon pathway. *Front Immunol.* (2018) 9:722. doi: 10.3389/fimmu.2018.00722
53. Kanthawong S, Bolscher JG, Veerman EC, van Marle J, de Soet HJ, Nazmi K, et al. Antimicrobial and antibiofilm activity of LL-37 and its truncated variants against *Burkholderia pseudomallei*. *Int J Antimicrob Agents.* (2012) 39:39–44. doi: 10.1016/j.ijantimicag.2011.09.010
54. Chen X, Takai T, Xie Y, Niyonsaba F, Okumura K, Ogawa H. Human antimicrobial peptide LL-37 modulates proinflammatory responses induced by cytokine milieus and double-stranded RNA in human keratinocytes. *Biochem Biophys Res Commun.* (2013) 433:532–7. doi: 10.1016/j.bbrc.2013.03.024
55. Torres-Juarez F, Cardenas-Vargas A, Montoya-Rosales A, González-Curiel I, Garcia-Hernandez MH, Enciso-Moreno JA, et al. LL-37 immunomodulatory activity during Mycobacterium tuberculosis infection in macrophages. *Infect Immun.* (2015) 83:4495–503. doi: 10.1128/IAI.00936-15
56. Tokumaru S, Sayama K, Shirakata Y, Komatsuzawa H, Ouhara K, Hanakawa Y, et al. Induction of keratinocyte migration *via* transactivation of the epidermal growth factor receptor by the antimicrobial peptide LL-37. *J Immunol.* (2005) 175:4662–8. doi: 10.4049/jimmunol.175.7.4662
57. Wu WK, Sung JJ, To KF Yu L, Li HT Li ZJ, et al. The host defense peptide LL-37 activates the tumor-suppressing bone morphogenetic protein signaling *via* inhibition of proteasome in gastric cancer cells. *J Cell Physiol.* (2010) 223:178–86. doi: 10.1002/jcp.22026
58. Domachowske JB, Dyer KD, Bonville CA, Rosenberg HF. Recombinant human eosinophil-derived neurotoxin/RNase 2 functions as an effective antiviral agent against respiratory syncytial virus. *J Infect Dis.* (1998) 177:1458–64. doi: 10.1086/515322
59. Domachowske JB, Dyer KD, Adams AG, Leto TL, Rosenberg HF. Eosinophil cationic protein/RNase 3 is another RNase A-family ribonuclease with direct antiviral activity. *Nucleic Acids Res.* (1998) 26:3358–63. doi: 10.1093/nar/26.14.3358
60. Lehrer RI, Szklarek D, Barton A, Ganz T, Hamann KJ, Gleich GJ. Antibacterial properties of eosinophil major basic protein and eosinophil cationic protein. *J Immunol.* (1989) 142:4428–34.
61. Ackerman SJ, Loegering DA, Venge P, Olsson I, Harley JB, Fauci AS, et al. Distinctive cationic proteins of the human eosinophil granule: major basic protein, eosinophil cationic protein, and eosinophil-derived neurotoxin. *J Immunol.* (1983) 131:2977–82.
62. Ackerman SJ, Gleich GJ, Loegering DA, Richardson BA, Butterworth AE. Comparative toxicity of purified human eosinophil granule cationic proteins for schistosomula of Schistosoma mansoni. *Am J Trop Med Hyg.* (1985) 34:735–45. doi: 10.4269/ajtmh.1985.34.735
63. Molina HA, Kierszenbaum F, Hamann KJ, Gleich GJ. Toxic effects produced or mediated by human eosinophil granule components on *Trypanosoma cruzi*. *Am J Trop Med Hyg.* (1988) 38:327–34. doi: 10.4269/ajtmh.1988.38.327
64. Lu L, Li J, Moussaoui M, Boix E. Immune modulation by human secreted RNases at the extracellular space. *Front Immunol.* (2018) 9:1012. doi: 10.3389/fimmu.2018.01012
65. Mohammed I, Yeung A, Abedin A, Hopkinson A, Dua HS. Signalling pathways involved in ribonuclease-7 expression. *Cell Mol Life Sci.* (2011) 68:1941–52. doi: 10.1007/s00018-010-0540-2
66. Otri AM, Mohammed I, Abedin A, Cao Z, Hopkinson A, Panjwani N, et al. Antimicrobial peptides expression by ocular surface cells in response to *Acanthamoeba castellanii*: an *in vitro* study. *Br J Ophthalmol.* (2010) 94:1523–7. doi: 10.1136/bjo.2009.178236
67. Yang D, Chen Q, Rosenberg HF, Rybak SM, Newton DL, Wang ZY, et al. Human ribonuclease A superfamily members, eosinophil-derived neurotoxin and pancreatic ribonuclease, induce dendritic cell maturation and activation. *J Immunol.* (2004) 173:6134–42. doi: 10.4049/jimmunol.173.10.6134
68. Yang D, Rosenberg HF, Chen Q, Dyer KD, Kurosaka K, Oppenheim JJ. Eosinophil-derived neurotoxin (EDN), an antimicrobial protein with chemotactic activities for dendritic cells. *Blood.* (2003) 102:3396–403. doi: 10.1182/blood-2003-01-0151
69. Li S, Sheng J, Hu JK Yu W, Kishikawa H, Hu MG, et al. Ribonuclease 4 protects neuron degeneration by promoting angiogenesis, neurogenesis, and neuronal survival under stress. *Angiogenesis.* (2013) 16:387–404. doi: 10.1007/s10456-012-9322-9
70. Ferguson R, Subramanian V. The cellular uptake of angiogenin, an angiogenic and neurotrophic factor is through multiple pathways and largely dynamin independent. *PLoS ONE.* (2018) 13:e0193302. doi: 10.1371/journal.pone.0193302
71. Kim KW, Park SH, Lee SJ, Kim JC. Ribonuclease 5 facilitates corneal endothelial wound healing *via* activation of PI3-kinase/Akt pathway. *Sci Rep.* (2016) 6:31162. doi: 10.1038/srep31162
72. Gläser R, Harder J, Lange H, Bartels J, Christophers E, Schröder JM. Antimicrobial psoriasin (S100A7) protects human skin from *Escherichia coli* infection. *Nat Immunol.* (2005) 6:57–64. doi: 10.1038/ni1142
73. Lee KC, Eckert RL. S100A7 (Psoriasin)–mechanism of antibacterial action in wounds. *J Invest Dermatol.* (2007) 127:945–57. doi: 10.1038/sj.jid.5700663
74. Jinquan T, Vorum H, Larsen CG, Madsen P, Rasmussen HH, Gesser B, et al. Psoriasin: a novel chemotactic protein. *J Invest Dermatol.* (1996) 107:5–10. doi: 10.1111/1523-1747.ep12294284
75. Zheng Y, Niyonsaba F, Ushio H, Ikeda S, Nagaoka I, Okumura K, et al. Microbicidal protein psoriasin is a multifunctional modulator of neutrophil activation. *Immunology.* (2008) 124:357–67. doi: 10.1111/j.1365-2567.2007.02782.x
76. Burian M, Schittek B. The secrets of dermcidin action. *Int J Med Microbiol.* (2015) 305:283–6. doi: 10.1016/j.ijmm.2014.12.012
77. Oppenheim FG, Xu T, McMillian FM, Levitz SM, Diamond RD, Offner GD, et al. Histatins, a novel family of histidine-rich proteins in human parotid secretion. Isolation, characterization, primary structure, and fungistatic effects on *Candida albicans*. *J Biolo Chem.* (1988) 263:7472–7. doi: 10.1016/S0021-9258(18)68522-9
78. Zolin GVS, Fonseca FHD, Zambom CR, Garrido SS. Histatin 5 metallopeptides and their potential against *Candida albicans* pathogenicity and drug resistance. *Biomolecules*. (2021) 11:1209. doi: 10.3390/biom11081209
79. Lee SM, Son KN, Shah D, Ali M, Balasubramaniam A, Shukla D, et al. Histatin-1 attenuates LPS-induced inflammatory signaling in RAW264.7 macrophages. *Int J Mol Sci*. (2021) 22:7856. doi: 10.3390/ijms22157856
80. Shah D, Ali M, Shukla D, Jain S, Aakalu VK. Effects of histatin-1 peptide on human corneal epithelial cells. *PLoS ONE.* (2017) 12:e0178030. doi: 10.1371/journal.pone.0178030

81. Shah D, Son KN, Kalmodia S, Lee BS, Ali M, Balasubramaniam A, et al. Wound Healing properties of histatin-5 and identification of a functional domain required for histatin-5-induced cell migration. *Mol Ther Methods Clin Dev.* (2020) 17:709–16. doi: 10.1016/j.omtm.2020.03.027
82. McDermott AM. Antimicrobial compounds in tears. *Exp Eye Res.* (2013) 117:53–61. doi: 10.1016/j.exer.2013.07.014
83. Tsai PS, Evans JE, Green KM, Sullivan RM, Schaumberg DA, Richards SM, et al. Proteomic analysis of human meibomian gland secretions. *Br J Ophthalmol.* (2006) 90:372–7. doi: 10.1136/bjo.2005.080846
84. Hao L, Shan Q, Wei J, Ma F, Sun P. Lactoferrin: major physiological functions and applications. *Curr Protein Pept Sci.* (2019) 20:139–44. doi: 10.2174/1389203719666180514150921
85. Gillette TE, Allansmith MR. Lactoferrin in human ocular tissues. *Am J Ophthalmol.* (1980) 90:30–7. doi: 10.1016/S0002-9394(14)75074-3
86. Santagati MG, La Terra Mule S, Amico C, Pistone M, Rusciano D, Enea V. Lactoferrin expression by bovine ocular surface epithelia: a primary cell culture model to study lactoferrin gene promoter activity. *Ophthalmic Res.* (2005) 37:270–8. doi: 10.1159/000087372
87. Samuelsen O, Haukland HH, Ulvatne H, Vorland LH. Anti-complement effects of lactoferrin-derived peptides. *FEMS Immunol Med Microbiol.* (2004) 41:141–8. doi: 10.1016/j.femsim.2004.02.006
88. Ramirez-Rico G, Martinez-Castillo M. de la Garza M, Shibayama M, Serrano-Luna J. *Acanthamoeba castellanii* proteases are capable of degrading iron-binding proteins as a possible mechanism of pathogenicity. *J Eukaryot Microbiol.* (2015) 62:614–22. doi: 10.1111/jeu.12215
89. Ashby B, Garrett Q, Willcox M. Bovine lactoferrin structures promoting corneal epithelial wound healing *in vitro*. *Invest Ophthalmol Vis Sci.* (2011) 52:2719–26. doi: 10.1167/iovs.10-6352
90. Hanstock HG, Edwards JP, Walsh NP. Tear lactoferrin and lysozyme as clinically relevant biomarkers of mucosal immune competence. *Front Immunol.* (2019) 10:1178. doi: 10.3389/fimmu.2019.01178
91. Ganz T. Defensins: antimicrobial peptides of innate immunity. *Nat Rev Immunol.* (2003) 3:710–20. doi: 10.1038/nri1180
92. Stotz HU, Thomson JG, Wang Y. Plant defensins: defense, development and application. *Plant Signal Behav.* (2009) 4:1010–2. doi: 10.4161/psb.4.11.9755
93. Bulet P, Stöcklin R, Menin L. Anti-microbial peptides: from invertebrates to vertebrates. *Immunol Rev.* (2004) 198:169–84. doi: 10.1111/j.0105-2896.2004.0124.x
94. Pazgier M, Hoover DM, Yang D, Lu W, Lubkowski J. Human beta-defensins. *Cell Mol Life Sci.* (2006) 63:1294–313. doi: 10.1007/s00018-005-5540-2
95. Weinberg A, Jin G, Sieg S, McCormick TS. The yin and yang of human Beta-defensins in health and disease. *Front Immunol.* (2012) 3:294. doi: 10.3389/fimmu.2012.00294
96. McIntosh RS, Cade JE, Al-Abed M, Shanmuganathan V, Gupta R, Bhan A, et al. The spectrum of antimicrobial peptide expression at the ocular surface. *Invest Ophthalmol Vis Sci.* (2005) 46:1379–85. doi: 10.1167/iovs.04-0607
97. Haynes RJ, Tighe PJ, Dua HS. Antimicrobial defensin peptides of the human ocular surface. *Br J Ophthalmol.* (1999) 83:737–41. doi: 10.1136/bjo.83.6.737
98. Ikeda A, Sakimoto T, Shoji J, Sawa M. Expression of alpha- and beta-defensins in human ocular surface tissue. *Jpn J Ophthalmol.* (2005) 49:73–8. doi: 10.1007/s10384-004-0163-y
99. Mohammed I, Suleman H, Otri AM, Kulkarni BB, Chen P, Hopkinson A, et al. Localization and gene expression of human beta-defensin 9 at the human ocular surface epithelium. *Invest Ophthalmol Vis Sci.* (2010) 51:4677–82. doi: 10.1167/iovs.10-5334
100. Abedin A, Mohammed I, Hopkinson A, Dua HS, A. novel antimicrobial peptide on the ocular surface shows decreased expression in inflammation and infection. *Invest Ophthalmol Vis Sci.* (2008) 49:28–33. doi: 10.1167/iovs.07-0645
101. Redfern RL, Reins RY, McDermott AM. Toll-like receptor activation modulates antimicrobial peptide expression by ocular surface cells. *Exp Eye Res.* (2011) 92:209–20. doi: 10.1016/j.exer.2010.12.005
102. Redfern RL, McDermott AM. Toll-like receptors in ocular surface disease. *Exp Eye Res.* (2010) 90:679–87. doi: 10.1016/j.exer.2010.03.012
103. Jiang Z, Mant CT, Vasil M, Hodges RS. Role of positively charged residues on the polar and non-polar faces of amphipathic alpha-helical antimicrobial peptides on specificity and selectivity for Gram-negative pathogens. *Chem Biol Drug Des.* (2018) 91:75–92. doi: 10.1111/cbdd.13058
104. Ting DSJ, Goh ETL, Mayandi V, Busoy JMF, Aung TT, Periayah MH, et al. Hybrid derivative of cathelicidin and human beta defensin-2 against Gram-positive bacteria: a novel approach for the treatment of bacterial keratitis. *Sci Rep.* (2021) 11:18304. doi: 10.1038/s41598-021-97821-3
105. Ong PY, Ohtake T, Brandt C, Strickland I, Boguniewicz M, Ganz T, et al. Endogenous antimicrobial peptides and skin infections in atopic dermatitis. *N Engl J Med.* (2002) 347:1151–60. doi: 10.1056/NEJMoa021481
106. Kiatsurayanon C, Ogawa H, Niyonsaba F. The role of host defense peptide human beta-defensins in the maintenance of skin barriers. *Curr Pharm Des.* (2018) 24:1092–9. doi: 10.2174/1381612824666180327164445
107. Daher KA, Selsted ME, Lehrer RI. Direct inactivation of viruses by human granulocyte defensins. *J Virol.* (1986) 60:1068–74. doi: 10.1128/jvi.60.3.1068-1074.1986
108. Lakshminarayanan R, Tan WX, Aung TT, Goh ET, Muruganantham N, Li J, et al. Branched peptide, B2088, disrupts the supramolecular organization of lipopolysaccharides and sensitizes the gram-negative bacteria. *Sci Rep.* (2016) 6:25905. doi: 10.1038/srep25905
109. Coorens M, Scheenstra MR, Veldhuizen EJ, Haagsman HP. Interspecies cathelicidin comparison reveals divergence in antimicrobial activity, TLR modulation, chemokine induction and regulation of phagocytosis. *Sci Rep.* (2017) 7:40874. doi: 10.1038/srep40874
110. Zanetti M, Gennaro R, Skerlavaj B, Tomasinsig L, Circo R. Cathelicidin peptides as candidates for a novel class of antimicrobials. *Curr Pharm Des.* (2002) 8:779–93. doi: 10.2174/1381612023395457
111. Cowland JB, Johnsen AH, Borregaard N. hCAP-18, a cathelin/pro-bactenecin-like protein of human neutrophil specific granules. *FEBS Lett.* (1995) 368:173–6. doi: 10.1016/0014-5793(95)00634-L
112. Larrick JW, Hirata M, Balint RF, Lee J, Zhong J, Wright SC. Human CAP18: a novel antimicrobial lipopolysaccharide-binding protein. *Infect Immun.* (1995) 63:1291–7. doi: 10.1128/iai.63.4.1291-1297.1995
113. Zasloff M. Antimicrobial peptides of multicellular organisms: my perspective. *Adv Exp Med Biol.* (2019) 1117:3–6. doi: 10.1007/978-981-13-3588-4_1
114. Gudmundsson GH, Agerberth B, Odeberg J, Bergman T, Olsson B, Salcedo R. The human gene FALL39 and processing of the cathelin precursor to the antibacterial peptide LL-37 in granulocytes. *Eur J Biochem.* (1996) 238:325–32. doi: 10.1111/j.1432-1033.1996.0325z.x
115. Sørensen OE, Gram L, Johnsen AH, Andersson E, Bangsbøll S, Tjabringa GS, et al. Processing of seminal plasma hCAP-18 to ALL-38 by gastricsin: a novel mechanism of generating antimicrobial peptides in vagina. *J Biol Chem.* (2003) 278:28540–6. doi: 10.1074/jbc.M301608200
116. Romeo D, Skerlavaj B, Bolognesi M, Gennaro R. Structure and bactericidal activity of an antibiotic dodecapeptide purified from bovine neutrophils. *J Biol Chem.* (1988) 263:9573–5. doi: 10.1016/S0021-9258(19)81553-3
117. Mookherjee N, Hancock RE. Cationic host defence peptides: innate immune regulatory peptides as a novel approach for treating infections. *Cell Mol Life Sci.* (2007) 64:922–33. doi: 10.1007/s00018-007-6475-6
118. Scheenstra MR, van Harten RM, Veldhuizen EJA, Haagsman HP, Coorens M. Cathelicidins modulate TLR-activation and inflammation. *Front Immunol.* (2020) 11:1137. doi: 10.3389/fimmu.2020.01137
119. Ren SX, Shen J, Cheng AS, Lu L, Chan RL Li ZJ, et al. FK-16 derived from the anticancer peptide LL-37 induces caspase-independent apoptosis and autophagic cell death in colon cancer cells. *PLoS ONE.* (2013) 8:e63641. doi: 10.1371/journal.pone.0063641
120. Ren SX, Cheng AS, To KF, Tong JH Li MS, Shen J, et al. Host immune defense peptide LL-37 activates caspase-independent apoptosis and suppresses colon cancer. *Cancer Res.* (2012) 72:6512–23. doi: 10.1158/0008-5472.CAN-12-2359
121. Lee PH, Ohtake T, Zaiou M, Murakami M, Rudisill JA, Lin KH, et al. Expression of an additional cathelicidin antimicrobial peptide protects against bacterial skin infection. *Proc Natl Acad Sci USA.* (2005) 102:3750–5. doi: 10.1073/pnas.0500268102
122. Huang LC, Reins RY, Gallo RL, McDermott AM. Cathelicidin-deficient (Cnlp -/-) mice show increased susceptibility to *Pseudomonas aeruginosa* keratitis. *Invest Ophthalmol Vis Sci.* (2007) 48:4498–508. doi: 10.1167/iovs.07-0274
123. Gordon YJ, Huang LC, Romanowski EG, Yates KA, Proske RJ, McDermott AM. Human cathelicidin (LL-37), a multifunctional peptide, is expressed by

ocular surface epithelia and has potent antibacterial and antiviral activity. *Curr Eye Res.* (2005) 30:385–94. doi: 10.1080/02713680590934111
124. Li X, Li Y, Han H, Miller DW, Wang G. Solution structures of human LL-37 fragments and NMR-based identification of a minimal membrane-targeting antimicrobial and anticancer region. *J Am Chem Soc.* (2006) 128:5776–85. doi: 10.1021/ja0584875
125. Wang G, Mishra B, Epand RF, Epand RM. High-quality 3D structures shine light on antibacterial, anti-biofilm and antiviral activities of human cathelicidin LL-37 and its fragments. *Biochim Biophys Acta.* (2014) 1838:2160–72. doi: 10.1016/j.bbamem.2014.01.016
126. Engelberg Y, Landau M. The human LL-37(17-29) antimicrobial peptide reveals a functional supramolecular structure. *Nat Commun.* (2020) 11:3894. doi: 10.1038/s41467-020-17736-x
127. Wang G. Structures of human host defense cathelicidin LL-37 and its smallest antimicrobial peptide KR-12 in lipid micelles. *J Biol Chem.* (2008) 283:32637–43. doi: 10.1074/jbc.M805533200
128. Wang G, Epand RF, Mishra B, Lushnikova T, Thomas VC, Bayles KW, et al. Decoding the functional roles of cationic side chains of the major antimicrobial region of human cathelicidin LL-37. *Antimicrob Agents Chemother.* (2012) 56:845–56. doi: 10.1128/AAC.05637-11
129. Rajasekaran G, Kim EY, Shin SY. LL-37-derived membrane-active FK-13 analogs possessing cell selectivity, anti-biofilm activity and synergy with chloramphenicol and anti-inflammatory activity. *Biochim Biophys Acta Biomembr.* (2017) 1859:722–33. doi: 10.1016/j.bbamem.2017.01.037
130. Ting DSJ, Beuerman RW, Dua HS, Lakshminarayanan R, Mohammed I. Strategies in translating the therapeutic potentials of host defense peptides. *Front Immunol.* (2020) 11:983. doi: 10.3389/fimmu.2020.00983
131. Mohammed I, Said DG, Nubile M, Mastropasqua L, Dua HS. Cathelicidin-derived synthetic peptide improves therapeutic potential of vancomycin against *Pseudomonas aeruginosa*. *Front Microbiol.* (2019) 10:2190. doi: 10.3389/fmicb.2019.02190
132. Rosenberg HF. RNase A ribonucleases and host defense: an evolving story. *J Leukoc Biol.* (2008) 83:1079–87. doi: 10.1189/jlb.1107725
133. Beintema JJ, Wietzes P, Weickmann JL, Glitz DG. The amino acid sequence of human pancreatic ribonuclease. *Anal Biochem.* (1984) 136:48–64. doi: 10.1016/0003-2697(84)90306-3
134. Raines RT. Ribonuclease A. *Chem Rev.* (1998) 98:1045–66. doi: 10.1021/cr960427h
135. Lu L, Arranz-Trullén J, Prats-Ejarque G, Pulido D, Bhakta S, Boix E. Human antimicrobial RNases inhibit intracellular bacterial growth and induce autophagy in mycobacteria-infected macrophages. *Front Immunol.* (2019) 10:1500. doi: 10.3389/fimmu.2019.01500
136. Donato R. Functional roles of S100 proteins, calcium-binding proteins of the EF-hand type. *Biochim Biophys Acta.* (1999) 1450:191–231. doi: 10.1016/S0167-4889(99)00058-0
137. Brodersen DE, Etzerodt M, Madsen P, Celis JE, Thøgersen HC, Nyborg J, et al. EF-hands at atomic resolution: the structure of human psoriasin (S100A7) solved by MAD phasing. *Structure.* (1998) 6:477–89. doi: 10.1016/S0969-2126(98)00049-5
138. Madsen P, Rasmussen HH, Leffers H, Honoré B, Dejgaard K, Olsen E, et al. Molecular cloning, occurrence, and expression of a novel partially secreted protein "psoriasin" that is highly up-regulated in psoriatic skin. *J Invest Dermatol.* (1991) 97:701–12. doi: 10.1111/1523-1747.ep12484041
139. Lei H, Li X, Jing B, Xu H, Wu Y. Human S100A7 induces mature interleukin1α expression by RAGE-p38 MAPK-CALPAIN1 PATHWAY IN PSORIASIS. *PLoS ONE.* (2017) 12:e0169788. doi: 10.1371/journal.pone.0169788
140. Garreis F, Gottschalt M, Schlorf T, Gläser R, Harder J, Worlitzsch D, et al. Expression and regulation of antimicrobial peptide psoriasin (S100A7) at the ocular surface and in the lacrimal apparatus. *Invest Ophthalmol Vis Sci.* (2011) 52:4914–22. doi: 10.1167/iovs.10-6598
141. Abtin A, Eckhart L, Mildner M, Gruber F, Schröder JM, Tschachler E. Flagellin is the principal inducer of the antimicrobial peptide S100A7c (psoriasin) in human epidermal keratinocytes exposed to *Escherichia coli*. *FASEB J.* (2008) 22:2168–76. doi: 10.1096/fj.07-104117
142. Murakami M, Ohtake T, Dorschner RA, Schittek B, Garbe C, Gallo RL. Cathelicidin anti-microbial peptide expression in sweat, an innate defense system for the skin. *J Invest Dermatol.* (2002) 119:1090–5. doi: 10.1046/j.1523-1747.2002.19507.x
143. Flad T, Bogumil R, Tolson J, Schittek B, Garbe C, Deeg M, et al. Detection of dermcidin-derived peptides in sweat by ProteinChip technology. *J Immunol Methods.* (2002) 270:53–62. doi: 10.1016/S0022-1759(02)00229-6
144. Song C, Weichbrodt C, Salnikov ES, Dynowski M, Forsberg BO, Bechinger B, et al. Crystal structure and functional mechanism of a human antimicrobial membrane channel. *Proc Natl Acad Sci USA.* (2013) 110:4586–91. doi: 10.1073/pnas.1214739110
145. Schittek B, Hipfel R, Sauer B, Bauer J, Kalbacher H, Stevanovic S, et al. Dermcidin: a novel human antibiotic peptide secreted by sweat glands. *Nat Immunol.* (2001) 2:1133–7. doi: 10.1038/ni732
146. You J, Fitzgerald A, Cozzi PJ, Zhao Z, Graham P, Russell PJ, et al. Post-translation modification of proteins in tears. *Electrophoresis.* (2010) 31:1853–61. doi: 10.1002/elps.200900755
147. Steffen H, Rieg S, Wiedemann I, Kalbacher H, Deeg M, Sahl HG, et al. Naturally processed dermcidin-derived peptides do not permeabilize bacterial membranes and kill microorganisms irrespective of their charge. *Antimicrob Agents Chemother.* (2006) 50:2608–20. doi: 10.1128/AAC.00181-06
148. Khurshid Z, Najeeb S, Mali M, Moin SF, Raza SQ, Zohaib S, et al. Histatin peptides: pharmacological functions and their applications in dentistry. *Saudi Pharm J.* (2017) 25:25–31. doi: 10.1016/j.jsps.2016.04.027
149. Kalmodia S, Son KN, Cao D, Lee BS, Surenkhuu B, Shah D, et al. Presence of histatin-1 in human tears and association with aqueous deficient dry eye diagnosis: a preliminary study. *Sci Rep.* (2019) 9:10304. doi: 10.1038/s41598-019-46623-9
150. Ting DSJ, Cairns J, Gopal BP, Ho CS, Krstic L, Elsahn A, et al. Risk factors, clinical outcomes, and prognostic factors of bacterial keratitis: the Nottingham Infectious Keratitis Study. *Front Med.* (2021) 8:715118. doi: 10.3389/fmed.2021.715118
151. Ung L, Chodosh J. Foundational concepts in the biology of bacterial keratitis. *Exp Eye Res.* (2021) 209:108647. doi: 10.1016/j.exer.2021.108647
152. Ting DSJ, Ho CS, Deshmukh R, Said DG, Dua HS. Infectious keratitis: an update on epidemiology, causative microorganisms, risk factors, and antimicrobial resistance. *Eye.* (2021) 35:1084–101. doi: 10.1038/s41433-020-01339-3
153. Collier SA, Gronostaj MP, MacGurn AK, Cope JR, Awsumb KL, Yoder JS, et al. Estimated burden of keratitis–United States, 2010. *MMWR Morb Mortal Wkly Rep.* (2014) 63:1027–30.
154. Song X, Xie L, Tan X, Wang Z, Yang Y, Yuan Y, et al. A multi-center, cross-sectional study on the burden of infectious keratitis in China. *PLoS ONE.* (2014) 9:e113843. doi: 10.1371/journal.pone.0113843
155. Ting DSJ, Settle C, Morgan SJ, Baylis O, Ghosh S. A 10-year analysis of microbiological profiles of microbial keratitis: the North East England Study. *Eye.* (2018) 32:1416–7. doi: 10.1038/s41433-018-0085-4
156. Khor WB, Prajna VN, Garg P, Mehta JS, Xie L, Liu Z, et al. The Asia Cornea Society Infectious Keratitis Study: a prospective multicenter study of infectious keratitis in Asia. *Am J Ophthalmol.* (2018) 195:161–70. doi: 10.1016/j.ajo.2018.07.040
157. Ung L, Bispo PJM, Shanbhag SS, Gilmore MS, Chodosh J. The persistent dilemma of microbial keratitis: global burden, diagnosis, and antimicrobial resistance. *Surv Ophthalmol.* (2019) 64:255–71. doi: 10.1016/j.survophthal.2018.12.003
158. Ting DSJ, Ho CS, Cairns J, Elsahn A, Al-Aqaba M, Boswell T, et al. 12-year analysis of incidence, microbiological profiles and *in vitro* antimicrobial susceptibility of infectious keratitis: the Nottingham Infectious Keratitis Study. *Br J Ophthalmol.* (2021) 105:328–33. doi: 10.1136/bjophthalmol-2020-316128
159. Ting DSJ, Ho CS, Cairns J, Gopal BP, Elsahn A, Al-Aqaba MA, et al. Seasonal patterns of incidence, demographic factors, and microbiological profiles of infectious keratitis: the Nottingham Infectious Keratitis Study. *Eye.* (2021) 35:2543–9. doi: 10.1038/s41433-020-01272-5
160. Ting DSJ, Galal M, Kulkarni B, Elalfy MS, Lake D, Hamada S, et al. Clinical characteristics and outcomes of fungal keratitis in the United Kingdom 2011-2020: a 10-year study. *J Fungi.* (2021) 7:966. doi: 10.20944/preprints202110.0104.v1

161. Brown L, Leck AK, Gichangi M, Burton MJ, Denning DW. The global incidence and diagnosis of fungal keratitis. *Lancet Infect Dis.* (2021) 21:e49–57. doi: 10.1016/S1473-3099(20)30448-5
162. Ting DSJ, Henein C, Said DG, Dua HS. Photoactivated chromophore for infectious keratitis - corneal cross-linking (PACK-CXL): a systematic review and meta-analysis. *Ocul Surf.* (2019) 17:624–34. doi: 10.1016/j.jtos.2019.08.006
163. Ting DSJ, McKenna M, Sadiq SN, Martin J, Mudhar HS, Meeney A, et al. Arthrographis kalrae keratitis complicated by endophthalmitis: a case report with literature review. *Eye Contact Lens.* (2020) 46:e59–65. doi: 10.1097/ICL.0000000000000713
164. Anshu A, Parthasarathy A, Mehta JS, Htoon HM, Tan DT. Outcomes of therapeutic deep lamellar keratoplasty and penetrating keratoplasty for advanced infectious keratitis: a comparative study. *Ophthalmology.* (2009) 116:615–23. doi: 10.1016/j.ophtha.2008.12.043
165. Ting DSJ, Henein C, Said DG, Dua HS. Amniotic membrane transplantation for infectious keratitis: a systematic review and meta-analysis. *Sci Rep.* (2021) 11:13007. doi: 10.1038/s41598-021-92366-x
166. Said DG, Rallis KI, Al-Aqaba MA, Ting DSJ, Dua HS. Surgical management of infectious keratitis. *Ocul Surf.* (2021). doi: 10.1016/j.jtos.2021.09.005. [Epub ahead of print].
167. Chen X, Niyonsaba F, Ushio H, Okuda D, Nagaoka I, Ikeda S, et al. Synergistic effect of antibacterial agents human beta-defensins, cathelicidin LL-37 and lysozyme against *Staphylococcus aureus* and *Escherichia coli*. *J Dermatol Sci.* (2005) 40:123–32. doi: 10.1016/j.jdermsci.2005.03.014
168. Singh PK, Tack BF, McCray PB Jr., Welsh MJ. Synergistic and additive killing by antimicrobial factors found in human airway surface liquid. *Am J Physiol Lung Cell Mol Physiol.* (2000) 279:L799–805. doi: 10.1152/ajplung.2000.279.5.L799
169. Mohammed I, Mohanty D, Said DG, Barik MR, Reddy MM, Alsaadi A, et al. Antimicrobial peptides in human corneal tissue of patients with fungal keratitis. *Br J Ophthalmol.* (2021) 105:1172–7. doi: 10.1136/bjophthalmol-2020-316329
170. Otri AM, Mohammed I, Al-Aqaba MA, Fares U, Peng C, Hopkinson A, et al. Variable expression of human Beta defensins 3 and 9 at the human ocular surface in infectious keratitis. *Invest Ophthalmol Vis Sci.* (2012) 53:757–61. doi: 10.1167/iovs.11-8467
171. Ting DSJ, Bignardi G, Koerner R, Irion LD, Johnson E, Morgan SJ, et al. Polymicrobial keratitis with *Cryptococcus curvatus*, *Candida parapsilosis*, and *Stenotrophomonas maltophilia* after penetrating keratoplasty: a rare case report with literature review. *Eye Contact Lens.* (2019) 45:e5–10. doi: 10.1097/ICL.0000000000000517
172. Asbell PA, Sanfilippo CM, Sahm DF, DeCory HH. Trends in antibiotic resistance among ocular microorganisms in the United States from 2009 to 2018. *JAMA Ophthalmol.* (2020) 138:439–50. doi: 10.1001/jamaophthalmol.2020.0155
173. Craig JP, Nichols KK, Akpek EK, Caffery B, Dua HS, Joo CK, et al. TFOS DEWS II definition and classification report. *Ocul Surf.* (2017) 15:276–83. doi: 10.1016/j.jtos.2017.05.008
174. Ting DSJ, Ghosh S. Acute corneal perforation 1 week following uncomplicated cataract surgery: the implication of undiagnosed dry eye disease and topical NSAIDs. *Ther Adv Ophthalmol.* (2019) 11:2515841419869508. doi: 10.1177/2515841419869508
175. Brito-Zerón P, Baldini C, Bootsma H, Bowman SJ, Jonsson R, Mariette X, et al. Sjögren syndrome. *Nat Rev Dis Primers.* (2016) 2:16047. doi: 10.1038/nrdp.2016.47
176. Sonobe H, Ogawa Y, Yamada K, Shimizu E, Uchino Y, Kamoi M, et al. A novel and innovative paper-based analytical device for assessing tear lactoferrin of dry eye patients. *Ocul Surf.* (2019) 17:160–6. doi: 10.1016/j.jtos.2018.11.001
177. Chao C, Tong L. Tear lactoferrin and features of ocular allergy in different severities of meibomian gland dysfunction. *Optom Vis Sci.* (2018) 95:930–6. doi: 10.1097/OPX.0000000000001285
178. Gerber-Hollbach N, Plattner K, O'Leary OE, Jenoe P, Moes S, Drexler B, et al. Tear film proteomics reveal important differences between patients with and without ocular GvHD after allogeneic hematopoietic cell transplantation. *Invest Ophthalmol Vis Sci.* (2018) 59:3521–30. doi: 10.1167/iovs.18-24433
179. Narayanan S, Miller WL, McDermott AM. Expression of human beta-defensins in conjunctival epithelium: relevance to dry eye disease. *Invest Ophthalmol Vis Sci.* (2003) 44:3795–801. doi: 10.1167/iovs.02-1301
180. Ohashi Y, Ishida R, Kojima T, Goto E, Matsumoto Y, Watanabe K, et al. Abnormal protein profiles in tears with dry eye syndrome. *Am J Ophthalmol.* (2003) 136:291–9. doi: 10.1016/S0002-9394(03)00203-4
181. Kuo MT, Fang PC, Chao TL, Chen A, Lai YH, Huang YT, et al. Tear proteomics approach to monitoring Sjögren syndrome or dry eye disease. *Int J Mol Sci.* (2019) 20:1932. doi: 10.3390/ijms20081932
182. Careba I, Chiva A, Totir M, Ungureanu E, Gradinaru S. Tear lipocalin, lysozyme and lactoferrin concentrations in postmenopausal women. *J Med Life.* (2015) 8(Spec Issue):94–8.
183. Narayanan S, Redfern RL, Miller WL, Nichols KK, McDermott AM. Dry eye disease and microbial keratitis: is there a connection? *Ocul Surf.* (2013) 11:75–92. doi: 10.1016/j.jtos.2012.12.002
184. Khoo P, Cabrera-Aguas M, Robaei D, Lahra MM, Watson S. Microbial keratitis and ocular surface disease: a 5-year study of the microbiology, risk factors and clinical outcomes in Sydney, Australia. *Curr Eye Res.* (2019) 44:1195–202. doi: 10.1080/02713683.2019.1631852
185. Godefrooij DA, de Wit GA, Uiterwaal CS, Imhof SM, Wisse RP. Age-specific incidence and prevalence of keratoconus: a Nationwide Registration Study. *Am J Ophthalmol.* (2017) 175:169–72. doi: 10.1016/j.ajo.2016.12.015
186. Kennedy RH, Bourne WM, Dyer JA. A 48-year clinical and epidemiologic study of keratoconus. *Am J Ophthalmol.* (1986) 101:267–73. doi: 10.1016/0002-9394(86)90817-2
187. Andreanos KD, Hashemi K, Petrelli M, Droutsas K, Georgalas I, Kymionis GD. Keratoconus treatment algorithm. *Ophthalmol Ther.* (2017) 6:245–62. doi: 10.1007/s40123-017-0099-1
188. Mohammadpour M, Heidari Z, Hashemi H. Updates on managements for keratoconus. *J Curr Ophthalmol.* (2018) 30:110–24. doi: 10.1016/j.joco.2017.11.002
189. Ting DSJ, Rana-Rahman R, Chen Y, Bell D, Danjoux JP, Morgan SJ, et al. Effectiveness and safety of accelerated (9 mW/cm) corneal collagen cross-linking for progressive keratoconus: a 24-month follow-up. *Eye.* (2019) 33:812–8. doi: 10.1038/s41433-018-0323-9
190. Ting DS, Sau CY, Srinivasan S, Ramaesh K, Mantry S, Roberts F. Changing trends in keratoplasty in the West of Scotland: a 10-year review. *Br J Ophthalmol.* (2012) 96:405–8. doi: 10.1136/bjophthalmol-2011-300244
191. Fasolo A, Frigo AC, Bohm E, Genisi C, Rama P, Spadea L, et al. The CORTES study: corneal transplant indications and graft survival in an Italian cohort of patients. *Cornea.* (2006) 25:507–15. doi: 10.1097/01.ico.0000214211.60317.1f
192. Mas Tur V, MacGregor C, Jayaswal R, O'Brart D, Maycock N. A review of keratoconus: diagnosis, pathophysiology, and genetics. *Surv Ophthalmol.* (2017) 62:770–83. doi: 10.1016/j.survophthal.2017.06.009
193. Pannebaker C, Chandler HL, Nichols JJ. Tear proteomics in keratoconus. *Mol Vis.* (2010) 16:1949–57.
194. Lema I, Duran JA. Inflammatory molecules in the tears of patients with keratoconus. *Ophthalmology.* (2005) 112:654–9. doi: 10.1016/j.ophtha.2004.11.050
195. Galvis V, Sherwin T, Tello A, Merayo J, Barrera R, Acera A. Keratoconus: an inflammatory disorder? *Eye.* (2015) 29:843–59. doi: 10.1038/eye.2015.63
196. Balasubramanian SA, Mohan S, Pye DC, Willcox MD. Proteases, proteolysis and inflammatory molecules in the tears of people with keratoconus. *Acta Ophthalmol.* (2012) 90:e303–9. doi: 10.1111/j.1755-3768.2011.02369.x
197. Yam GH, Fuest M, Zhou L, Liu YC, Deng L, Chan AS, et al. Differential epithelial and stromal protein profiles in cone and non-cone regions of keratoconus corneas. *Sci Rep.* (2019) 9:2965. doi: 10.1038/s41598-019-39182-6
198. Balasubramanian SA, Pye DC, Willcox MD. Levels of lactoferrin, secretory IgA and serum albumin in the tear film of people with keratoconus. *Exp Eye Res.* (2012) 96:132–7. doi: 10.1016/j.exer.2011.12.010
199. Pastori V, Tavazzi S, Lecchi M. Lactoferrin-loaded contact lenses counteract cytotoxicity caused *in vitro* by keratoconic tears. *Cont Lens Anterior Eye.* (2019) 42:253–7. doi: 10.1016/j.clae.2018.12.004
200. Rezvan F, Khabazkhoob M, Hooshmand E, Yekta A, Saatchi M, Hashemi H. Prevalence and risk factors of pterygium: a systematic review and meta-analysis. *Surv Ophthalmol.* (2018) 63:719–35. doi: 10.1016/j.survophthal.2018.03.001
201. Ting DSJ, Liu YC, Patil M, Ji AJS, Fang XL, Tham YC, et al. Proposal and validation of a new grading system for pterygium (SLIT2). *Br J Ophthalmol.* (2021) 105:921–4. doi: 10.1136/bjophthalmol-2020-315831

202. Liu T, Liu Y, Xie L, He X, Bai J. Progress in the pathogenesis of pterygium. *Curr Eye Res.* (2013) 38:1191–7. doi: 10.3109/02713683.2013.823212
203. Zhou L, Beuerman RW, Ang LP, Chan CM Li SF, Chew FT, et al. Elevation of human alpha-defensins and S100 calcium-binding proteins A8 and A9 in tear fluid of patients with pterygium. *Invest Ophthalmol Vis Sci.* (2009) 50:2077–86. doi: 10.1167/iovs.08-2604
204. Abubakar SA, Isa MM, Omar N, Tan SW. Relative quantification of human β-defensins gene expression in pterygium and normal conjunctiva samples. *Mol Med Rep.* (2020) 22:4931–7. doi: 10.3892/mmr.2020.11560
205. Ljubimov AV, Saghizadeh M. Progress in corneal wound healing. *Prog Retin Eye Res.* (2015) 49:17–45. doi: 10.1016/j.preteyeres.2015.07.002
206. Zhou L, Huang LQ, Beuerman RW, Grigg ME Li SF, Chew FT, et al. Proteomic analysis of human tears: defensin expression after ocular surface surgery. *J Proteome Res.* (2004) 3:410–6. doi: 10.1021/pr034065n
207. McDermott AM, Redfern RL, Zhang B. Human beta-defensin 2 is up-regulated during re-epithelialization of the cornea. *Curr Eye Res.* (2001) 22:64–7. doi: 10.1076/ceyr.22.1.64.6978
208. Reins RY, Hanlon SD, Magadi S, McDermott AM. Effects of topically applied vitamin d during corneal wound healing. *PLoS ONE.* (2016) 11:e0152889. doi: 10.1371/journal.pone.0152889
209. Lu X, Vick S, Chen Z, Chen J, Watsky MA. Effects of vitamin D receptor knockout and vitamin D deficiency on corneal epithelial wound healing and nerve density in diabetic mice. *Diabetes.* (2020) 69:1042–51. doi: 10.2337/db19-1051
210. Elizondo RA, Yin Z, Lu X, Watsky MA. Effect of vitamin D receptor knockout on cornea epithelium wound healing and tight junctions. *Invest Ophthalmol Vis Sci.* (2014) 55:5245–51. doi: 10.1167/iovs.13-13553
211. Weidinger S, Beck LA, Bieber T, Kabashima K, Irvine AD. Atopic dermatitis. *Nat Rev Dis Primers.* (2018) 4:1. doi: 10.1038/s41572-018-0001-z
212. Kumar S. Vernal keratoconjunctivitis: a major review. *Acta Ophthalmol.* (2009) 87:133–47. doi: 10.1111/j.1755-3768.2008.01347.x
213. Takahashi T, Gallo RL. The critical and multifunctional roles of antimicrobial peptides in dermatology. *Dermatol Clin.* (2017) 35:39–50. doi: 10.1016/j.det.2016.07.006
214. Chen JJ, Applebaum DS, Sun GS, Pflugfelder SC. Atopic keratoconjunctivitis: a review. *J Am Acad Dermatol.* (2014) 70:569–75. doi: 10.1016/j.jaad.2013.10.036
215. Ikeda A, Nakanishi Y, Sakimoto T, Shoji J, Sawa M, Nemoto N. Expression of beta defensins in ocular surface tissue of experimentally developed allergic conjunctivitis mouse model. *Jpn J Ophthalmol.* (2006) 50:1–6. doi: 10.1007/s10384-005-0262-4
216. Hida RY, Ohashi Y, Takano Y, Dogru M, Goto E, Fujishima H, et al. Elevated levels of human alpha -defensin in tears of patients with allergic conjunctival disease complicated by corneal lesions: detection by SELDI ProteinChip system and quantification. *Curr Eye Res.* (2005) 30:723–30. doi: 10.1080/02713680591005986
217. Rapacz P, Tedesco J, Donshik PC, Ballow M. Tear lysozyme and lactoferrin levels in giant papillary conjunctivitis and vernal conjunctivitis. *CLAO J.* (1988) 14:207–9.
218. Gether L, Overgaard LK, Egeberg A, Thyssen JP. Incidence and prevalence of rosacea: a systematic review and meta-analysis. *Br J Dermatol.* (2018) 179:282–9. doi: 10.1111/bjd.16481
219. Rainer BM, Kang S, Chien AL. Rosacea: epidemiology, pathogenesis, and treatment. *Dermatoendocrinol.* (2017) 9:e1361574. doi: 10.1080/19381980.2017.1361574
220. Yamasaki K, Di Nardo A, Bardan A, Murakami M, Ohtake T, Coda A, et al. Increased serine protease activity and cathelicidin promotes skin inflammation in rosacea. *Nat Med.* (2007) 13:975–80. doi: 10.1038/nm1616
221. Koczulla R, von Degenfeld G, Kupatt C, Krotz F, Zahler S, Gloe T, et al. An angiogenic role for the human peptide antibiotic LL-37/hCAP-18. *J Clin Invest.* (2003) 111:1665–72. doi: 10.1172/JCI17545
222. Kiratli H, Irkec M, Orhan M. Tear lactoferrin levels in chronic meibomitis associated with acne rosacea. *Eur J Ophthalmol.* (2000) 10:11–4.
223. Hancock RE, Sahl HG. Antimicrobial and host-defense peptides as new anti-infective therapeutic strategies. *Nat Biotechnol.* (2006) 24:1551–7. doi: 10.1038/nbt1267
224. Fjell CD, Hiss JA, Hancock RE, Schneider G. Designing antimicrobial peptides: form follows function. *Nat Rev Drug Discov.* (2011) 11:37–51. doi: 10.1038/nrd3591
225. Christoffersen RE. Antibiotics–an investment worth making? *Nat Biotechnol.* (2006) 24:1512–4. doi: 10.1038/nbt1206-1512
226. Zhou L, Liu SP, Chen LY Li J, Ong LB, Guo L, et al. The structural parameters for antimicrobial activity, human epithelial cell cytotoxicity and killing mechanism of synthetic monomer and dimer analogues derived from hBD3 C-terminal region. *Amino Acids.* (2011) 40:123–33. doi: 10.1007/s00726-010-0565-8
227. Kolar SSN, Luca V, Baidouri H, Mannino G, McDermott AM, Mangoni ML. Esculentin-1a(1-21)NH2: a frog skin-derived peptide for microbial keratitis. *Cell Mol Life Sci.* (2015) 72:617–27. doi: 10.1007/s00018-014-1694-0
228. Luca V, Stringaro A, Colone M, Pini A, Mangoni ML. Esculentin(1-21), an amphibian skin membrane-active peptide with potent activity on both planktonic and biofilm cells of the bacterial pathogen *Pseudomonas aeruginosa*. *Cell Mol Life Sci.* (2013) 70:2773–86. doi: 10.1007/s00018-013-1291-7
229. Casciaro B, Dutta D, Loffredo MR, Marcheggiani S, McDermott AM, Willcox MD, et al. Esculentin-1a derived peptides kill *Pseudomonas aeruginosa* biofilm on soft contact lenses and retain antibacterial activity upon immobilization to the lens surface. *Biopolymers.* (2017) 110:e23074. doi: 10.1002/bip.23074
230. Clemens LE, Jaynes J, Lim E, Kolar SS, Reins RY, Baidouri H, et al. Designed host defense peptides for the treatment of bacterial keratitis. *Invest Ophthalmol Vis Sci.* (2017) 58:6273–81. doi: 10.1167/iovs.17-22243
231. Dutta D, Zhao T, Cheah KB, Holmlund L, Willcox MDP. Activity of a melimine derived peptide Mel4 against *Stenotrophomonas*, *Delftia*, *Elizabethkingia*, *Burkholderia* and biocompatibility as a contact lens coating. *Cont Lens Anterior Eye.* (2017) 40:175–83. doi: 10.1016/j.clae.2017.01.002
232. Yasir M, Dutta D, Willcox MDP. Mode of action of the antimicrobial peptide Mel4 is independent of *Staphylococcus aureus* cell membrane permeability. *PLoS ONE.* (2019) 14:e0215703. doi: 10.1371/journal.pone.0215703
233. Kalaiselvan P, Konda N, Pampi N, Vaddavalli PK, Sharma S, Stapleton F, et al. Effect of antimicrobial contact lenses on corneal infiltrative events: a randomized clinical trial. *Transl Vis Sci Technol.* (2021) 10:32. doi: 10.1167/tvst.10.7.32
234. Mayandi V, Xi Q, Leng Goh ET, Koh SK, Jie Toh TY, Barathi VA, et al. Rational substitution of ε-lysine for α-lysine enhances the cell and membrane selectivity of pore-forming melittin. *J Med Chem.* (2020) 63:3522–37. doi: 10.1021/acs.jmedchem.9b01846
235. Ting DSJ Li J, Verma CS, Goh ETL, Nubile M, Mastropasqua L, et al. Evaluation of host defense peptide (CaD23)-antibiotic interaction and mechanism of action: insights from experimental and molecular dynamics simulations studies. *Front Pharmacol.* (2021) 12:731499. doi: 10.3389/fphar.2021.731499
236. Liu S, Zhou L, Li J, Suresh A, Verma C, Foo YH, et al. Linear analogues of human beta-defensin 3: concepts for design of antimicrobial peptides with reduced cytotoxicity to mammalian cells. *Chembiochem.* (2008) 9:964–73. doi: 10.1002/cbic.200700560
237. Bai Y, Liu S, Jiang P, Zhou L, Li J, Tang C, et al. Structure-dependent charge density as a determinant of antimicrobial activity of peptide analogues of defensin. *Biochemistry.* (2009) 48:7229–39. doi: 10.1021/bi900670d
238. Ladram A, Nicolas P. Antimicrobial peptides from frog skin: biodiversity and therapeutic promises. *Front Biosci.* (2016) 21:1341–71. doi: 10.2741/4461
239. Willcox MD, Hume EB, Aliwarga Y, Kumar N, Cole N, A. novel cationic-peptide coating for the prevention of microbial colonization on contact lenses. *J Appl Microbiol.* (2008) 105:1817–25. doi: 10.1111/j.1365-2672.2008.03942.x
240. Cole N, Hume EB, Vijay AK, Sankaridurg P, Kumar N, Willcox MD. *In vivo* performance of melimine as an antimicrobial coating for contact lenses in models of CLARE and CLPU. *Invest Ophthalmol Vis Sci.* (2010) 51:390–5. doi: 10.1167/iovs.09-4068
241. Dutta D, Ozkan J, Willcox MD. Biocompatibility of antimicrobial melimine lenses: rabbit and human studies. *Optom Vis Sci.* (2014) 91:570–81. doi: 10.1097/OPX.0000000000000232

242. Dutta D, Vijay AK, Kumar N, Willcox MD. Melimine-coated antimicrobial contact lenses reduce microbial keratitis in an animal model. *Invest Ophthalmol Vis Sci.* (2016) 57:5616–24. doi: 10.1167/iovs.16-19882
243. Yasir M, Dutta D, Willcox MDP. Comparative mode of action of the antimicrobial peptide melimine and its derivative Mel4 against *Pseudomonas aeruginosa*. *Sci Rep.* (2019) 9:7063. doi: 10.1038/s41598-019-42440-2
244. Jin L, Bai X, Luan N, Yao H, Zhang Z, Liu W, et al. A designed tryptophan- and lysine/arginine-rich antimicrobial peptide with therapeutic potential for clinical antibiotic-resistant *Candida albicans* vaginitis. *J Med Chem.* (2016) 59:1791–9. doi: 10.1021/acs.jmedchem.5b01264
245. Mishra B, Wang G. The importance of amino acid composition in natural AMPs: an evolutional, structural, and functional perspective. *Front Immunol.* (2012) 3:221. doi: 10.3389/fimmu.2012.00221
246. Shukla SC, Singh A, Pandey AK, Mishra A. Review on production and medical applications of ε-polylysine. *Biochem Eng J.* (2012) 65:70–81. doi: 10.1016/j.bej.2012.04.001
247. Geornaras I, Yoon Y, Belk KE, Smith GC, Sofos JN. Antimicrobial activity of epsilon-polylysine against *Escherichia coli* O157:H7, *Salmonella* Typhimurium, and *Listeria monocytogenes* in various food extracts. *J Food Sci.* (2007) 72:M330–4. doi: 10.1111/j.1750-3841.2007.00510.x
248. Shima S, Matsuoka H, Iwamoto T, Sakai H. Antimicrobial action of epsilon-poly-L-lysine. *J Antibiot.* (1984) 37:1449–55. doi: 10.7164/antibiotics.37.1449
249. Venkatesh M, Barathi VA, Goh ETL, Anggara R, Fazil M, Ng AJY, et al. Antimicrobial activity and cell selectivity of synthetic and biosynthetic cationic polymers. *Antimicrob Agents Chemother.* (2017) 61:e00469-17. doi: 10.1128/AAC.00469-17
250. Clausen ML, Slotved HC, Krogfelt KA, Andersen PS, Agner T. *In vivo* expression of antimicrobial peptides in atopic dermatitis. *Exp Dermatol.* (2016) 25:3–9. doi: 10.1111/exd.12831
251. Liu PT, Stenger S, Li H, Wenzel L, Tan BH, Krutzik SR, et al. Toll-like receptor triggering of a vitamin D-mediated human antimicrobial response. *Science.* (2006) 311:1770–3. doi: 10.1126/science.1123933
252. Albenali LH, Danby S, Moustafa M, Brown K, Chittock J, Shackley F, et al. Vitamin D and antimicrobial peptide levels in patients with atopic dermatitis and atopic dermatitis complicated by eczema herpeticum: a pilot study. *J Allergy Clin Immunol.* (2016) 138:1715–9.e4. doi: 10.1016/j.jaci.2016.05.039
253. Javanbakht MH, Keshavarz SA, Djalali M, Siassi F, Eshraghian MR, Firooz A, et al. Randomized controlled trial using vitamins E and D supplementation in atopic dermatitis. *J Dermatolog Treat.* (2011) 22:144–50. doi: 10.3109/09546630903578566
254. Amestejani M, Salehi BS, Vasigh M, Sobhkhiz A, Karami M, Alinia H, et al. Vitamin D supplementation in the treatment of atopic dermatitis: a clinical trial study. *J Drugs Dermatol.* (2012) 11:327−30.
255. https://clinicaltrials.gov/ct2/show/results/NCT01590758 (accessed November 02, 2021).
256. https://www.fiercebiotech.com/biotech/dipexium-plummets-total-phiii-failure (accessed November 02, 2021).
257. Roudi R, Syn NL, Roudbary M. Antimicrobial peptides as biologic and immunotherapeutic agents against cancer: a comprehensive overview. *Front Immunol.* (2017) 8:1320. doi: 10.3389/fimmu.2017.01320
258. Das P, Sercu T, Wadhawan K, Padhi I, Gehrmann S, Cipcigan F, et al. Accelerated antimicrobial discovery *via* deep generative models and molecular dynamics simulations. *Nat Biomed Eng.* (2021) 5:613–23. doi: 10.1038/s41551-021-00689-x
259. Biswaro LS, da Costa Sousa MG, Rezende TMB, Dias SC, Franco OL. Antimicrobial peptides and nanotechnology, recent advances and challenges. *Front Microbiol.* (2018) 9:855. doi: 10.3389/fmicb.2018.00855
260. Tangpricha V, Judd SE, Ziegler TR, Hao L, Alvarez JA, Fitzpatrick AM, et al. LL-37 concentrations and the relationship to vitamin D, immune status, and inflammation in HIV-infected children and young adults. *AIDS Res Hum Retroviruses.* (2014) 30:670–6. doi: 10.1089/aid.2013.0279
261. Mily A, Rekha RS, Kamal SM, Akhtar E, Sarker P, Rahim Z, et al. Oral intake of phenylbutyrate with or without vitamin D3 upregulates the cathelicidin LL-37 in human macrophages: a dose finding study for treatment of tuberculosis. *BMC Pulm Med.* (2013) 13:23. doi: 10.1186/1471-2466-13-23
262. Yeung ATY, Choi YH, Lee AHY, Hale C, Ponstingl H, Pickard D, et al. A genome-wide knockout screen in human macrophages identified host factors modulating *Salmonella* infection. *mBio.* (2019) 10:e02169-19. doi: 10.1128/mBio.02169-19
263. Pajor M, Sogin J, Worobo RW, Szweda P. Draft genome sequence of antimicrobial producing *Paenibacillus alvei* strain MP1 reveals putative novel antimicrobials. *BMC Res Notes.* (2020) 13:280. doi: 10.1186/s13104-020-05124-z

Conflict of Interest: The authors declare that the research was conducted in the absence of any commercial or financial relationships that could be construed as a potential conflict of interest.

The reviewer HO declared a shared parent affiliation with the authors RL and RB to the handling editor at the time of review.

Publisher's Note: All claims expressed in this article are solely those of the authors and do not necessarily represent those of their affiliated organizations, or those of the publisher, the editors and the reviewers. Any product that may be evaluated in this article, or claim that may be made by its manufacturer, is not guaranteed or endorsed by the publisher.

frontiers | Frontiers in Medicine

PERSPECTIVE
published: 28 June 2022
doi: 10.3389/fmed.2022.845522

The Ethical and Societal Considerations for the Rise of Artificial Intelligence and Big Data in Ophthalmology

T. Y. Alvin Liu[1]* *and Jo-Hsuan Wu*[2]

[1] Wilmer Eye Institute, Johns Hopkins University, Baltimore, MD, United States, [2] Shiley Eye Institute and Viterbi Family Department of Ophthalmology, University of California, San Diego, La Jolla, CA, United States

Medical specialties with access to a large amount of imaging data, such as ophthalmology, have been at the forefront of the artificial intelligence (AI) revolution in medicine, driven by deep learning (DL) and big data. With the rise of AI and big data, there has also been increasing concern on the issues of bias and privacy, which can be partially addressed by low-shot learning, generative DL, federated learning and a "model-to-data" approach, as demonstrated by various groups of investigators in ophthalmology. However, to adequately tackle the ethical and societal challenges associated with the rise of AI in ophthalmology, a more comprehensive approach is preferable. Specifically, AI should be viewed as sociotechnical, meaning this technology shapes, and is shaped by social phenomena.

Keywords: ethics, bias, artificial intelligence, fairness, privacy

OPEN ACCESS

Edited by:
Jorge L. Alió Del Barrio, Miguel Hernández University of Elche, Spain

Reviewed by:
Gilbert Yong San Lim, SingHealth, Singapore
Dinesh Gunasekeran, National University of Singapore, Singapore

***Correspondence:**
T. Y. Alvin Liu
tliu25@jhmi.edu

Specialty section:
This article was submitted to Ophthalmology, a section of the journal Frontiers in Medicine

Received: *29 December 2021*
Accepted: *10 June 2022*
Published: *28 June 2022*

Citation:
Liu TYA and Wu J-H (2022) The Ethical and Societal Considerations for the Rise of Artificial Intelligence and Big Data in Ophthalmology. Front. Med. 9:845522. doi: 10.3389/fmed.2022.845522

INTRODUCTION

The rise of artificial intelligence (AI) and big data has been hailed as the 4th Industrial Revolution. Recent advancement in AI, in the form of deep learning (DL) which is a subtype of machine learning (ML), and improvement in hardware such as graphic processing units (GPU), have propelled medical AI applications to the forefront of the public discourse. This is because DL has been shown to be on par with human experts in analyzing medical images across different specialties, especially in medical specialties that interact with and have access to a large number of images, such as dermatology, radiology, and ophthalmology (1–10). In addition, "super-human" feats achieved by DL, such as the robust prediction of age, gender, blood pressure and smoking status of a person from a color fundus photograph alone (11), have captured the public's imagination and sparked a debate on the role and impact of AI on medicine.

Ophthalmology, being at the forefront of this AI revolution in medicine, is well-positioned to actively participate in and be a thought-leader on the societal implications for the rise of AI and big data in medicine. In the following perspective piece, we will highlight the ethical controversies and considerations from an ophthalmological perspective. The two major concerns regarding the rise of AI in medicine and ophthalmology center on bias and privacy.

DISCUSSION

Bias and Fairness

AI has the potential to entrench, or even exacerbate, existing biases in the healthcare system *via* unfair recommendations or decision-making. Fairness can be defined as "the absence of any prejudice or favoritism toward an individual or a group based on their inherent or acquired characteristics" (12). A prominent example of a medical AI algorithm providing unfair recommendations and exacerbating biases was highlighted by a study by Obermeyer at al. (13) showing that an AI algorithm systematically biased against Black patients, by erroneously using previous health costs as a proxy for predicting health needs and illness severity.

Bias in the training data is one of the most common reasons for a ML algorithm to produce unfair downstream predictions or recommendations. Many types of bias in ML exist. A comprehensive discussion of the different kinds of bias is beyond the scope of the current paper, but is nicely summarized here (14, 15). Specifically, within the context of ophthalmology DL studies, imbalance in training images is a common, yet addressable, reason that can lead to biases against a patient subgroup, such as patients of a certain race. For example, the AREDS image dataset (16), generated from a landmark longitudinal clinical trial and used in numerous important ophthalmology DL studies, was derived primarily from Caucasian patients (about 96% of participants). While age-related macular degeneration (AMD) is more prevalent in Caucasian patients (prevalence of 5.4% vs. 4.2% in Hispanic, 2.4% in Black and 4.6% in Asian) (17–19), the difference in prevalence on a population level does not explain fully the extreme imbalance in the AREDS dataset. Additional factors, such as unequal access to or interest in participating in clinical trials, likely also played a role.

However, such imbalance in training data can be addressed in three different ways. First, patient recruitment in prospective studies can be planned to ensure equal enrollment numbers for different pre-specified patient subgroups, e.g., based on sex, age, race, ethnicity, socioeconomic status and disease severity, etc. Second, if the recruitment of a certain patient subgroup is limited by practicality or natural prevalence of the disease, e.g., Black patients with AMD, then low-shot DL can be attempted. Low-shot DL, in contrast to traditional DL which requires a large amount of data for training, can be trained with relatively few samples (20), and can outperform traditional DL approaches when the available training dataset is small (5). Third, the patient subgroup that is under-represented in the training samples can be augmented by generative DL, a DL technique that can generate synthetic data. It has been shown that retinal images, created by generative DL, can be used to train a robust DL system for AMD classification (21). Specifically, in the context of DL-based detection of referable diabetic retinopathy, generative DL has been used to increase the training image samples of an under-represented patient subgroup and has been shown to decrease the bias against that particular under-represented patient subgroup during testing (22).

In addition to addressing the data distribution, the model itself can be fine-tuned to improve fairness. For example, instead of minimizing the average error across all statistics, we could aim to minimize the maximum error of a subset of statistics as evaluated across different demographic groups of interest.

A recent scoping review on digital health solutions (23) found that AI health applications generally lacked vigorous pragmatic prospective real-world validations. Addressing training data imbalance during model development should produce more generalizable ophthalmic AI applications that perform more robustly in real-world validations.

Privacy

DL models typically require a large amount of data for training, and the rise of DL in ophthalmology coincided with the rise of big data, both in the form of images and tabular data. The training and testing of DL models often involve combining ophthalmic images from different sources, and there is increasing concern that such transfer of data represents an unacceptable risk of privacy breach, especially since fundus images are now considered protected health information.

Such concerns can be addressed in two ways: federated learning and differential privacy. The training of DL models can be facilitated by federated learning, which allows model training in a decentralized fashion, takes advantage of the data heterogeneity from disparate sources, and does not require actual transfer of data between the sources (24). This approach has been successfully implemented in the context of retinal microvasculature segmentation and referable diabetic retinopathy detection on optical coherence tomography (OCT) and OCT angiography images. The authors demonstrated that a federated learning approach achieved similar results as a traditional centralized learning approach (25). Similarly, instead of transferring data to train a DL model, the model itself can be "brought" to the data for retraining. This concept has been successfully demonstrated in the context of DL-based intraretinal fluid segmentation on OCT images, in which the parameters of a pre-trained DL model were frozen, transferred to and retrained at a different institution. The authors showed that such a "model-to-data" work flow could update a model and improve the model's performance, without the transfer of actual data (26).

Besides image databases, ophthalmology is also at the forefront of establishing massive tabular databases. The Intelligent Research in Sight (IRIS) Registry, spearheaded by the American Academy of Ophthalmology, is the largest specialty database in all of medicine in the world. The data collected to date has been invaluable, and led to numerous new insights and publications. Without a question, the IRIS Registry will be indispensable in developing the next-generation predictive ML algorithms. The data collected in IRIS is first de-identified, before being distributed to researchers. Traditional data de-identification methods include complete removal of all unique identifiers or coarsening of the original dataset. Data coarsening is achieved by providing the exact values of only a subset of the original sample and thus creating an incomplete dataset (27, 28). What remains to be seen is whether traditional data de-identification methods will be sufficient for protecting the privacy of data in the IRIS registry or similar tabular databases. Traditional de-identification methods are vulnerable to linkage

and other re-identification attacks, in which third parties correlate the supposedly anonymized data with unanticipated sources of auxiliary information to learn sensitive information about data participants. Examples of de-identification failure include the re-identification of "anonymized" hospital records released by Massachusetts' Group Insurance Commission and the re-identification of Netflix users' movie reviews from a dataset released as part of a ML challenge that Netflix hosted in 2006. A promising avenue of research is the application of differential privacy to large ophthalmic databases, such as IRIS.

Differential privacy is the only principled solution for releasing aggregate information about a statistical database, with provable guarantees that no information attributable to any individual in the dataset will be revealed. Briefly, differential privacy employs randomization to guarantee that the log odds ratio of any output of the analysis is bounded by and compared to a counterfactual world, in which any given participant has been entirely removed from the dataset, thereby formally limiting what inferences an arbitrarily well-informed observer can make about the data of any single participant (29). By definition, differential privacy prevents membership inference attacks as discussed above and provides a general umbrella of protection. However, the exact methods to create a differentially private dataset of unstructured data, e.g., ophthalmic images, are not currently available. This a major limitation of differential privacy as most recent advances in ML applications to ophthalmology have been in DL applications to ophthalmic images.

Finally, next-generation data infrastructure, specifically geared toward big data, ML and data privacy, is being developed, and a cutting-edge example is swarm learning. Swarm learning (30) is a decentralized data infrastructure that uses blockchain technology to ensure peer-to-peer data security. In contrast to federated learning which still requires a central parameter server, swarm learning is completely decentralized and, in addition, could inherit and be compatible with aforementioned differential privacy algorithms.

CONCLUSION

We are in the midst of the 4th Industrial Revolution, and ophthalmology has been at the forefront of the rise in AI/ML/DL and big data in medicine, and encountered various ethical and societal implications of this trend. While the concerns surrounding bias, fairness and privacy can be partially addressed by the strategies outlined above, a more comprehensive approach is preferable. This shift in mentality is best demonstrated by a recently announced special funding opportunity that was offered by the National Institute of Health as part of the Bridge2AI Common Fund[1]. The funding opportunity aims to produce Data Generation Projects that prospectively curate AI/ML ready data based on ethical principles. Multi-disciplinary teams, comprised of physicians, computer scientists and ethicists, are expected to promote a culture of ethical inquiry and consider ethical issues throughout the entire lifecycle of the project. Such an approach is grounded in the emerging view that AI is a sociotechnical issue: that is, AI shapes, and is shaped by social phenomena. The acknowledgment that the successful application of AI to medicine hinges on the holistic tackling of the associated ethical and societal implications is indeed a huge step forward, and we predict ophthalmologists in particular will play an important role in this regard in the years to come.

DATA AVAILABILITY STATEMENT

The original contributions presented in the study are included in the article/supplementary materials, further inquiries can be directed to the corresponding author.

AUTHOR CONTRIBUTIONS

All authors listed have made a substantial, direct, and intellectual contribution to the work and approved it for publication.

[1]https://commonfund.nih.gov/bridge2ai

REFERENCES

1. Bridge J, Harding S, Zheng Y. Development and validation of a novel prognostic model for predicting AMD progression using longitudinal fundus images. *BMJ Open Ophthalmol.* (2020) 5:e000569. doi: 10.1136/bmjophth-2020-000569
2. Peng Y, Keenan TD, Chen Q, et al. Predicting risk of late age-related macular degeneration using deep learning. *NPJ Digit Med.* (2020) 3:111. doi: 10.1038/s41746-020-00317-z
3. Bhuiyan A, Wong TY, Ting DSW, Govindaiah A, Souied EH, Smith RT. Artificial intelligence to stratify severity of Age-Related Macular Degeneration (AMD) and predict risk of progression to late AMD. *Transl Vis Sci Technol.* (2020) 9:25. doi: 10.1167/tvst.9.2.25
4. Ludwig CA, Perera C, Myung D, Greven MA, Smith SJ, Chang RT, et al. Automatic identification of referral-warranted diabetic retinopathy using deep learning on mobile phone images. *Transl Vis Sci Technol.* (2020) 9:60. doi: 10.1167/tvst.9.2.60
5. Burlina P, Paul W, Mathew P, Joshi N, Pacheco KD, Bressler NM. Low-shot deep learning of diabetic retinopathy with potential applications to address artificial intelligence bias in retinal diagnostics and rare ophthalmic diseases. *JAMA Ophthalmol.* (2020) 138:1070–7. doi: 10.1001/jamaophthalmol.2020.3269
6. Ting DSW, Cheung CY, Lim G, Tan GSW, Quang ND, Gan A, et al. Development and validation of a deep learning system for diabetic retinopathy and related eye diseases using retinal images from multiethnic populations with diabetes. *JAMA.* (2017) 318:2211–23. doi: 10.1001/jama.2017.18152
7. Brown JM, Campbell JP, Beers A, Chang K, Ostmo S, Chan RVP, et al. Automated diagnosis of plus disease in retinopathy of prematurity using deep convolutional neural networks. *JAMA Ophthalmol.* (2018) 136:803–10. doi: 10.1001/jamaophthalmol.2018.1934
8. Campbell JP, Kim SJ, Brown JM, Ostmo S, Chan RVP, Kalpathy-Cramer J, et al. Evaluation of a deep learning-derived quantitative retinopathy of prematurity severity scale. *Ophthalmology.* (2020) 128:1070–6. doi: 10.1016/j.ophtha.2020.10.025
9. Liu TYA, Wei J, Zhu H, Subramanian PS, Myung D, Yi PH, et al. Detection of optic disc abnormalities in color fundus photographs using deep learning. *J Neuroophthalmol.* (2021) 41:368–74. doi: 10.1097/WNO.0000000000001358
10. Liu TYA, Zhu H, Chen H, Arevalo JF, Hui FK, Yi PH, et al. Gene expression profile prediction in uveal melanoma using deep learning: a pilot study for

the development of an alternative survival prediction tool. *Ophthalmol Retina.* (2020) 4:1213–5. doi: 10.1016/j.oret.2020.06.023
11. Poplin R, Varadarajan AV, Blumer K, Liu Y, McConnell MV, Corrado GS, et al. Prediction of cardiovascular risk factors from retinal fundus photographs via deep learning. *Nat Biomed Eng.* (2018) 2:158–64. doi: 10.1038/s41551-018-0195-0
12. Mehrabi N, Morstatter F, Saxena N, Lerman K, Galstyan A. A survey on bias and fairness in machine learning. *arXiv:1908.09635v3.* (2019). doi: 10.48550/arXiv.1908.09635
13. Obermeyer Z, Powers B, Vogeli C, Mullainathan S. Dissecting racial bias in an algorithm used to manage the health of populations. *Science.* (2019) 366:447–53. doi: 10.1126/science.aax2342
14. Olteanu A, Castillo C, Diaz F, Kiciman E. Social data: Biases, methodological pitfalls, and ethical boundaries. (2016) 2:13. doi: 10.2139/ssrn.2886526
15. Suresh H, Guttag J. A framework for understanding sources of harm throughout the machine learning life cycle. In: *Equity and Access in Algorithms, Mechanisms, and Optimization (EAAMO '21).* New York, NY: Association for Computing Machinery (2021). p. 1–9. doi: 10.1145/3465416.3483305
16. Age-Related Eye Disease Study Research Group. The Age-Related Eye Disease Study (AREDS): design implications. AREDS report no 1. *Control Clin Trials.* (1999) 20:573–600. doi: 10.1016/S0197-2456(99)00031-8
17. Klein R, Klein BE, Knudtson MD, Wong TY, Cotch MF, Liu K, et al. Prevalence of age-related macular degeneration in 4 racial/ethnic groups in the multi-ethnic study of atherosclerosis. *Ophthalmology.* (2006) 113:373–80. doi: 10.1016/j.ophtha.2005.12.013
18. Friedman DS, Katz J, Bressler NM, Rahmani B, Tielsch JM. Racial differences in the prevalence of age-related macular degeneration: the Baltimore Eye Survey. *Ophthalmology.* (1999) 106:1049–55. doi: 10.1016/S0161-6420(99)90267-1
19. Zhou M, Duan P-C, Liang J-H, Zhang X-F, Pan C-W. Geographic distributions of age-related macular degeneration incidence: a systematic review and meta-analysis. *Br J Ophthalmol.* (2021) 105:1427–34. doi: 10.1136/bjophthalmol-2020-316820
20. Wang Y, Yao Q, Kwok J, Ni LM. Generalizing from a few examples: a survey on few-shot learning. *arXiv:1904.05046v3* (2020).
21. Burlina PM, Joshi N, Pacheco KD, Liu TYA, Bressler NM. Assessment of deep generative models for high-resolution synthetic retinal image generation of age-related macular degeneration. *JAMA Ophthalmol.* (2019) 137:258–64. doi: 10.1001/jamaophthalmol.2018.6156
22. Burlina P, Joshi N, Paul W, Pacheco KD, Bressler NM. Addressing artificial intelligence bias in retinal diagnostics. *Transl Vis Sci Technol.* (2021) 10:13. doi: 10.1167/tvst.10.2.13
23. Gunasekeran DV, Tseng RMWW, Tham Y-C, Wong TY. Applications of digital health for public health responses to COVID-19: a systematic scoping review of artificial intelligence, telehealth and related technologies. *NPJ Digital Med.* (2021) 4:40. doi: 10.1038/s41746-021-00412-9
24. Sheller MJ, Edwards B, Reina GA, Martin J, Pati S, Kotrotsou A, et al. Federated learning in medicine: facilitating multi-institutional collaborations without sharing patient data. *Sci Rep.* (2020) 10:12598. doi: 10.1038/s41598-020-69250-1
25. Lo J, Timothy TY, Ma D, Zang P, Owen JP, Zhang Q, et al. Federated learning for microvasculature segmentation and diabetic retinopathy classification of OCT data. *Ophthalm Sci.* (2021) 1:100069. doi: 10.1016/j.xops.2021.100069
26. Mehta N, Lee CS, Mendonça LSM, Raza K, Braun PX, Duker JS, et al. Model-to-data approach for deep learning in optical coherence tomography intraretinal fluid segmentation. *JAMA Ophthalmol.* (2020) 138:1017–24. doi: 10.1001/jamaophthalmol.2020.2769
27. Heitjan DF. Ignorability and coarse data: some biomedical examples. *Biometrics.* (1993) 49:1099–109. doi: 10.2307/2532251
28. Shardell M, El-Kamary SS. Sensitivity analysis of informatively coarsened data using pattern mixture models. *J Biopharm Stat.* (2009) 19:1018–38. doi: 10.1080/10543400903242779
29. Dwork C, Roth A. The algorithmic foundations of differential privacy. *Found Trends Theor Comput Sci.* (2013) 9:211–407. doi: 10.1561/9781601988195
30. Warnat-Herresthal S, Schultze H, Shastry KL, Manamohan S, Mukherjee S, Garg V, et al. Swarm learning for decentralized and confidential clinical machine learning. *Nature.* (2021) 594, 265–270. doi: 10.1038/s41586-021-03583-3

Conflict of Interest: The authors declare that the research was conducted in the absence of any commercial or financial relationships that could be construed as a potential conflict of interest.

frontiers | Frontiers in Medicine

ORIGINAL RESEARCH
published: 04 July 2022
doi: 10.3389/fmed.2022.860371

Widefield Optical Coherence Tomography in Pediatric Retina: A Case Series of Intraoperative Applications Using a Prototype Handheld Device

*Thanh-Tin P. Nguyen[1], Shuibin Ni[1,2], Guangru Liang[1,2], Shanjida Khan[1,2], Xiang Wei[1,2], Alison Skalet[1,3,4,5], Susan Ostmo[1], Michael F. Chiang[6], Yali Jia[1,2], David Huang[1,2], Yifan Jian[1,2] and J. Peter Campbell[1]**

[1] Casey Eye Institute, Oregon Health and Science University, Portland, OR, United States, [2] Department of Biomedical Engineering, Oregon Health and Science University, Portland, OR, United States, [3] Knight Cancer Institute, Oregon Health and Science University, Portland, OR, United States, [4] Department of Radiation Medicine, Oregon Health and Science University, Portland, OR, United States, [5] Department of Dermatology, Oregon Health and Science University, Portland, OR, United States, [6] National Eye Institute, National Institutes of Health, Bethesda, MD, United States

OPEN ACCESS

Edited by:
Jorge L. Alió Del Barrio, Miguel Hernández University of Elche, Spain

Reviewed by:
Magdy Moussa, Tanta University, Egypt
Simar Rajan Singh, Post Graduate Institute of Medical Education and Research (PGIMER), India

***Correspondence:**
J. Peter Campbell
campbelp@ohsu.edu

Specialty section:
This article was submitted to Ophthalmology, a section of the journal Frontiers in Medicine

Received: *22 January 2022*
Accepted: *15 June 2022*
Published: *04 July 2022*

Citation:
Nguyen TTP, Ni S, Liang G, Khan S, Wei X, Skalet A, Ostmo S, Chiang MF, Jia Y, Huang D, Jian Y and Campbell JP (2022) Widefield Optical Coherence Tomography in Pediatric Retina: A Case Series of Intraoperative Applications Using a Prototype Handheld Device. Front. Med. 9:860371. doi: 10.3389/fmed.2022.860371

Optical coherence tomography (OCT) has changed the standard of care for diagnosis and management of macular diseases in adults. Current commercially available OCT systems, including handheld OCT for pediatric use, have a relatively narrow field of view (FOV), which has limited the potential application of OCT to retinal diseases with primarily peripheral pathology, including many of the most common pediatric retinal conditions. More broadly, diagnosis of all types of retinal detachment (exudative, tractional, and rhegmatogenous) may be improved with OCT-based assessment of retinal breaks, identification of proliferative vitreoretinopathy (PVR) membranes, and the pattern of subretinal fluid. Intraocular tumors both benign and malignant often occur outside of the central macula and may be associated with exudation, subretinal and intraretinal fluid, and vitreoretinal traction. The development of wider field OCT systems thus has the potential to improve the diagnosis and management of myriad diseases in both adult and pediatric retina. In this paper, we present a case series of pediatric patients with complex vitreoretinal pathology undergoing examinations under anesthesia (EUA) using a portable widefield (WF) swept-source (SS)-OCT device.

Keywords: retina, pediatric retina, optical coherence tomography, handheld optical coherence tomography, optical coherence tomography with angiography

INTRODUCTION

Optical coherence tomography (OCT) is an essential diagnostic tool in the management of retinal disease. There are trade-offs in the acquisition of OCT images between speed of acquisition, field of view (FOV), and image resolution and quality. Over the last two decades, despite significant advances in imaging speed and the transition from time-domain to spectral domain (SD)-OCT, the vast majority of OCT applications are for macular diseases in adults. OCT has proven ability

to detect subclinical disease, often resulting in new disease classifications and earlier treatment, facilitate objective assessment of macular thickness and pathologic fluid, and improve visualization of the vitreoretinal interface. As a result, it is not possible to provide the standard of care for many adult retinal diseases without OCT.

These same advances in clinical diagnosis and management would likely benefit pediatric retina patients. In retinopathy of prematurity (ROP), the most common pediatric retinal disease, OCT has revealed the normal spectrum of macular development in prematurely born infants (1, 2), identified the presence of intraretinal fluid (3, 4), and demonstrated the ability to objectively assess changes at the vitreoretinal interface (5). However, early work has been limited by the specifications of commercially available devices. Over the past few years, a number of groups have explored the advantages of arm-mounted SD-OCT (6) and prototype swept-source (SS)-OCT in pediatric retinal diseases (7–10). With the versatility of a handheld probe and faster image acquisition times, SS-OCT has improved the ease of imaging in both awake and sedated children.

We have developed a handheld SS-OCT device with two imaging configurations, one with a 55° FOV and higher resolution for OCTA imaging (11), and one with a 105° FOV for OCT structural imaging only (12). Our 55° FOV system generates OCTA volumes concurrently with OCT, and both imaging configurations allow for real time *en face* visualization to allow the physician to position the probe optimally for image acquisition. The 105° FOV system has potential to provide objective diagnosis in pediatric retinal diseases with predominantly extramacular pathology, like ROP, and contribute to new insight in these disease processes. We recently described our experience using these devices for ROP screening in the neonatal intensive care unit (NICU) in awake infants (13, 14). Here, we present a review of the potential clinical benefits and applications of widefield (WF) and ultra-widefield (UWF) handheld OCT in pediatric retina patients undergoing examinations under anesthesia (EUA) for a variety of conditions.

MATERIALS AND METHODS

This study was approved by the Institutional Review Board (IRB) at Oregon Health and Science University (OHSU) and adheres to all tenets of the Declaration of Helsinki. Consent for imaging was obtained from parents. Pupils were pharmacologically dilated per routine clinical care. Infants were imaged in the operating room (OR) after the induction of general anesthesia and placement of an eyelid speculum with a 400-kHz portable handheld SS-OCT system, shown in **Figure 1**, using a modular lens system providing up to a 105° FOV. A display screen on the probe provides real-time *en face* visualization of the retina and allows for efficient positioning of the probe (15–17). The probe was operated by the examining ophthalmologist, whilst another operator controlled the software. Image acquisition time was 1.5 s per volume. Patients were imaged between November of 2020 to October 2021.

Optical coherence tomography volumes were processed and presented in linear scale. Mean-intensity *en face* projections were calculated with custom software coded in MATLAB (18). B-scans presented in this manuscript were produced *via* image registration and averaging of adjacent B-scans. Three-dimensional image rendering was performed *via* the Volume Viewer plugin of Fiji, a distribution of ImageJ after pre-processing using a combination of thresholding and manual image segmentation (19). OCTA images were generated using a novel phase-stabilized complex-decorrelation methodology (20), with automated segmentation performed using a guided bidirectional graph search method (21), both of which were designed specifically for use in swept-source, widefield applications.

RESULTS

During the study period, we obtained images in 20 patients undergoing EUA in the operating room, as seen in **Table 1**. Here, we present a variety of pathologies and examples to illustrate some potential applications in pediatric retina.

Retinal Detachments

Portable widefield OCT facilitates the evaluation of tractional, exudative, rhegmatogenous (and combined mechanism) retinal detachments (RDs) in children. The most common visualization of OCT is the cross-sectional scan (B-scan) that reveals axial anatomy within a single imaging slice. However, SS-OCT can facilitate real-time *en-face* visualization of the entire imaging range. **Figure 2** reveals *en face* and selected B-scans from several children with tractional retinal detachment (TRD). TRDs are most commonly related to peripheral epiretinal neovascularization with fibrosis, with the resulting vitreoretinal traction leading to macular dragging (as seen in **Figure 2A**), distortion of the normal retinal architecture, and if there is sufficient anterior-posterior traction, separation of the retina from the retinal pigment epithelium (RPE). OCT is more sensitive for detection of this spectrum of changes, as seen in **Figure 2C** which reveals an early stage 4a detachment in ROP with the selected B-scan demonstrating tractional schisis but no subretinal fluid. It is important to note that the transverse resolution of these B-scans is relatively low, the result of expanding FOV while maintaining efficient imaging time (1.5 s). Resolution can be improved with either longer imaging time, which is challenging in children, or narrower FOV, as previously seen with our 55° FOV prototype (11). **Figure 3** demonstrates a rhegmatogenous retinal detachment (RRD) with a large temporal retinal break in a 5-year-old girl. Exudative retinal detachments (ERDs) may be relatively more common in pediatric retinal diseases such as in ROP after laser treatment or in severe Coats' disease, which means they are often diagnosed clinically rather than with OCT imaging due to

TABLE 1 | Patient ages and diagnoses.

	Diagnosis	Figure	Age
Case 1	Tractional retinal detachment (TRD) secondary to Familial Exudative Vitreoretinopathy (FEVR)	2A	3 years, 6 months
Case 2	TRD secondary to incontinentia pigmenti (IP)	2B, 8A	2B: 1 year, 6 months; 8A: 1 year
Case 3	TRD secondary to retinopathy of prematurity (ROP), Stage 4A	2C	4 months
Case 4	Rhegmatogenous retinal detachment (RRD)	3	5 years, 10 months
Case 5	Tractional and exudative retinal detachment (ERD) secondary to vasoproliferative lesion	4A	15 years
Case 6	Chronic exudative retinopathy	4B	16 years
Case 7	ERD secondary to ROP after laser	4C	5 months
Case 8	Coats disease	5	2 years, 3 months
Case 9	Retinoblastoma with calcified, partially calcified, and atrophic regressed tumors after completion of therapy	6A	3 years
Case 10	Retinoblastoma with partially calcified tumor in patient undergoing chemotherapy	6B	5 months
Case 11	Retinoblastoma with vitreous seeding and multifocal tumors	6C	7 months
Case 12	X-linked retinoschisis (XLRS)	7A	8 years
Case 13	Chorioretinal scarring with retinal traction secondary to non-accidental trauma (NAT)	7B	7 months
Case 14	ROP with regressed Stage 3 ROP with vitreoretinal traction	7C	2 months
Case 15	Persistent fetal vasculature (PFV)	7D	1 year, 7 months
Case 16	IP with peripheral avascular retina and neovascularization	8B	2 years, 7 months
Case 17	Hemangioblastomas in the setting of Von Hippel Lindau syndrome	9	15 years
Case 18	Central cataract in the setting of PFV	10A, 10B	6 months
Case 19	Retained silicone oil in the anterior chamber	10C	14 years
Case 20	TRD secondary to FEVR	11	4 months

Patient ages are at the time of OCT imaging.

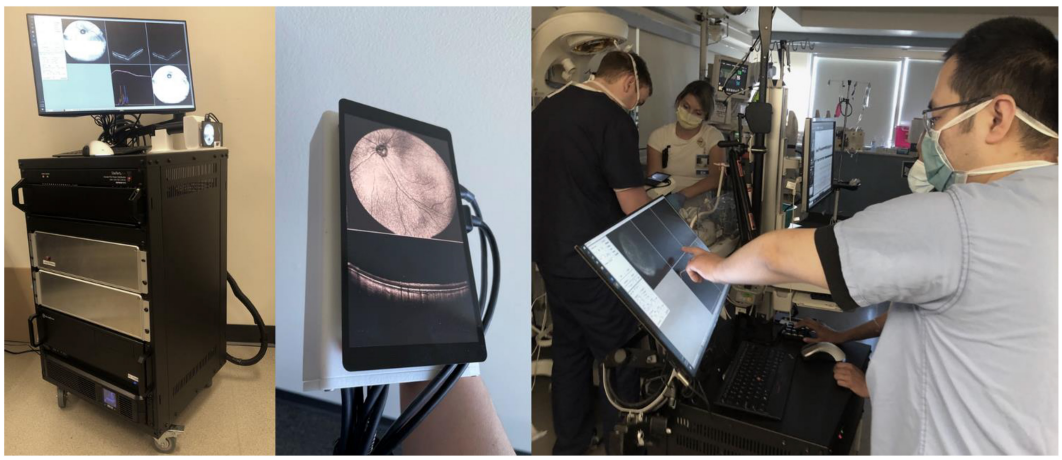

FIGURE 1 | Handheld, SS-OCT device. From left: portable prototype device, imaging probe with real-time *en face* display, and process of obtaining OCT volumes of an infant in the NICU.

the limitations of existing commercially available devices. Yet accurate diagnosis is critical because the management of exudative detachments is often different than if the primary mechanism is tractional or rhegmatogenous. **Figure 4** provides several examples ERDs and combined tractional and exudative RDs in children.

Macular Exudation

While WF-OCT is critical for visualization of the retinal periphery, it can still be used to diagnose and monitor exudation in the macula in many diseases. **Figure 5** demonstrates several examples of the visualization of subretinal exudative in Coats' disease, including the potential benefit of *en face* visualization with topographic volume rendering. There are many previous publications focusing on the role of OCT in pediatric macular disease (2, 3, 22).

Intraocular Tumors

A number of retinal tumors can present in childhood including retinoblastoma (RB), retinal hemangioblastoma as part of Von-Hippel Lindau (VHL) disease, vasoproliferative tumor, and a variety of benign hamartomas such as choroidal hemangioma and congenital hypertrophy of the retina and RPE. The

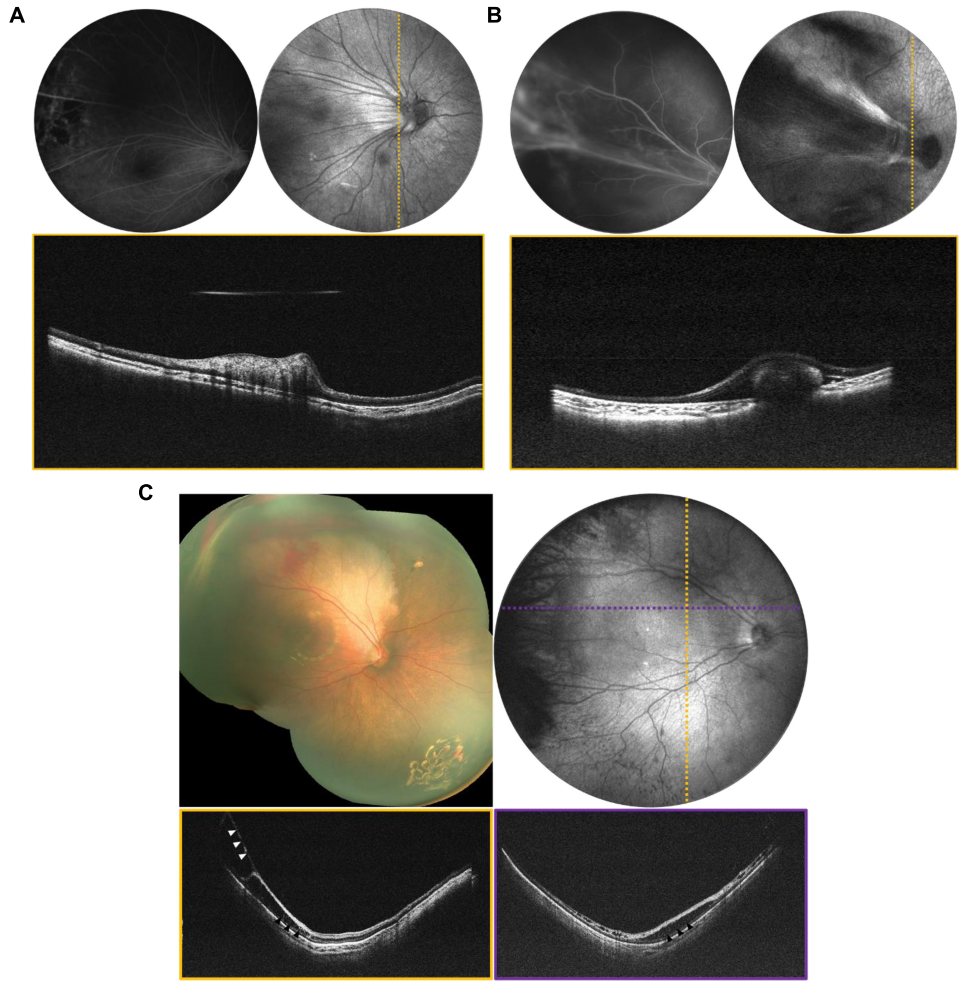

FIGURE 2 | Tractional retinal disease evaluated *via* OCT. **(A)** Tractional retinal fold secondary to FEVR in a 3-year-old patient. **(B)** Tractional fold with peripheral detachment secondary to IP in a 1-year-old patient. For **(A,B)**, top left is the FA, top right is the mean-intensity *en face* projection taken with the 55° FOV configuration, and bottom is the B-scan corresponding to the dotted line. **(C)** Stage 4a ROP in a 4-month-old born at 24 weeks gestation. Top left image is a montage of fundus photographs. Top right is a 105° FOV OCT *en face* with dotted lines indicating the locations of the color-coded B-scans in the bottom row. Vitreoretinal traction is indicated by white arrows, and areas of schisis are indicated by black arrows.

most serious of these is RB, which is both vision- and life-threatening. The current standard of care requires careful documentation of all tumors in the retina, including their size, location and the presence of any associated vitreous seeding, and subretinal fluid. Fundus photos are used to document these findings. Commercially available OCT systems are also widely used in retinoblastoma care, but have significant limitations due to their narrow field of view and narrow depth of focus (23–26). Retinoblastoma tumors are often highly elevated, multifocal and arise in the peripheral retina as well as the posterior pole. There is considerable potential for the use of WF-OCT in retinoblastoma care. **Figure 6** demonstrates several examples of RB documented with our device during routine RB EUAs. The WF-OCT system was successful in capturing three dimensional images of elevated tumors, including those in the far periphery, and provided better images than traditional fundus photography in the setting of diffuse vitreous seeding (**Figure 6C**). WF-OCT was also able to identify very small subclinical tumors (27), indicating that it may prove useful in surveillance for new tumors in children with known RB or in those being screened due to family history of the disease.

Vitreoretinal Interface Disorders

Changes at the vitreoretinal interface are better diagnosed with OCT than ophthalmoscopy and are common in pediatric proliferative retinopathies, some inherited retinal degenerations, and disorders of ocular development. **Figure 7A** shows an example of X-linked retinoschisis (XLRS), in which retinoschisis may manifest both in the macula and periphery. Many conditions demonstrate an abnormally adherent vitreoretinal interface. An abnormal vitreoretinal interface may be associated with prior trauma, as in **Figure 7B**, and regressed neovascularization in ROP, as in **Figure 7C**. Finally, in persistent fetal vasculature

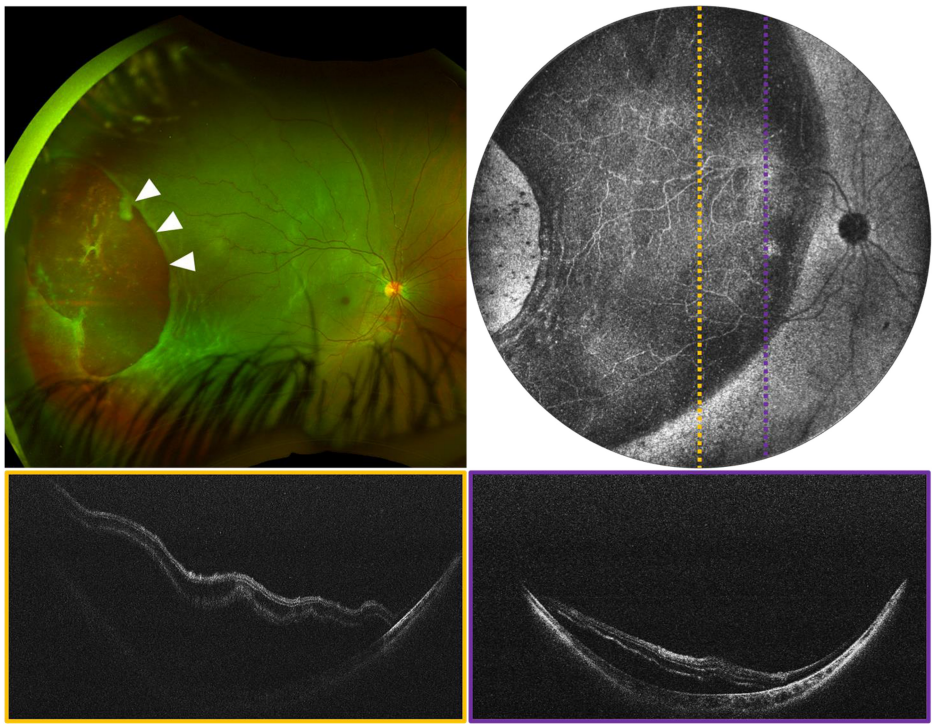

FIGURE 3 | Rhegmatogenous retinal detachment (RRD) in a 5-year-old girl, evaluated using widefield OCT. **(Top left)** Image is an ultra-widefield fundus photograph, with white arrows indicating a large temporal break. **(Top right)** Image is the 105° FOV OCT *en face*, with dotted lines indicating the locations of the color-coded B-scans shown below.

(PFV), there is a cellular connection through the vitreous cavity that connects the retina to the anterior segment, which can be associated with traction at the nerve or in an extramacular location, as seen in **Figure 7D**.

Vascular Disorders

Obtaining high quality OCTA is challenging even in cooperative adults, more so in children, and even more so with wider field of view. Nontheless, particularly under anesthesia, it is possible to explore the potential role OCTA may play in the diagnosis of pediatric retinal diseases when used in conjunction with structural OCT (**Figure 8A**). **Figure 8B** demonstrates an OCTA taken during an EUA for a child with incontinentia pigmenti (IP), revealing both non-perfusion and neovascularization without the need for fluorescein dye. **Figure 9** demonstrates several VHL tumors visualized with *en face* OCT and OCTA.

Anterior Segment Optical Coherence Tomography

Anterior segment (AS)-OCT has demonstrated a number of potential uses in adults, including evaluation of corneal curvature and pathology, angle structures, and iris and lens abnormalities (28). We have included a few examples of AS-OCT obtained in our practice, but believe that the most significant potential application of this imaging may be in the evaluation and management of pediatric glaucoma in which anterior segment dysgenesis is typical (29). **Figure 10** reveals *en face* and cross-sectional AS-OCT in several patients with both preoperative and post-operative abnormalities of the anterior segment.

DISCUSSION

In this paper, we reviewed our experience using WF-OCT in the management of patients with a variety of pediatric retinal diseases undergoing EUA. Compared to the highest resolution commercially available adult OCT devices, our prototype uses a faster, swept-source laser, which facilitates efficient imaging of the retina even in awake neonates and children. These results demonstrate the tradeoff between FOV and resolution, which is necessary when trying to keep imaging time to a minimum.

Retinopathy of Prematurity

The diagnosis of ROP relies on subjective assessment of clinical features on ophthalmoscopic exam or fundus photography, despite significant inter-observer variability in diagnosis, practice, and outcomes. Most of the early work using OCT work has focused on macular manifestations of ROP, such as the presence of macular edema, vitreous opacities, and the presence of retinoschisis posterior to the ridge (3, 4, 30). Widefield OCT has demonstrated the potential to provide real-time *en face* visualization, objective assessment of the peripheral stage, longitudinal monitoring of disease progression and regression,

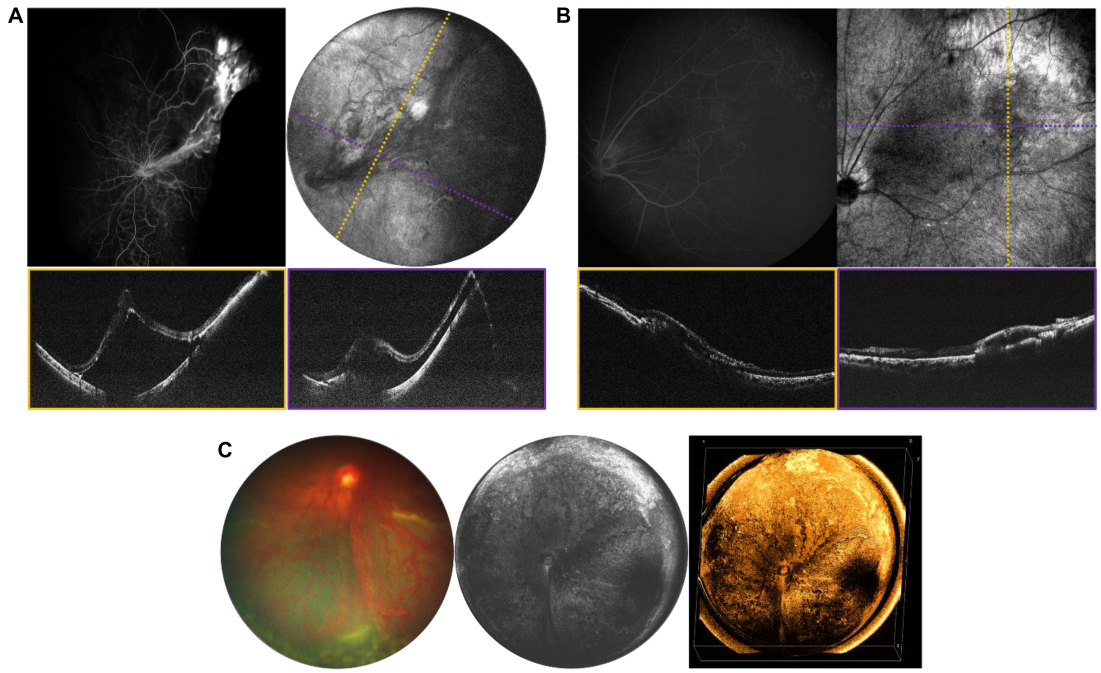

FIGURE 4 | Tractional and exudative retinal detachments. **(A)** ERD in a 15-year-old girl in the setting of a vasoproliferative lesion. **(B)** Chronic exudative retinopathy in a 16-year-old girl. For **(A,B)**, top left image is fluorescein angiography (FA), top right is the mean-intensity *en face* projection [105° FOV for panel **(A)** and 40° FOV for panel **(B)**], with dotted lines indicating the locations of the color-coded B-scans shown below. **(C)** ERD in a 5-month-old patient with ROP. From left: fundus photograph, 105° FOV OCT en face, and three-dimensional rendering of the same OCT volume.

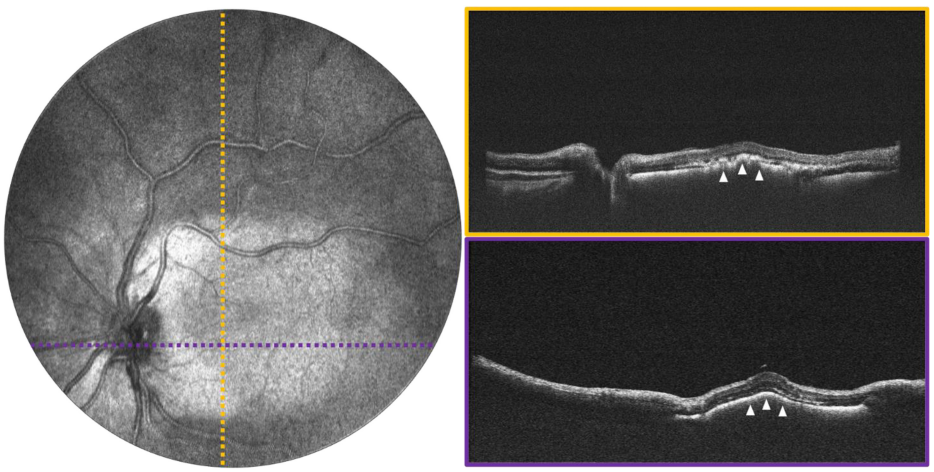

FIGURE 5 | Macular exudation in a 2-year-old with Coats disease. **(Left)** Image shows 55° FOV OCT *en face* projection, with dotted lines indicating the locations of the color-coded B-scans shown on the **(right)**. White arrows point to the area of subretinal exudation.

and detection of early vitreoretinal interface abnormalities (13, 14, 31).

Tractional, Exudative, and Rhegmatogenous Retinal Detachments

Differentiating the cause of retinal detachment is key for proper management of retinal detachments in children, and OCT may be a pivotal tool. RRD repair depends on accurate identification of breaks, and the identification and management of proliferative vitreoretinopathy (PVR) membranes, which may be above or below the retinal surface. The standard of care is to carefully observe the entire retina with ophthalmoscopy and scleral depression for the presence of breaks. However, clinical diagnosis is not perfect and OCT may be superior for identification of peripheral pathology (32, 33). In this paper, we have presented several examples of tractional, rhegmatogenous, and exudative

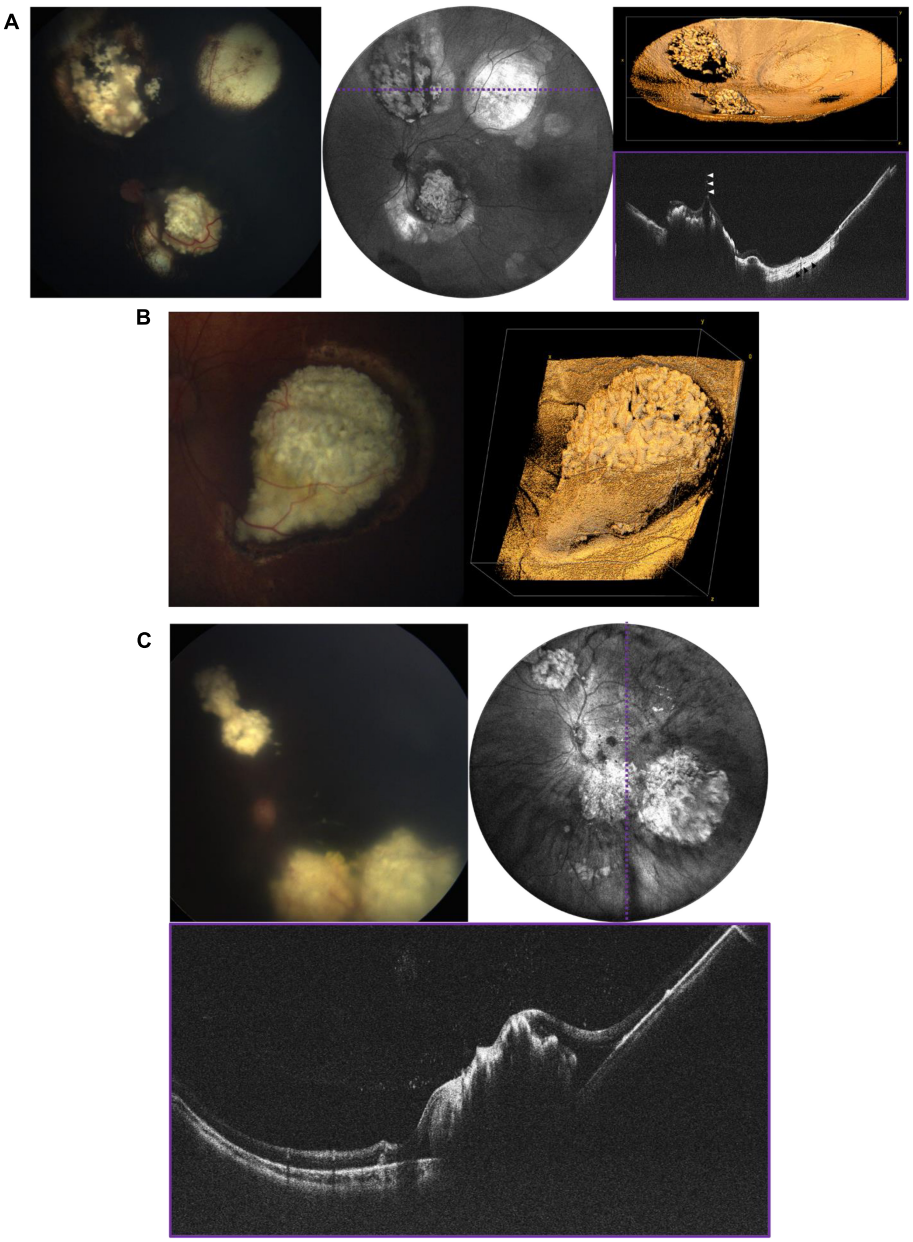

FIGURE 6 | Retinoblastoma evaluated with OCT in three patients with bilateral disease. **(A)** 3-year-old with multifocal RB in the left eye who has completed therapy. Left image is the fundus photograph, middle image is the 105° FOV OCT *en face* projection showing multiple regressed tumors, with dashed purple line corresponding to the location of the B-scan on the bottom right. White arrows point toward a vitreous band, while black arrows point to an area of retinal atrophy. Top right image shows three-dimensional rendering of the same volume shown in the middle panel. **(B)** Large partially calcified retinoblastoma in a 5-month-old patient undergoing systemic chemotherapy. Fundus photograph is shown on the left, and three-dimensional rendering of 40° FOV, high-resolution OCT volume is shown on the right. **(C)** 7-month-old undergoing systemic chemotherapy with active RB including diffuse vitreous seeding and multifocal tumors in the left eye. Top left image shows the fundus photograph, top right shows the 105° FOV OCT *en face* projection, with dashed purple line corresponding to the B-scan below.

detachments and highlighted ways in which WF-OCT may be utilized in the diagnosis and monitoring of these diseases in the future. One example of a potential use of WF-OCT is in monitoring the resolution of subretinal fluid following RD surgery. **Figure 11** reveals pre- and post-operative *en face* OCT and B-scans for a child with familial exudative vitreoretinopathy (FEVR) who presented shortly after birth with bilateral retinal folds and tractional-exudative RDs. Post-operative scans reveal improved exudation and subretinal fluid.

Intraocular Tumors

In retinoblastoma (RB), the most common primary intraocular malignancy in children, the value of OCT has been demonstrated, however, there are known challenges

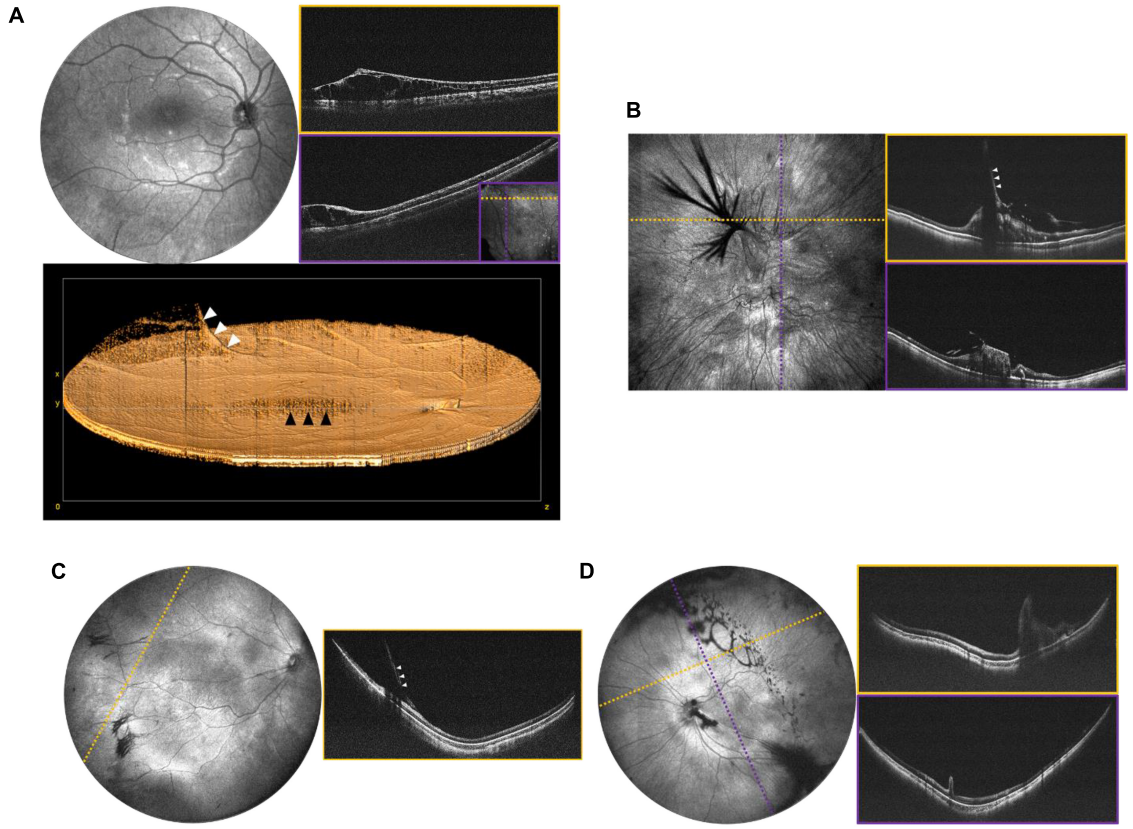

FIGURE 7 | Peripheral retinal and vitreoretinal interface abnormalities. **(A)** OCT evaluation in an 8-year-old patient with XLRS. Top left shows the 55° FOV *en face* projection, with corresponding volume rendering shown below. White arrows denote a blood vessel extending into the area of vitreoschisis (vitreous veils) and black arrows denote the area of foveoschisis. Top right images show high-resolution scans of an area of retinoschisis taken with 40° FOV. The inset in the bottom-right corner of the purple B-scan shows the locations of the cross-sections in dotted lines. **(B)** OCT evaluation of 7-month-old patient with history of non-accidental trauma, displaying disorganization of the retinal architecture, as well as vitreoretinal traction in region of prior breakthrough vitreous hemorrhage. Left image shows a 40° FOV *en face* projection, with dashed yellow and purple lines denoting the location of the corresponding B-scans on the right. White arrows denote vitreoretinal traction. **(C)** Vitreoretinal traction in a 2-month-old at site of regressed stage 3 extraretinal neovascularization in ROP. Left image shows 105° FOV *en face* view with dashed line indicating the location of the cross-sectional B-scan pictured on the right. White arrows denote vitreoretinal traction. **(D)** 1-month-old with ectopic PFV. Top left image shows the 105° FOV *en face* projection with complex oval-shaped vitreoschisis. Dotted lines correspond to B-scan locations demonstrating retinal fold through the macula.

with commercially available OCT systems (23–26). The potential value for WF-OCT to image and document tumor location and size, to monitor treatment response to laser, cryotherapy and chemotherapy, and to evaluate for newly emerging tumors is clear. A system which could combine structural images with OCTA would be of particular interest. House et al. (34) utilized OCTA to evaluate irregular tumor vasculature, with the advantage of depth resolution compared to fluorescein angiography (FA). As tumor vascular density in RB has been found to correlate significantly with a greater risk of metastasis (35), OCTA imaging could be useful in providing prognostic information. Beyond RB, there is considerable potential for WF-OCTA in the management of a wide variety of elevated and/or peripheral tumors involving the choroid and retina. In retinal hemangioblastomas, which may be associated with Von Hippel Lindau (VHL) syndrome, OCTA has been useful to differentiate non-vascular lesions from the vascular tumors, but the limited FOV has been a comparative disadvantage versus FA (36).

Inherited Retinal Dystrophies and Congenital Anomalies

In the realm of inherited retinal dystrophies (IRDs), OCT has been useful in identifying prognostic indicators, such as foveal cavitation (37), and the extent of photoreceptor atrophy. Spectral-domain (SD-OCT) technology has provided adequate axial resolution to evaluate X-linked retinoschisis in greater detail, elucidating the precise layers where retinal separation tends to occur (38). OCTA has also been utilized to evaluate choroidal neovascularization in IRDs, with advances in automated image segmentation capable of accurately delineating vascular plexuses even

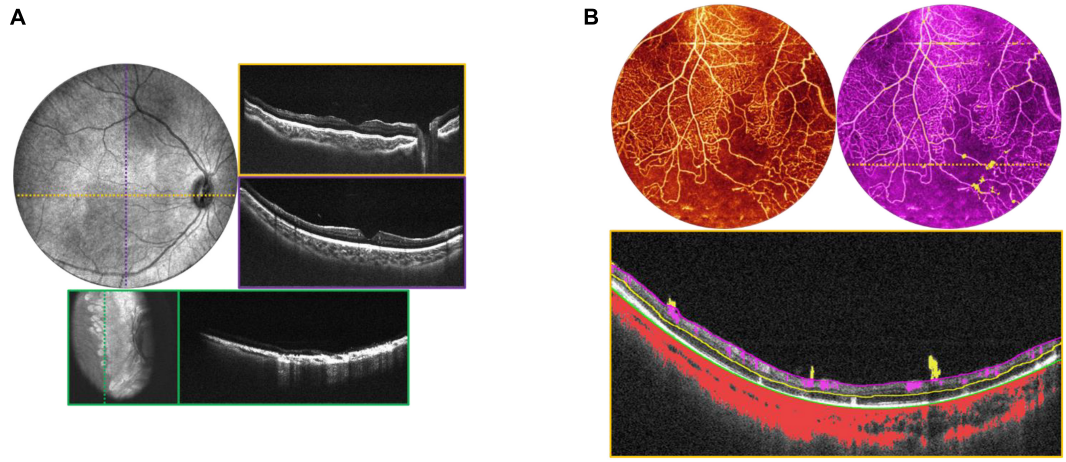

FIGURE 8 | Incontinentia pigmenti (IP). **(A)** OCT volume of a 1-year-old with IP. Top left image is the OCT 55° FOV *en face* projection. Corresponding color-coded B-scans at top right show irregularities in the nerve fiber layer and retinal surface. Bottom image in teal shows the retina after laser treatment, with *en face* view on the left, and corresponding B-scan on the right. **(B)** OCTA evaluation of a 2-year-old patient with IP. Top left image shows the OCTA en face projection with 55° FOV, while top right image shows the same volume with extraretinal neovascularization highlighted in bright yellow. Bottom image is the B-scan corresponding to the dashed yellow line above, showing automated segmentation of capillary plexus layers.

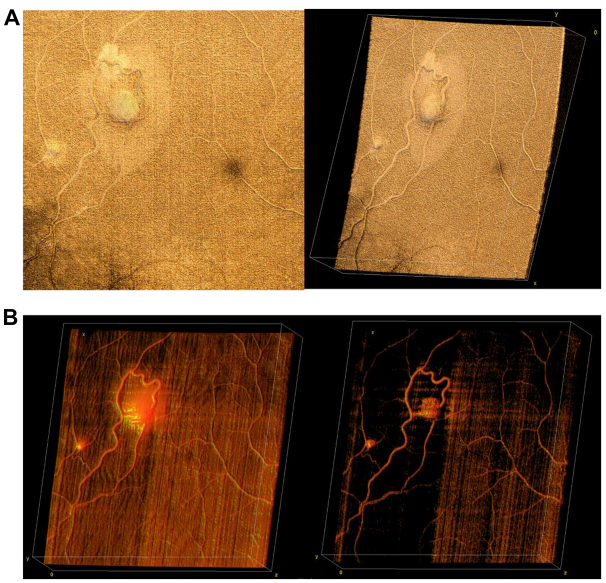

FIGURE 9 | Retinal hemangioblastomas in the setting of Von Hippel Lindau (VHL) syndrome. **(A)** Volume rendering of retinal hemangioblastomas in a 15-year-old. Left image shows an *en face* of a three-dimensional volume rendering of the tumors taken with a 40° FOV, while image on the right shows an angled view of the same volume. **(B)** Three-dimensional visualization of vessels generated from OCTA of the same volume as in panel **(A)**. The image on the left shows a three-dimensional rendering of the OCTA volume, showing flow signal within the tumors. Image on the right shows the same volume with higher contrast between vessels and surrounding tissue.

in the setting of distorted retinal architecture (39). In FEVR, OCTA has shown vascular abnormalities in the deep and superficial vascular complexes (40), and for both FEVR and PFV, handheld OCT has been used to detect optic nerve head dragging and associated vitreous bands (41, 42). In IP, OCT has illustrated subclinical change to foveal structure, including inner and outer retinal thinning associated with retinal ischemia in IP (43–46).

Limitations of Widefield Optical Coherence Tomography Imaging

As mentioned throughout, there is a tradeoff between FOV, resolution, and acquisition speed, therefore the transverse resolution is lower for a given laser when expanding the FOV for a given amount of imaging time. Practically speaking, that means that individual B-scans may be lower resolution using this approach compared to commercially available systems with narrower FOV, such as the Heidelberg Flex system, although the acquisition time is faster (6). Other limitations to this approach overlap with those found in comparable commercial OCT systems, and include motion artifacts and shadow which often necessitate the capture of multiple redundant volumes per region of interest. Current OCT systems are also limited by the potential axial imaging range, which limits the ability to obtain UWF imaging in larger eyes.

CONCLUSION

In summary, the use of WF-OCT has several potential advantages compared to the clinical exam and fundus photography in the setting of pediatric retinal diseases. As in adults, the axial resolution is superior to what our eyes can see, enabling earlier detection of retinal abnormalities in multiple diseases. *En face* visualization can provide the same benefit as fundus

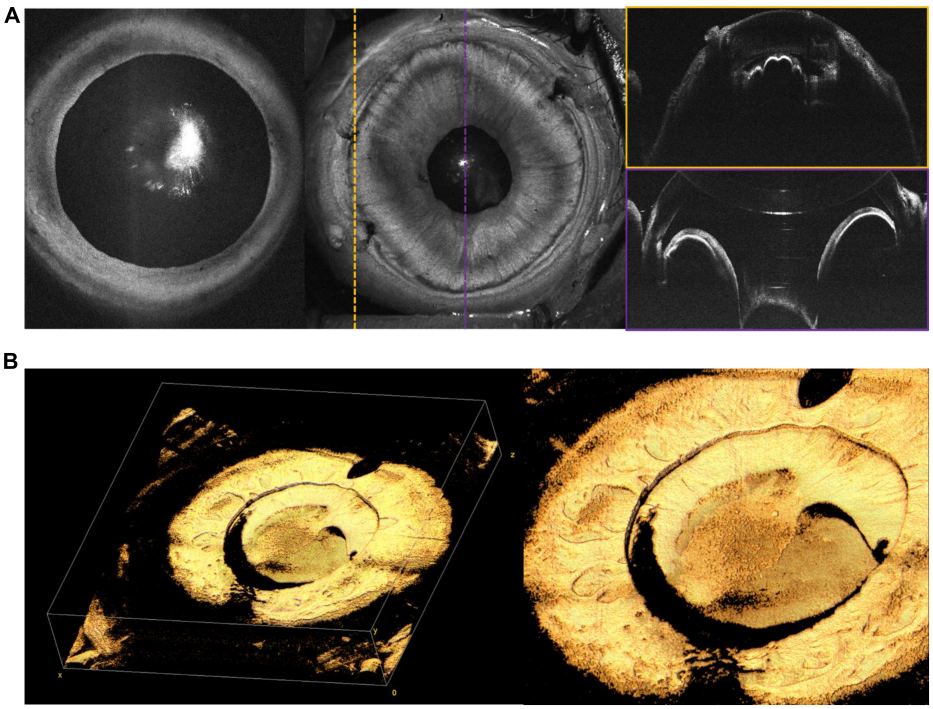

FIGURE 10 | Anterior segment (AS)-OCT. **(A)** AS-OCT in a 6-month-old with PFV. Leftmost *en face* OCT demonstrates good pupillary dilation and central cataract. Middle image shows *en face* of AS-OCT, with corresponding color-coded B-scans on the right. The scan outlined in yellow was taken at the limbus, providing visualization of the ciliary body. The scan outlined in purple shows the iris, with a reflection artifact affecting the cornea. **(B)** Silicone oil in the anterior chamber on AS-OCT in a 14-year-old. Leftmost image shows three-dimensional rendering of the iris and anterior chamber, while rightmost image shows a close up of retained oil above the lens. Both **(A,B)** were captured with a 105° FOV.

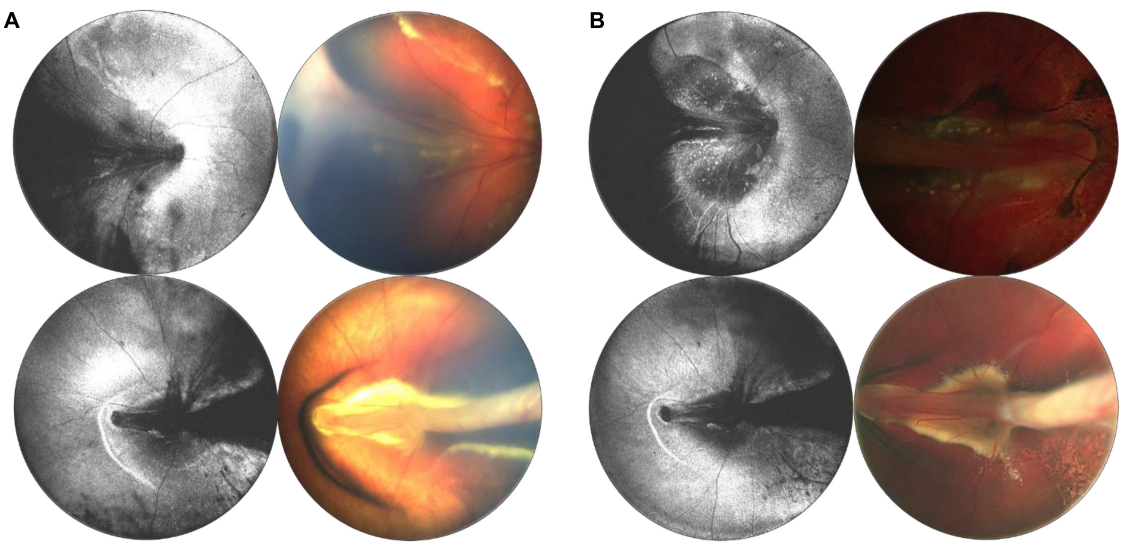

FIGURE 11 | Longitudinal monitoring of a patient with familial exudative vitreoretinopathy (FEVR). **(A)** Pre-surgical repair of bilateral tractional retinal detachments secondary to FEVR in a 4-month-old patient taken with 55° FOV device. **(B)** Post-surgical repair images, with OCT *en face* taken 1 week after surgery, and fundus photographs taken 3 months after surgery. For panels **(A,B)**, left column are OCT en face projections, whilst right column are color fundus photographs.

photography, but with volumetric structural and angiographic information as well. Finally, OCT facilitates objective assessment of retinal structures that can be used to monitor disease stability. The challenges to widespread adoption of this technology remain the lack of commercially available OCT devices of sufficient speed and FOV to be effective in capturing images

outside of the macula. As the costs of lasers come down with time, our hope is that the market will facilitate the routine use of this technology in the care of children with retinal disease.

DATA AVAILABILITY STATEMENT

The original contributions presented in this study are included in the article/supplementary material, further inquiries can be directed to the corresponding author.

ETHICS STATEMENT

The studies involving human participants were reviewed and approved by the Oregon Health and Science University Institutional Review Board. Written informed consent was obtained from the minor(s)' legal guardian/next of kin for the publication of any potentially identifiable images or data included in this article.

AUTHOR CONTRIBUTIONS

JC, MC, DH, YaJ, and YiJ designed the study and obtained the funding. SO developed and maintained the patient database and consented all patients. AS contributed to the data and critically reviewed the manuscript. T-TN, GL, SN, SK, and XW identified, processed, and contributed to the images to the final manuscript. All authors reviewed and approved of the final version of the manuscript.

FUNDING

This work was supported by grants R01 HD107494 and P30 EY10572 from the National Institutes of Health (Bethesda, MD), by unrestricted departmental funding, a Career Development Award (JC) and a Career Advancement Award (YiJ) from Research to Prevent Blindness (New York, NY), and the West Coast Consortium for Technology and Innovations in Pediatrics.

REFERENCES

1. Maldonado RS, O'Connell RV, Sarin N, Freedman SF, Wallace DK, Cotten CM, et al. Dynamics of human foveal development after premature birth. *Ophthalmology.* (2011) 118:2315–25. doi: 10.1016/j.ophtha.2011.05.028
2. Lee H, Proudlock FA, Gottlob I. Pediatric optical coherence tomography in clinical practice—recent progress. *Invest Ophthalmol Vis Sci.* (2016) 57:OCT69–79. doi: 10.1167/iovs.15-18825
3. Vinekar A, Avadhani K, Sivakumar M, Mahendradas P, Kurian M, Braganza S, et al. Understanding clinically undetected macular changes in early retinopathy of prematurity on spectral domain optical coherence tomography. *Invest Ophthalmol Vis Sci.* (2011) 52:5183–8. doi: 10.1167/iovs.10-7155
4. Muni RH, Kohly RP, Charonis AC, Lee TC. Retinoschisis detected with handheld spectral-domain optical coherence tomography in neonates with advanced retinopathy of prematurity. *Arch Ophthalmol.* (2010) 128:57–62. doi: 10.1001/archophthalmol.2009.361
5. Joshi MM, Trese MT, Capone A Jr. Optical coherence tomography findings in stage 4A retinopathy of prematurity: a theory for visual variability. *Ophthalmology.* (2006) 113:657–60. doi: 10.1016/j.ophtha.2006.01.007
6. Hsu ST, Ngo HT, Stinnett SS, Cheung NL, House RJ, Kelly MP, et al. Assessment of macular microvasculature in healthy eyes of infants and children using OCT angiography. *Ophthalmology.* (2019) 126:1703–11. doi: 10.1016/j.ophtha.2019.06.028
7. Viehland C, Chen X, Tran-Viet D, Jackson-Atogi M, Ortiz P, Waterman G, et al. Ergonomic handheld OCT angiography probe optimized for pediatric and supine imaging. *Biomed Opt Express.* (2019) 10:2623–38. doi: 10.1364/BOE.10.002623
8. Jin P, Zou H, Zhu J, Xu X, Jin J, Chang TC, et al. Choroidal and retinal thickness in children with different refractive status measured by swept-source optical coherence tomography. *Am J Ophthalmol.* (2016) 168:164–76.
9. Campbell JP, Nudleman E, Yang J, Tan O, Chan RP, Chiang MF, et al. Handheld optical coherence tomography angiography and ultra–wide-field optical coherence tomography in retinopathy of prematurity. *JAMA Ophthalmol.* (2017) 135:977–81.
10. Chen X, Viehland C, Carrasco-Zevallos OM, Keller B, Vajzovic L, Izatt JA, et al. Microscope-integrated optical coherence tomography angiography in the operating room in young children with retinal vascular disease. *JAMA Ophthalmol.* (2017) 135:483–6. doi: 10.1001/jamaophthalmol.2017.0422
11. Ni S, Wei X, Ng R, Ostmo S, Chiang MF, Huang D, et al. High-speed and widefield handheld swept-source OCT angiography with a VCSEL light source. *Biomed Opt Express.* (2021) 12:3553–70. doi: 10.1364/BOE.425411
12. Ni S, Nguyen T-TP, Ng R, Khan S, Ostmo S, Jia Y, et al. 105° field of view non-contact handheld swept-source optical coherence tomography. *Opt Lett.* (2021) 46:5878–81. doi: 10.1364/OL.443672
13. Nguyen T-TP, Ni S, Khan S, Wei X, Ostmo S, Chiang MF, et al. Advantages of widefield optical coherence tomography in the diagnosis of retinopathy of prematurity. *Front Pediatr.* (2022) 9:797684. doi: 10.3389/fped.2021.797684
14. Scruggs BA, Ni S, Nguyen T-TP, Ostmo S, Chiang MF, Jia Y, et al. Peripheral optical coherence tomography assisted by scleral depression in retinopathy of prematurity. *Ophthalmol Sci.* (2021) 2:100094. doi: 10.1016/j.xops.2021.100094
15. Borkovkina S, Camino A, Janpongsri W, Sarunic MV, Jian Y. Real-time retinal layer segmentation of OCT volumes with GPU accelerated inferencing using a compressed, low-latency neural network. *Biomed Opt Exp.* (2020) 11:3968–84. doi: 10.1364/BOE.395279
16. Jian Y, Wong K, Sarunic MV. Graphics processing unit accelerated optical coherence tomography processing at megahertz axial scan rate and high resolution video rate volumetric rendering. *J Biomed Opt.* (2013) 18:026002. doi: 10.1117/1.JBO.18.2.026002
17. Xu J, Wong K, Jian Y, Sarunic MV. Real-time acquisition and display of flow contrast using speckle variance optical coherence tomography in a graphics processing unit. *J Biomed Opt.* (2014) 19:026001. doi: 10.1117/1.JBO.19.2.026001
18. MathWorks. *MATLAB and Statistics Release*. Natick, MA: The MathWorks Inc (2021).
19. Abràmoff MD, Magalhães PJ, Ram SJ. Image processing with ImageJ. *Biophotonics Int.* (2004) 11:36–42.
20. Wei X, Hormel TT, Jia Y. Phase-stabilized complex-decorrelation angiography. *Biomed Opt Express.* (2021) 12:2419–31. doi: 10.1364/BOE.420503
21. Guo Y, Camino A, Zhang M, Wang J, Huang D, Hwang T, et al. Automated segmentation of retinal layer boundaries and capillary plexuses in wide-field optical coherence tomographic angiography. *Biomed Opt Exp.* (2018) 9:4429–42. doi: 10.1364/BOE.9.004429
22. Ecsedy M, Szamosi A, Karkó C, Zubovics L, Varsányi B, Németh J, et al. A comparison of macular structure imaged by optical coherence tomography in preterm and full-term children. *Invest Ophthalmol Vis Sci.* (2007) 48:5207–11.
23. Cao C, Markovitz M, Ferenczy S, Shields CL. Hand-held spectral-domain optical coherence tomography of small macular retinoblastoma in infants before and after chemotherapy. *J Pediatr Ophthalmol Strabismus.* (2014) 51:230–4. doi: 10.3928/01913913-20140603-01

24. Rootman DB, Gonzalez E, Mallipatna A, VandenHoven C, Hampton L, Dimaras H, et al. Hand-held high-resolution spectral domain optical coherence tomography in retinoblastoma: clinical and morphologic considerations. *Br J Ophthalmol.* (2013) 97:59–65. doi: 10.1136/bjophthalmol-2012-302133
25. Nadiarnykh O, McNeill-Badalova NA, Gaillard MC, Bosscha MI, Fabius AW, Verbraak FD, et al. Optical coherence tomography (OCT) to image active and inactive retinoblastomas as well as retinomas. *Acta Ophthalmol.* (2020) 98:158–65. doi: 10.1111/aos.14214
26. Soliman SE, VandenHoven C, MacKeen LD, Héon E, Gallie BL. Optical coherence tomography–guided decisions in retinoblastoma management. *Ophthalmology.* (2017) 124:859–72. doi: 10.1016/j.ophtha.2017.01.052
27. Skalet AH, Campbell JP, Jian Y. Ultra-widefield Optical Coherence Tomography for Retinoblastoma. *Ophthalmology.* (2022). 129:718.
28. Ang M, Baskaran M, Werkmeister RM, Chua J, Schmidl D, Dos Santos VA, et al. Anterior segment optical coherence tomography. *Prog Retin Eye Res.* (2018) 66:132–56.
29. Pilat AV, Proudlock FA, Shah S, Sheth V, Purohit R, Abbot J, et al. Assessment of the anterior segment of patients with primary congenital glaucoma using handheld optical coherence tomography. *Eye.* (2019) 33:1232–9. doi: 10.1038/s41433-019-0369-3
30. Legocki AT, Zepeda EM, Gillette TB, Grant LE, Shariff A, Touch P, et al. Vitreous findings by handheld spectral-domain oct correlate with retinopathy of prematurity severity. *Ophthalmol Retina.* (2020) 4:1008–15. doi: 10.1016/j.oret.2020.03.027
31. Chen X, Mangalesh S, Dandridge A, Tran-Viet D, Wallace DK, Freedman SF, et al. Spectral-domain OCT findings of retinal vascular–avascular junction in infants with retinopathy of prematurity. *Ophthalmol Retina.* (2018) 2:963–71. doi: 10.1016/j.oret.2018.02.001
32. Ansari WH, Blackorby BL, Shah GK, Blinder KJ, Dang S. OCT Assistance in identifying retinal breaks in symptomatic posterior vitreous detachments. *Ophthalmic Surg Lasers Imaging Retina.* (2020) 51:628–32.
33. Choudhry N, Golding J, Manry MW, Rao RC. Ultra-widefield steering-based spectral-domain optical coherence tomography imaging of the retinal periphery. *Ophthalmology.* (2016) 123:1368–74. doi: 10.1016/j.ophtha.2016.01.045
34. House RJ, Hsu ST, Thomas AS, Finn AP, Toth CA, Materin MA, et al. Vascular findings in a small retinoblastoma tumor using OCT angiography. *Ophthalmol Retina.* (2019) 3:194. doi: 10.1016/j.oret.2018.09.018
35. Rössler J, Dietrich T, Pavlakovic H, Schweigerer L, Havers W, Schüler A, et al. Higher vessel densities in retinoblastoma with local invasive growth and metastasis. *Am J Pathol.* (2004) 164:391–4. doi: 10.1016/S0002-9440(10)63129-X
36. Sagar P, Rajesh R, Shanmugam M, Konana VK, Mishra D. Comparison of optical coherence tomography angiography and fundus fluorescein angiography features of retinal capillary hemangioblastoma. *Indian J Ophthalmol.* (2018) 66:872.
37. Parodi MB, Cicinelli MV, Iacono P, Bolognesi G, Bandello F. Multimodal imaging of foveal cavitation in retinal dystrophies. *Graefes Arch Clin Exp Ophthalmol.* (2017) 255:271–9.
38. Yu J, Ni Y, Keane PA, Jiang C, Wang W, Xu G. Foveomacular schisis in juvenile X-linked retinoschisis: an optical coherence tomography study. *Am J Ophthalmol.* (2010) 149:973–978.e2. doi: 10.1016/j.ajo.2010.01.031
39. Patel RC, Gao SS, Zhang M, Alabduljalil T, Al-Qahtani A, Weleber RG, et al. Optical coherence tomography angiography of choroidal neovascularization in four inherited retinal dystrophies. *Retina.* (2016) 36:2339–47. doi: 10.1097/IAE.0000000000001159
40. Hsu ST, Finn AP, Chen X, Ngo HT, House RJ, Toth CA, et al. Macular microvascular findings in familial exudative vitreoretinopathy on optical coherence tomography angiography. *Ophthalmic Surg Lasers Imaging Retina.* (2019) 50:322–9.
41. Lee J, El-Dairi MA, Tran-Viet D, Mangalesh S, Dandridge A, Jiramongkolchai K, et al. Longitudinal changes in the optic nerve head and retina over time in very young children with familial exudative vitreoretinopathy. *Retina.* (2019) 39:98. doi: 10.1097/IAE.0000000000001930
42. De la Huerta I, Mesi O, Murphy B, Drenser KA, Capone A Jr, Trese MT. Spectral domain optical coherence tomography imaging of the macula and vitreomacular interface in persistent fetal vasculature syndrome with posterior involvement. *Retina.* (2019) 39:581–6. doi: 10.1097/IAE.0000000000001993
43. Mangalesh S, Chen X, Tran-Viet D, Viehland C, Freedman SF, Toth CA. Assessment of the retinal structure in children with incontinentia pigmenti. *Retina.* (2017) 37:1568.
44. McClintic SM, Wilson LB, Campbell JP. Novel macular findings on optical coherence tomography in incontinentia pigmenti. *JAMA Ophthalmol.* (2016) 134:e162751. doi: 10.1001/jamaophthalmol.2016.2751
45. Kim SJ, Yang J, Liu G, Huang D, Campbell JP. Optical coherence tomography angiography and ultra-widefield optical coherence tomography in a child with Incontinentia pigmenti. *Ophthalmic Surg Lasers Imaging Retina.* (2018) 49:273–5. doi: 10.3928/23258160-20180329-11
46. Kunkler AL, Patel NA, Russell JF, Fan KC, Al-Khersan H, Iyer PG, et al. Intraoperative optical coherence tomography angiography in children with Incontinentia pigmenti. *Ophthalmol Retina.* (2022) 6:330–2. doi: 10.1016/j.oret.2022.01.001

Conflict of Interest: Oregon Health and Science University (OHSU), DH, and YaJ have significant financial interests in Optovue, a company that may have a commercial interest in the results of this research and technology. These potential conflicts of interest have been reviewed and managed by OHSU. DH and YaJ have received royalties for patent files through OHSU, as well as loaned equipment for research from Optovue.

The remaining authors declare that the research was conducted in the absence of any commercial or financial relationships that could be construed as a potential conflict of interest.

Publisher's Note: All claims expressed in this article are solely those of the authors and do not necessarily represent those of their affiliated organizations, or those of the publisher, the editors and the reviewers. Any product that may be evaluated in this article, or claim that may be made by its manufacturer, is not guaranteed or endorsed by the publisher.

Advantages of publishing in Frontiers

OPEN ACCESS
Articles are free to read for greatest visibility and readership

FAST PUBLICATION
Around 90 days from submission to decision

HIGH QUALITY PEER-REVIEW
Rigorous, collaborative, and constructive peer-review

TRANSPARENT PEER-REVIEW
Editors and reviewers acknowledged by name on published articles

Frontiers
Avenue du Tribunal-Fédéral 34
1005 Lausanne | Switzerland

Visit us: www.frontiersin.org
Contact us: frontiersin.org/about/contact

REPRODUCIBILITY OF RESEARCH
Support open data and methods to enhance research reproducibility

DIGITAL PUBLISHING
Articles designed for optimal readership across devices

FOLLOW US
@frontiersin

IMPACT METRICS
Advanced article metrics track visibility across digital media

EXTENSIVE PROMOTION
Marketing and promotion of impactful research

LOOP RESEARCH NETWORK
Our network increases your article's readership